Current Topics in Microbiology and Immunology

Friedrich Koch-Nolte *Editor*

Endogenous ADP-Ribosylation

Springer

Current Topics in Microbiology and Immunology

Volume 384

More information about this series at http://www.springer.com/series/82

Friedrich Koch-Nolte
Editor

Endogenous ADP-Ribosylation

Responsible Series Editor: Klaus Aktories

Springer

Editor
Friedrich Koch-Nolte
Institute of Immunology
University Medical Center
Hamburg
Germany

ISSN 0070-217X
ISBN 978-3-319-10770-7
DOI 10.1007/978-3-319-10771-4

ISSN 2196-9965 (electronic)
ISBN 978-3-319-10771-4 (eBook)

Library of Congress Control Number: 2014948775

Springer Cham Heidelberg New York Dordrecht London

Printed on acid-free paper

Springer is part of Springer Science+Business Media (www.springer.com)

Preface

ADP-ribosylation was originally discovered as a posttranslational protein modification catalyzed by Diphtheria Toxin (DT) and Cholera Toxin (CT). These toxins are secreted by *Corynebacterium diphtheriae* and *Vibrio cholera* as a multidomain protein (DT) or as a binary AB_5 protein complex (CT). Each of these toxins harbors a catalytic ADP-ribosyltransferase (ART) domain. Structurally, the enzymatic domains of DT and CT are related, even though they show very limited sequence similarity. Following translocation across cellular membranes to the cytosol of mammalian cells, the ART domains of these toxins transfer ADP-ribose from NAD^+ to a specific amino acid in a specific target protein; in case of DT to Diphthamide 687 (a modified histidine residue) of elongation factor 2, in case of CT to Arginine 187 in the alpha subunit of heterotrimeric G proteins. Due to their high specificity, these toxins are still widely used today as tools to delete specific cell types (DT) or to study signaling via G-protein coupled receptors (CT).

Molecular cloning and 3D-structure analyses have uncovered endogenous enzymes related to DT and CT in many organisms from all kingdoms of life. Remarkably, these endogenous ARTs fall into two major subclasses that are distinguished by conserved structural motifs: H-Y-E in the ART**D** subfamily (related to **D**iphtheria Toxin), R-S-E in the ART**C** subfamily (related to C2 and C3 **C**lostridial Toxins).

Biochemical analyses have uncovered ARTs that ADP-ribosylate amino acids other than diphthamide and arginine, the targets of DT and CT. These include cysteine, asparagine, threonine, glutamine, lysine, and glutamate. Moreover, structurally related ARTs have been discovered that ADP-ribosylate nucleotides or antibiotics. ADP-ribosylation is a potentially reversible modification. Two distinct enzyme families are known that catalyze de-ADP-ribosylation of ADP-ribosylated proteins. These include ADP-ribosylhydrolases (ARHs) and macro-domain/poly-ADP-ribosylglycohydrolases (PARGs).

Database and structural analyses indicate that endogenous ARTs, ARHs, and PARGs in plants and animals have been acquired by lateral gene transfer from procaryotes. Indeed, as laid out in the chapter by L. Aravind, the origin of these enzymes seems to lie in polymorphic prokaryotic biological conflict systems.

This volume brings together ten papers from renowned experts in the field that review exciting recent findings on ADP-ribosylation. This field is important not only because it delivers a better understanding of ADP-ribosylating toxins and their endogenous relatives, but also because this understanding provides a basis for developing toxin-neutralizing drugs and drugs that target endogenous ART relatives. I am confident that the reader will enjoy the interesting contributions in this special issue on endogenous ADP-ribosylation.

Hamburg Friedrich Koch-Nolte

Contents

Part I
Evolution and Detection of Endogenous ADP-Ribosylation

The Natural History of ADP-Ribosyltransferases and the ADP-Ribosylation System

L. Aravind, Dapeng Zhang, Robson F. de Souza, Swadha Anand and Lakshminarayan M. Iyer

Abstract Catalysis of NAD^+-dependent ADP-ribosylation of proteins, nucleic acids, or small molecules has evolved in at least three structurally unrelated superfamilies of enzymes, namely ADP-ribosyltransferase (ART), the Sirtuins, and probably TM1506. Of these, the ART superfamily is the most diverse in terms of structure, active site residues, and targets that they modify. The primary diversification of the ART superfamily occurred in the context of diverse bacterial conflict systems, wherein ARTs play both offensive and defensive roles. These include toxin–antitoxin systems, virus-host interactions, intraspecific antagonism (polymorphic toxins), symbiont/parasite effectors/toxins, resistance to antibiotics, and repair of RNAs cleaved in conflicts. ARTs evolving in these systems have been repeatedly acquired by lateral transfer throughout eukaryotic evolution, starting from the PARP family, which was acquired prior to the last eukaryotic common ancestor. They were incorporated into eukaryotic regulatory/epigenetic control systems (e.g., PARP family and NEURL4), and also used as defensive (e.g., pierisin and CARP-1 families) or immunity-related proteins (e.g., *Gig2*-like ARTs). The ADP-ribosylation system also includes other domains, such as the Macro, ADP-ribosyl glycohydrolase, NADAR, and ADP-ribosyl cyclase, which appear to have initially diversified in bacterial conflict-related systems. Unlike ARTs, sirtuins appear to have a much smaller presence in conflict-related systems.

Supplementary MaterialA list of Genbank identifier and domain architectures of the proteins discussed in this chapter might be found at: ftp://ftp.ncbi.nih.gov/pub/aravind/ADPR/ADPR.html

L. Aravind (✉) · D. Zhang · S. Anand · L. M. Iyer
National Center for Biotechnology Information, National Library of Medicine, National Institutes of Health, Bethesda, MD 20894, USA
e-mail: aravind@ncbi.nlm.nih.gov

R. F. de Souza
Microbiology Department, Biomedical Sciences Institute, University of Sao Paulo, Av. Prof. Lineu Prestes, 1374-Biomédicas II-Sala 250, Cidade Universitária, São Paulo 05508-900, Brazil

Current Topics in Microbiology and Immunology (2015) 384: 3–32
DOI: 10.1007/82_2014_414

Published Online: 16 July 2014

Contents

1 Introduction

Nicotinamide adenine dinucleotide (NAD^+) is a versatile metabolite that is at the center of a large array of biochemical processes across all domains or superkingdoms of life (Belenky et al. 2007; Gazzaniga et al. 2009; Sorci et al. 2010). Its most widespread and best understood role is that of a redox cofactor (along with its phosphorylated derivative $NADP^+$) for diverse dehydrogenases of the Rossmann fold, which utilizes the facile transition between the hydrogenated and dehydrogenated states of the nicotinamide ring (Berg et al. 2012). The role of NAD^+ as a substrate for diverse protein- and nucleic acid-modifying enzymes has also become increasingly apparent in a striking array of subcellular contexts. In these latter reactions, rather than undergoing reversible oxidation state changes, different fragments of the NAD^+ molecule are transferred to substrate molecules resulting in specific modifications. One of these, catalyzed by the DNA ligase, which is observed in all bacteria, is the transfer of the adenylate moiety from NAD^+ to the 5′ phosphate of DNA (Park et al. 1989). This adenylated DNA serves as an intermediate for the ligation of polynucleotides. Another class of transfer reactions targets the bond between the nicotinamide ring and the ADP-ribose moiety transferring the latter moiety to targets with the release of nicotinamide. Such ADP-ribose transfer reactions are catalyzed by at least three evolutionarily unrelated superfamilies of enzymes, namely the ADP-ribosyltransferase (ART), the Sirtuins, and the obscure TM1506 superfamilies (Corda and Di Girolamo 2003; Hassa et al. 2006; Hawse and Wolberger 2009; Iyer et al. 2011).

2 The Many Faces of ADP-Ribosylation

ADP-ribosylation catalyzed by the ART superfamily first came to light in two independent studies in the 1960s, which respectively identified a novel biopolymer in vertebrate cells (Chambon et al. 1963) and showed the need for NAD^+ for the action of the diphtheria toxin produced by *Corynebacterium diphtheria* (Collier and Pappenheimer 1964). A flurry of investigations in the next 5 years showed that the common theme unifying these disparate activities was the enzymatic conjugation of ADP-ribose (hereinafter ADPR) derived from NAD^+ to proteins and/or other ADPR moieties (Sugimura and Miwa 1994; Ueda and Hayaishi 1985). Over the next 20 years it became firmly established that NAD^+-dependent ADP-ribosylation was a widespread phenomenon across diverse lineages of life as well as viruses (Sugimura and Miwa 1994; Ueda and Hayaishi 1985). Among the key issues that became clear was that this modification came in two basic forms: polyADP-ribosylation, where long-branched polymers of ADP-ribose are generated and added to target proteins, and mono-ADP-ribosylation, which involved transfer of a single ADP-ribose moiety to the target (Sugimura and Miwa 1994; Ueda and Hayaishi 1985). It was also established that this modification targets several distinct amino acid side chains and termini resulting in the ribose being linked via *N*-, *O*- or *S*- glycosidic bonds (Corda and Di Girolamo 2003; Laing et al. 2011) (Fig. 1).

It was also seen that these modifications catalyzed by ARTs were at the center of a wide range of biological phenomena. Of these, the first to be described in detail were the mono-ADP-ribosylation activities of diverse bacterial toxins (Corda and Di Girolamo 2003; Ueda and Hayaishi 1985). Around the same time, it also became apparent that the bacteriophage T4 encodes one or more ARTs, which are deployed to mono-ADP-ribosylate host proteins, such as the RNA polymerase α subunit (Koch and Ruger 1994; Ueda and Hayaishi 1985). In parallel, there was also accumulating evidence for the roles of cellular ARTs. For example, the ART-ADP-ribosyl glycohydrolase pair, DraT and DraG was found to alternately modify or demodify dinitrogenase reductase and regulate its activity (Ludden 1994). In more recent times the roles of such ARTs and polyADP-ribosyltransferases (PARPs/PARTs) have become increasingly evident in diverse eukaryotic processes (Hassa et al. 2006). Modifications of nuclear proteins (e.g., histones) by PARPs, cytoskeletal (e.g., actin) by intracellular ARTs and surface proteins (e.g., nucleotide-gated ion channels and integrins) by ecto-ARTs play important roles in epigenetics, regulation of DNA repair, apoptosis, signaling, and complex biological processes, such as long-term memory in animals (Cohen-Armon et al. 2004; Hassa et al. 2006; Koch-Nolte et al. 2008).

Sirtuins, whose activities have come to light relatively recently, were first identified as protein ADP-ribosyltransferases (Frye 1999). However, this activity has not been much studied; rather they are best known for their action as protein deacylases—in these reactions they transfer the ADPR from NAD^+ to acylated lysines in proteins (Smith et al. 2002). As a consequence, the acyl group is removed in the form of an *O*-acylated ADP-ribose (OAADPR; Fig. 1). In addition

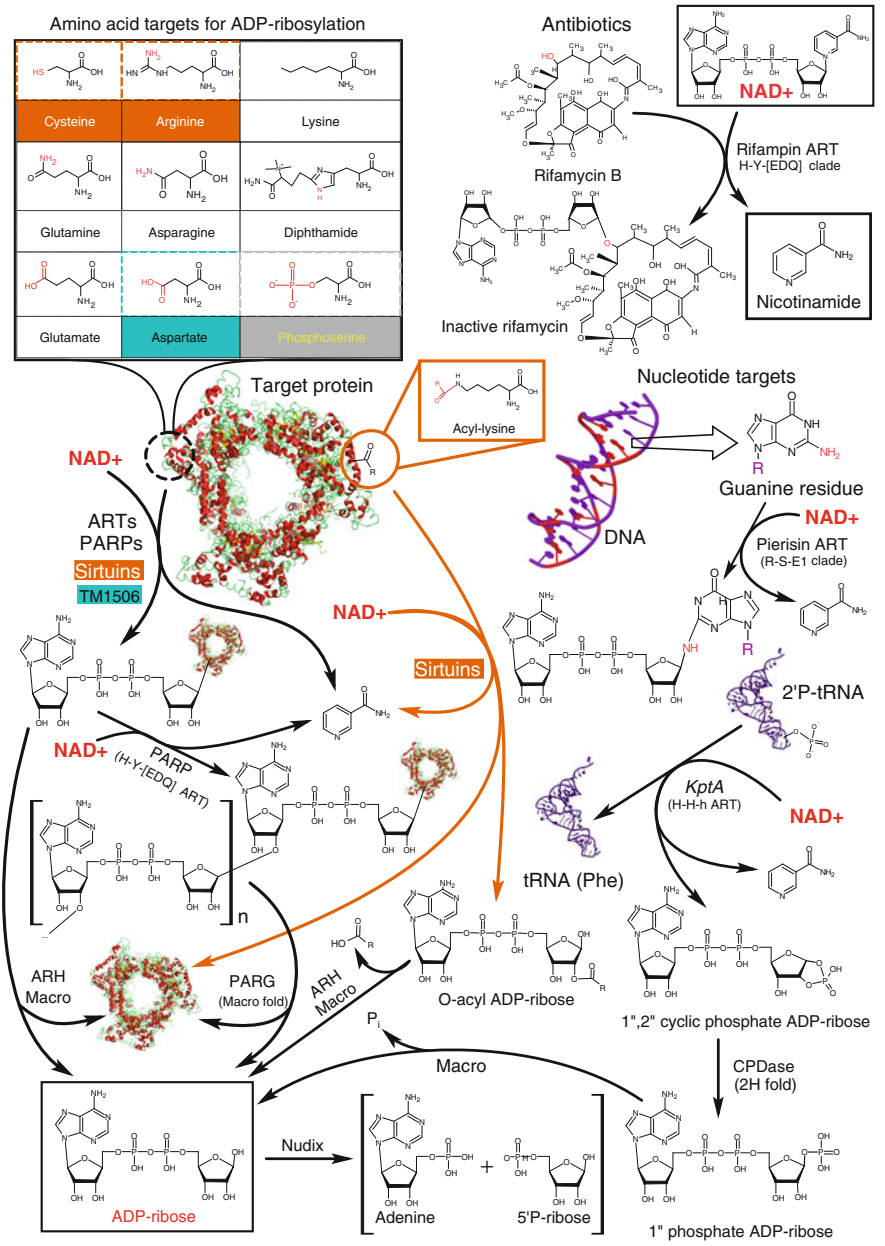
Amino acid targets for ADP-ribosylation
Cysteine
Arginine
Lysine
Glutamine
Asparagine
Diphthamide
Glutamate
Aspartate
Phosphoserine
Antibiotics
NAD+
Rifampin ART
H-Y-[EDQ] clade
Rifamycin B
Inactive rifamycin
Nicotinamide
Target protein
Acyl-lysine
Nucleotide targets
Guanine residue
NAD+
Pierisin ART
(R-S-E1 clade)
DNA
2'P-tRNA
ARTs
PARPs
Sirtuins
TM1506
NAD+
Sirtuins
NAD+
PARP
(H-Y-[EDQ] ART)
n
KptA
(H-H-h ART)
NAD+
tRNA (Phe)
ARH
Macro
PARG
(Macro fold)
ARH
Macro
O-acyl ADP-ribose
1",2" cyclic phosphate ADP-ribose
P i
Macro
CPDase
(2H fold)
ADP-ribose
Nudix
Adenine
5'P-ribose
1" phosphate ADP-ribose

◀ **Fig. 1** Summary of known ADP-ribosylation targets and pathways. Most substrates are tagged by ADP-ribose by different members of the ADP-ribosyltransferase fold (ARTs and PARPs). Cysteine and arginine residues (*orange*) may also serve as substrates for reactions catalyzed by members of the sirtuin family and aspartate (*turquoise*) is possibly a substrate of the TM1506 family. The enzyme responsible for phosphoserine (*gray*) ADP-ribosylation remains unknown. At the bottom of the figure, some key reactions for processing ADP-ribose derivatives are represented. *ART* ADP-ribosyltransferase, *PARP* poly(ADP-ribosyl) polymerase, *CDPase* 2′-cyclic phosphate hydrolase, *KptA/Tpt1* RNA 2′-phosphotransferase (ART fold), *Pierisin* lepidopteran cytotoxin (ART fold), *ARH* ADP-ribosylglycohydrolase, *PARG* poly(ADP-ribosyl)-glycohydrolase, *Macro* ADP-ribose associated Macro domain, *Nudix* "nucleotide diphosphate linked to X" hydrolase domain. Sirtuins might deacylate proteins with several distinct acyl groups (show as R-), such as acetyl, malonyl, crotonyl, succinyl or palmitoyl groups

to ARTs and sirtuins, a variety of other enzymes have been characterized as belonging to the ADPR-centered systems, such as ADP-ribosyl glycohydrolases (ARHs), which deconjugate ADP-ribose from targets (Koch-Nolte et al. 2008), polyADP-ribosyl glycohydrolases (PARGs) which hydrolyze ADPR polymers (Slade et al. 2011), ADP-ribosyl cyclase/cyclic-ADP-ribose hydrolase (e.g., CD38) (Guse and Lee 2008) and binding domains, which recognize ADPR and its derivatives generated by the action of the above enzymes (de Souza and Aravind 2012). In the past two decades, the advent of genome sequencing, structural genomics, and development of sensitive sequence analysis methods have greatly advanced our understanding of these proteins: First, new sequence and structure analysis methods have helped identify new members using sensitive similarity searches (Bazan and Koch-Nolte 1997; de Souza and Aravind 2012; Fieldhouse et al. 2010; Otto et al. 2005; Pallen et al. 2001). Second, they have given us an unprecedented window into the evolution of these enzymes and helped us understand their origins (de Souza and Aravind 2012; Zhang et al. 2012). Finally, they have also opened the door for new approaches to the understanding of their functions in experimentally difficult or less-studied organisms (e.g., algae such as *Emiliania*, apicomplexan parasites like *Plasmodium*, trypanosomes, and bacterial pathogens such *as Mycobacterium tuberculosis*) (Garcia-Salcedo et al. 2003; Merrick and Duraisingh 2007).

In this chapter, we provide an overview of the biochemical diversity and evolutionary history of ADPR-transferring enzymes in light of recent advances in genomics and computational sequence analysis. We also summarize new functional insights and possible new directions offered by these studies.

3 The ART Superfamily

3.1 Biochemical Diversity in the ART Superfamily

Members of the ART superfamily (hereinafter ARTs) can catalyze the transfer of ADPR from NAD^+ to diverse substrates resulting in *N*- *O*- or *S*- glycosidic linkages with the 1″ position of ribose (Fig. 1). This reaction proceeds via the SN1

mechanism: the nicotinamide leaves first with the generation of a reactive oxacarbenium ion as an intermediate, which is presented for nucleophilic attack by the target moiety at the 1″ position (Jorgensen et al. 2008a). The transfer is accompanied by an anomeric inversion of the newly formed glycosidic bond at the 1″ position with respect to the linkage of nicotinamide in NAD^+ (Ueda and Hayaishi 1985). The reaction mechanism, wherein nicotinamide leaves first, is consistent with the proposal that some members of the ART superfamily such as the halovibirins and the streptococcal NADase (SPN) toxins act primarily as NAD^+-glycohydrolases (Smith et al. 2011; Stabb et al. 2001). However, in the former case the released ADPR is noncatalytically conjugated to arginines in proteins (Stabb et al. 2001), suggesting that even the latter enzymes could potentially use the same mechanism to generate products effectively same as *bona fide* ARTs. In contrast to enzyme superfamilies catalyzing most other protein modifications, ARTs modify a striking variety of side chains and terminal positions in proteins (Fig. 1) (Corda and Di Girolamo 2003; Hassa et al. 2006; Koch-Nolte et al. 2001; Laing et al. 2011; Ueda and Hayaishi 1985). To date, ARTs have been shown to modify: (1) the terminal NH_2 of the guanidino group of arginine (e.g., the bacterial DraT which ADP-ribosylates the dinitrogen reductase, the T4 proteins Alt, ModA and ModB, several bacterial toxins directed at eukaryotic hosts such as the cholera, *Bacillus sphaericus* mosquitocidal toxin (MTX), *Bacillus cereus* VIP2, *Clostridium difficile* CDT and *C. perfringens* iota toxins, as well as eukaryotic mono-ARTs (ARTC1-ARTC5) modifying endogenous proteins such as actins, integrins, and nucleotide-gated ion channels); (2) The intracyclic NH in diphthamide, which is a highly modified amino acid derived from histidine in eukaryotic EF2 (e.g., the diphtheria and *P. aeruginosa* toxin A); (3) The NH_2 of the amide group of the glutamine side chain (e.g., the *Photorhabdus luminescens* ART toxin); (4) The NH_2 of the amide group of the asparagine side chain (e.g., the *Clostridium botulinum* C3 toxin); (5) The SH group in the side chain of cysteine (e.g., the pertussis toxin which targets cysteines in multiple vertebrate Gα proteins); (6) The COOH group of glutamate [e.g., PARP10/ARTD10 ADP-ribosylates itself on glutamate 882 (Kleine et al. 2008)]. The COOH group of the aspartate side chain has also been proposed as a potential mono-ART substrate in eukaryotes, although to date the responsible enzyme remains unidentified (Hassa et al. 2006). Early studies also detected ADP-ribosylation of phosphoserine in Histone H1 but again the enzyme remains unknown (Smith and Stocken 1974). Furthermore, given this diversity it is conceivable that there might be ART domains which modify side chains of serine or threonine, especially among versions found in bacterial toxins.

In the case of PARPs, successive ADPR chains might be added via *O*-glycosidic linkages between the 2′ or 2″ positions and 1″ positions of successive ADPR units. As each unit has two ribose moieties successive links to either of them can result in large branched molecules with up to 200 units that can be visualized via electron microscopy (Hassa et al. 2006; Ueda and Hayaishi 1985). In eukaryotes, these poly ADPR (pADPR) molecules apparently modify a wide range of nuclear proteins including core and linker histones, chromatin proteins like HMGA/B, transcription factors like p53, RNA-binding proteins such hnRNPs and DNA

repair/replication factors like topoisomerases and PCNA (Hassa et al. 2006; Ueda and Hayaishi 1985). It is widely believed that in these substrate proteins the side chain COOH of glutamate, the terminal COOH and/or perhaps aspartate are modified by pADPR. However, recent studies have shown that the automodification of PARP1 (ARTD1) occurs via lysine epsilon-NH_2 groups (Altmeyer et al. 2009).

In addition to proteins, ARTs modify nucleic acids: cytotoxic ARTs of lepidopterans and molluscs modify the exo-cyclic amino group at the second position of guanine in DNA to induce apoptosis (Carpusca et al. 2006; Nakano et al. 2006). Another nucleic acid-modifying ART is the RNA 2′-phosphotransferase KptA/Tpt1 (ARTD18), an enzyme that repairs the 2′-phosphate generated as a result of tRNA splicing and RNA ligase action (Spinelli et al. 1999). Here, the ADPR is added to 2′ phosphate which then leaves as ADP-ribose 1″-2″ cyclic diphosphate (Appr>p). ARTs also modify low molecular weight substrates, such as the rifamycin antibiotics, which are inactivated by ADP-ribosylation of an OH group on carbon 23 (Baysarowich et al. 2008) (Fig. 1).

3.2 *Structural and Catalytic Features of the ART Superfamily*

The ART superfamily is characterized by extreme divergence at the sequence level often making it difficult to identify new members through sequence analysis alone (Bazan and Koch-Nolte 1997; de Souza and Aravind 2012; Fieldhouse et al. 2010). However, at the structural level all members of the superfamily show a strongly conserved core fold (Figs. 2 and 3) (Bazan and Koch-Nolte 1997; de Souza and Aravind 2012). This core consists of a split β-sheet formed by two distinct units of three strands each, with most strands being alternately interleaved between the two units (i.e., strand order in the sheet is 4-5-2|1-3-6, where "|" represents the split in the sheet; Fig. 2 bottom panel). Typically, most of these strands are followed by a downstream helical element suggesting that the entire fold emerged through a series of duplications of a strand-helix element with the strands being distributed alternately between two units of the split sheet. In most members of the family the key active site residues emerge from the "lower" surface of strand 1, and the "upper" surface of strands 2 and 5 (Fig. 3). As a result the NAD^+ molecule is sterically constrained between the lower and upper surfaces respectively of the two units of the split sheet with the central diphosphate being wedged in the central split in the sheet (Jorgensen et al. 2008a). The characteristic loop between helix 1 and strand 2 is observed throughout the fold and forms a "wall" of the NAD^+-binding pocket (Fig. 3). The active site residues from strand 1 typically contact the ribose linked to the adenine and also the nicotinamide moiety. Those from strands 2 and 5 contact the ribose linked to the nicotinamide. This conformational constraining of NAD^+ between the two elements of the split sheet appears to be critical for catalysis by these enzymes for it appears to strain the substrate to facilitate its cleavage.

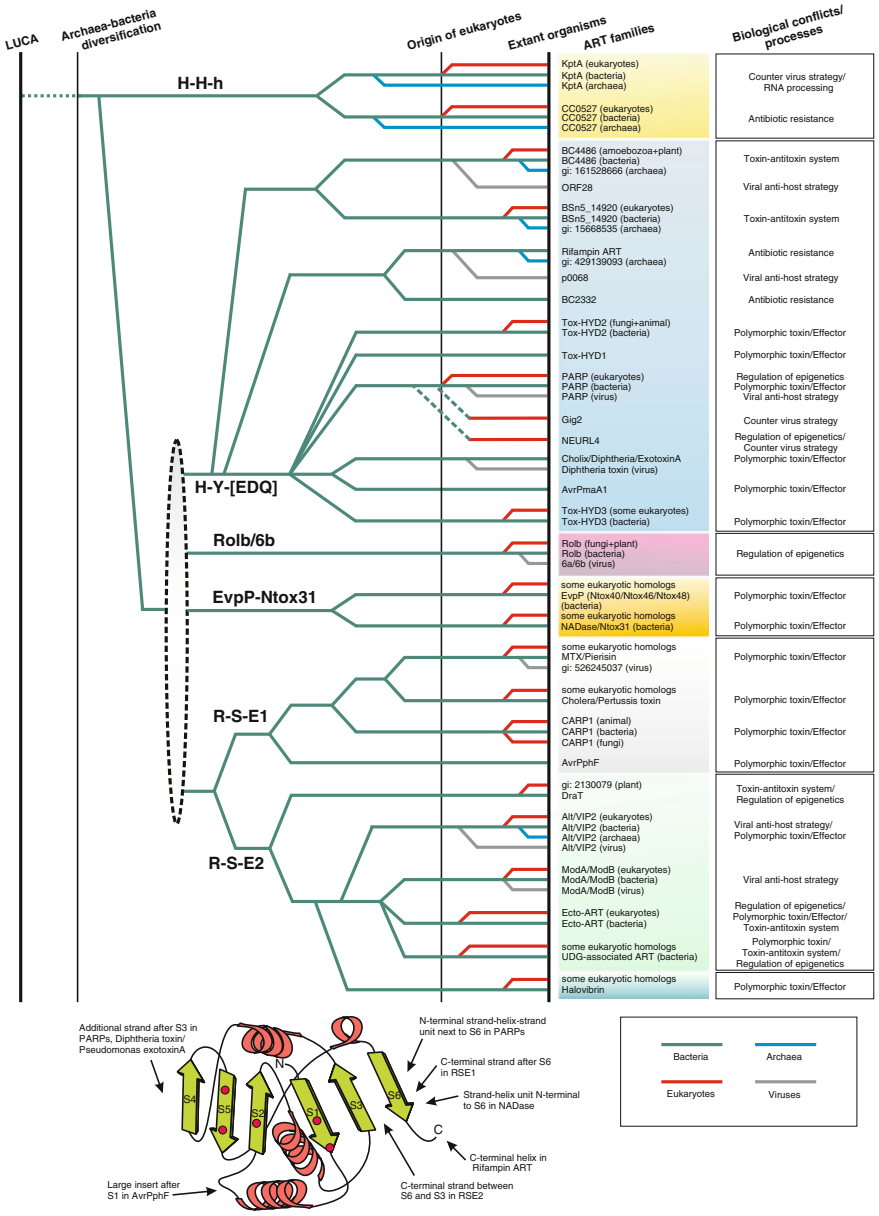

Fig. 2 Reconstructed evolutionary history for the different members of ART superfamily. Horizontal lines are colored according to their observed phyletic distributions (key: *bottom right*). *Dashes* indicate uncertainty in terms of the origins of a family, while the *gray ellipse* indicates that the RolB/6b clade likely underwent rapid divergence from either the H-Y-[EDQ] or R-S-E clade. The H-H-h and H-Y-[EDQ] include the ARTD proteins, while the R-S-E clade includes the ARTC proteins in the previously presented nomenclature for ART domains (Hottiger et al. 2010). For each family the known or inferred functional role in biological conflicts or processes is indicated (*right column*). Representatives of each family are shown in Figs. 4 and 5. In the bottom panel shows the idealized topology of the ART fold with markup indicating specific structural features associated with certain ART families and positions of active site residues

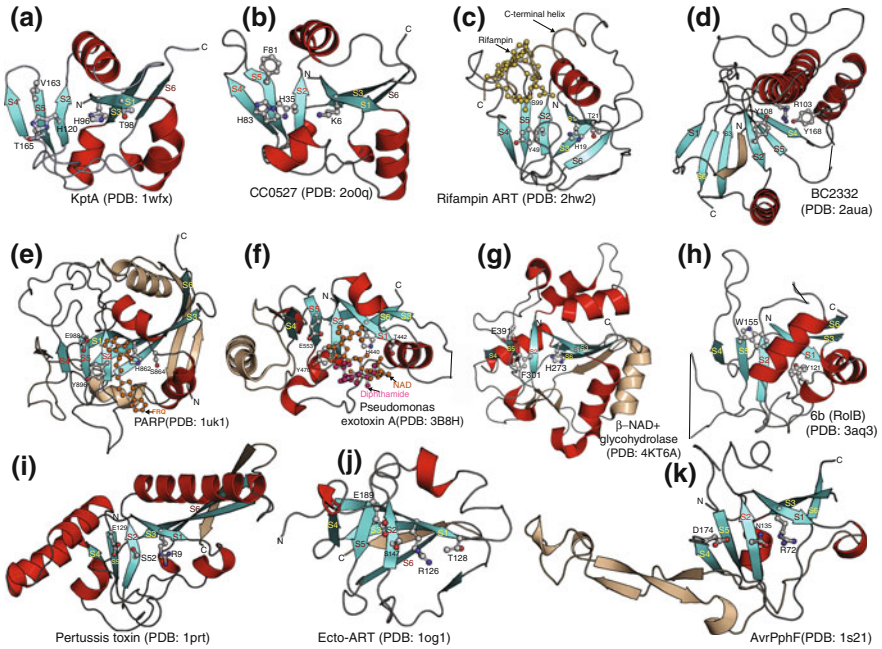

Fig. 3 Cartoon structures of diverse members of the ART superfamily. Conserved strands and helices of the core fold are shown in *aquamarine* and *red*, respectively. Additional strands that pack with the sheets and inserts are shown in *wheat color*. Conserved strands of the core are labeled, as also active site residues and ligands. **a** KptA (PDB: 1wfx). **b** CC0527 (PDB: 2o0q). **c** Rifampin ART (PDB: 2hw2). **d** BC2332 (PDB: 2aua). **e** PARP (PDB: 1uk1). **f** Pseudomonas exotoxin A (PDB: 3B8H). **g** β-NAD$^+$ glycohydrolyase (PDB: 4KT6A). **h** 6b (RolB) (PDB: 3aq3). **i** Pertussis toxin (PDB: 1prt). **j** Ecto-ART (PDB: log1). **k** AvrPphF (PDB: 1s21)

Examination of the active site residues reveals three widespread configurations which are described in terms of the consensus conserved residue supplied by strands 1, 2, and 5 of the core:

(1) *H-H-h*: This is seen primarily in two families, namely the KptA (ARTD18) or tRNA 2′ phosphotransferase family and the CC0527 family (Fig. 3a, b), which has been largely obscure prior to this chapter (see below). Here, the first strand supplies a conserved H, which is usually in a HX[ST] motif, where both the H and the downstream alcoholic residue might make polar contacts with the 2′ and 3′ OH of ribose groups. Strand-2 supplies a histidine and strand-5 has just a hydrophobic residue (h), which contacts the ribose linked to the nicotinamide. In these ARTs the hydrophobic residue in strand 5 is followed by an additional polar residue two residues downstream, typically [TS] in KptA or H in CC0527, which is also likely to contribute to the active site (Fig. 3a, b).

(2) *H-Y-[QED]*: This is seen in several families such as diphtheria toxin-like ARTs, PARPs, and related mono-ARTs (Figs. 2 and 3c–f). Domains with this

active site configuration and those with the above configuration have been previously designated as ARTD (Hottiger et al. 2010). Here, the strand 1 histidine occurs in the same motif as observed in the H-H-h configuration. The residue from strand 2 is an aromatic residue which is typically tyrosine and less frequently phenylalanine. That from the beginning of strand 5 is acidic or in some cases a glutamine and it typically makes a polar contact with the 2″ OH (Jorgensen et al. 2008a). It often occurs as the downstream residue in a [QE]X[QED] motif, with the first [QE] position playing a role in recognition of the target moiety that is ADP-ribosylated (Baysarowich et al. 2008; Jorgensen et al. 2008a, b). A variation on this theme is seen in the rifamycin ART family, where the strand 5 displays a TXSXR motif, where the TXS maps to the [QE]X[QED] in the above motif (Fig. 3c). Similarly, in a related novel family of ARTs prototyped by the version from the *Acinetobacter* phage ZZ1 (p0068; gi: 570033484) the acidic residue is often absent, being replaced by a tyrosine.

(3) *R-[ST]-E*: This configuration is seen in several bacterial toxins, like the heat labile toxin of *E. coli*, the cholera toxin, bacteriophage ARTs, like Alt, ModA and ModB, and certain eukaryotic intracellular (e.g., molluscan CARP-1) and extracellular ARTs (Fig. 3). Domains with this active site configuration have been previously designated as ARTC (Hottiger et al. 2010). In this configuration, the arginine plays the equivalent role as the histidine in strand 1 and the [ST] plays a role comparable to the aromatic residue (Y) in strand 2. The E from strand 5 is identical in function to the equivalent residue in those showing the H-Y-E configuration (Figs. 2 and 3).

(4) *Aberrant configurations*: Several of members of the ART superfamily show highly derived active site configurations that do not match any of the above patterns. The previously unrecognized clade of ARTs typified by the *Edwardsiella tarda* EvpP toxin (Zheng and Leung 2007) and the SPN toxins (Smith et al. 2011) (see below) displays either an arginine (rarely histidine; e.g., NADase) or no specific conserved residue in strand 1, an aromatic position (usually Y or F) equivalent to the Y or [ST] in strand 2 and a glutamate/glutamine at the beginning of strand-5. Thus this clade displays a hybrid between the H-Y-[QED] and R-[ST]-E configurations. The RolB family of ARTs prototyped by the *Agrobacterium* Ti plasmid (T-DNA) 6b-related proteins (Wang et al. 2011) represents another aberrant configuration (Fig. 3h), where most residues corresponding to any of the above configurations are not conserved. The only exception is a highly conserved aromatic residue from strand-5 that corresponds to the hydrophobic residue in the H-H-h configuration (Fig. 3h). This residue along with another residue (typically tyrosine or arginine) from the helical insert upstream of strand 3 is likely to constitute a novel active site in this family. Another novel family, the BC2332 (Pfam: DUF2441) family has undergone an even more drastic modification, both in structural and sequence terms (Fig. 3d). It appears to have emerged via triplication of the ancestral ART fold followed by reconstitution of a domain by elements drawn from each of the three repeats. As a

consequence, the strand order is re-organized, now adopting a 4-1-2-6-3-5 linear sequence from the N- to C-terminus, where the numbers stand for the strand numbers in the typical ART domain. This is concomitantly accompanied by the emergence of a completely new active site that is unrelated to all other members of the fold (Fig. 3d). This pervasive plasticity in the active site of the ARTs lends further support to the proposal that the conformation in which NAD^+ is "wedged" in the split sheet is probably more critical for the catalytic mechanism than the strict presence of particular residues.

The minimal version of the fold with just six strands and no extended inserts between the elements is seen only in the KptA and CC0527 families (Hottiger et al. 2010). The core split β-sheet is often augmented by N-terminal (e.g., RolB family) (Wang et al. 2011) or C-terminal extensions (e.g., diphtheria toxin-like ARTs) or internal insertions (e.g.,an inserted strand after strand 3 in PARPs) (Hottiger et al. 2010). A subset of ARTs showing the R-S-E configuration shows an additional C-terminal strand 7, which forms a hairpin with core strand-6 and stacks against strand 3 in a parallel configuration (Fig. 3j). The rifamycin ART family shows a C-terminal helix which plays a key role in substrate recognition by forming a "cap" over the active site (Baysarowich et al. 2008). Additionally, several versions might show inserted elements. The characteristic loop between helix 1 and strand 2 is a frequent site for independent insertions in different families and some of these inserts play a role in substrate recognition (e.g., rifamycin and diphtheria toxin-like ART families). Some PARPs display an insert of a Zn-cluster just N-terminal to strand 3, which might also play a role in substrate recognition (Hottiger et al. 2010). The dramatic structural reorganization in the BC2332 family has resulted in the emergence of unprecedented large inserts between some of the elements drawn from the different copies of the above mentioned triplication. Thus, emergence of lineage-specific inserts appears to have played an important role in the origin of distinct substrate specificities in the superfamily.

4 Evolutionary History and Diversity of the ART Superfamily

Availability of multiple structures from distant members of the ART superfamily, sensitive sequence profile searches to identify novel versions, and determination of phyletic patterns have resulted in a new and detailed understanding of the evolutionary history of the ART superfamily (Bazan and Koch-Nolte 1997; de Souza and Aravind 2012; Finn et al. 2010; Schaffer et al. 2001; Soding et al. 2005). In particular the above-described structural features and active site configurations help establish the higher-order relationships between distantly related families (Fig. 2). Within families, higher levels of sequence conservation allow establishment of relationships based on conventional phylogenetic analysis (Price et al. 2010).

By combining these, we present below an evolutionary reconstruction reflecting the current state of the data (Fig. 2).

Broadly, the ART superfamily can be divided into three major higher-order clades that more-or-less reflect the above-described three basic active site configurations. The most primitive or earliest branching clade appears to be the H-H-h clade followed by a crown group comprised of the H-Y-[EDQ] and the R-S-E clades (Fig. 2). Thus, the presence of an active site H in the first strand appears to be the ancestral feature of the ART superfamily, with the R in the R-S-E clade being a derived feature. The acidic residue at the beginning of the strand 5 appears to be a shared derived character unifying the crown clades. Below, we briefly describe the various constituent families of within each of these major clades.

4.1 The H-H-h Clade

This is the most primitive or basal clade of the ART superfamily as indicated by an unelaborated structure and active site lacking an acidic position in strand 5 (Figs. 2 and 3a, b). This clade contains only two families the KptA and CC0527 (Pfam: DUF952) which are unified by above-described active site features associated with strand 5. Of these, KptA represents the most widely distributed lineage of the ART superfamily and is typically present in a single copy in organisms that encode it (de Souza and Aravind 2012). This family is seen in most eukaryotes barring the basal-most branches (parabasalids and diplomonads), several euryarchaeal and crenarchaeal clades and representatives of most major bacterial lineages albeit in a somewhat patchy distribution. This widespread phyletic pattern suggests that KptA could have potentially been present in the last universal common ancestor (LUCA). However, phylogenetic analysis suggests that both the archaeal and eukaryotic branches are nested within the bacterial radiation making it possible that it actually emerged in bacteria and was independently transferred to the former two lineages (Fig. 2). Nevertheless, its wide distribution and structural simplicity suggest that it is close to the ancestral version of the entire ART superfamily and that other ARTs were likely derived from it by extensive and rapid divergence. In eukaryotes and archaea, it appears to be part of the core RNA-processing mechanism required for tRNA maturation following removal of the intron (Spinelli et al. 1999). Interestingly, knockout of the sole mouse representative of this family Trpt1 did not apparently result in RNA-processing defects (Harding et al. 2008), suggesting that despite its strong conservation in eukaryotes it might be a nonessential gene in mammals. However, its function in bacteria is less understood. Its presence in operons where it is combined with the RNA repair $5' \rightarrow 3'$ polymerase Thg1 suggests that it might be involved in RNA repair, perhaps as strategy against bacteriophage or toxin attack on tRNAs (de Souza and Aravind 2012) (Fig. 4). However, in several bacteria it occurs as part of large NAD^+/ADPR metabolism operon combined with genes for several other enzymes which use these metabolites, such as sirtuins, Macro, PARG (also belonging to Macro

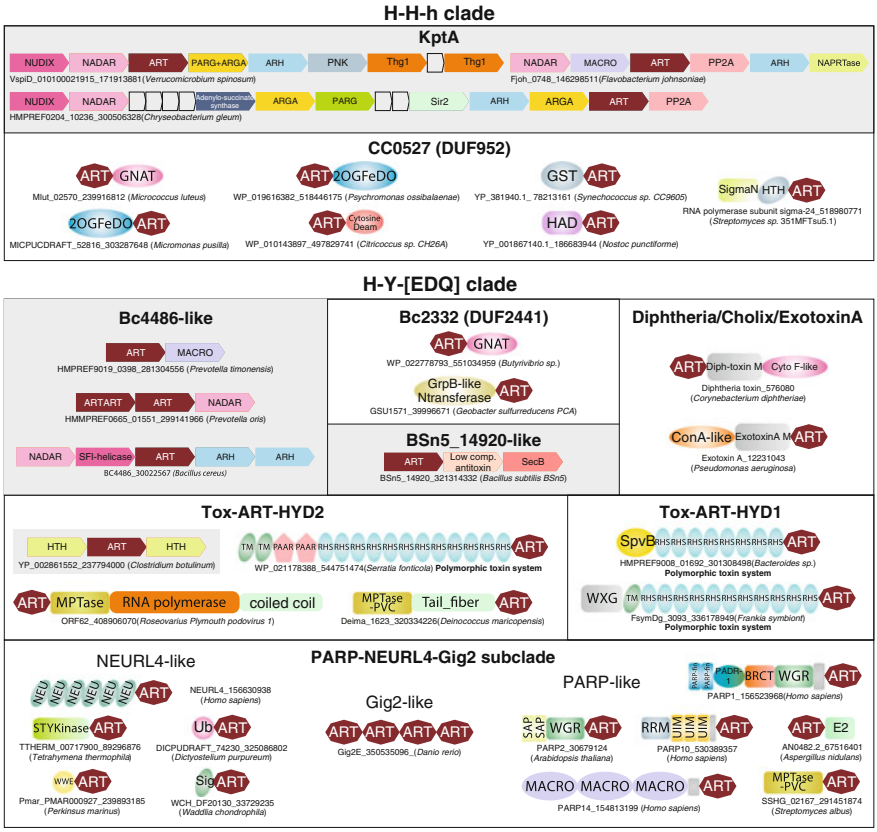

Fig. 4 Domain architectures and gene neighborhoods of ARTs of the H-H-h and H-Y-[EDQ] clades. Gene neighborhoods and domain architectures are labeled with the gene name, Genbank index (gi) number and the species name, which is shown in brackets. For domain architectures, the label corresponds to the ART containing gene. Gene neighborhoods are shown as *box-arrows* with the *arrowhead* pointing to the gene in the 3′ direction of the coding strand. These are further shaded *gray*. The architectures are grouped based on the type of ART. Standard domain abbreviations are used to label genes and domains

superfamily), NADAR, and ARHs but no RNA-related genes (de Souza and Aravind 2012) (Fig. 4). This raises the possibility that a subset of the bacterial KptAs might modify substrates other than RNA.

The CC0527 family is widely but patchily distributed across the bacterial superkingdom. It appears to have also been independently transferred to several eukaryotes such as fungi, viridiplantae, stramenopile algae *Emiliania*, and *Naegleria* (Fig. 2). While its structure is available (PDB: 2o0q), its function has remained obscure. Examination of its domain architectures reveals fusions to glutathione S-transferases, GCN5-like NH_2 acetyltransferases (GNAT superfamily), cytosine deaminases, or 2 oxoglutarate/Fe-dependent dioxygenases (Fig. 4).

All these associated enzymes have been previously implicated in modification and detoxification of antibiotics by respectively adding, glutathione and acetyl groups, deaminating cytosine in Blasticidin S-like compounds and hydroxylation (Ramirez and Tolmasky 2010; Walsh 2003). Thus, by the principle of "guilt by association" (Aravind 2000) it is likely that the CC0527 ADP-ribosylates antibiotics or other toxic compounds in a reaction comparable to the rifamycin ARTs.

4.2 The H-Y-[EDQ] Clade

The primary and explosive diversification of this clade appears to have occurred in the context of several prokaryotic conflict systems (Zhang et al. 2012). These include intragenomic conflict systems such as type-II Toxin–Antitoxin (T–A) systems, intergenomic conflicts between bacteriophages and their host genome, olecule toxins or antibiotics, and interorganismal conflict using proteinaceous effectors (Aravind et al. 2012; Zhang et al. 2012). Indeed, in each of these conflict systems ARTs of this clade have been extensively deployed as toxins to target proteins (Fig. 2). Three families belonging to this clade are encountered in T–A systems that are widely distributed across the bacterial tree (Fig. 4). The first of these is the recently described BC4486 family (prototyped by BC4486 from *Bacillus cereus*), which is typically found in a two gene T–A system, where the second gene encodes either a member of the NADAR superfamily (BC4488) or a member of the Macro superfamily (de Souza and Aravind 2012). These two genes follow a strict gene order with that encoding the BC4486 family ART always occurring as the first gene in the operon (Fig. 4). Based on this, it has been suggested that the BC4486 protein functions as an ADP-ribosylating toxin while the Macro or the NADAR protein function as antitoxins that counter the former's action by removing the ADP-ribose moiety. Thus, they might be seen as analogous to the DraG-DraT system (see below). Also belonging to this family is a subfamily of ARTs prototyped by ORF28 (gi: 46309426) of *Agrotis segetum* granulovirus, which is encoded by certain arthropod DNA viruses such as baculoviruses, ascoviruses, and iridoviruses (Fig. 2).

The second of the T–A-associated families, the BSn5_14920 family (prototyped by the eponymous protein from *Bacillus subtilis* BSn5) is encoded by a 3-gene T–A wherein the ART is again encoded by the first gene (Fig. 4). This is followed by a gene for the antitoxin which assumes the form of a low complexity or intrinsically disordered protein with two highly conserved hydrophobic residues at the C-terminus and the third gene encoding the chaperone SecB (Sala et al. 2013). In these systems, the intrinsically disordered antitoxin is postulated to bind SecB by the C-terminal hydrophobic residues, while SecB stabilizes it, allowing it to inhibit the toxin ART. If under protein unfolding stress conditions the SecB is drawn away toward other unfolded proteins, then the antitoxin is destabilized (Sala et al. 2013), unleashing the action of the ART, which presumably induces dormancy by modifying certain targets. The third T–A-associated family is the

Tox-ART-HYD2 family prototyped by a version from a *Clostridium botulinum* T–A system (gi: 237794000; Fig. 4). In these, the postulated toxin ART is typically accompanied by two predicted antitoxins, which are DNA-binding helix-turn-helix proteins (HTH) proteins, encoded by flanking genes (Fig. 4). Outside TA systems, ARTs of this family are also encountered in bacterial polymorphic toxin systems with variable C-terminal domains that are likely to be used in intraspecific conflicts by bacteria (e.g., gi: 544751474 from *Serratia fonticola* (Zhang et al. 2012)). Here, the ART occurs as one of the variable C-terminal toxin tips preceded by a long stretch of RHS repeats which help present the toxin on cell-surfaces of bacteria. Other members occur in phages such as *Roseovarius* Plymouth podovirus 1(gi: 408906070) where they are fused to the viral RNA polymerase and might help regulate transcription in course of infection (Fig. 4). Members of this family have also been transferred to and expanded in eukaryotes such as *Acanthamoeba* (gi: 470494435), choanoflagellates, and the fungal plant pathogen *Puccinia*. The Tox-ART-HYD1 family is another ART family with comparable features, which is found in several polymorphic toxin systems from several bacterial lineages (Fig. 4) (Zhang et al. 2012).

The family typified by the p0068 protein of the *Acinetobacter* phage ZZ1 appears to be involved in phage-host conflicts and is found in several bacteriophage genomes, including a lineage-specific expansion in *Bacillus* phage G (10 paralogs) (de Souza and Aravind 2012). These phage versions are predicted to act similarly to the T4 and N4 phage ARTs (see below for details) in modifying host proteins to facilitate viral replication (Koch and Ruger 1994; Tiemann et al. 2004). Cellular versions are found in cyanobacteria and the nanohaloarchaeon *Haloredivivus*. This family is further related to another family, rifamycin ART (Figs. 2 and 3c), which is implicated as a defensive element in interorganismal conflict by neutralizing rifamycin antibiotics (Baysarowich et al. 2008). The spread of this family across bacteria through lateral transfer appears to have been a key determinant of resistance toward this class of antibiotics. The structurally highly modified BC2332 family is likely to have been derived from this assemblage and its domain fusions and operonic associations (Fig. 4) are also suggestive of a role comparable to the rifamycin ART family in detoxification of small molecules. Most families discussed thus far are characterized by more or less a minimal ART domain with few or no additional structural inserts. This suggests that they are likely to represent the basal-most lineages within the H-Y-[EDQ] clade (Fig. 2).

The remaining families of this clade appear to constitute a monophyletic assemblage, which appears to have initially diversified in toxin systems that are used as effectors by bacteria in interorganismal conflicts (Fig. 2). Of these, the PARP-NEURL4-*Gig2* subclade is a major monophyletic assemblage that includes several bacterial effectors, such as one encoded by the intracellular chlamydia-like pathogen of animals and amoebae, *Waddlia chondrophila* (gi: 337292305) (de Souza and Aravind 2012). PARP family includes both *bona fide* PARPs (e.g., human PARP1-3/ARTD1-3, vPARP/ARTD4, and the tankyrases/ARTD5-6) and related mono-ARTS (ARTD7-17; also called Pl-MARTs) (Citarelli et al. 2010; Hassa et al. 2006; Otto et al. 2005). The eukaryotic versions are closely related to

effectors encoded by bacteria such as *Legionella drancourtii* (gi: 363538754) and *Vibrio caribbenthicus* (gi: 497289311) and appear to have been derived from such precursors (Zhang et al. 2012). At least two PARP family members, including the histone-modifying PARP1 can be reconstructed as being present in the last eukaryotic common ancestor LECA (Citarelli et al. 2010). In course of eukaryotic evolution they expanded extensively to spawn several distinct lineages such as the telomere-protein-modifying tankyrases and the vPARP, which is a subunit of the vault, an organelle associated with small noncoding RNAs. Thus, the PARP family was incorporated into a diverse set of eukaryotic systems ranging from epigenetic regulation to control of RNA-processing and chromosome dynamics (Hottiger et al. 2010). This was accompanied by fusion to several distinct domains such as the PARP-Zn-finger, WGR (also of bacterial origin) and SAP domains, all involved in DNA binding, and the phosphopeptide binding BRCT domain in *bona fide* PARPs and domains such as the E2 ubiqutin ligase, peptide-binding WWE, ubiquitin-binding UIM and RNA-binding RRM domains in the case of the mono-ARTs from this family (Fig. 4). The eukaryotic *Gig2* family (Jiang et al. 2009) shows lineage-specific expansions in fishes, *Oxytricha trifallax*, and the haptophyte alga *Emiliania huxleyi* and includes proteins which may possess multiple tandem ART domains (Fig. 4). In fishes, it has been shown to be induced by interferon as part of the antiviral response (Jiang et al. 2009; Krasnov et al. 2011). Hence, these ARTs might have been recruited by eukaryotes to counter viruses by modifying their proteins. The NEURL4 family typified by the eponymous human protein is found in most animal lineages and several more basal eukaryotic lineages (de Souza and Aravind 2012). They are typically fused to other domains such as neuralized repeats, ubiquitin, WWE, and MORN-repeats and have undergone independent lineage-specific expansions in the fungus *Rhizophagus irregularis*, slime molds, sponges, crustaceans, amphioxus, and ciliates (Fig. 4). While NEURL4 itself has been implicated in centrosomal assembly (Al-Hakim et al. 2012), these expanded versions might have roles in antiviral responses similar to the *Gig2* family. Another more divergent family in this subclade is the Tox-ART-HYD3 family, which is present as the toxin tip of a recently identified class of bacterial cell surface effectors (Fig. 2; DZ, LMI, LA unpublished).

The large assembly of effectors deployed by both animal and plant-pathogenic bacteria comprises the final major family in the H-Y-[EDQ] clade (Fig. 2) (Corda and Di Girolamo 2003; Hassa et al. 2006; Koch-Nolte et al. 2001). The precise relationships in this family are difficult to discern due to their rapid sequence divergence as a consequence of adaptation against host immune responses and the selection for targeting different host proteins. One distinct monophyletic lineage within this group includes the diphthamide-targeting ARTs such as diphtheria toxin, the *Vibrio cholerae* cholix toxin, and the *P. aeruginosa* Exotoxin A. A more divergent version of this group is the ART domain of the AvrPm1 of the plant pathogen *Pseudomonas syringae* (Rohmer et al. 2003). This assemblage of toxins might have originated from phage ARTs used in intergenomic conflicts as suggested by the fact that several are encoded by temperate phages (Boyd 2012).

4.3 The R-S-E Clade

The diversification of the R-S-E clade closely parallels that of the above clade in that it primarily occurred in the context of the same bacterial conflict systems as those discussed above. On structural grounds the R-S-E clade can be divided into two major subclades (Figs. 2 and 3i–k). The first retains the ancestral state of the split β-sheet of the ARTs, with the core 6 strands. The second subclade is characterized by the above-described additional seventh strand that is spatially inserted between the core strand 3 and strand 6 (the additional strand subclade).

The first subclade contains five families of bacterial effectors deployed both in intraspecific conflict (polymorphic toxins) and against more distantly related organisms and hosts (Fig. 2). The first of these families is the MTX/Pierisin family, which is typified by the arthropod-killing toxin deployed by *Bacillus sphaericus* and the apoptotic pierisin-like cytotoxin from lepidopterans (Carpusca et al. 2006; Nakano et al. 2006; Takahashi-Nakaguchi et al. 2013). Interestingly, this family has evolved a wide range of substrate specificities which include both protein and DNA. The close relationship between lepidopteran cytotoxins like pierisin and the insecticidal effectors encoded *Paenibacillus larvae* temperate bacteriophage phiIBB_Pl23 (gi: 526245037; Fig. 5) suggest they were acquired by insects from their bacterial symbionts/pathogens and incorporated in their cellular systems as mediators of apoptosis or as defensive toxins against parasitoids (Takahashi-Nakaguchi et al. 2013). Similar to the lateral transfers to insects, members of this family have also been transferred to several plants such as the dicot *Medicago truncatula* and the grass *Aegilops tauschii*, where they appear to be seed-associated albumins which might play a role in defense against seed-eating animals (Fig. 5). Members of this family are also found as toxin tips of polymorphic toxin-like proteins such as a toxin from *Pseudomonas fluorescens* (gi: 515906858), where it occurs C-terminal to series of RHS repeats (Fig. 5). Two other closely related families in this subclade are the cholera toxin-heat-labile enterotoxin A (CTXA/LTA) and the pertussis toxin (PTX) families, which are prototyped by the eponymous proteins (Fig. 2) (Corda and Di Girolamo 2003; Laing et al. 2011). The former family, widely disseminated across pathogenic bacteria, includes effectors of forms infecting both animals and plants (e.g., *Xanthomonas fuscans* gi: 495244509), and symbionts such as *Sodalis* (gi: 573023525) which colonizes the tsetse fly (Snyder and Rio 2013). Interestingly, members of the CTXA/LTA family also appear to have been transferred to the plant *Selaginella* (gi: 302792354), and several insect- and plant-pathogenic fungi (e.g., *Metarhizium* and *Colletotrichum* respectively), where they have undergone lineage-specific expansion (Fig. 5). These latter ART domains are on occasions fused to a C-terminal conserved, apparently enzymatic domain, which is also found fused to ricin-like RNA-targeting toxins of these fungi and in several plant proteins (e.g., gi: 629706939); we predict that they might function as secreted effectors deployed in defensive interactions (Fig. 5). PTX family shows a similar distribution in bacteria but is mainly limited to animal pathogens.

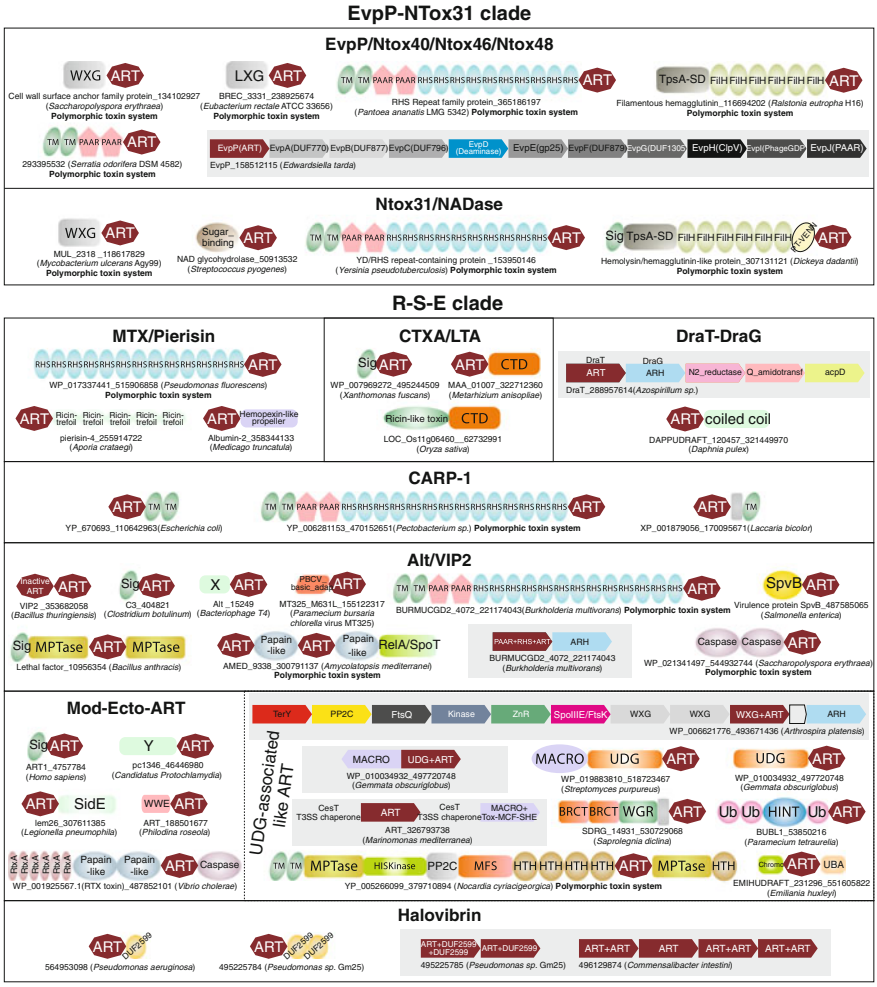

Fig. 5 Domain architectures and gene neighborhoods of ARTs of the R-S-E clade. The labeling scheme and grouping of proteins and gene neighborhoods are as described in Fig. 4. Standard domain abbreviations are used to label genes and domains. Additionally, X and Y are uncharacterized domains

The fourth family in the first subclade is typified by the molluscan DNA-modifying toxin CARP-1 from the clam *Meretrix lamarckii* (Nakano et al. 2006). We also found four members of this family in the oyster *Crassostrea gigas*, suggesting a more widespread presence of these proteins in bivalves. Members of the CARP-1 family are conserved in most filamentous fungi of both ascomycete and basidiomycete lineages (Fig. 5) and certain other eukaryotes such as the choanoflagellate *Monosiga* and the stramenopile *Phytophthora*. In bacteria, they are found as toxin tips of polymorphic toxins (Zhang et al. 2012) (e.g., gi:

470152651 from *Pectobacterium*; Fig. 5) or certain membrane-associated proteins (e.g., gi: 110642963 from *Escherichia coli* 536). The eukaryotic versions appear to have been acquired from the bacterial version by lateral transfer on multiple occasions. Interestingly, DNA-modifying activity has emerged in this family independently of the pierisin family. A divergent and distinctive family within the first subclade is the distinctive AvrPphF family that is prototyped by the eponymous effector of the plant pathogen *P. syringae* (Singer et al. 2004). This family is typified by a large insert after the first strand-helix unit (Fig. 3k). Moreover, other than the arginine from the first strand the remaining active site residues have undergone drastic modification: the S in strand 2 is replaced by a polar residue often asparagine or arginine while the acidic residue from strand 5 is entirely lost. Instead its place appears to be taken by a similarly positioned aspartate from the end of strand 4.

The second subclade represents another extensive radiation of the R-S-E clade and includes four major families (Fig. 2). The first, the DraT family, contains the structurally and architecturally least elaborated versions. These are represented by T–A systems prototyped by the DraT-DraG system, which itself appears to be a "domesticated" T–A system exapted for dinitrogen reductase regulation (de Souza and Aravind 2012; Ludden 1994). Here, the ART (DraT) acts as the protein-modifying toxin, while the ARH (DraG) acts as the demodifying antitoxin that reverses the action of the former. A member of this family has been horizontally transferred to the crustacean *Daphnia pulex* (gi: 321449970; Fig. 5), where it appears to have been incorporated into a much larger polypeptide. The second family is typified by the secreted halovibrins (HvnA and HvnB) of *Vibrio fischeri*, the extracellular symbiont that confers bioluminescence to the squid *Euprymna scolopes* by residing in its light organ (Stabb et al. 2001). This family is marked by a large central insert in the ART domain and conserved cysteine residues that are predicted to form two disulfide bridges. In addition to symbiotic and pathogenic bacteria (e.g., *Erwinia amylovora*, *P. aeruginosa*, and *P. syringae*) it also found in *Perkinsus marinus* the eukaryotic parasite of oysters and clams (Fig. 5), suggesting that modification via action of halovibrins might play a role in host interactions of multiple unrelated pathogens. The third family in this subclade is the large Alt/VIP2 family (Corda and Di Girolamo 2003; Han et al. 1999; Koch-Nolte et al. 2001; Laing et al. 2011). This includes phage T4 Alt which is packaged into the virion and deployed upon infection to hijack the host transcription machinery by modifying the RNA polymerase α subunit (Koch and Ruger 1994). Interestingly, certain eukaryotic DNA viruses, such as the *Paramecium bursaria Chlorella* virus (PBCV1_A092/093L) also encode an ART belonging to this family, which is packaged into the virion (Dunigan et al. 2012), suggesting that it might be deployed right after infection just as with the bacteriophage versions. Other members are toxins deployed by various animal pathogenic bacteria such as *B. cereus* VIP2, *C. perfringens* iota, *C. botulinum* C2 and C3, *B. anthracis* lethal factor, *Aeromonas hydrophila* VahC and *Salmonella* SpvB (Corda and Di Girolamo 2003; Fieldhouse et al. 2010; Shniffer et al. 2012; Ueda and Hayaishi 1985). These proteins frequently target specific host proteins such as actin and the small GTPase

Rho. This family also contains several polymorphic toxins, which are typically distinguished by N-terminal RHS repeats as in the case of other versions found in polymorphic toxins (e.g., gi: 221174043 from *Burkholderia multivorans*; Fig. 5) (Zhang et al. 2012). Interestingly, the immunity proteins for these toxins are ARHs (e.g., gi: 221174044) suggesting that their action is reversed by hydrolytic removal of the ADPR modification by the latter. A related group of toxins from actinobacteria (e.g., gi: 300791137) contains several tandem copies of the ART domain combined with other enzymatic domains such as metallopeptidases, papain-like and caspase-like thiol peptidases, and RelA/SpoT-like nucleotidyltransferases (Zhang et al. 2012) (Fig. 5).

The fourth, the Mod-Ecto-ART family is also large and like the previous one includes both phage versions and those deployed as toxins in interorganismal conflicts. The phage-encoded ARTs in this family are prototyped by the T4 Mod proteins (ModA and ModB), which are expressed post-infection and catalyze host RNA polymerase subunit modifications to facilitate transcriptional switching to the late genes of T4 (Tiemann et al. 2004). The effectors belonging to this family include a novel effector (pc1346; gi: 46446980) encoded by the endosymbiont *Protochlamydia,* which resides in amoebae, and various type-III secretion system effectors of *Pseudomonas syringae*, namely hopO1-1/2/3, and HopU1, *Xanthomonas axonopodis* effector XopA1 and a *Legionella pneumophila* T4SS effector (gi: 307611385) (de Souza and Aravind 2012; Fu et al. 2007; Zhang et al. 2012). Certain RTX toxins (Linhartova et al. 2010), which are secreted by means of ABC ATPases, by pathogenic bacteria like *V. cholerae* also contain ART domains of this family (e.g., gi: 487852101). Another interesting member of this family predicted to be involved in intragenomic conflicts in bacteria is fused to a DNA glycosylase of the UDG superfamily (e.g., gi: 497720748; Fig. 5). These are encoded in operons along with a gene for a Macro protein and in some cases an ARH. These are predicted to modify DNA and introduce abasic sites in conjunction with the fused DNA glycosylase domain, whereas the Macro and ARH might counter these modifications. Thus, they could function as a potential DNA-modifying restriction system. Related ART proteins are also encoded as part of a mobile novel T7SS and might be deployed as toxins exported by them (Anantharaman et al. 2012). Yet other related ART domains also occur as part of large actinobacterial proteins with several other enzymatic and helix-turn-helix domains (e.g., gi: 379710894; *Nocardia cyriacigeorgica*; Fig. 5); these proteins might represent a multipronged defensive and signaling strategy against antibiotics. Members of this lineage have been transferred to eukaryotes on several occasions, and include a version from oomycetes (e.g., *Saprolegnia diclina* gi: 530729068), where they have displaced the PARP family catalytic domain within a PARP-like polypeptide (Fig. 5). Other members include the BUBL1-like proteins fused to ubiquitin and HINT autopeptidase domains in ciliates (Dassa et al. 2004) and versions fused to methylated peptide-binding chromodomains in *Emiliania* (Fig. 5).

Also included in the above family are the ecto-ARTs of eukaryotes which are secreted proteins that add a single ADPR moiety to extracellular proteins

(Glowacki et al. 2002; Pallen et al. 2001). These ecto-ARTs show a patchy distribution in eukaryotes being found in the animal lineage as well as groups such as the haptophyte alga *Emiliania* and the rhizarian *Reticulomyxa filosa*. In the latter two taxa they show massive lineage-specific expansions. Certain mammalian versions (ARTC2) function as "toxins" for T cells by inducing their apoptosis (Adriouch et al. 2001; Hassa et al. 2006; Seman et al. 2003). This raises the possibility that the expanded version in the more basal eukaryotic lineages might have a role in defense or cell surface organization by modifying extracellular targets. Rotifers display an expansion of intracellular members of this clade, including versions which appear to have displaced the PARP-like H-Y-[EDQ] clade catalytic domain to associate with the N-terminal WWE domain (gi: 188501623; Fig. 5). All these eukaryotic ARTs are nested within the radiation of bacterial effectors, being particularly close to certain versions such as the *P. syringae* effectors hopO1-1/2/3, suggesting that they were acquired by lateral transfer from bacterial symbionts or parasites (Glowacki et al. 2002; Pallen et al. 2001).

4.4 The Aberrant Clades

The most extensive of these is the EvpP-NTox31 clade, which contains secreted ARTs with a "hybrid" active site. Hence, it is unclear if they are derived versions of either the H-Y-[EDQ] or R-S-E clades, or represent a distinct transitional clade (Fig. 2). This clade includes two distinct sub-clades, of which the EvpP sub-clade is constituted by three families of toxin tips of polymorphic toxins (NTox40, NTox46, and NTox48) (Zhang et al. 2012), and the effectors of pathogenic bacteria, such as EvpP of *E. tarda* (Zheng and Leung 2007). Those occurring with polymorphic toxins are characterized by neighboring immunity protein genes and are associated with several distinct secretory systems such as T7SS and T5SS in Gram-positive and proteobacteria, respectively (Fig. 5). Several of the host-targeting effectors, such as EvpP, are associated with T6SS (Zheng and Leung 2007). The second subclade includes Ntox31 that is found in polymorphic toxin systems and SPNs. SPNs from *Streptococcus pyogenes* and related species appear to be derived from polymorphic toxin systems and are reused as host-directed toxins. Polymorphic tips of systems featuring EvpP-NTox31 domains often display toxin cassettes coding for multiple distinct members of this clade, classical R-S-E clade ARTs or ADP-ribosyl cyclases (Fig. 5). Extensive sequence divergence also precludes precise phylogenetic placement of the RolB family (Fig. 2).

5 Sirtuins and TM1506

The ADP-ribosylation activity of the sirtuins is generally believed to be much weaker than that of the ART superfamily (Frye 1999; Hawse and Wolberger 2009). ADP-ribosylation by sirtuins has been shown to be specific for arginine in

nuclear proteins like histones and perhaps tubulin α/β in the cytoskeleton (Hassa et al. 2006; Hawse and Wolberger 2009). Mitochondrial sirtuins (SIRT3, SIRT4, and SIRT5 in humans) have been implicated in mono-ADP-ribosylation of cysteine-119 in glutamate dehydrogenase (Haigis et al. 2006). The conservation of ADP-ribosylation by sirtuins across eukaryotes (confirmed in animals, apicomplexans, and kinetoplastids) (Garcia-Salcedo et al. 2003; Merrick and Duraisingh 2007) and the coupling of bacterial sirtuins in operons with ADP-ribosyl glycohydrolases (de Souza and Aravind 2012) suggests that this activity might indeed be widely functionally relevant, even if less understood. The ADPR transfer-associated deacylation of lysines by sirtuins is conserved in both prokaryotes and eukaryotes and targets the entire spectrum of acyl modifications ranging from the simple acetyl group, through mid-sized propionyl, crotonyl, malonyl, and succinyl groups, all the way to long-chained moieties like the myristoyl group (Belenky et al. 2007; Jiang et al. 2013; Smith et al. 2002).

Sirtuins display a classical α/β Rossmann fold that had diversified prior to the LUCA into two distinct assemblages of enzymes (de Souza and Aravind 2012; Smith et al. 2002). The first of these includes all classical $NAD^+/NADP^+$-dependent dehydrogenases (Andreeva et al. 2008; de Souza and Aravind 2012; Ronimus and Morgan 2003). The sirtuins however belong to the second assemblage along with the deoxyhypusine synthase and the NAD^+–$NADP^+$ transhydrogenases (Andreeva et al. 2008; de Souza and Aravind 2012; Smith et al. 2002). While topologically similar to the former, this version of the Rossmann fold binds NAD+ in the reverse configuration. Moreover, sirtuins have evolved an additional set of catalytic residues (usually a conserved histidine), which are absent in the others dehydrogenases, that have allowed the sirtuins to utilize NAD^+ as a substrate to transfer ADP-ribose to target moieties rather than as a redox cofactor. Sirtuins are present in all the three superkingdoms of life, with phylogenetic analysis suggesting that majority of archaeal sirtuins from euryarchaea, crenarchaea, and korarchaea form a slow-evolving monophyletic clade (de Souza and Aravind 2012). They are also widespread in bacteria where they have undergone a notable diversification. Hence, the ancestral sirtuin was likely to have been present in the LUCA (de Souza and Aravind 2012). While eukaryotes might have inherited at least one sirtuin from their archaeal progenitor, several of the eukaryotic sirtuins appear to have been acquired via lateral transfer from bacteria (Iyer et al. 2008). In particular, sirtuin 4, 5, and 6 appear to have been independently acquired relatively early in eukaryotic evolution from bacterial precursors. Like the PARP family, eukaryotic sirtuins also developed fusions to several distinct domains such as the ubiquitin-binding Ubp-ZnF domain, tetratricopeptide and kelch repeats, and the Macro domain (Iyer et al. 2008), which might play a role in further processing of OAADPR or allosteric regulation by it (Peterson et al. 2011; Timinszky et al. 2009). In some bacteria, sirtuins occur as part of large operons with several other NAD^+-utilizing and ADPR-processing enzymes such as KptA, ARHs, and Macro (de Souza and Aravind 2012) (Fig. 4). This suggests that NAD^+ utilization and ADPR metabolism by a diverse array of enzymes might be coordinately regulated in these organisms. Several bacteria also possess a functionally enigmatic family

of sirtuins, which occur in operons for diverse restriction systems in place of the restriction DNases (Burroughs et al. 2013; Iyer et al. 2004). This suggests that they are functionally equivalent to the restriction enzymes raising the possibility that they target DNA, perhaps via ADP-ribosylation of DNA bases or have undergone a functional shift to catalyze an unrelated reaction, such as DNase activity.

The TM1506 family is prototyped by the eponymous protein from *Thermotoga maritima* (Iyer et al. 2011). This protein was shown to be ADP-ribosylated at aspartate-56 (Xu et al. 2008). Analysis of the structure of this protein showed that it contains a deaminase-like fold and possesses the characteristic active site pocket of this fold with a distinctive set of conserved residues that are likely to support catalytic activity. The crystal structure of TM1506 also showed diffraction density for a ligand in this active site that is consistent with an ADP-ribose linked to D56 or its precursor NAD^+ (Xu et al. 2008). This suggests that it might be a novel ADP-ribosylating enzyme with auto-activity. Thus far, this family is only found in bacteria. TM1506-like genes are often linked in predicted operons to genes encoding a Rossmann fold aldo/keto reductase fused to a rubredoxin-like zinc ribbon and a 5TM protein that is predicted to form a transmembrane channel (Iyer et al. 2011). In bacteroidetes, the domain is also fused to a TonB-like receptor, which is usually involved in the trafficking of small molecules, such as siderophores and peptide antibiotics (Noinaj et al. 2010). Thus, it is conceivable that the activity of the TM1506 family regulates transmembrane trafficking of molecules by the products of associated genes.

6 A Synthetic Overview of the Tendencies in the Diversification of the ADP-Ribosylation System

It is currently not clear if there were any member of the ART superfamily in the LUCA or whether they arose first in bacteria (Fig. 2). Nevertheless, KptA appears closest to the ancestral version of this superfamily suggesting that it first arose in the context of RNA repair. From that point on the ART superfamily diverged rapidly and explosively in the bacterial superkingdom in terms of sequence, structure, and active site residues, and evolved a wide range of substrates specificities, albeit without any notable diversification in terms of the basic reaction type they catalyze. Second, as noted in the above discussion the primary diversification of ARTs appears to have taken place in bacteria among diverse systems involved in defensive and offensive strategies in intragenomic, intergenomic, and intraorganismal conflicts (Fig. 2) (Fieldhouse et al. 2010; Glowacki et al. 2002; Pallen et al. 2001; Zhang et al. 2012). This suggests it took place under the combination of the intense selective pressures arising from development of resistance to their action and defensive counter strategies directed against them in such conflict systems, and relaxation of selection for specific interactions with multiple cellular molecules beyond substrates and immunity proteins (Aravind et al. 2012). Strikingly,

eukaryotes have repeatedly (more than 20 distinct occasions) acquired ARTs from these prokaryotic conflict systems (Fig. 2). While some of these like the PARP family were acquired prior to the LECA (Citarelli et al. 2010), others seems to have been sporadically acquired throughout eukaryotic evolution. These ARTs appear to have been deployed in two distinct modes: (1) they appear to more or less retain their ancestral toxin function upon transfer to the eukaryotes. Thus, they appear to be utilized as mediators of apoptosis as seen in the case of pierisin, CARP-1, and certain ecto-ARTs. (2) They are incorporated as components of core regulatory systems, where they modify proteins as part of quintessentially eukaryotic regulatory and epigenetic processes. This process was usually accompanied by fusion to several distinct domains, some of which are unique to eukaryotes (e.g., WWE and PARP-ZnF; Fig. 4), in domain architectures that are unparalleled in prokaryotic counterparts (Hottiger et al. 2010). Another, unique aspect of the evolution of eukaryotic ARTs is the lineage-specific expansions that have occurred on several independent occasions. Given the possible role of unrelated lineage-specifically expanded families in anti-pathogen defenses in eukaryotes (Jiang et al. 2009; Krasnov et al. 2011; Rosado et al. 2013), it is conceivable that ARTs have repeatedly been deployed as part of anti-pathogen strategies of eukaryotes.

The above-described evolutionary tendencies of ART superfamily are in contrast with those observed for the sirtuins (de Souza and Aravind 2012). Sirtuins show only a limited presence in the above-described conflict-related systems. The only such versions are those occurring in restriction systems, wherein they take the place of restriction endoDNases. However, they are currently not known in secreted effectors involved in interorganismal conflict. Most conserved versions of sirtuins appear to be forms that are involved in regulation of intracellular proteins by deacylation or perhaps ADP-ribosylation (Garcia-Salcedo et al. 2003; Haigis et al. 2006; Hassa et al. 2006; Merrick and Duraisingh 2007; Smith et al. 2002). Consistent with this, sirtuins show greater conservation at the sequence level and little variation in their active site residues. Notably, unlike the ARTs they also show little diversity in their domain architectures. Like the ARTs, eukaryotes have acquired sirtuins on multiple occasions from bacteria (Iyer et al. 2008); however, there is no evidence that any of these were acquired from conflict-related systems. Moreover, unlike the ARTs, sirtuins show little propensity for lineage-specific expansions in eukaryotes. These differences suggest that the ART fold is probably more suited for structural diversification; thus it tended to be selected repeatedly as a scaffold for evolving different ADP-ribosylation activities.

However, four other superfamilies of domains in the ADP-ribosylation system, namely the ADP-ribosyl cyclase, Macro, NADAR, and ARH appear to have evolutionary histories comparable to that of the ART superfamily (de Souza and Aravind 2012; Zhang et al. 2012). Of these, Macro NADAR and ARH appear to have emerged in type-II T–A and polymorphic toxin systems as enzymatic antitoxins or immunity proteins removing ADP-ribosyl modifications. Moreover, Macro, NADAR and the ARH domain also appear to have diversified in bacterial systems to cleave ADPR modifications from macromolecules and process other ADPR derivatives such as OAADPR (generated by sirtuins during deacylation)

and ADP-ribose 1″-phosphate (Appr1″p) generated during RNA repair (Guse and Lee 2008; Hofmann et al. 2000; Karras et al. 2005; Koch-Nolte et al. 2008; Slade et al. 2011). All these versions were incorporated into eukaryotic systems upon being acquired by lateral transfer. De-ADP-ribosylating Macro domains were recruited as the PARGs as well as mono-ADP-ribosyl hydrolases of the eukaryotes (de Souza and Aravind 2012; Slade et al. 2011). Similarly, the ARG domain was recruited both in de-ADP-ribosylation and processing of OAADPRs in eukaryotes (Koch-Nolte et al. 2008; Ono et al. 2006). The ADP-ribosyl cyclase (ARC) has previously only been characterized in animals and generates cyclic-ADP-ribose (cADPr) and nicotinic acid adenine dinucleotide phosphate (NAADP), respectively from NAD^+ and NADP (Guse and Lee 2008). cADPr and NAADP have been shown to function as potent inducers of calcium influx via the ryanodine receptors. At the same time by channeling NAD^+, ARCs might also affect protein deacylation by sirtuins and other processes requiring NAD^+ (Guse and Lee 2008). Polymorphic toxins with ARC domains occur in free-living bacteria and are predicted to be delivered via T5SS, T6SS, and T7SS (Zhang et al. 2012). This suggests that they are used in intraspecific conflict rather than against eukaryotes. It remains to be seen if some of these ARC domains might function as NADases or ADP ribosyltransferases. Bacterial ARCs appear to have been transferred to eukaryotes on at least two occasions, namely to animals and fungi, where they function as membrane-associated enzymes (Zhang et al. 2012). Thus, majority of enzymes of the eukaryotic ADPR system might have originally emerged in the context of bacterial conflict systems and were then acquired via lateral transfer by eukaryotes. This pattern resembles another large superfamily of proteins namely the deaminases, which likewise diversified in comparable bacterial contexts and were incorporated into eukaryotic nucleic acid modification and anti-pathogen defense systems on several occasions (Iyer et al. 2011). More generally, it adds further evidence to the recently proposed hypothesis that the rapid evolution of novel biochemical capabilities in bacterial conflict systems has been a major supplier of innovations in the evolution of eukaryotic regulatory systems (Aravind et al. 2012).

7 Conclusion

Little over 50 years after its discovery we have a fairly detailed view of the evolutionary history of the ADP-ribosylation system and the functioning of its various components at the molecular level. While considerable progress has been made in terms of the biochemistry and biology of this system, several new questions have been raised by recent studies. First, identification of new ARTs through sequence and structure analysis has emphasized the diversity of the ART active site. This calls for new understanding of the ART reaction mechanism, especially in cases like RolB or BC2332 where the active site is completely remodeled. Second, newly identified ARTs like NEURL4, plant pierisin-like,

fungal CARP-1-like ARTs, and the various lineage-specifically expanded versions in eukaryotes are interesting targets for discovery of new biological roles for ARTs in both model and nonmodel organisms. Finally, bacterial versions of ART, sirtuin, Macro, NADAR, and ARH domains in diverse conflict systems offer the potential for understanding both the nature of these conflict systems and the true extent of the diversity of biochemical activities in the ADPR system.

Acknowledgments Work by the authors is supported by the Intramural Research Program of the National Library of Medicine, the National Institutes of Health, USA.

References

Adriouch S, Ohlrogge W, Haag F, Koch-Nolte F, Seman M (2001) Rapid induction of naive T cell apoptosis by ecto-nicotinamide adenine dinucleotide: requirement for mono(ADP-ribosyl)transferase 2 and a downstream effector. J Immunol 167(1):196–203

Al-Hakim AK, Bashkurov M, Gingras AC, Durocher D, Pelletier L (2012) Interaction proteomics identify NEURL4 and the HECT E3 ligase HERC2 as novel modulators of centrosome architecture. Mol Cell Proteomics 11(6):M111 014233

Altmeyer M, Messner S, Hassa PO, Fey M, Hottiger MO (2009) Molecular mechanism of poly(ADP-ribosyl)ation by PARP1 and identification of lysine residues as ADP-ribose acceptor sites. Nucleic Acids Res 37(11):3723–3738

Anantharaman V, Iyer LM, Aravind L (2012) Ter-dependent stress response systems: novel pathways related to metal sensing, production of a nucleoside-like metabolite, and DNA-processing. Mol Biosyst 8(12):3142–3165

Andreeva A, Howorth D, Chandonia JM, Brenner SE, Hubbard TJ, Chothia C, Murzin AG (2008) Data growth and its impact on the SCOP database: new developments. Nucleic Acids Res 36(Database issue):D419–D425

Aravind L (2000) Guilt by association: contextual information in genome analysis. Genome Res 10(8):1074–1077

Aravind L, Anantharaman V, Zhang D, de Souza RF, Iyer LM (2012) Gene flow and biological conflict systems in the origin and evolution of eukaryotes. Front Cell Infect Microbiol 2:89

Baysarowich J, Koteva K, Hughes DW et al (2008) Rifamycin antibiotic resistance by ADP-ribosylation: structure and diversity of Arr. Proc Natl Acad Sci U S A 105(12):4886–4891

Bazan JF, Koch-Nolte F (1997) Sequence and structural links between distant ADP-ribosyltransferase families. Adv Exp Med Biol 419:99–107

Belenky P, Bogan KL, Brenner C (2007) NAD^+ metabolism in health and disease. Trends Biochem Sci 32(1):12–19

Berg JM, Tymoczko JL, Stryer L (2012) Biochemistry, 7th edn. W.H. Freeman, New York

Boyd EF (2012) Bacteriophage-encoded bacterial virulence factors and phage-pathogenicity island interactions. Adv Virus Res 82:91–118

Burroughs AM, Ando Y, Aravind L (2013) New perspectives on the diversification of the RNA interference system: insights from comparative genomics and small RNA sequencing. Wiley Interdiscip Rev RNA 5(2):141–181

Carpusca I, Jank T, Aktories K (2006) *Bacillus sphaericus* mosquitocidal toxin (MTX) and pierisin: the enigmatic offspring from the family of ADP-ribosyltransferases. Mol Microbiol 62(3):621–630

Chambon P, Weil J, Mandel P (1963) Nicotinamide mononucleotide activation of a new DNA-dependent polyadenylic acid synthesizing nuclear enzyme. Biochem Biophys Res Commun 11:39–43

Citarelli M, Teotia S, Lamb RS (2010) Evolutionary history of the poly(ADP-ribose) polymerase gene family in eukaryotes. BMC Evol Biol 10:308

Cohen-Armon M, Visochek L, Katzoff A et al (2004) Long-term memory requires polyADP-ribosylation. Science 304(5678):1820–1822

Collier R, Pappenheimer A (1964) Studies on the mode of action of diphtheria toxin. II. Effect of toxin on amino acid incorporation in cell-free systems. J Exp Med 120:1019–1039

Corda D, Di Girolamo M (2003) Functional aspects of protein mono-ADP-ribosylation. EMBO J 22(9):1953–1958

Dassa B, Yanai I, Pietrokovski S (2004) New type of polyubiquitin-like genes with intein-like autoprocessing domains. Trends Genet 20(11):538–542

de Souza RF, Aravind L (2012) Identification of novel components of NAD-utilizing metabolic pathways and prediction of their biochemical functions. Mol Biosyst 8(6):1661–1677

Dunigan DD, Cerny RL, Bauman AT et al (2012) *Paramecium bursaria* chlorella virus 1 proteome reveals novel architectural and regulatory features of a giant virus. J Virol 86(16):8821–8834

Fieldhouse RJ, Turgeon Z, White D, Merrill AR (2010) Cholera- and anthrax-like toxins are among several new ADP-ribosyltransferases. PLoS Comput Biol 6(12):e1001029

Finn RD, Mistry J, Tate J, et al (2010) The Pfam protein families database. Nucleic Acids Res 38(Database issue):D211–D222

Frye RA (1999) Characterization of five human cDNAs with homology to the yeast SIR2 gene: Sir2-like proteins (sirtuins) metabolize NAD and may have protein ADP-ribosyltransferase activity. Biochem Biophys Res Commun 260(1):273–279

Fu ZQ, Guo M, Jeong BR et al (2007) A type III effector ADP-ribosylates RNA-binding proteins and quells plant immunity. Nature 447(7142):284–288

Garcia-Salcedo JA, Gijon P, Nolan DP, Tebabi P, Pays E (2003) A chromosomal SIR2 homologue with both histone NAD-dependent ADP-ribosyltransferase and deacetylase activities is involved in DNA repair in *Trypanosoma brucei*. EMBO J 22(21):5851–5862

Gazzaniga F, Stebbins R, Chang SZ, McPeek MA, Brenner C (2009) Microbial NAD metabolism: lessons from comparative genomics. Microbiol Mol Biol Rev 73(3):529–541 (Table of Contents)

Glowacki G, Braren R, Firner K et al (2002) The family of toxin-related ecto-ADP-ribosyltransferases in humans and the mouse. Protein Sci 11(7):1657–1670

Guse AH, Lee HC (2008) NAADP: a universal Ca^{2+} trigger. Sci Signal 1(44):re10

Haigis MC, Mostoslavsky R, Haigis KM et al (2006) SIRT4 inhibits glutamate dehydrogenase and opposes the effects of calorie restriction in pancreatic beta cells. Cell 126(5):941–954

Han S, Craig JA, Putnam CD, Carozzi NB, Tainer JA (1999) Evolution and mechanism from structures of an ADP-ribosylating toxin and NAD complex. Nat Struct Biol 6(10):932–936

Harding HP, Lackey JG, Hsu HC et al (2008) An intact unfolded protein response in Trpt1 knockout mice reveals phylogenic divergence in pathways for RNA ligation. RNA 14(2):225–232

Hassa PO, Haenni SS, Elser M, Hottiger MO (2006) Nuclear ADP-ribosylation reactions in mammalian cells: where are we today and where are we going? Microbiol Mol Biol Rev 70(3):789–829

Hawse WF, Wolberger C (2009) Structure-based mechanism of ADP-ribosylation by sirtuins. J Biol Chem 284(48):33654–33661

Hofmann A, Zdanov A, Genschik P, Ruvinov S, Filipowicz W, Wlodawer A (2000) Structure and mechanism of activity of the cyclic phosphodiesterase of Appr>p, a product of the tRNA splicing reaction. EMBO J 19(22):6207–6217

Hottiger MO, Hassa PO, Luscher B, Schuler H, Koch-Nolte F (2010) Toward a unified nomenclature for mammalian ADP-ribosyltransferases. Trends Biochem Sci 35(4):208–219

Iyer LM, Makarova KS, Koonin EV, Aravind L (2004) Comparative genomics of the FtsK-HerA superfamily of pumping ATPases: implications for the origins of chromosome segregation, cell division and viral capsid packaging. Nucleic Acids Res 32(17):5260–5279

Iyer LM, Anantharaman V, Wolf MY, Aravind L (2008) Comparative genomics of transcription factors and chromatin proteins in parasitic protists and other eukaryotes. Int J Parasitol 38(1):1–31

Iyer LM, Zhang D, Rogozin IB, Aravind L (2011) Evolution of the deaminase fold and multiple origins of eukaryotic editing and mutagenic nucleic acid deaminases from bacterial toxin systems. Nucleic Acids Res 39(22):9473–9497

Jiang H, Khan S, Wang Y et al (2013) SIRT6 regulates TNF-alpha secretion through hydrolysis of long-chain fatty acyl lysine. Nature 496(7443):110–113

Jiang J, Zhang YB, Li S, Yu FF, Sun F, Gui JF (2009) Expression regulation and functional characterization of a novel interferon inducible gene *Gig2* and its promoter. Mol Immunol 46(15):3131–3140

Jorgensen R, Wang Y, Visschedyk D, Merrill AR (2008a) The nature and character of the transition state for the ADP-ribosyltransferase reaction. EMBO Rep 9(8):802–809

Jorgensen R, Purdy AE, Fieldhouse RJ, Kimber MS, Bartlett DH, Merrill AR (2008b) Cholix toxin, a novel ADP-ribosylating factor from *Vibrio cholerae*. J Biol Chem 283(16): 10671–10678

Karras GI, Kustatscher G, Buhecha HR et al (2005) The macro domain is an ADP-ribose binding module. EMBO J 24(11):1911–1920

Kleine H, Poreba E, Lesniewicz K et al (2008) Substrate-assisted catalysis by PARP10 limits its activity to mono-ADP-ribosylation. Mol Cell 32(1):57–69

Koch-Nolte F, Reche P, Haag F, Bazan F (2001) ADP-ribosyltransferases: plastic tools for inactivating protein and small molecular weight targets. J Biotechnol 92(2):81–87

Koch-Nolte F, Kernstock S, Mueller-Dieckmann C, Weiss MS, Haag F (2008) Mammalian ADP-ribosyltransferases and ADP-ribosylhydrolases. Front Biosci 13:6716–6729

Koch T, Ruger W (1994) The ADP-ribosyltransferases (gpAlt) of bacteriophages T2, T4, and T6: sequencing of the genes and comparison of their products. Virology 203(2):294–298

Krasnov A, Timmerhaus G, Schiotz BL et al (2011) Genomic survey of early responses to viruses in Atlantic salmon, *Salmo salar* L. Mol Immunol 49(1–2):163–174

Laing S, Unger M, Koch-Nolte F, Haag F (2011) ADP-ribosylation of arginine. Amino Acids 41(2):257–269

Linhartova I, Bumba L, Masin J et al (2010) RTX proteins: a highly diverse family secreted by a common mechanism. FEMS Microbiol Rev 34(6):1076–1112

Ludden PW (1994) Reversible ADP-ribosylation as a mechanism of enzyme regulation in prokaryotes. Mol Cell Biochem 138(1–2):123–129

Merrick CJ, Duraisingh MT (2007) *Plasmodium falciparum* Sir2: an unusual sirtuin with dual histone deacetylase and ADP-ribosyltransferase activity. Eukaryot Cell 6(11):2081–2091

Nakano T, Matsushima-Hibiya Y, Yamamoto M et al (2006) Purification and molecular cloning of a DNA ADP-ribosylating protein, CARP-1, from the edible clam *Meretrix lamarckii*. Proc Natl Acad Sci U S A 103(37):13652–13657

Noinaj N, Guillier M, Barnard TJ, Buchanan SK (2010) TonB-dependent transporters: regulation, structure, and function. Annu Rev Microbiol 64:43–60

Ono T, Kasamatsu A, Oka S, Moss J (2006) The 39-kDa poly(ADP-ribose) glycohydrolase ARH3 hydrolyzes O-acetyl-ADP-ribose, a product of the Sir2 family of acetyl-histone deacetylases. Proc Natl Acad Sci U S A 103(45):16687–16691

Otto H, Reche PA, Bazan F, Dittmar K, Haag F, Koch-Nolte F (2005) In silico characterization of the family of PARP-like poly(ADP-ribosyl)transferases (pARTs). BMC Genomics 6:139

Pallen MJ, Lam AC, Loman NJ, McBride A (2001) An abundance of bacterial ADP-ribosyltransferases—implications for the origin of exotoxins and their human homologues. Trends Microbiol 9(7):302–307 (discussion 308)

Park UE, Olivera BM, Hughes KT, Roth JR, Hillyard DR (1989) DNA ligase and the pyridine nucleotide cycle in *Salmonella typhimurium*. J Bacteriol 171(4):2173–2180

Peterson FC, Chen D, Lytle BL, Rossi MN, Ahel I, Denu JM, Volkman BF (2011) Orphan macrodomain protein (human C6orf130) is an O-acyl-ADP-ribose deacylase: solution structure and catalytic properties. J Biol Chem 286(41):35955–35965

Price MN, Dehal PS, Arkin AP (2010) FastTree 2: approximately maximum-likelihood trees for large alignments. PLoS One 5(3):e9490

Ramirez MS, Tolmasky ME (2010) Aminoglycoside modifying enzymes. Drug Resist Updat 13(6):151–171

Rohmer L, Kjemtrup S, Marchesini P, Dangl JL (2003) Nucleotide sequence, functional characterization and evolution of pFKN, a virulence plasmid in *Pseudomonas syringae* pathovar maculicola. Mol Microbiol 47(6):1545–1562

Ronimus RS, Morgan HW (2003) Distribution and phylogenies of enzymes of the Embden-Meyerhof-Parnas pathway from archaea and hyperthermophilic bacteria support a gluconeogenic origin of metabolism. Archaea 1(3):199–221

Rosado MM, Bennici E, Novelli F, Pioli C (2013) Beyond DNA repair, the immunological role of PARP-1 and its siblings. Immunology 139(4):428–437

Sala A, Calderon V, Bordes P, Genevaux P (2013) TAC from *Mycobacterium tuberculosis*: a paradigm for stress-responsive toxin-antitoxin systems controlled by SecB-like chaperones. Cell Stress Chaperones 18(2):129–135

Schaffer AA, Aravind L, Madden TL et al (2001) Improving the accuracy of PSI-BLAST protein database searches with composition-based statistics and other refinements. Nucleic Acids Res 29(14):2994–3005

Seman M, Adriouch S, Scheuplein F et al (2003) NAD-induced T cell death: ADP-ribosylation of cell surface proteins by ART2 activates the cytolytic P2X7 purinoceptor. Immunity 19(4):571–582

Shniffer A, Visschedyk DD, Ravulapalli R et al (2012) Characterization of an actin-targeting ADP-ribosyltransferase from *Aeromonas hydrophila*. J Biol Chem 287(44):37030–37041

Singer AU, Desveaux D, Betts L et al (2004) Crystal structures of the type III effector protein AvrPphF and its chaperone reveal residues required for plant pathogenesis. Structure 12(9): 1669–1681

Slade D, Dunstan MS, Barkauskaite E et al (2011) The structure and catalytic mechanism of a poly(ADP-ribose) glycohydrolase. Nature 477(7366):616–620

Smith CL, Ghosh J, Elam JS, Pinkner JS, Hultgren SJ, Caparon MG, Ellenberger T (2011) Structural basis of *Streptococcus pyogenes* immunity to its NAD^+ glycohydrolase toxin. Structure 19(2):192–202

Smith JA, Stocken LA (1974) Chemical and metabolic properties of adenosine diphosphate ribose derivatives of nuclear proteins. Biochem J 147:523–529

Smith JS, Avalos J, Celic I, Muhammad S, Wolberger C, Boeke JD (2002) SIR2 family of NAD(+)-dependent protein deacetylases. Methods Enzymol 353:282–300

Snyder AK, Rio RV (2013) Interwoven biology of the tsetse holobiont. J Bacteriol 195(19):4322–4330

Soding J, Biegert A, Lupas AN (2005) The HHpred interactive server for protein homology detection and structure prediction. Nucleic Acids Res 33(Web Server issue):W244–W248

Sorci L, Kurnasov OV, Rodionov DA, Osterman A (2010) Genomics and enzymology of NAD biosynthesis. In: Mander LN, Lui HW (eds) Comprehensive natural products II : chemistry and biology, vol 7. Elsevier, Amsterdam, pp 213–257

Spinelli SL, Kierzek R, Turner DH, Phizicky EM (1999) Transient ADP-ribosylation of a 2′-phosphate implicated in its removal from ligated tRNA during splicing in yeast. J Biol Chem 274(5):2637–2644

Stabb EV, Reich KA, Ruby EG (2001) *Vibrio fischeri* genes *hvnA* and *hvnB* encode secreted NAD(+)-glycohydrolases. J Bacteriol 183(1):309–317

Sugimura T, Miwa M (1994) Poly(ADP-ribose): historical perspective. Mol Cell Biochem 138(1–2):5–12

Takahashi-Nakaguchi A, Matsumoto Y, Yamamoto M, Iwabuchi K, Totsuka Y, Sugimura T, Wakabayashi K (2013) Demonstration of cytotoxicity against wasps by pierisin-1: a possible defense factor in the cabbage white butterfly. PLoS One 8(4):e60539

Tiemann B, Depping R, Gineikiene E, Kaliniene L, Nivinskas R, Ruger W (2004) ModA and ModB, two ADP-ribosyltransferases encoded by bacteriophage T4: catalytic properties and mutation analysis. J Bacteriol 186(21):7262–7272

Timinszky G, Till S, Hassa PO et al (2009) A macrodomain-containing histone rearranges chromatin upon sensing PARP1 activation. Nat Struct Mol Biol 16(9):923–929

Ueda K, Hayaishi O (1985) ADP-ribosylation. Annu Rev Biochem 54:73–100

Walsh C (2003) Antibiotics : actions, origins, resistance. ASM Press, Washington, D.C.

Wang M, Soyano T, Machida S, Yang JY, Jung C, Chua NH, Yuan YA (2011) Molecular insights into plant cell proliferation disturbance by *Agrobacterium* protein 6b. Genes Dev 25(1):64–76

Xu Q, Kozbial P, McMullan D et al (2008) Crystal structure of an ADP-ribosylated protein with a cytidine deaminase-like fold, but unknown function (TM1506), from *Thermotoga maritima* at 2.70 A resolution. Proteins 71(3):1546–1552

Zhang D, de Souza RF, Anantharaman V, Iyer LM, Aravind L (2012) Polymorphic toxin systems: comprehensive characterization of trafficking modes, processing, mechanisms of action, immunity and ecology using comparative genomics. Biol Direct 7:18

Zheng J, Leung KY (2007) Dissection of a type VI secretion system in *Edwardsiella tarda*. Mol Microbiol 66(5):1192–1206

Identification and Analysis of ADP-Ribosylated Proteins

Friedrich Haag and Friedrich Buck

Abstract The analysis of ADP-ribosylated proteins is a challenging task, on the one hand because of the diversity of the target proteins and the modification sites, on the other hand because of the particular problems posed by the analysis of ADP-ribosylated peptides. ADP-ribosylated proteins can be detected in in vitro experiments after the incorporation of radioactively labeled or chemically modified ADP-ribose. Endogenously ADP-ribosylated proteins may be detected and enriched by antibodies directed against the ADP-ribosyl moiety or by ADP-ribosyl binding macro domains. The determination of the exact attachment site of the modification, which is a prerequisite for the understanding of the specificity of the various ADP-ribosyl transferases and the structural consequences of ADP-ribosylation, necessitates the proteolytic cleavage of the proteins. The resulting peptides can afterwards be enriched either by IMAC (using the affinity of the pyrophosphate group for heavy metal ions) or by immobilized boronic acid beads (using the affinity of the vicinal ribose hydroxy groups for boronic acid). The identification of the modified peptides usually requires tandem mass spectrometric measurements. Problems that hamper the mass spectrometric analysis by collision-induced decay (CID) can be circumvented either by the application of different fragmentation techniques (electron transfer or electron capture dissociation; ETD or ECD) or by enzymatic cleavage of the ADP-ribosyl group to ribosyl-phosphate.

F. Haag · F. Buck
Institute of Immunology, University Medical Center Hamburg-Eppendorf,
Martinistr. 52, 20246 Hamburg, Germany

F. Buck (✉)
Institute of Clinical Chemistry, University Medical Center Hamburg-Eppendorf,
Martinistr. 52, 20246 Hamburg, Germany
e-mail: buck@uke.de

Current Topics in Microbiology and Immunology (2015) 384: 33–50
DOI: 10.1007/82_2014_424

Published Online: 12 August 2014

Abbreviations

ADP	Adenosine diphosphate
CID	Collision-induced decay
IMAC	Immobilized metal ion affinity chromatography
ECD	Electron capture dissociation
ETD	Electron transfer dissociation
GAPDH	Glyceraldehyde-3-phosphate dehydrogenase
HNP-1	Human neutrophil peptide-1
LC/MS	Liquid chromatography/mass spectrometry
MS/MS	Tandem mass spectrometry
NAD	Nicotinamide adenine dinucleotide
QTOF	Quadrupol time-of-flight
SDS-PAGE	Sodium dodecyl sulfate polyacrylamide gel electrophoresis

Contents

1 Introduction

The analysis of any post-translational modification crucially depends upon the methods available for the detection of modified substrates. The requirement profile for an ideal method for the detection of a post-translational modification is complex, and cannot be fulfilled by any single technique. An ideal method should be

sensitive and specific, allow the visualization of modified proteins both within analytical procedures such as SDS-PAGE or gel chromatography as well as within their native cellular environment, and give information about the number and intramolecular location of the attached modifications.

The term ADP-ribosylation describes the transfer of an ADP-ribose moiety from NAD+ to a target structure under the release of nicotinamide. Although this review focuses on the analysis of ADP-ribosylated proteins, it is important to bear in mind that other structures such as DNA, RNA, antibiotics, and water may also serve as acceptors of ADP-ribose. Since its discovery in the late 1960s, a variety of methods have been developed to visualize the incorporation of ADP-ribose into proteins, including the introduction of chemical modifications into the substrate NAD^+, the development of antibodies and natural ligands to detect the modification, and the refinement of mass spectrometry techniques to identify ADP-ribosylated proteins and to determine the modification site.

However, in comparison to phosphorylation, another post-translational modification that profoundly impacts target protein function, the development of methods to identify and analyze ADP-ribosylated substrates lags far behind. Two factors have greatly helped to analyze the role of phosphorylation in signal transduction pathways that are not available in a comparable manner for ADP-ribosylation: the development of algorithms to define consensus sequence motifs that allow the prediction of potential phosphorylation sites (He et al. 2011; Ubersax and Ferrell 2007), and the increased availability of phosphorylation site-specific antibodies that are able to directly report the presence or absence of a phosphorus residue at a specific site within a protein substrate (Macek et al. 2009). Importantly, the availability of site-specific antibodies permits the identification and analysis of endogenously phosphorylated proteins, whereas the field of ADP-ribosylation is still largely dependent on analyzing the products of ADP-ribosylation reactions performed in vitro using chemically modified versions of the substrate NAD^+.

A further complication in the analysis of ADP-ribosylated proteins is the heterogeneity of ADP-ribosylation reactions. ADP-ribosyltransferases have been divided into the two families of ARTC (C2/C3 toxin-like) and ARTD (diphtheria toxin-like) enzymes. While all known poly-ADP-ribosyltransferases belong to the ARTD family, and mono-ADP-ribosylation has traditionally been the domain of the ARTC transferases, it has recently been appreciated that some ARTD family members and even some family members of the structurally unrelated sirtuin family can mediate mono-ADP-ribosylation (Feijs et al. 2013). In addition, ADP-ribose may be attached to proteins by nonenzymatic means (McDonald and Moss 1994). These different reaction types result in a wide spectrum of amino acid specificities that complicate the analysis of their products.

The aim of this review is to provide an overview of current methods for the identification and analysis of ADP-ribosylated proteins, beginning with the characterization of the products of in vitro ADP-ribosylation reactions using modified versions of NAD^+ as a substrate, and continuing to recent advances in the identification and analysis of endogenously modified ADP-ribosylated proteins and of the respective modification sites.

2 Strategies for the Identification of ADP-Ribosylated Proteins

2.1 Using Modified NAD$^+$ to Identify ADP-Ribosylated Proteins in In vitro Reactions

2.1.1 Use of Radiolabeled NAD$^+$

The use of radioactive NAD$^+$ as a substrate was the first, and for a long time the only means to visualize ADP-ribosylated proteins. The first ADP-ribosylation reaction ever observed was detected following the incubation of nuclear extracts from liver cells with radioactive ATP in the presence of nicotinamide mononucleotide (Chambon et al. 1963). However, in this case the modified high-molecular weight substrate resulting from the reaction was not correctly identified as polymeric ADP-ribose, but at first misinterpreted to be polyadenylic acid. Only some years later was it realized that the radioactive ATP might have been converted to NAD$^+$ by NAD$^+$ pyrophosphorylase present in the nuclear extract. Similar experiments using radiolabeled NAD$^+$ that had been synthesized prior to incubation were performed almost simultaneously by several groups, and led to the realization that NAD$^+$ and not ATP was the immediate substrate and to the identification of polymeric ADP-ribose as the product of the reaction (Chambon et al. 1966; Fujimura et al. 1967; Nishizuka et al. 1967). The radioactive NAD$^+$ species developed for these experiments subsequently were used by Honjo et al. to discover ADP-ribosylation as the mechanism causing the inactivation of elongation factor 2 by diphtheria toxin (Honjo et al. 1968). By incubating target and toxin with NAD$^+$ carrying radiolabels at different positions within the molecule, these authors found that NAD$^+$ labeled at any position outside of nicotinamide caused incorporation of radioactivity into the target protein.

This brief historic introduction may serve to illustrate one of the pitfalls that may be associated with the use of radioactive (or otherwise modified) metabolites to visualize post-translational modifications. The detection of radiolabel does not give any information about whether and how the radioactive substrate has been processed before incorporation into the protein. We will return to this below. However, the use of radioactive NAD$^+$ has many advantages that make it a method of choice for the visualization of ADP-ribosylation reactions in many experimental contexts. First, enzymes are usually indifferent to isotope exchanges within their substrates, so radioactive NAD$^+$ may be expected to faithfully mimic the behavior of unmodified NAD$^+$. Radioactively labeled proteins can be visualized directly with a high sensitivity in many detection systems, such as SDS-PAGE or gel chromatography, that give biochemical information such as molecular size about the target protein.

The incorporation of radioactive ADP-ribose is less useful for the identification of ADP-ribosylation in the context of living cells or for the affinity purification of ADP-ribosylated substrates. In the latter case, it can be used as a tracer to follow the

progress of modified proteins during the purification procedure, but, in contrast to other forms of modified NAD^+ discussed below, by itself does not provide any mechanism facilitating enrichment.

Radioactive NAD^+ is commercially readily available in various species differing in the isotopes used for labeling and the positions where the label is incorporated. Most applications use NAD^+ carrying a radioactive phosphorus atom within the diphosphate bridge at the position proximal to the adenosine moiety ([α^{32}P]-NAD^+). However, NAD^+ species labeled at other positions are also available and may be useful for certain applications. Especially, NAD^+ labeled by ^{14}C within the nicotinamide moiety has been used to differentiate genuine ADP-ribosylation from the formation of unconventional adducts of NAD^+ with target proteins (McDonald and Moss 1993).

2.1.2 Use of Nonradioactive NAD^+ Derivatives

Several modifications have been incorporated into the adenosyl moiety of NAD^+ with the aim of introducing detectable chemical "tags" into ADP-ribosylated target proteins. This approach offers several advantages over the use of radioactivity to label NAD^+. These tags are recognized by highly specific ligands such as antibodies or streptavidin that can be conjugated to fluorochromes, thus permitting the visualization of ADP-ribosylated proteins by immunofluorescence. In addition, this approach allows ADP-ribosylation reactions occurring on cell surfaces to be followed by flow cytometry (Krebs et al. 2003).

Zhang and Snyder conjugated NAD^+ to biotin, and reported that biotinylated NAD^+ could be used by diphtheria toxin to modify elongation factor 2, and by an unknown endogenous nitric oxide-inducible ADP-ribosyltransferase to modify GAPDH (Zhang and Snyder 1993). However, this latter case was later found not to be due to genuine ADP-ribosylation, but to represent unconventional covalent attachments of either NAD^+ or ADP-ribosyl to GAPDH (McDonald and Moss 1993). In a similar fashion, Takei and colleagues used digoxigenin to label NAD^+ and showed that the resulting DIG-NAD was incorporated by pertussis toxin into its target protein $G_{i\alpha}$ (Takei et al. 1994). The modified protein was then visualized by immunofluorescence microscopy using anti-digoxigenin antibodies, and found to be localized in the plasma membrane and the nucleus. However, it is important to note that other authors have contested the validity of using biotinylated or digoxigenin-conjugated NAD^+ as surrogate substrates for ADP-ribosyltransferases. Klebl et al. found that the pattern of target proteins labeled by either pertussis toxin or arginine-specific ADP-ribosyltransferase from skeletal muscle was different when using biotinylated or digoxigenin-conjugated NAD^+ as compared to that obtained using [^{32}P]-NAD^+ (Klebl et al. 1997).

An interesting alternative to the above-mentioned chemical modifications is the introduction of an etheno group into the adenine moiety of NAD^+. The NAD^+-analog 1,N6-etheno-NAD^+ (etheno-NAD^+) is readily accepted as a substrate for ADP-ribosylation by a broad spectrum of bacterial and eukaryotic ADP-ribosyltransferases

(Armstrong and Merrill 2001; Davis et al. 1998; Giovane et al. 1985; Hingorani and Ho 1988; Klebl and Pette 1996; Krebs et al. 2003; Lowery and Ludden 1988). An antibody (1G4) is available that specifically recognizes 1,N6-ethenoadenosine. This originally had been developed to detect ethenoadenosine as an adduct in DNA resulting from the exposure of workers to vinyl chloride (Young and Santella 1988). The 1G4 antibody detects etheno-ADP-ribose incorporated into both poly- and mono-ADP-ribosylated proteins, and can be used in a variety of assay systems including Western blot and immunofluorescence (Bannas et al. 2005; Davis et al. 1998; Krebs et al. 2003; Liao and Puro 2006). Importantly, fluorochrome-conjugated 1G4 antibody has been used as a flow cytometric assay to monitor cell surface ADP-ribosyltransferase activity (Grahnert et al. 2002; Krebs et al. 2003; Scheuplein et al. 2009; Seman et al. 2003). Recently, 1G4 coupled to superparamagnetic iron oxide (SPIO) particles has been used to detect cells carrying etheno-ADP-ribosylated proteins in vivo by magnetic resonance imaging (Bannas et al. 2010).

2.2 Determining the Specificity of ADP-Ribosylation Sites

ADP-ribosyltransferases have been divided into the two families of ARTC and ARTD enzymes (Hottiger et al. 2010). While all molecularly identified mammalian ARTC transferases are specific for arginine as the acceptor residue (Seman et al. 2004), mammalian ARTD transferases preferentially seem to modify lysine, glutamic or aspartic acid, or serine/threonine residues (Feijs et al. 2013). ADP-ribosylation on cysteine and asparagine residues has also been detected biochemically, although the responsible enzymes have not been molecularly defined.

The stability of the ADP-ribosyl-protein bond in different chemical environments can help to elucidate the amino acid linkage of the modification (Cervantes-Laurean et al. 1993; Feijs et al. 2013). The O-glycosidic linkage to acidic residues is more sensitive to neutral hydroxylamine than the N-glycosidic bond to arginine or lysine (Moss et al. 1983). ADP-ribosyl bonds to cysteine are uniquely sensitive to mercuric chloride (Meyer et al. 1988). However, while the enzymatic ADP-ribosyl-cysteine linkage catalyzed by pertussis toxin is resistant to neutral hydroxylamine, the nonenzymatic covalent attachment of free ADP-ribose to cysteine is sensitive to both mercuric chloride and hydroxylamine (McDonald and Moss 1994; McDonald et al. 1992).

2.3 Detection of Endogenously ADP-Ribosylated Proteins

While many tools are available to visualize and identify the products of in vitro ADP-ribosylation reactions via the use of labeled analogs of NAD^+, it is much more difficult to detect ADP-ribosylated proteins that have been endogenously modified by living cells using their own unlabeled pool of NAD^+. This section outlines some of the approaches that have been taken to achieve this aim.

2.3.1 Anti-ADP-Ribosyl Antibodies

Already early in the history of ADP-ribosylation several groups made antibodies designed to detect endogenously ADP-ribosylated proteins. Meyer and Hilz immunized rabbits with a nonhydrolyzable ADP-ribose analog or ADP-ribose coupled to bovine serum albumin, and then purified the resulting serum on an affinity column containing ADP-ribosyl-guanidinobutyrate, formed by ADP-ribosylating guanodinobutyrate by cholera toxin. The resulting serum recognized ADP-ribosylated elongation factor 2 in immunoblots and revealed the ADP-ribosylation of nuclear proteins in response to chemical stress by immunofluorescence (Meyer and Hilz 1986). Spiegel and co-workers immunized with ADP-ribose chemically coupled to carrier proteins. The resulting serum recognized G-proteins modified by pertussis toxin and ADP-ribosylated elongation factor 2 on immunoblots (Eide et al. 1986). McMahon and co-workers immunized rabbits with ADP-ribosylated polyarginine and used the resulting serum to detect arginine-ADP-ribosylated proteins in subcellular fractions of quail cardiac muscle by immunoblot (Schwab et al. 2000). More recently, the group of Tsuchiya raised an antiserum to ADP-ribosylated histones, and purified anti-ADP-ribosyl antibodies on an affinity column containing ADP-ribosylated protamine. The resulting serum was used in immunoblot and immunofluorescence to detect ADP-ribosylation on lymphocytes and in skeletal muscle (Osago et al. 2008). Although these attempts have created valuable tools for the detection of endogenously ADP-ribosylated proteins, they have not gained wide distribution. To date, no monoclonal antibody recognizing ADP-ribosyl-arginine or any other ADP-ribosyl linkage is available.

2.3.2 Recombinant Macro Domains as Sensors for ADP-Ribosylated Proteins

Recently, macro domains contained in some intracellular proteins have been identified as binding domains for polymeric and monomeric ADP-ribose (Karras et al. 2005). This property has been exploited to precipitate ADP-ribosylated proteins from extracts of CHO and HL-60 cells using recombinant macro domains from human ARTD9 and the archaeal protein Afl521 (Dani et al. 2009). Subsequent analysis of the precipitated proteins by mass spectrometry revealed several known target proteins of intracellular ADP-ribosylation (see Sect. 3).

2.3.3 Antibodies Against Epitopes Sensitive to ADP-Ribosylation on Target Proteins

In selected cases, antibodies that recognize target proteins of ADP-ribosylation at their modification site have been used to monitor the state of endogenous ADP-ribosylation of the respective protein. For example, integrin α_L/β_2 (LFA-1, CD11a/CD18) can be ADP-ribosylated on both of its two chains. ADP-ribosylation of

LFA-1 interfered with the binding of some antibodies (i.e., mAb 2D7 that recognizes CD11a and mAb C71/16 that recognizes CD18), while the binding of other antibodies was not affected [Nemoto 1996]. Similarly, recognition of CD8 by mAb YTS156.7.7, but not by mAb H35–17.2, was blocked when murine T cells were exposed to extracellular NAD^+, suggesting that binding of YTS156.7.7 was sensitive to the ADP-ribosylation of its cognate epitope. Further experiments revealed that NAD^+ released from lymph node cells during cell preparation was sufficient to mediate the ADP-ribosylation of CD8 (Lischke et al. 2013).

3 Strategies for the Enrichment of ADP-Ribosylated Proteins

Some of the procedures described above for the detection of ADP-ribosylated proteins can also be used for their specific enrichment in pulldown experiments, either after the introduction of modified NAD^+ in vitro or by the use of antibodies or macro domains for the binding of endogenously ADP-ribosylated proteins.

3.1 Use of Nonradioactive NAD^+ Derivatives in Pulldown Experiments

The NAD^+ derivatives described in Sect. 2.1.2 can be used to purify or enrich ADP-ribosylated proteins by affinity chromatography. As a proof of principle, Zhang and Snyder showed that diphtheria toxin could utilize biotinylated NAD^+ as a substrate to incorporate biotin-ADP-ribose into EF2, and used streptavidin beads to isolate the modified protein from cell extracts. They then used the same methodology to purify an unknown protein that was ADP-ribosylated in response to nitric oxide, which they then identified as glyceraldehyde-3-phosphate dehydrogenase (Zhang 1997; Zhang and Snyder 1993). In a similar fashion, we have used the 1G4 antibody specific for ethenoadenosine to purify etheno-ADP-ribosylated membrane proteins from detergent extracts of cells expressing cell surface ARTC2 and incubated with etheno-NAD^+ (our own unpublished observations).

3.2 Pulldown of Endogenously ADP-Ribosylated Proteins

Antibodies directed against the ADP-ribosyl moiety (see Sect. 2.3.1) could, in general, be used for the enrichment of ADP-ribosylated proteins in immunoprecipitation experiments. However, the lack of easily available antibodies, particularly monoclonal antibodies, has hampered this approach. Furthermore, single-step immunoprecipitations are prone to a high load of contaminations (Mellacheruvu et al. 2013).

An alternative approach is the pulldown of ADP ribosylated proteins with recombinant macro domains (see Sect. 2.3.2). The use of a recombinant macro domain from the Archaeon *Archaeglobus fulgidus* for the enrichment of ADP-ribosylated proteins in a pulldown experiment has been described (Dani et al. 2009). The authors used a non-ADP-ribosyl binding mutant of the macro domain for pre-clearing of the extract and in a second step the wild-type macro domain for the specific binding of ADP-ribosylated proteins. Both macro domain constructs carried His_6- or GST-tags for immobilization onto beads. After separation by SDS gel electrophoresis a number of known target proteins for ADP-ribosylation were identified by mass spectrometry (e.g., the heatshock protein GRP78, mitochondrial glutamate dehydrogenase, G protein β subunits, EF 1α, GAPDH), demonstrating the feasibility of the method for the isolation of proteins ADP-ribosylated at different amino acid side chains.

4 Strategies for the Enrichment of ADP Ribosylated Peptides After Proteolytic Digestion

Post-translational modifications are, in general, not stoichiometric. Furthermore, ADP-ribosylated peptides, just as phosphopeptides, are prone to losses during sample preparation and their mass spectrometric detection poses particular problems (see Regulation of nitrogenase by reversible mono-ADP-ribosylation). Thus, specific enrichment is advisable at the protein level (see *Photorhabdus luminescens* Toxins TccC3 and TccC5: Insecticidal ADP-Ribosyltransferases that Modify Threonine and Glutamine) or after proteolytic digestion at the peptide level.

Both the pyrophosphate and the ribosyl moiety of the ADP-ribosyl group can be used for the enrichment of modified peptides. However, both procedures are of limited specificity, since the affinity materials also exhibit an affinity for phosphorylated or glycosylated peptides, respectively.

After any enrichment procedure, the eluted peptide fractions should be desalted by reverse-phase materials (e.g., ZipTips), dried down and redissolved in an appropriate buffer for mass spectrometric analysis (See Regulation of nitrogenase by reversible mono-ADP-ribosylation).

4.1 Enrichment by Phosphate-Binding Affinity Materials

Affinity enrichment by IMAC or by TiO_2 beads are standard procedures in the analysis of phosphopeptides (Macek et al. 2009; Rosenqvist et al. 2011). In spite of the differences in the chemical structure of the phosphate bonds, similar affinities as for phosphopeptides have been demonstrated for the binding of ADP-ribosylated peptides onto IMAC or TiO_2 beads (Laing et al. 2011). The binding mode of the ADP-ribosyl group to Fe^{3+}-IMAC beads is shown schematically in Fig. 1a.

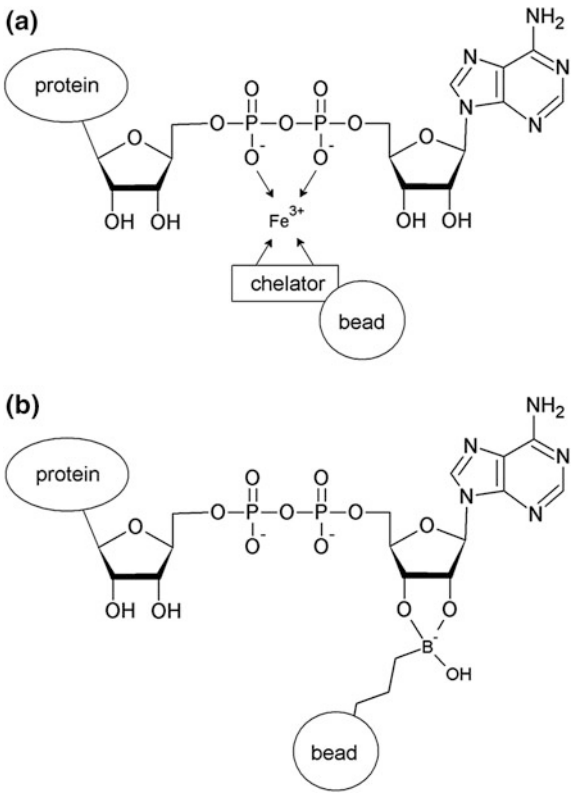

Fig. 1 Enrichment of ADP-ribosylated peptides by binding to solid phase matrices. Schematic showing the interaction of an ADP-ribosylated protein with an IMAC affinity matrix (**a**) or a boronic acid resin (**b**)

Enrichment was tested for beads loaded with Fe^{3+} and for magnetic TiO_2 beads using ADP-ribosylated TNFα (double digest with trypsin and Glu-C (synonym: V8 protease)), tryptically digested ADP-ribosylated HNP-1, a well characterized substrate for ADP-ribosylation (Paone et al. 2006)), mono- and doubly ADP-ribosylated Kemptide (LRRASLG, a model substrate for both kinases and ADP-ribosyl transferases) and, as a phosphopeptide control, tryptically digested α-casein. All test samples contained an excess of tryptically digested BSA. The results demonstrated clearly that IMAC as well as binding to TiO_2 are suited for the enrichment of ADP-ribosylated peptides. While both methods gave comparable yields for the phosphopeptide controls, Fe^{3+}-IMAC enrichment gave more consistent results and higher yields compared with the enrichment by TiO_2 magnetic beads. However, as often observed for the enrichment of phosphopeptides, the yields varied highly between the different ADP-ribosylated peptides. Therefore, it is not clear whether the superior performance of IMAC can be generalized. For the enrichment of peptides ADP-ribosylated at Asp or Glu side chains the elution conditions have to be modified, since ADP-ribosylated carboxylate side chains are susceptible to hydrolysis at basic pH values (Cervantes-Laurean et al. 1997).

Finally, it should be noted that, since ADP-ribosylated peptides are copurified with phosphopeptides in IMAC and TiO_2 enrichment experiments (as outlined above), ADP-ribosylation sites can be identified in phosphoproteomics data sets (Matic et al. 2012).

4.2 Enrichment by Boronate Affinity Materials

Boronate affinity chromatography is an established method for the isolation of 1,2-cis-diol-containing compounds (Liu and Scouten 2000, 2005). Even though its application for the purification of ADP-ribosylated peptides has been described early on (Okayama et al. 1978), the method has rarely been used. A detailed description is given by Rosenthal and colleagues (Rosenthal et al. 2011). In short, ADP-ribosylated peptides are bound to boronic acid resins at moderately basic conditions and high ionic strength (pH 8.7–8.8, 0.5–1 M NaCl, 0–50 mM $MgCl_2$). The binding mode of the ADP-ribosyl group to boronic acid beads is shown schematically in Fig. 1b. The bound peptides are eluted at low pH (e.g., 0.1 M acetic acid) or by competition with a diol-containing compound (e.g., 50 mM sorbitol).

5 Identification of Protein ADP-Ribosylation Sites

The identification of protein post-translational modification sites in modern proteome analysis relies almost exclusively on the mass spectrometric analysis after proteolytic digestion. If the ADP-ribosylated protein can be isolated and identified, the detection of a peptide with a mass increment of 541.06 Da can provide a strong hint at the site of a mono-ADP-ribosylation (Margarit et al. 2006). Putative ADP-ribosylation sites can be confirmed by site-directed mutagenesis (Ganesan et al. 1998). Similar to phosphopeptides, ADP-ribosylated peptides have a high affinity for mono- and divalent cations, and even after careful purification, sodium and potassium adducts are usually detected in addition to the protonated species (unpublished observation) in positive mode mass spectrometry. While this effect on the one hand hampers the detection by decreasing the sensitivity, it corroborates, on the other hand, the presence of a phosphate group in the respective peptide. However, the definite proof of an ADP-ribosyl modification and its exact location can only be obtained from the analysis of the fragment pattern in MS/MS mass spectrometric experiments (for a review see (Hengel and Goodlett 2012)).

5.1 Identification by MS/MS Fragment Analysis

5.1.1 Collision-induced Decay

The standard technique for the analysis of peptides by tandem mass spectrometry is CID, (synonymous: collision-activated decay, CAD). In a collision cell filled with an inert gas (mostly argon or helium), analytes are accelerated by an applied voltage. Collision with the inert gas molecules results in the conversion of kinetic into vibrational energy until chemical bonds are broken. The analyte is then identified by its fragmentation pattern. Peptides typically fragment at peptide bonds, while most post-translational modifications are either stable in a CID experiment (e.g., phosphotyrosine, acetyllysine) or the modification is eliminated as a neutral leaving group ("neutral loss", e.g., phosphoric acid from phosphoserine, monosaccharides from glycopeptides). ADP-ribosylated peptides, however, display a different behavior, which poses a considerable obstacle to their detection and identification: upon fragmentation, ADP-ribosylated peptides release predominantly not the modifying ADP-ribosyl group, but the peptide as a neutral loss, while the ADP-ribose group or its fragments carry the charge(s) (Hengel et al. 2009). These authors have proposed a nomenclature for the fragments of the ADP-ribosyl group that are typically detected upon fragmentation of ADP-ribosylated peptides. These are listed in Table 1. Peptide fragments needed for sequence identification are small or not detectable. The extent of this problem is controversial and may depend on the experimental setting. Upon fragmentation in an ion trap instrument, the neutral loss of the peptide component was found to be pronounced only for smaller peptides, while fragmentation of larger ADP-ribosylated peptides resulted in the detection of both peptide and ADP-ribose fragments (Hengel et al. 2010). By contrast, in a QTOF instrument the fragmentation pattern of all ADP-ribosylated peptides was dominated by fragments of ADP-ribose (Laing et al. 2011).

While the fragmentation pattern of ADP-ribosylated peptides hampers the unambiguous identification of the site of modification, the strong fragment signals of the ADP-ribosyl group can, on the other hand, be used for the sensitive detection of the ADP-ribosylated peptides in LC/MS experiments. In samples of moderate complexity ADP-ribosylated peptides can also be identified by the alternating acquisition of spectra at low and high collision energy in LC/MS experiments. In the spectra recorded at high collision energy, ADP-ribosylated peptides give rise to a series of characteristic fragments (Table 1), the signals of which can be traced in the respective extracted ion chromatograms. In the spectra recorded at low collision energy the candidate peptides can be identified and validated (Laing et al. 2011). This approach is essentially an application of the general approach described for the identification of labile post-translational modifications (Carapito et al. 2009).

Osago and colleagues studied the CID fragmentation of ADP-ribosylated peptides in positive and negative mode in a quadrupol tandem instrument (Osago et al. 2009). In addition to the fragments listed in Table 1 the authors describe a singly charged fragment with m/z = 582.4 (negative mode) or m/z = 584.4 (positive mode),

Table 1 Fragments detected after CID fragmentation of ADP-ribosylated peptides

Theoret. mass as MH^+ [Da]	Assignment	Fragment type[a]
136.06	Adenine	m_1
250.09	Adenosine-18	m_3
348.07	Adenosine-monophosphate	m_6
428.04	Adenosine diphosphate	m_8

[a] Nomenclature according to Hengel et al. (2009)

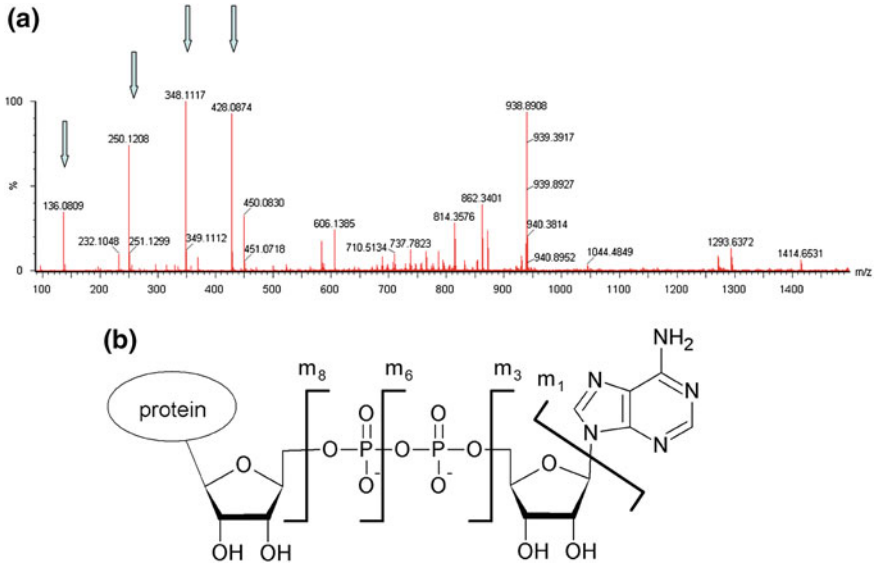

Fig. 2 Fragmentation of ADP-ribosylated peptides in CID fragmentation experiments. **a**. MS/MS spectrum of di-ADP-ribosylated Kemptide after CID fragmentation. Fragments of the ADP-ribosyl groups (listed in Table 1) are marked by *arrows*. Nanospray ESI experiments were performed on a QTOF II instrument (Waters), using 500 fMol Kemptide/µl in 60 % MeOH/5 % HCOOH; precursor selection: m/z = 927.3 (MH_2^{2+}); for further experimental details see (Laing et al. 2010). **b**. Fragmentation pattern of the ADP-ribosyl group in CID fragmentation experiments

which can be attributed to the carbodiimide derivative of the ADP-ribosyl group, and results from a cleavage within the arginine guanidinium group. This fragment can be used for the identification of ADP-ribosylated peptides in a precursor ion scanning experiment. It should, however, be noted that it can be detected only if arginine is the site of ADP-ribosylation (Fig. 2).

5.1.2 Fragmentation by ECD or ETD

Electron capture dissociation and electron transfer dissociation are fragmentation techniques in which low energy electrons are transferred onto multiply charged peptides either directly (ECD) or chemically mediated by a radical anion (ETD). The radical cation analytes that arise from this process fragment by a mechanism different from CID and give rise to different fragmentation products. Most notably, ECD and ETD lead preferentially to peptide backbone fragmentation while leaving side chain modifications intact. This has been shown for phosphorylations and has been demonstrated to be the case also for ADP-ribosylations in ECD (Hengel et al. 2009) and ETD (Zee and Garcia 2009) experiments. Thus, ECD or ETD can be used in different experimental schemes for the simultaneous identification of the ADP-ribosyl group and the peptide to which it is attached. This has also been shown for peptides, which are ADP-ribosylated at lysine side chains by a nonenzymatic reaction (Fedorova et al. 2010).

In CID experiments, potentially ADP-ribosylated peptides can be identified in precursor ion scanning experiments (Osago et al. 2009), in MS/MS experiments (Hengel et al. 2009), or by data-independent acquisition (Laing et al. 2011). The respective peptide sequence can then unambiguously be determined by ECD or ETD.

5.2 Identification of ADP-Ribosylation Sites After Enzymatic or Chemical Cleavage of the ADP-Ribosyl Group

While the removal of the modifying group is mandatory for the analysis of poly (ADP-ribosyl)ated proteins due to the complex structure of the modification, this may also facilitate the detection of mono-ADP-ribosylation sites. Any treatment should reduce the complexity of the modification in order to make it more manageable, while leaving a tag on the modified amino acid side chain to unambiguously identify the site of modification.

It has long been known that poly(ADP-ribose) can be digested by snake venom phosphodiesterase (Matsubara et al. 1970). The pyrophosphate bond between the ADP-ribosyl-phosphate groups is cleaved by the phosphodiesterase, leaving a phosphoribosyl group attached to the amino acid side chain.

Recently the use of this reaction for the identification of auto-ADP-ribosylation sites in PARP1 (ARTD1) has been described and the applicability for both mono- and poly-ADP-ribosylated peptides has been demonstrated (Chapman et al. 2013). Phosphoribosylated peptides exhibit properties comparable to phosphopeptides insofar as they can be enriched by standard phosphoproteomics procedures (e.g., IMAC) and show similar fragmentation characteristics upon CID in mass spectrometric experiments, providing, in contrast to ADP-ribosylated peptides, ample fragment signals for peptide identification.

For the analysis of ADP-ribosylated peptides modified at Asp or Glu side chains, the ADP-ribosyl group can be cleaved by treatment with hydroxylamine (Zhang et al. 2013), leaving a hydroxamic acid derivative at the modified side chain. The mass increment of + 15 Da serves as a tag for ADP-ribosylation. ADP-ribosylated Arg is cleaved only slowly (Moss et al. 1983) and all other ADP-ribosylated amino acid side chains are refractory to hydroxylamine treatment (Cervantes-Laurean et al. 1997).

6 Conclusion

ADP-ribosylated proteins can be identified after in vitro labeling with radioactively labeled or chemically modified ADP-ribosyl derivatives. Endogenously ADP-ribosylated proteins can be identified with anti-ADP-ribosyl antibodies or ADP-ribosyl binding macro domains. Some of these techniques can also be used for enrichment.

After proteolytic cleavage, ADP-ribosylated peptides can be enriched by binding to immobilized metal ion (IMAC) beads or to boronic acid beads.

In tandem mass spectrometric experiments, fragmentation by CID typically results in characteristic fragments of the ADP-ribosyl moiety, while only weak signals of peptide fragments are detected. Thus, CID experiments are useful for the detection of an ADP-ribosyl modification, but often do not allow the identification of the peptide to which it is attached. This problem can be overcome by alternative fragmentation techniques (ECD or ETD). Another option is the phosphodiesterase treatment of the sample, converting ADP-ribosylated peptides into phosphoribosylated peptides (which have properties comparable to phosphopeptides, or, in the case of ADP-ribosylated Asp or Glu side chains, the treatment with hydroxylamine, coverting ADP-ribosyl groups into hydroxamic acid derivatives (which are stable upon CID fragmentation).

References

Armstrong S, Merrill AR (2001) Application of a fluorometric assay for characterization of the catalytic competency of a domain III fragment of Pseudomonas aeruginosa exotoxin A. Anal Biochem 292:26–33

Bannas P, Adriouch S, Kahl S, Braasch F, Haag F, Koch-Nolte F (2005) Activity and specificity of toxin-related mouse T cell ecto-ADP-ribosyltransferase ART2.2 depends on its association with lipid rafts. Blood 105:3663–3670

Bannas P, Graumann O, Balcerak P, Peldschus K, Kaul MG, Hohenberg H, Haag F, Adam G, Ittrich H, Koch-Nolte F (2010) Quantitative magnetic resonance imaging of enzyme activity on the cell surface: in vitro and in vivo monitoring of ADP-ribosyltransferase 2 on T cells. Mol Imaging 9:211–222

Carapito C, Klemm C, Aebersold R, Domon B (2009) Systematic LC-MS analysis of labile post-translational modifications in complex mixtures. J Proteome Res 8:2608–2614

Cervantes-Laurean D, Jacobson EL, Jacobson MK (1997) Preparation of low molecular weight model conjugates for ADP-ribose linkages to protein. Methods Enzymol 280:275–287

Cervantes-Laurean D, Minter DE, Jacobson EL, Jacobson MK (1993) Protein glycation by ADP-ribose: studies of model conjugates. Biochemistry 32:1528–1534

Chambon P, Weill JD, Doly J, Strosser MT, Mandel P (1966) On the formation of a novel adenylic compound by enzymatic extracts of liver nuclei. Biochem Biophys Res Commun 25:638–643

Chambon P, Weill JD, Mandel P (1963) Nicotinamide mononucleotide activation of new DNA-dependent polyadenylic acid synthesizing nuclear enzyme. Biochem Biophys Res Commun 11:39–43

Chapman JD, Gagne JP, Poirier GG, Goodlett DR (2013) Mapping PARP-1 Auto-ADP-ribosylation sites by liquid chromatography-Tandem Mass Spectrometry. J Proteome Res 12 (4):1868–1880

Dani N, Stilla A, Marchegiani A, Tamburro A, Till S, Ladurner AG, Corda D, Di Girolamo M (2009) Combining affinity purification by ADP-ribose-binding macro domains with mass spectrometry to define the mammalian ADP-ribosyl proteome. Proc Natl Acad Sci U S A 106:4243–4248

Davis RE, Mysore V, Browning JC, Hsieh JC, Lu QA, Katsikis PD (1998) In situ staining for poly(ADP-ribose) polymerase activity using an NAD analogue. J Histochem Cytochem 46:1279–1289

Eide B, Gierschik P, Spiegel A (1986) Immunochemical detection of guanine nucleotide binding proteins mono-ADP-ribosylated by bacterial toxins. Biochemistry 25:6711–6715

Fedorova M, Frolov A, Hoffmann R (2010) Fragmentation behavior of Amadori-peptides obtained by non-enzymatic glycosylation of lysine residues with ADP-ribose in tandem mass spectrometry. J Mass Spectrom 45:664–669

Feijs KL, Verheugd P, Luscher B (2013) Expanding functions of intracellular resident mono-ADP-ribosylation in cell physiology. FEBS J 280:3519–3529

Fujimura S, Hasegawa S, Shimizu Y, Sugimura T (1967) Polymerization of the adenosine 5'-diphosphate-ribose moiety of nicotinamide-adenine dinucleotide by nuclear enzyme. I. Enzymatic reactions. Biochim Biophys Acta 145:247–259

Ganesan AK, Frank DW, Misra RP, Schmidt G, Barbieri JT (1998) Pseudomonas aeruginosa exoenzyme S ADP-ribosylates Ras at multiple sites. J Biol Chem 273:7332–7337

Giovane A, Balestrieri C, Quagliuolo L, Servillo L (1985) 1-N6-Etheno-ADP-ribosylation of elongation factor-2 by diphtheria toxin. FEBS Lett 191:191–194

Grahnert A, Friedrich M, Pfister M, Haag F, Koch-Nolte F, Hauschildt S (2002) Mono-ADP-ribosyltransferases in human monocytes: regulation by lipopolysaccharide. Biochem J 362:717–723

He Z, Yang C, Guo G, Li N, Yu W (2011) Motif-All: discovering all phosphorylation motifs. BMC Bioinform 12(Suppl 1):S22

Hengel SM, Goodlett DR (2012) A review of tandem mass spectrometry characterization of adenosine diphosphate-ribosylated peptides. Int J Mass Spectrom 312:114–121

Hengel SM, Icenogle L, Collins C, Goodlett DR (2010) Sequence assignment of ADP-ribosylated peptides is facilitated as peptide length increases. Rapid Commun Mass Spectrom 24:2312–2316

Hengel SM, Shaffer SA, Nunn BL, Goodlett DR (2009) Tandem mass spectrometry investigation of ADP-ribosylated kemptide. J Am Soc Mass Spectrom 20:477–483

Hingorani VN, Ho YK (1988) Fluorescent labeling of signal-transducing G-proteins. Pertussis toxin-catalyzed etheno-ADP ribosylation of transducin. J Biol Chem 263:19804–19808

Honjo T, Nishizuka Y, Hayaishi O (1968) Diphtheria toxin-dependent adenosine diphosphate ribosylation of aminoacyl transferase II and inhibition of protein synthesis. J Biol Chem 243:3553–3555

Hottiger MO, Hassa PO, Luscher B, Schuler H, Koch-Nolte F (2010) Toward a unified nomenclature for mammalian ADP-ribosyltransferases. Trends Biochem Sci 35:208–219

Karras GI, Kustatscher G, Buhecha HR, Allen MD, Pugieux C, Sait F, Bycroft M, Ladurner AG (2005) The macro domain is an ADP-ribose binding module. EMBO J 24:1911–1920

Klebl BM, Gopel SO, Pette D (1997) Specificity and target proteins of arginine-specific mono-ADP-ribosylation in T-tubules of rabbit skeletal muscle. Arch Biochem Biophys 347:155–162
Klebl BM, Pette D (1996) A fluorometric assay for measurement of mono-ADP-ribosyltransferase activity. Anal Biochem 239:145–152
Krebs C, Koestner W, Nissen M, Welge V, Parusel I, Malavasi F, Leiter EH, Santella RM, Haag F, Koch-Nolte F (2003) Flow cytometric and immunoblot assays for cell surface ADP-ribosylation using a monoclonal antibody specific for ethenoadenosine. Anal Biochem 314:108–115
Laing S, Koch-Nolte F, Haag F, Buck F (2011) Strategies for the identification of arginine ADP-ribosylation sites. J Proteomics 75:169–176
Laing S, Unger M, Koch-Nolte F, Haag F (2010) ADP-ribosylation of arginine. Amino Acids 41:257–269
Liao SD, Puro DG (2006) NAD+-induced vasotoxicity in the pericyte-containing microvasculature of the rat retina: effect of diabetes. Invest Ophthalmol Vis Sci 47:5032–5038
Lischke T, Schumacher V, Wesolowski J, Hurwitz R, Haag F, Koch-Nolte F, Mittrucker HW (2013) CD8-beta ADP-ribosylation affects CD8(+) T-cell function. Eur J Immunol 43:1828–1838
Liu XC, Scouten WH (2000) Boronate affinity chromatography. Methods Mol Biol 147:119–128
Liu XC, Scouten WH (2005) Boronate affinity chromatography. In: Hage DS (ed) Handbook of affinity chromatography. CRC Press, Boca Raton, pp 215–229
Lowery RG, Ludden PW (1988) Purification and properties of dinitrogenase reductase ADP-ribosyltransferase from the photosynthetic bacterium Rhodospirillum rubrum. J Biol Chem 263:16714–16719
Macek B, Mann M, Olsen JV (2009) Global and site-specific quantitative phosphoproteomics: principles and applications. Annu Rev Pharmacol Toxicol 49:199–221
Margarit SM, Davidson W, Frego L, Stebbins CE (2006) A steric antagonism of actin polymerization by a salmonella virulence protein. Structure 14:1219–1229
Matic I, Ahel I, Hay RT (2012) Reanalysis of phosphoproteomics data uncovers ADP-ribosylation sites. Nat Methods 9:771–772
Matsubara H, Hasegawa S, Fujimura S, Shima T, Sugimura T (1970) Studies on poly (adenosine diphosphate ribose). V. Mechanism of hydrolysis of poly (adenosine diphosphate ribose) by snake venom phosphodiesterase. J Biol Chem 245:3606–3611
McDonald LJ, Moss J (1993) Stimulation by nitric oxide of an NAD linkage to glyceraldehyde-3-phosphate dehydrogenase. Proc Natl Acad Sci U S A 90:6238–6241
McDonald LJ, Moss J (1994) Enzymatic and nonenzymatic ADP-ribosylation of cysteine. Mol Cell Biochem 138:221–226
McDonald LJ, Wainschel LA, Oppenheimer NJ, Moss J (1992) Amino acid-specific ADP-ribosylation: structural characterization and chemical differentiation of ADP-ribose-cysteine adducts formed nonenzymatically and in a pertussis toxin-catalyzed reaction. Biochemistry 31:11881–11887
Mellacheruvu D, Wright Z, Couzens AL, Lambert JP, St-Denis NA, Li T, Miteva YV, Hauri S, Sardiu ME, Low TY, Halim VA, Bagshaw RD, Hubner NC, Al-Hakim A, Bouchard A, Faubert D, Fermin D, Dunham WH, Goudreault M, Lin ZY, Badillo BG, Pawson T, Durocher D, Coulombe B, Aebersold R, Superti-Furga G, Colinge J, Heck AJ, Choi H, Gstaiger M, Mohammed S, Cristea IM, Bennett KL, Washburn MP, Raught B, Ewing RM, Gingras AC, Nesvizhskii AI (2013) The CRAPome: a contaminant repository for affinity purification-mass spectrometry data. Nat Methods 10:730–736
Meyer T, Hilz H (1986) Production of anti-(ADP-ribose) antibodies with the aid of a dinucleotide-pyrophosphatase-resistant hapten and their application for the detection of mono(ADP-ribosyl) ated polypeptides. Eur J Biochem 155:157–165
Meyer T, Koch R, Fanick W, Hilz H (1988) ADP-ribosyl proteins formed by pertussis toxin are specifically cleaved by mercury ions. Biol Chem Hoppe Seyler 369:579–583
Moss J, Yost DA, Stanley SJ (1983) Amino acid-specific ADP-ribosylation. J Biol Chem 258:6466–6470

Nishizuka Y, Ueda K, Nakazawa K, Hayaishi O (1967) Studies on the polymer of adenosine diphosphate ribose. I. Enzymic formation from nicotinamide adenine dinuclotide in mammalian nuclei. J Biol Chem 242:3164–3171

Okayama H, Ueda K, Hayaishi O (1978) Purification of ADP-ribosylated nuclear proteins by covalent chromatography on dihydroxyboryl polyacrylamide beads and their characterization. Proc Natl Acad Sci U S A 75:1111–1115

Osago H, Terashima M, Hara N, Yamada K, Tsuchiya M (2008) A new detection method for arginine-specific ADP-ribosylation of protein – a combinational use of anti-ADP-ribosylarginine antibody and ADP-ribosylarginine hydrolase. J Biochem Biophys Methods 70:1014–1019

Osago H, Yamada K, Shibata T, Yoshino K, Hara N, Tsuchiya M (2009) Precursor ion scanning and sequencing of arginine-ADP-ribosylated peptide by mass spectrometry. Anal Biochem 393:248–254

Paone G, Stevens LA, Levine RL, Bourgeois C, Steagall WK, Gochuico BR, Moss J (2006) ADP-ribosyltransferase-specific modification of human neutrophil peptide-1. J Biol Chem 281:17054–17060

Rosenqvist H, Ye J, Jensen ON (2011) Analytical strategies in mass spectrometry-based phosphoproteomics. Methods Mol Biol 753:183–213

Rosenthal F, Messner S, Roschitzki B, Gehrig P, Nanni P, Hottiger MO (2011) Identification of distinct amino acids as ADP-ribose acceptor sites by mass spectrometry. Methods Mol Biol 780:57–66

Scheuplein F, Schwarz N, Adriouch S, Krebs C, Bannas P, Rissiek B, Seman M, Haag F, Koch-Nolte F (2009) NAD+ and ATP released from injured cells induce P2X7-dependent shedding of CD62L and externalization of phosphatidylserine by murine T cells. J Immunol 182:2898–2908

Schwab CJ, Colville MJ, Fullerton AT, McMahon KK (2000) Evidence of endogenous mono-ADP-ribosylation of cardiac proteins via anti-ADP-ribosylarginine immunoreactivity. Proc Soc Exp Biol Med 223:389–396

Seman M, Adriouch S, Haag F, Koch-Nolte F (2004) Ecto-ADP-ribosyltransferases (ARTs): emerging actors in cell communication and signaling. Curr Med Chem 11:857–872

Seman M, Adriouch S, Scheuplein F, Krebs C, Freese D, Glowacki G, Deterre P, Haag F, Koch-Nolte F (2003) NAD-induced T cell death: ADP-ribosylation of cell surface proteins by ART2 activates the cytolytic P2X7 purinoceptor. Immunity 19:571–582

Takei Y, Takahashi K, Kanaho Y, Katada T (1994) Pertussis toxin-catalyzed ADP-ribosylation of GTP-binding proteins with digoxigenin-conjugated NAD. Identification of the proteins in plasma membranes and nuclei. FEBS Lett 338:264–266

Ubersax JA, Ferrell JE Jr (2007) Mechanisms of specificity in protein phosphorylation. Nat Rev Mol Cell Biol 8:530–541

Young TL, Santella RM (1988) Development of techniques to monitor for exposure to vinyl chloride: monoclonal antibodies to ethenoadenosine and ethenocytidine. Carcinogenesis 9:589–592

Zee BM, Garcia BA (2009) Electron transfer dissociation facilitates sequencing of adenosine diphosphate-ribosylated peptides. Anal Chem 82:28–31

Zhang J (1997) Use of biotinylated NAD to label and purify ADP-ribosylated proteins. Methods Enzymol 280:255–265

Zhang J, Snyder SH (1993) Purification of a nitric oxide-stimulated ADP-ribosylated protein using biotinylated beta-nicotinamide adenine dinucleotide. Biochemistry 32:2228–2233

Zhang Y, Wang J, Ding M, Yu Y (2013) Site-specific characterization of the Asp- and Glu-ADP-ribosylated proteome. Nat Methods 10:981–984

Part II
ADP-Ribosylation by ARTCs (R-S-E ARTs)

Photorhabdus luminescens Toxins TccC3 and TccC5: Insecticidal ADP-Ribosyltransferases that Modify Threonine and Glutamine

Klaus Aktories, Gudula Schmidt and Alexander E. Lang

Abstract The ADP-ribosyltransferases TccC3 and TccC5 are the biologically active TcC components of the tripartite *Photorhabdus luminescens* Tc toxin, which consist of TcA, TcB, and TcC components. TcA is the binding and membrane translocation component. TcB is a functional linker between TcC and TcA and also involved in the translocation of the toxin. While TccC3 ADP-ribosylates actin at threonine 148, TccC5 modifies Rho proteins at glutamine 61/63. Both modifications result in major alteration of the actin cytoskeleton. Here we discuss structure and function of the Tc toxin and compare its ADP-ribosyltransferase activities with other types of actin and Rho modifying toxins.

Contents

K. Aktories (✉) · G. Schmidt · A. E. Lang
Institut für Experimentelle und Klinische Pharmakologie und Toxikologie, Albert-Ludwigs-Universität Freiburg, Albertstr. 25, 79104 Freiburg, Germany
e-mail: klaus.aktories@pharmakol.uni-freiburg.de

Current Topics in Microbiology and Immunology (2015) 384: 53–67
DOI: 10.1007/82_2014_382

Published Online: 8 June 2014

1 Introduction

Mono-ADP-ribosylation is a frequently used molecular mechanism by which bacterial toxins affect eukaryotic target proteins. The list of these bacterial toxins increased during recent years (Pallen et al. 2001; de Souza and Aravind 2012). The first toxin identified to utilize this type of modification was diphtheria toxin, which ADP-ribosylates eukaryotic elongation factor 2 (EF-2) (Honjo et al. 1968; Gill et al. 1969). Diphtheria toxin ADP-ribosylates elongation factor 2 at a post-translationally modified histidine residue called diphthamide. Its modification by ADP-ribosylation results in inhibition of protein synthesis. *Pseudomonas* exotoxin A and *Vibrio cholerae* toxin cholix exhibit an identical mechanism of action. Both toxins target the same diphthamide residue of EF-2 and like diphtheria toxin cause inhibition of protein synthesis (Iglewski and Kabat 1975; Collier 1968; Jorgensen et al. 2008). Heterotrimeric G proteins are the targets of cholera toxin and pertussis toxin, which activate or inactivate G proteins. Cholera toxin and the related *Escherichia coli* heat-labile enterotoxin ADP-ribosylate the α-subunit of Gs proteins at a crucial arginine residue, thereby inhibiting the switch-off mechanism of Gs (Cassel and Pfeuffer 1978; Moss and Vaughan 1977; Gill and Richardson 1980). On the other hand, pertussis toxin ADP-ribosylates a cysteine residue of the α-subunit of Gi/o proteins (West et al. 1985; Ui 1984). This inhibits the interaction of the G protein with G-protein-coupled receptors and prevents G protein activation.

Also, small GTPases are targets of ADP-ribosylating toxins. *Clostridium botulinum* C3 exoenzyme (C3bot) ADP-ribosylates asparagine 41 of RhoA, B, and C (Aktories et al. 1987; Sekine et al. 1989). This modification blocks Rho signaling by inhibition of Rho activation and stabilization of the Rho/GDI complex (Sehr et al. 1998; Barth et al. 1999; Genth et al. 2003). Similar targets and effects were shown for C3-related bacterial toxin isoforms, such as *Clostridium limosum* C3lim (Just et al. 1992), *Bacillus cereus* C3cer (Just et al. 1995) and various *Staphylococcus aureus* C3stau isoforms (Wilde et al. 2002) also known as EDINs (Sugai et al. 1990). Small GTPases are also targeted by *Pseudomonas* effector ExoS, which modifies arginine residues of Ras, Rac, and various Rab proteins (Fraylick et al. 2002). In addition, ezrin, radixin, and moesin are targeted by this bacterial ADP-ribosyltransferase (Maresso et al. 2004). The related *Pseudomonas* effector ExoT ADP-ribosylates the kinase regulators CrKI and II at arginine (Sun and Barbieri 2003).

A large group of bacterial ADP-ribosylating toxins targets actin at arginine 177, thereby inhibiting actin polymerization. Among these are the binary toxins from *C. botulinum* (C2 toxin) (Aktories et al. 1986), *Clostridium perfringens* (iota toxin) (Schering et al. 1988), *Clostridium spiroforme* (CST) (Simpson et al. 1989), *Clostridium difficile* (CDT) (Gülke et al. 2001; Perelle et al. 1997), and *B. cereus* vegetative insecticidal protein (VIP) (Han et al. 1999). While the binary toxins consist of a binding and translocation component, which is physically separated from the biologically active enzyme component, various bacterial effectors have been described, which share a similar ADP-ribosyltransferase domain and modify also arginine 177 (Pallen et al. 2001). Among these effectors, which are translocated into

Table 1 Bacterial actin-ADP-ribosyltransferases

Toxin	Bacterium	Components	Substrate specificity	Acceptor amino acid
C2 toxin	*Clostridium botulinum*	C2I (enzyme) C2II (binding)	β/γ-actin	Arg-177
Iota toxin	*Clostridium perfringens*	Ia (enzyme) Ib (binding)	α- and β/γ-actin	Arg-177
CST	*Clostridium spiroforme*	Sa (enzyme) Sb (binding)	α- and β/γ-actin	Arg-177
CDT	*Clostridium difficile*	CDTa (enzyme) CDTb (binding)	α- and β/γ-actin	Arg-177
VIP	*Bacillus cereus*	VIP2 (enzyme) VIP1 (binding)	α- and β/γ-actin	Arg-177
SpvB	*Salmonella enterica*	SpvB (enzyme)	α- and β/γ-actin	Arg-177
Photox	*Photorhabdus luminescens*	Photox (enzyme)	α- and β/γ-actin	Arg-177
AexT	*Aeromonas salmonicida*	AexT (enzyme)	α- and β/γ-actin	Arg-177
PTC3	*Photorhabdus luminescens*	TccC3 (enzyme) TcdB2 (linker) TcdA1 (binding)	α- and β/γ-actin	Thr-148

target cells by type-III or type-VI secretion, are *Salmonella enterica* effector SpvB (Otto et al. 1995), *Aeromonas salmonicida* effector AexT (Braun et al. 2002), and *Photorhabdus luminescens* toxin Photox (Visschedyk et al. 2010), respectively (Table 1).

Highly effective new methods of genome analyses allowed identification of numerous additional bacterial ADP-ribosyltransferases, which are probably protein toxins and important for host-pathogen interactions (Pallen et al. 2001; Fieldhouse and Merrill 2008), but are not fully characterized so far. Recently, two novel bacterial ADP-ribosyltransferases, TccC3, and TccC5, have been described, which are produced by insecticidal *P. luminescens* bacteria (Lang et al. 2010). These enzymes are the biologically active parts of large toxin complexes (Waterfield et al. 2001; ffrench-Constant and Waterfield 2006). Although elucidation of the structure and functions of these ADP-ribosylating toxins has just started, it is already clear that the mode of action of these toxins allow exciting new insights into the molecular mechanisms by which bacterial toxins targets their hosts. In the following part, we will review structure and function of these remarkable ADP-ribosylating toxins.

2 Toxins Are Essential for the Life Cycle of *Photorhabdus luminescens*

Photorhabdus luminescens are entomopathogenic bacteria, which need toxins to kill insects. They produce a large array of different toxins. Toxin production by *Photorhabdus* has to be adapted to the complicated life cycle of the gram-negative

enterobacterium and their tight symbiosis with nematodes. *P. luminescens* lives in the gut of nematodes of the family *Heterorhabditidae*. After invasion of insect larvae by the nematodes, *Photorhabdus* bacteria are released from the worms by regurgitation (Forst et al. 1997; Waterfield et al. 2009; Ciche 2007; Ciche et al. 2008). In the larvae, the bacteria start to produce a large number of different virulence factors, including various toxins, proteases, lipases, hemolysins, and antibiotics.

One of the most potent agents produced by the bacteria are Tc (toxin complex) toxins, which occur in several homologs and isoforms. Eventually, production of toxins cause death of insects within few days, thereby a source of nourishment is produced, which allows establishment of an optimal environment for growth, proliferation, and multiplication of nematodes and bacteria. When the insect cadaver is exhausted of nutrients, the nematodes take up *Photorhabdus* bacteria and leave the depleted larvae to invade a new insect prey (Waterfield et al. 2009; ffrench-Constant et al. 2003).

2.1 Structure of Tc Toxins

The *Photorhabdus* toxin complexes (Tc) are essential for insecticidal activity and productive symbiosis with nematodes. The toxin complex is very large (>1.7 MDa) (Sheets et al. 2011) and consists of the three components TcA, TcB, and TcC (ffrench-Constant and Bowen 2000; ffrench-Constant and Waterfield 2006; Waterfield et al. 2001) (Fig. 1). TcA (∼285 kDa) is the cell-binding component and TcC (∼112 kDa), the biologically active component. TcB (∼170 kDa) acts as a linker between TcA and TcC (see below). Recent cryo-electron microscopy and crystal structure analyses revealed major insights into organization of the toxin and the translocation of the enzyme component into the cytosol (Gatsogiannis et al. 2013; Busby et al. 2013; Landsberg et al. 2011).

Initial cryo-electron microscopic studies revealed the structure of the binding and translocation domain TcA (isoform TcdA1) at a resolution of 6.3 Å and already suggested a novel syringe-like injection mechanism for Tc toxins (Gatsogiannis et al. 2013). According to these data, TcdA1 forms a pentameric prepore structure, consisting of a central channel, shaped like a flared funnel, with an outer shell compartment resulting in a bell-like structure of the TcA component (Fig. 2). The central channel structure is formed by very long helices. Studies at different pH and with liposomes revealed a conformational change of the TcA component with movement of the outer shell to the upper side of TcA and formation of a transmembrane channel part and channel opening (Fig. 2). Similar data were obtained by cryo-electron microscopic studies with the related *Yersinia entomophaga* toxin complex (Landsberg et al. 2011). More recent studies from the *Y. entomophaga* toxin show that TcB and the conserved N-terminal part of TcC form a huge β-barrel-shaped cage. The connection of TcB to the TcA pentamer is via a six-bladed β-propeller structure. The top of the barrel cage is closed by a highly

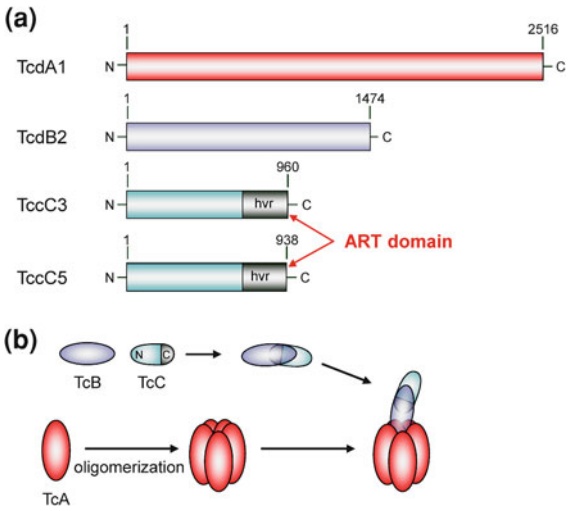

Fig. 1 Tc proteins and model of the *Photorhabdus* toxin complex. **a** Tc proteins located on the Tcd locus (Waterfield et al. 2001). A toxin complex consists of the TcA cell binding and translocation component TcdA1, the TcB linker component TcdB2 and one of the TcC components TccC3 or TccC5. The N-terminal regions of these TcC components are very similar but the C-terminal parts designated hypervariable region (hvr) differ between the toxins and harbor the ADP-ribosyltransferase (ART) domain. **b** Model of the interaction of TcA with TcB and TcC. TcB and TcC form a 1:1 complex that binds to the pentameric TcA

conserved RHS (Rearrangement HotSpots)-repeat associated domain. Here is an aspartate protease domain located, which probably cleaves the C-terminal ADP-ribosyltransferase domain of TcC components and releases it into the β-barrel-shaped cage ready for microinjection into host cells by means of the TcA pentamer syringe (Busby et al. 2013).

2.2 Cellular Factors Involved in TcC Translocation

Intracellular factors are involved in cellular uptake of the ADP-ribosyltransferase domain of Tc toxins. By using pharmacological inhibitors, heat shock protein 90 (Hsp90) and peptidyl prolyl cis/trans isomerases (PPIases) have been identified to be involved in the uptake of the ADP-ribosylating toxins TccC3 and TccC5 into the host cell cytosol (Lang et al. 2013). Inhibition of Hsp90 by radicicol or by the geldanamycin derivative 17-DMAG decreases intoxication of target cells by *Photorhabdus* toxin complexes. Similarly, cyclosporin A and FK506 (Tacrolimus), which inhibit the PPIases cyclophilin and FK506-binding protein (FKBPs), respectively, reduce cell intoxication by TccC3 and TccC5. This effect is suggested to be due to a role of HSP90 and PPIases in translocation of the toxins into target cells. The inhibiting compounds do not affect the ADP-ribosyltransferase

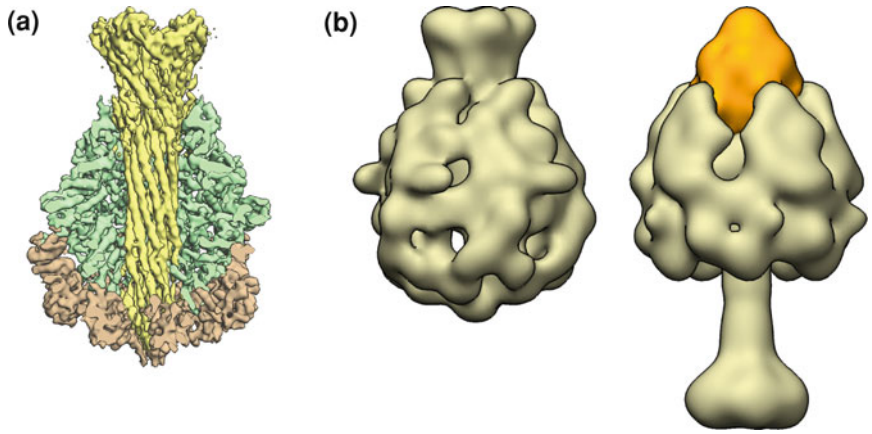

Fig. 2 Structure of TcdA1 and the holotoxin PTC3. **a** Cryo-electron microscopy structure of the TcdA1 prepore (6.3 Å) at pH 5. The outer shell is depicted in *green* and *brown* and the inner channel in *yellow*. **b** Model of the three-dimensional structures derived from electron microscopy pictures of negatively stained TcdA1 and the holotoxin PTC3 (complex of TcdA1, TcdB2, and TccC3). TcdA1 and TcdB2–TccC3 (TcB and TcC components were covalently linked to allow expression in *E. coli*) are shown in *khaki* and *orange*, respectively (Gatsogiannis et al. 2013). The *left picture* gives the prepore conformation of the binding and translocation component TcdA1 with the docking side for TcdB2–TccC3 on the *top*. After binding of TcdB2–TccC3 and under the influence of a pH change, a conformational change occurs with formation of a stem-like structure at the bottom of the molecule (*right*). This part is suggested to cross the membrane of vesicles of target cells to release the ADP-ribosyltransferase domain into the cytosol. Figures are from (Gatsogiannis et al. 2013)

activity in vitro and have no effect on binding to target cells or in pore formation. Because Hsp90-inhibitors and PPIases-inhibitors exhibits similar effects on other toxin ADP-ribosyltransferases (e.g., binary actin-ADP-ribosylating toxins), it is suggested that this is a group effect and is relevant for the toxin uptake of all ADP-ribosyltransferases but not of others types of intracellularly acting toxins such as Rho-glucosylating *C. difficile* toxins A and B (Lang et al. 2013).

3 Biological Activities of Tc Components

As mentioned above, several isoforms of Tc toxins exist. This is especially true for the TcC components. Already from the primary sequence, it is obvious that TcC components consist of an N-terminal core-domain, which is highly conserved between the isoforms and a C-terminal hypervariable region (hvr-region). From the various TcC components identified, the biological activities of TccC3 and TccC5 were studied in more detail, recently.

When hemocytes isolated from the hemolymph of larvae of the greater wax moth (*Galleria mellonella*) are treated with TcA (isoform TcdA1), TcB (isoform TcdB2), and TccC3 or TccC5, the ability of the cells to phagocyte *E. coli* particles

is blocked (Lang et al. 2010). This effect is most prominent when both enzyme components are combined (TccC3 and TccC5). By contrast, the single components TcdA1, TcdB2, or TccC3/TccC5 exhibit no inhibiting effects, indicating that the toxin activities depend on the tripartite toxin complex. Inhibition of phagocytosis of hemocytes by Tc is the result of its action on the actin cytoskeleton. This is obvious from the effects of the toxin complexes on the morphology of the actin cytoskeleton. The combination of TcdA1, TcdB2, and TccC3 induces redistribution of the actin cytoskeleton labeled with FITC-phalloidin. Actin aggregates are observed and the submembranous cortical actin is diminished. TcdA1, TcdB2, and TccC5 cause a completely different effect on the actin cytoskeleton of hemocytes. This toxin combination results in strong formation of stress fibers. When both active components (TccC3 and TccC5) are combined with TcdA1, TcdB2, the effect on the actin cytoskeleton is even more drastic and results in total loss of normal actin structures and in formation of actin clusters (Lang et al. 2010).

4 TccC3 ADP-Ribosylates Actin

What is the reason for the Tc effects on the actin cytoskeleton? Initial studies showed that the variable domain of TccC3 exhibits distant sequence similarities with toxin ADP-ribosyltransferases (Fig. 3). Especially, the three amino acids, designated as RSE group are found in TccC3 with R probably involved in NAD^+ binding, S as a part of a ST or STS motif also involved in NAD^+ binding and E as the so-called catalytic glutamate, which is conserved in all bacterial ADP-ribosyltransferases (Otto et al. 2005; Fieldhouse and Merrill 2008; Hottiger et al. 2010). In fact, in the presence of [^{32}P]NAD^+ the toxin component TccC3 labels an $\sim$45 kDa protein in lysates of HeLa cells and insect Sf9 cells. Mass spectrometric analysis revealed that the substrate of TccC3 is actin, which is modified at threonine-148 (Lang et al. 2010).

Skeletal muscle α-actin as well as $\beta\gamma$-non-muscle actin is modified. Moreover, modification occurs with nonpolymerized and with polymerized actin. These findings are remarkable for at least two reasons: Firstly, threonine as the acceptor site for ADP-ribosylation is not shared by any other ADP-ribosyltransferase. All other bacterial protein toxins modify actin at arginine 177 (Vandekerckhove et al. 1987, 1988). Secondly, while TccC3 modifies polymerized actin, all other bacterial transferases ADP-ribosylate monomeric G-actin only (Schering et al. 1988; Aktories et al. 1986). Accordingly, the functional consequences of modification of actin catalyzed by TccC3 are completely different from those resulting from modification of arginine 177. Toxin-induced modification of actin at arginine 177 inhibits actin polymerization because the ADP-ribose attached to actin blocks polymerization by steric hindrance (Holmes et al. 1990; Perieteanu et al. 2010; Aktories et al. 2011). Modification of actin at arginine 177 is incompatible with the double-helix structure of F-actin. The only position where actin-ADP-ribosylated at arginine 177 can interact with F-actin is the barbed end of actin filaments. There, ADP-ribosylated acts like a capping protein to block polymerization even of

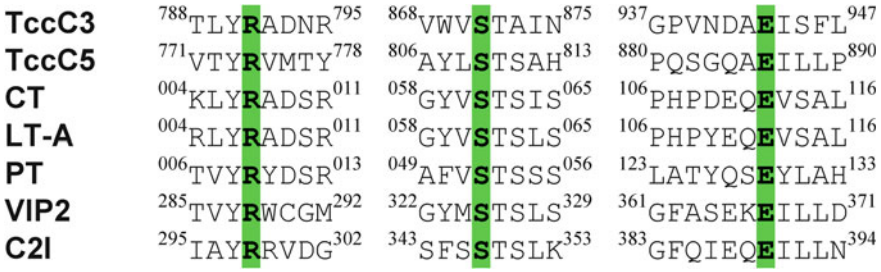

Fig. 3 Sequence alignment of bacterial ADP-ribosyltransferases. Highly-conserved residues of different bacterial actin-ARTCs are shown and *numbers* indicate position of amino acid residues. Sequences of following enzymes are shown: *Photorhabdus luminescens* TccC3 (Acc. No. Q8GF97), *Photorhabdus luminescens* TccC5 (Acc. No. Q8GF91), cholera toxin (CT; Acc. No. D30052), *E. coli* heat-labile enterotoxin A chain (LT-A; Acc. No. P06717), pertussis toxin (PT; Acc. No. P04977), *Bacillus cereus* insecticidal toxin (VIP2; Acc. No. 1QS2) and *Clostridium botulinum* C2I toxin (Acc. No. D4N871). *Note* Numbering of CT, LT-A, and PT is without signal sequences. Residues forming the RSE-motif of ADP-ribosyltransferases are highlighted: the arginine residue (R) probably involved in NAD^+ binding, the first serine residue (S) from the ST or STS motif also involved in NAD^+ binding and the so-called catalytic glutamate (E)

unmodified G-actin (Wegner and Aktories 1988; Weigt et al. 1989; Aktories and Wegner 1989). By contrast, TccC3 ADP-ribosylates actin at threonine 148 (Lang et al. 2010). ADP-ribosylation of actin at this position was verified by site directed mutagenesis. To this end, in vitro transcription/translation of mutagenized actin was employed, showing that change of threonine 148 to alanine prevented modification by TccC3. Threonine 148 is located in a region of actin, which is responsible for the interaction of actin with thymosin-β4 (Mannherz and Hannappel 2009; Safer 1992). Accordingly, cross-linking of actin with thymosin-β4 is blocked after ADP-ribosylation of actin at this site (Lang et al. 2010). The functional consequences are remarkable. Normally, binding of thymosin-β4 to actin causes sequestration of monomeric G-actin and prevents actin polymerization (Mannherz and Hannappel 2009). After TccC3-induced ADP-ribosylation at threonine 148, however, thymosin-β4 is no longer able to block actin polymerization. Thus, ADP-ribosylation of actin at threonine 148 and arginine 177 causes opposite effects with induction of polymerization in the first case and inhibition of polymerization in the latter case.

4.1 Comparison of Iota Toxin with TccC3

Recently, the enzyme component of iota toxin (Ia), which modifies actin at arginine 177, was crystallized in complex with actin by Tsurumura and coworkers (Tsurumura et al. 2013). Moreover, several crystallized snapshots of the interaction of the ADP-ribosylation of actin by Ia were obtained showing the toxin in complex with actin and NAD^+, and, excitingly, also in a complex with ADP-ribosylated

actin. These data revealed a "strain alleviation model" of ADP-ribosylation, which was previously proposed by the group. All arginine-modifying ADP-ribosylating toxins are characterized by an EXE motif (e.g., 378Glu-X-Glu380 in Ia or 365Glu-X-Glu367 in VIP2; see also Fig. 3). This motif is the core of the ADP ribosylation turn–turn (ARTT) loop found in this family of actin-modifying enzymes and has an essential role in catalysis and protein substrate recognition (Han and Tainer 2002). While the second Glu (e.g., Glu380 of Ia) is essential for ADP-ribosylation and NADase activity, the first Glu (e.g., Glu378 of Ia) is needed for the ADP-ribosyltransferase reaction but not for NAD^+ hydrolysis (Barth et al. 1998). By exchanging Glu380 to serine, hydrolysis of NAD^+ was blocked and an iota toxin–actin complex with NAD^+ bound could be crystallized (Tsurumura et al. 2013). The data show that the ADP-ribose moiety of NAD^+ is in a tight grip of Ia, while the nicotinamide mononucleotide (NMN) ribose interacts with the EXE motif resulting in a distorted and strained structure of the NMN portion of NAD^+. For ADP-ribosylation of arginine 177 of actin, NAD^+ has to rotate around its pyrophosphate axes resulting in "strain alleviation" and covalent modification of actin.

The precise action of the ADP-ribosylation of actin by TccC3 is not known. The different site of modification of actin by TccC3 (ADP-ribosylation of threonine 148) suggests that the mechanism of ADP-ribosylation differs. Moreover, the ARTT loop of TccC3 differs from that of iota toxin or other binary actin-ADP-ribosylating toxins. The EXE motif of Ia is an DXE motif in TccC3. Again, this is a remarkable change, because other known ADP-ribosylating toxins of the R-S-E family which do not have the E-X-E motif, possess a Q-X-E motif and modify amino acids other than arginine, e.g., cysteine (PT) or asparagine (C3). Therefore, additional structural data of TccC3 are highly desired.

5 TccC5 ADP-Ribosylates Rho Proteins

As mentioned above, the treatment of *G. mellonella* hemocytes or HeLa cells with the combination of TccC5, the binding component TcdA1 and the linker TcdB2 results in strong formation of stress fibers. Induction of stress fiber formation is a typical feature of RhoA activation (Ridley and Hall 1992, 1994; Nobes and Hall 1995; Lim et al. 1996). Therefore, the hypothesis that TccC5 interacts with Rho to induce stress fiber formation was a straight forward hypothesis. Because TccC5 exhibits some sequence similarities with ADP-ribosyltransferases and shares with these enzymes, the RSE amino acid motif discussed above, it was logical to test TccC5 for ADP-ribosyltransferase activity. When lysates from HeLa cells or *G. mellonella* hemocytes were incubated with [^{32}P]NAD^+ and TccC5 labeling of 20–25 kDa proteins were identified. Later, it was shown that TccC5 modifies RhoA, Rac, and Cdc42 by ADP-ribosylation (Lang et al. 2010).

Rho proteins comprise a family of small GTP-binding proteins with about 20 family members (Hall 1993; Takai et al. 1993; Nobes and Hall 1994; Heasman and Ridley 2008; Burridge and Wennerberg 2004). Best studied are Rho, Rac, and

Cdc42 isoforms. They are involved in regulation of the actin cytoskeleton. Classical studies showed that RhoA is involved in stress fiber formation, whereas Rac organizes membrane ruffling and lamellipodia formation and Cdc42 participate in filopodia formation (Hall 1994, 1998). However, they are characterized by a multitude of essential cellular functions, which are largely conserved within the whole animal kingdom, including nematodes insects and mammals (Jaffe and Hall 2005). Rho proteins are regulated by GTPase cycle. They are inactive in the GDP-bound form. Nucleotide exchange of GDP to GTP by guanine nucleotide exchange factors (GEFs) turn Rho proteins into their active form and allow interaction with numerous cellular effectors to regulate the cytoskeleton, motility functions, cellular traffic, but also transcription or proliferation (Jaffe and Hall 2005). The active state of Rho proteins is terminated by GTP hydrolysis, caused by endogenous GTPase activity and facilitated by GTPase activating proteins (GAPs).

Interestingly, TccC5 ADP-ribosylates glutamine 63 of RhoA and glutamine 61 of Rac and Cdc42 (Lang et al. 2010). These glutamine residues are essential for the function of Rho proteins. They play a pivotal role in the turn-off mechanism of GTPase cycle of Rho proteins (Vetter and Wittinghofer 2001). The glutamines are crucial for the proper positioning of GTP within the GTPase catalytic side of Rho proteins and allow the nucleophilic attack of water to eventually hydrolyze GTP. Modification of this residue blocks endogenous and GAP-stimulated GTP hydrolysis (Lang et al. 2010). Therefore, after TccC5-induced ADP-ribosylation Rho proteins are persistently activated. This was verified by studying the interaction of RhoA with its effector rhotekin. For this type of experiments, the Rho-binding domains of rhotekin or mDIA are employed (Lang et al. 2010). TccC5-induced ADP-ribosylation of RhoA enhances its interaction with the effector rhotekin, indicating the activation of the GTPase. Increase in RhoA-rhotekin interaction is observed in vitro with isolated proteins as well as after treatment of intact cells with the toxin. Similar to RhoA, Rac, and Cdc42 are activated by TccC5. In these cases, glutamine 61 is ADP-ribosylated, the GTP hydrolysis is blocked and thereby the interaction of Rac or Cdc42 with effectors (e.g., PAK-kinase) is enhanced. As mentioned above, TccC5 causes stress fiber formation in intact cells. This effect is typical for activation of RhoA (Ridley and Hall 1992), whereas cellular consequences of the activation of Rac and Cdc42 are membrane ruffling, lamellipodia and filopodia formation, respectively (Ridley et al. 1992). Why TccC5 induces a dominant effect on stress fiber formation without major effects on lamellipodia or filopodia formation is not clear.

Activation of Rho proteins is also caused by *E. coli* cytotoxic necrotizing factors 1, 2, and 3 (CNFs1–3) or *Yersinia enterocolitica* CNFY (Schmidt et al. 1997; Hoffmann et al. 2004; Hoffmann and Schmidt 2004; Stoll et al. 2009). These toxins cause deamidation of the same glutamine residue of RhoA, which is ADP-ribosylated by TccC5. The functional consequences of the deamidation of glutamine 63 to glutamate for the GTPase of RhoA are essentially the same: GTP hydrolysis is blocked and RhoA is persistently activated, because the nitrogen of glutamine is crucial for the right positioning of GTP in the catalytic side of Rho

proteins. However, effects of CNFs on target cells apparently differ from those of TccC5. For example, CNF1-induced stress fiber formation are observed only during a relative short time (up to 3–4 h), then membrane ruffling and lamellipodia formation is predominant. Moreover, after long-term treatment (>24 h) of cells with CNF1 Rac proteins are strongly degraded (Pop et al. 2004). Whether this effect is relevant for TccC5 has to be studied.

6 Conclusions

TccC3 and TccC5 are novel ADP-ribosylating toxins, which are the biological active components of the tripartite *P. luminescens* Tc toxins. The toxins modify unique amino acid residues in target proteins, which have not been reported to be acceptors for ADP-ribosylating toxins previously. While TccC3 ADP-ribosylates actin at threonine 148, TccC5 modifies Rho proteins (Rho, Rac, and Cdc42) at glutamine 63/61. Both modifications activate the target proteins, resulting in polymerization of actin and in persistent activation of Rho proteins. Eventually, both effects cause increase in actin polymerization and restructuring of the actin cytoskeleton. While recent structure analyses of main parts of the tripartite toxins have been elucidated, showing a novel type of toxin and a novel type of toxin delivery into target cells, the structure analysis of the ADP-ribosylating domains of the toxins is still missing. Studies on the structure and interaction of TccC5 and TccC3 with their targets allow new insights into the molecular reaction mechanism of bacterial ADP-ribosylating toxins, which are still not well understood.

Acknowledgments This work was supported by the German Research Foundation (DFG) and the Center for Biological Signaling Studies (BIOSS) in Freiburg (Germany).

References

Aktories K, Wegner A (1989) ADP-ribosylation of actin by clostridial toxins. J Cell Biol 109:1385–1387

Aktories K, Bärmann M, Ohishi I, Tsuyama S, Jakobs KH, Habermann E (1986) Botulinum C2 toxin ADP-ribosylates actin. Nature 322:390–392

Aktories K, Weller U, Chhatwal GS (1987) *Clostridium botulinum* type C produces a novel ADP-ribosyltransferase distinct from botulinum C2 toxin. FEBS Lett 212:109–113

Aktories K, Lang AE, Schwan C, Mannherz HG (2011) Actin as target for modification by bacterial protein toxins. FEBS J 278:4526–4543

Barth H, Preiss JC, Hofmann F, Aktories K (1998) Characterization of the catalytic site of the ADP-ribosyltransferase *Clostridium botulinum* C2 toxin by site-directed mutagenesis. J Biol Chem 273:29506–29511

Barth H, Olenik C, Sehr P, Schmidt G, Aktories K, Meyer DK (1999) Neosynthesis and activation of Rho by *Escherichia coli* cytotoxic necrotizing factor (CNF1) reverse cytopathic effects of ADP-ribosylated Rho. J Biol Chem 274:27407–27414

Braun M, Stuber K, Schlatter Y, Wahli T, Kuhnert P, Frey J (2002) Characterization of an ADP-ribosyltransferase toxin (AexT) from *Aeromonas salmonicida* subsp. salmonicida. J Bacteriol 184:1851–1858

Burridge K, Wennerberg K (2004) Rho and Rac take center stage. Cell 116:167–179

Busby JN, Panjikar S, Landsberg MJ, Hurst MR, Lott JS (2013) The BC component of ABC toxins is an RHS-repeat-containing protein encapsulation device. Nature 501:547–550

Cassel D, Pfeuffer T (1978) Mechanism of cholera toxin action: Covalent modification of the guanyl nucleotide-binding protein of the adenylate cyclase system. Proc Natl Acad Sci USA 75:2669–2673

Ciche T (2007) The biology and genome of *Heterorhabditis bacteriophora*. WormBook, pp 1–9

Ciche TA, Kim KS, Kaufmann-Daszczuk B, Nguyen KC, Hall DH (2008) Cell invasion and matricide during *Photorhabdus luminescens* transmission by *Heterorhabditis bacteriophora* nematodes. Appl Environ Microbiol 74:2275–2287

Collier RJ (1968) Effect of diphtheria toxin on protein synthesis: inactivation of one of the transfer factors. J Mol Biol 25:83–98

de Souza RF, Aravind L (2012) Identification of novel components of NAD-utilizing metabolic pathways and prediction of their biochemical functions. Mol BioSyst 8:1661–1677

ffrench-Constant RH, Bowen DJ (2000) Novel insecticidal toxins from nematode-symbiotic bacteria. Cell Mol Life Sci 57:828–833

ffrench-Constant R, Waterfield N (2006) An ABC guide to the bacterial toxin complexes. Adv Appl Microbiol 58:169–183

ffrench-Constant R, Waterfield N, Daborn P, Joyce S, Bennett H, Au C, Dowling A, Boundy S, Reynolds S, Clarke D (2003) Photorhabdus: towards a functional genomic analysis of a symbiont and pathogen. FEMS Microbiol Rev 26:433–456

Fieldhouse RJ, Merrill AR (2008) Needle in the haystack: structure-based toxin discovery. Trends Biochem Sci 33:546–556

Forst S, Dowds B, Boemare N, Stackebrandt E (1997) *Xenorhabdus* and *Photorhabdus* spp.: bugs that kill bugs. Annu Rev Microbiol 51:47–72

Fraylick JE, Rucks EA, Greene DM, Vincent TS, Olson JC (2002) Eukaryotic cell determination of ExoS ADP-ribosyltransferase substrate specificity. Biochem Biophys Res Commun 291:91–100

Gatsogiannis C, Lang AE, Meusch D, Pfaumann V, Hofnagel O, Benz R, Aktories K, Raunser S (2013) A syringe-like injection mechanism in *Photorhabdus luminescens* toxins. Nature 495:520–523

Genth H, Gerhard R, Maeda A, Amano M, Kaibuchi K, Aktories K, Just I (2003) Entrapment of Rho ADP-ribosylated by *Clostridium botulinum* C3 exoenzyme in the Rho-guanine nucleotide dissociation inhibitor-1 complex. J Biol Chem 278:28523–28527

Gill DM, Richardson SH (1980) Adenosine diphosphate-ribosylation of adenylate cyclase catalyzed by heat-labile enterotoxin of Escherichia coli: comparison with cholera toxin. J Infect Dis 141:64–70

Gill DM, Pappenheimer JAM, Brown R, Kurnick JT (1969) Studies on the mode of action of diphtheria toxin. VII. Toxin-stimulated hydrolysis of nicotinamide adenine dinucleotide in mammalian cell extracts. J Exp Med 129:1–21

Gülke I, Pfeifer G, Liese J, Fritz M, Hofmann F, Aktories K, Barth H (2001) Characterization of the enzymatic component of the ADP-ribosyltransferase toxin CDTa from *Clostridium difficile*. Infect Immun 69:6004–6011

Hall A (1993) Ras-related proteins. Curr Opin Cell Biol 5:265–268

Hall A (1994) Small GTP-binding proteins and the regulation of the actin cytoskeleton. Annu Rev Cell Biol 10:31–54

Hall A (1998) Rho GTPases and the actin cytoskeleton. Science 279:509–514

Han S, Tainer JA (2002) The ARTT motif and a unified structural understanding of substrate recognition in ADP-ribosylating bacterial toxins and eukaryotic ADP-ribosyltransferases. Int J Med Microbiol 291:523–529

Han S, Craig JA, Putnam CD, Carozzi NB, Tainer JA (1999) Evolution and mechanism from structures of an ADP-ribosylating toxin and NAD complex. Nat Struct Biol 6:932–936

Heasman SJ, Ridley AJ (2008) Mammalian Rho GTPases: new insights into their functions from in vivo studies. Nat Rev Mol Cell Biol 9:690–701

Hoffmann C, Schmidt G (2004) CNF and DNT. Rev Physiol Biochem Pharmacol 152:49–63

Hoffmann C, Pop M, Leemhuis J, Schirmer J, Aktories K, Schmidt G (2004) The *Yersinia pseudotuberculosis* cytotoxic necrotizing factor (CNFY) selectively activates RhoA. J Biol Chem 279:16026–16032

Holmes KC, Popp D, Gebhard W, Kabsch W (1990) Atomic model of the actin filament. Nature 347:44–49

Honjo T, Nishizuka Y, Hayaishi O (1968) Diphtheria toxin-dependent adenosine diphosphate ribosylation of aminoacryl transferase II and inhibition of protein synthesis. J Biol Chem 243:3553–3555

Hottiger MO, Hassa PO, Luscher B, Schuler H, Koch-Nolte F (2010) Toward a unified nomenclature for mammalian ADP-ribosyltransferases. Trends Biochem Sci 35:208–219

Iglewski BH, Kabat D (1975) NAD-dependent inhibition of protein synthesis by *Pseudomonas aeruginosa* toxin. Proc Natl Acad Sci USA 72:2284–2288

Jaffe AB, Hall A (2005) Rho GTPases: biochemistry and biology. Annu Rev Cell Dev Biol 21:247–269

Jorgensen R, Purdy AE, Fieldhouse RJ, Kimber MS, Bartlett DH, Merrill AR (2008) Cholix toxin, a novel ADP-ribosylating factor from *Vibrio cholerae*. J Biol Chem 283:10671–10678

Just I, Schallehn G, Aktories K (1992) A novel C3-like ADP-ribosyltransferase produced by *Clostridium limosum*. In: Poirier GG, Moreau P (eds) ADP-ribosylation reactions. Springer, New York, pp 373–376

Just I, Selzer J, Jung M, van Damme J, Vandekerckhove J, Aktories K (1995) Rho-ADP-ribosylating exoenzyme from *Bacillus cereus*—purification, characterization and identification of the NAD-binding site. Biochemistry 34:334–340

Landsberg MJ, Jones SA, Rothnagel R, Busby JN, Marshall SD, Simpson RM, Lott JS, Hankamer B, Hurst MR (2011) 3D structure of the *Yersinia entomophaga* toxin complex and implications for insecticidal activity. Proc Natl Acad Sci USA 108:20544–20549

Lang AE, Schmidt G, Schlosser A, Hey TD, Larrinua IM, Sheets JJ, Mannherz HG, Aktories K (2010) *Photorhabdus luminescens* toxins ADP-ribosylate actin and RhoA to force actin clustering. Science 327:1139–1142

Lang AE, Ernst K, Lee H, Papatheodorou P, Schwan C, Barth H, Aktories K (2013) The chaperone Hsp90 and PPIases of the cyclophilin and FKBP families facilitate membrane translocation of *Photorhabdus luminescens* ADP-ribosyltransferases. Cell Microbiol

Lim L, Hall C, Monfries C (1996) Regulation of actin cytoskeleton by Rho-family GTPases and their associated proteins. Cell Dev Biol 7:699–706

Mannherz HG, Hannappel E (2009) The beta-thymosins: intracellular and extracellular activities of a versatile actin binding protein family. Cell Motil Cytoskelet 66:839–851

Maresso AW, Baldwin MR, Barbieri JT (2004) Ezrin/radixin/moesin proteins are high affinity targets for ADP-ribosylation by *Pseudomonas aeruginosa* ExoS. J Biol Chem 279:38402–38408

Moss J, Vaughan M (1977) Mechanism of action of choleragen. Evidence for ADP-ribosyltransferase activity with arginine as an acceptor. J Biol Chem 252:2455–2457

Nobes C, Hall A (1994) Regulation and function of the Rho subfamily of small GTPases. Curr Opin Genet Dev 4:77–81

Nobes CD, Hall A (1995) Rho, Rac, and Cdc42 GTPases regulate the assembly of multimolecular focal complexes associated with actin stress fibers, lamellipodia, and filopodia. Cell 81:53–62

Otto H, Hanson PI, Chapman ER, Blasi J, Jahn R (1995) Poisoning by botulinum neurotoxin A does not inhibit formation or disassembly of the synaptosomal fusion complex. Biochem Biophys Res Commun 212:945–952

Otto H, Reche PA, Bazan F, Dittmar K, Haag F, Koch-Nolte F (2005) In silico characterization of the family of PARP-like poly(ADP-ribosyl)transferases (pARTs). BMC Genom 6:139

Pallen MJ, Lam AC, Loman NJ, McBride A (2001) An abundance of bacterial ADP-ribosyltransferases—implications for the origin of exotoxins and their human homologues. Trends Microbiol 9:302–307

Perelle S, Gibert M, Bourlioux P, Corthier G, Popoff MR (1997) Production of a complete binary toxin (actin-specific ADP-ribosyltransferase) by *Clostridium difficile* CD196. Infect Immun 65:1402–1407

Perieteanu AA, Visschedyk DD, Merrill AR, Dawson JF (2010) ADP-ribosylation of cross-linked actin generates barbed-end polymerization-deficient F-actin oligomers. Biochemistry 49:8944–8954

Pop M, Aktories K, Schmidt G (2004) Isotype-specific degradation of Rac activated by the cytotoxic necrotizing factor 1 (CNF1). J Biol Chem 279:35840–35848

Ridley AJ, Hall A (1992) The small GTP-binding protein rho regulates the assembly of focal adhesions and actin stress fibers in response to growth factors. Cell 70:389–399

Ridley AJ, Hall A (1994) Signal transduction pathways regulating Rho-mediated stress fibre formation: requirement for a tyrosine kinase. EMBO J 13:2600–2610

Ridley AJ, Paterson HF, Johnston CL, Diekmann D, Hall A (1992) The small GTP-binding protein rac regulates growth factor-induced membrane ruffling. Cell 70:401–410

Safer D (1992) The interaction of actin with thymosin β_4. J Muscle Res Cell Motil 13:269–271

Schering B, Bärmann M, Chhatwal GS, Geipel U, Aktories K (1988) ADP-ribosylation of skeletal muscle and non-muscle actin by *Clostridium perfringens* iota toxin. Eur J Biochem 171:225–229

Schmidt G, Sehr P, Wilm M, Selzer J, Mann M, Aktories K (1997) Gln63 of Rho is deamidated by *Escherichia coli* cytotoxic necrotizing factor 1. Nature 387:725–729

Sehr P, Joseph G, Genth H, Just I, Pick E, Aktories K (1998) Glucosylation and ADP-ribosylation of Rho proteins—effects on nucleotide binding, GTPase activity, and effector-coupling. Biochemistry 37:5296–5304

Sekine A, Fujiwara M, Narumiya S (1989) Asparagine residue in the rho gene product is the modification site for botulinum ADP-ribosyltransferase. J Biol Chem 264:8602–8605

Sheets JJ, Hey TD, Fencil KJ, Burton SL, Ni W, Lang AE, Benz R, Aktories K (2011) Insecticidal toxin complex proteins from *Xenorhabdus nematophilus*: structure and pore formation. J Biol Chem 286:22742–22749

Simpson LL, Stiles BG, Zepeda H, Wilkins TD (1989) Production by *Clostridium spiroforme* of an iotalike toxin that possesses mono(ADP-ribosyl)transferase activity: Identification of a novel class of ADP-ribosyltransferases. Infect Immun 57:255–261

Stoll T, Markwirth G, Reipschlager S, Schmidt G (2009) A new member of a growing toxin family—*Escherichia coli* cytotoxic necrotizing factor 3 (CNF3). Toxicon 54:745–753

Sugai M, Enomoto T, Hashimoto K, Matsumoto K, Matsuo Y, Ohgai H, Hong Y-M, Inoue S, Yoshikawa K, Suginaka H (1990) A novel epidermal cell differentiation inhibitor (EDIN): Purification and characterization from *Staphylococcus aureus*. Biochem Biophys Res Commun 173:92–98

Sun J, Barbieri JT (2003) *Pseudomonas aeruginosa* ExoT ADP-ribosylates CT10-regulator of kinase (Crk). J Biol Chem 278:32794–32800

Takai Y, Kaibuchi K, Kikuchi A, Sasaki T, Shirataki H (1993) Regulators of small GTPases. Ciba Found Symp 176:128–138

Tsurumura T, Tsumori Y, Qiu H, Oda M, Sakurai J, Nagahama M, Tsuge H (2013) Arginine ADP-ribosylation mechanism based on structural snapshots of iota-toxin and actin complex. Proc Natl Acad Sci USA 110:4267–4272

Ui M (1984) Islet-activating protein, pertussis toxin: A probe for functions of the inhibitory guanine nucleotide regulatory component of adenylate cyclase. Trends Pharmacol Sci 5:277–279

Vandekerckhove J, Schering B, Bärmann M, Aktories K (1987) *Clostridium perfringens* iota toxin ADP-ribosylates skeletal muscle actin in Arg-177. FEBS Lett 225:48–52

Vandekerckhove J, Schering B, Bärmann M, Aktories K (1988) Botulinum C2 toxin ADP-ribosylates cytoplasmic β/g-actin in arginine 177. J Biol Chem 263:696–700

Vetter IR, Wittinghofer A (2001) The guanine nucleotide-binding switch in three dimensions. Science 294:1299–1304

Visschedyk DD, Perieteanu AA, Turgeon ZJ, Fieldhouse RJ, Dawson JF, Merrill AR (2010) Photox, a novel actin-targeting mono-ADP-ribosyltransferase from *Photorhabdus luminescens*. J Biol Chem 285:13525–13534

Waterfield NR, Bowen DJ, Fetherston JD, Perry RD, ffrench-Constant RH (2001) The tc genes of *Photorhabdus*: a growing family. Trends Microbiol 9:185–191

Waterfield NR, Ciche T, Clarke D (2009) Photorhabdus and a host of hosts. Annu Rev Microbiol 63:557–574

Wegner A, Aktories K (1988) ADP-ribosylated actin caps the barbed ends of actin filaments. J Biol Chem 263:13739–13742

Weigt C, Just I, Wegner A, Aktories K (1989) Nonmuscle actin ADP-ribosylated by botulinum C2 toxin caps actin filaments. FEBS Lett 246:181–184

West RE, Moss J, Vaughan M, Liu T, Liu T-Y (1985) Pertussis toxin-catalyzed ADP-ribosylation of transducin. J Biol Chem 260:14428–14430

Wilde C, Chhatwal GS, Aktories K (2002) C3stau, a new member of the family of C3-like ADP-ribosyltransferases. Trends Microbiol 10:5–7

Reaction Mechanism of Mono-ADP-Ribosyltransferase Based on Structures of the Complex of Enzyme and Substrate Protein

Hideaki Tsuge and Toshiharu Tsurumura

Abstract Mono-ADP-ribosylation is a post-translational protein modification catalyzed by bacterial toxins and exoenzymes that function as ADP-ribosyltransferases. Despite the importance of this modification, the reaction mechanism remains poorly understood due to a lack of information on the crystal structure of these enzymes in complex with a substrate protein. Recently, the structures of two such complexes became available, which shed new light on the mechanisms of mono-ADP-ribosylation. In this review, we consider the reaction mechanism based on the structures of ADP-ribosyltransferases in complex with a substrate protein.

Contents

H. Tsuge (✉) · T. Tsurumura
Faculty of Life Sciences, Kyoto Sangyo University, Kamigamo-Motoyama, Kyoto 603-8555, Japan
e-mail: tsuge@cc.kyoto-su.ac.jp

Current Topics in Microbiology and Immunology (2015) 384: 69–87
DOI: 10.1007/82_2014_415

Published Online: 3 July 2014

1 Introduction

ADP-ribosylation is an important post-translational protein modification known to be catalyzed by bacterial toxins as well as eukaryotic endogenous ADP-ribosyltransferases (ARTs). Mono-ARTs exhibit ART activity toward substrate proteins, but also show weak NAD-glycohydrolase (NADase) activity in the absence of a substrate protein. In both reactions, the enzyme cleaves the nicotinamide-ribosyl bond of βNAD$^+$; the difference is that in the former the ADP-ribosyl moiety is transferred to one of several amino acid acceptors on target proteins, while in the latter it is transferred to a water molecule. Based on their target specificity, bacterial ARTs are traditionally classified into four types: type I includes cholera toxin (CT), which ADP-ribosylates Gsα (Cassel and Pfeuffer 1978), and pertussis toxin, which ADP-ribosylates both Gi and Go (Katada and Ui 1982; Bokoch et al. 1983; Sternweis and Robishaw 1984); type II includes diphtheria toxin (DT) (Honjo et al. 1968, 1971) and exotoxin A (ExoA) from *Pseudomonas aeruginosa* (Iglewski and Kabat 1975; Chung and Collier 1977), which modify elongation factor 2 (eEF2), type III includes C3 toxin (C3) from *Clostridium botulinum*, which ADP-ribosylates Rho (Aktories and Frevert 1987); and type IV includes C2 toxin (C2) from *C. botulinum*, which ADP-ribosylates actin (Aktories et al. 1986, 1989) (Fig. 1). It is noteworthy that all of the target proteins function as ATPases or GTPases, which play critical roles within host cells. In other words, bacteria appear to "conquer" host cells using toxins that pinpoint critical components. In addition, the number of known members of the bacterial ART family continues to increase. For example, toxin complex component C3 (TccC3) and C5 (TccC5) from *Photorhabdus luminescens* are recently identified ARTs that modify actin and RhoA, but their target residues differ from other type IV and type III toxins, respectively (Lang et al. 2010). A review of this novel family is available elsewhere in this book. In addition, there is Certhrax toxin from *Bacillus cereus*, a novel ART with an unknown host factor (Visschedyk et al. 2012), and HopU1 from *Pseudomonas syringae*, which modifies an RNA-binding protein in plants (Fu et al. 2007).

It was recently proposed that mammalian ARTs could be classified into two groups based on their structural features. One class, ARTD (related to DT), contains a conserved H-Y-E motif, while the other class, ARTC (related to the C2 and C3 Clostridial toxins, including CT), contains a conserved R-S-E motif (Hottiger et al. 2010).

Among all these ARTs, there are conserved sequence motifs and strong structural similarities that suggest they make use of a common reaction mechanism (Domenighini et al. 1994). However, the catalytic mechanism of ARTs is still poorly understood, as there is little available information on the structures of these enzymes in complex with a substrate protein. That said, our group recently reported the crystal structure of an actin-specific ART (Ia) in complex with actin (Tsuge et al. 2008; Tsurumura et al. 2013). In addition, Jørgensen et al. reported the structure of ExoA complexed with eEF2 (Jørgensen et al. 2005; Jørgensen

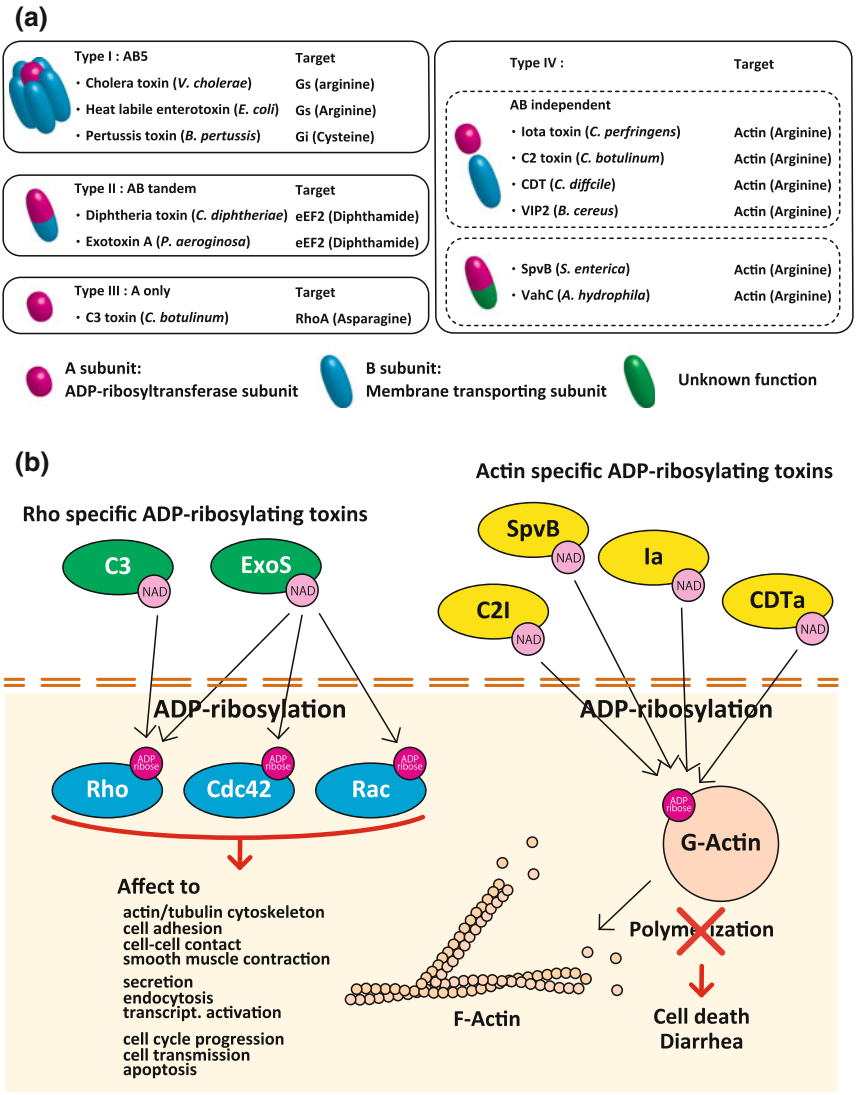

Fig. 1 **a** Classification of ARTs based on their target specificity. ADP-ribosyltransferase subunit (*A subunit*), membrane transporting subunit (*B subunit*) and a component with unknown function are in magenta, blue and green, respectively. **b** Effect of ADP-ribosylation by *Type III* and *Type IV* ADPRTs

et al. 2008). The structures of these two complexes provide novel insight into the reaction mechanism of ADP-ribosylation. In this review, we focus on the structure and the reaction mechanism of ARTC.

2 The Structure and Reaction Mechanism of Actin- and Rho-Targeting ARTs

Although the C2-like and C3-like ARTs modify different target proteins and act toward different amino acids within those proteins, their tertiary structures show strong similarities. The actin-targeting, C2-like ARTs include iota toxin (Ia) from *Clostridium perfringens* (Vandekerckhove et al. 1987), C2 (C2I) from *C. botulinum* (Aktories et al. 1986), *Clostridium spiroforme* toxin (Popoff et al. 1989) and *Clostridium difficile* toxin (Popoff et al. 1988), all of which ADP-ribosylate actin at Arg177. The ADP-ribosylated G-actin can bind to F-actin at the plus (barbed) end of the filament as a capping protein, but depolymerization occurs at the minus (pointed) end, and the newly released G-actin is then ADP-ribosylated by the toxin. Such toxin-induced actin depolymerization has dramatic effects on target cells, including remodeling of their microtubules and destruction of the actin cytoskeleton with subsequent apoptosis (Aktories et al. 2011).

The Rho-targeting, C3-like ARTs include enzymes produced by *C. botulinum, Clostridium limosum*, *Bacillus cereus* and *Staphylococcus aureus*. C3-like ARTs modify Asn41 of RhoA, B and C (Sekine et al. 1989; Aktories et al. 1989). Rho GTPases are master regulators of the actin cytoskeleton (Etienne-Manneville and Hall 2002), and their C3-catalyzed ADP-ribosylation causes their biological inactivation and thus inhibition of downstream signaling and its consequences.

In the time since the first actin-targeting C2 ART was identified (Aktories et al. 1986), numerous functional studies have been carried out examining the C2-like ARTs. The enzymatic subunits of C2, Ia and CDT consist of two similar repeated domains. The C-terminal domain harbors NAD^+ binding and ART activity, while the N-terminal domain lacks both NAD^+ binding and ART activity but binds the complementary B subunit. Based on the reported structures of the type I and type II enzymes, it was proposed that three motifs are conserved among ARTs; these include the (i) aromatic-Arg/His motif, (ii) STS motif, and (iii) E(Q)XE motif (Domenighini and Rappuoli 1996). Replacement of Arg with Ala in the aromatic-Arg/His motif leads to a complete loss of the enzymes' ART and NADase activities, their cytotoxic activities and thus their lethality (Perelle et al. 1996; Nagahama et al. 2000). Mutation of the first glutamate in the EXE motif prevents ART activity but not NADase activity, while mutation of the second glutamate diminishes both the ART and NADase activities (Nagahama et al. 2000; Perelle et al. 1996; Barth et al. 1998). Mutation of first serine in the STS motif drastically reduces ART activity (Barth et al. 1998; Nagahama et al. 2000).

The functional studies outlined above were subsequently confirmed by X-ray structural studies. The first resolved structure of a C2-like ART, VIP2 from *Bacillus cereus*, revealed that it is a mixed α/β protein and is divided into an N-domain and a C-domain with similar structures (Han et al. 1999) (Fig. 2). VIP2 belongs to the binary toxin family, which consists of VIP1 (membrane binding unit) and VIP2 (enzymatic unit) as well as iota-toxin (Ib (membrane binding unit) and Ia (enzymatic unit)) and C2 (C2II (membrane binding unit) and C2I

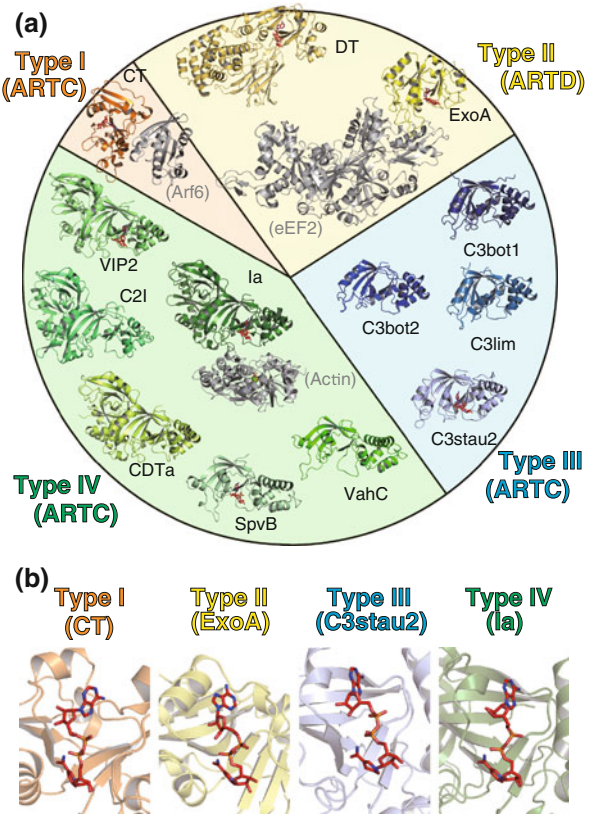

Fig. 2 Structures of ARTs and its NAD^+ binding of each type. **a** Structures of Ia (with actin), C2I, VIP2, CDTa, SpvB, VahC, C3, and CT (with ARF6) are shown, which are classified as ARTCs. The structures of DT and ExoA (with eEF2) are shown, which are classified as ARTDs. There is strong structural similarity in all ART domains with NAD^+ binding. The overall structures of type I, II, III and IV are depicted in *orange, yellow, blue*, and *green*, respectively. Binding proteins are depicted in *gray*. **b** The conformations of the bound NAD^+ in each ART type are shown. The NMN moiety binds in a similarly compact fashion (the NMN ring-like conformation) in all ARTs. The color coding for carbon atoms of NAD^+ is depicted in *red*. Accession number in PDB of shown structures are: NAD^+-CT-Arf6 (2A5F), NAD^+-DT (1TOX), NAD^+-ExoA-eEF2 (2ZIT), C3bot1 (1UZI), C3bot2 (1R45), C3lim (3BW8), NAD^+-C3stau2 (1OJZ), NAD^+-Ia-actin (4T03), NAD^+-VIP2 (1QS2), CDTa (2WN4), C2I (2J3X), NAD^+-SpvB (2GWL), and VahC (4FML)

(enzymatic unit)). Ia and C2I have been characterized using mutagenesis and biochemical methods, though VIP2 has not. On the other hand, the crystal structure of VIP2 complexed with NAD^+ has provided not only the structural framework of the enzyme but also a possible reaction mechanism. The second glutamate (Glu428) in the EXE motif of VIP2 interacts with the 2'hydroxyl of the nicotinamide sugar. The first glutamate (Glu426) is situated outside the NAD^+-binding cleft, where it may act in the deprotonation of actin on Arg177 to increase Arg177

nucleophilicity for the attack on the C1' of the oxocarbenium ion within the VIP2-NAD^+ complex. Successive papers examining the structure of C3 have shown (1) that the C3 structure is very similar to the C-domain of VIP2 and (2) that the ADP-ribosylating toxin turn-turn (ARTT) motif places VIP2 and C3 toxin into a single ARTT family characterized by analogous target protein recognition via a turn 1 aromatic and turn 2 hydrogen-bonding side-chain moiety (Han et al. 2001) (Fig. 3). It was proposed that the turn 2 Gln in C3 and Glu in VIP2 recognize the side-chain of Asn41 and Arg177, respectively. Structural and functional studies of several toxins in this class, including Ia from *C. perfringens* (Tsuge et al. 2003), C2 from *C. botulinum* (Schleberger et al. 2006), and CDTa from *C. difficile* (Sundriyal et al. 2009), are presently available. Also available are several C3 structures, including C3bot from *C. botulinum,* C3stau2 (EDIN2) from *Staphylococcus aureus* (Evans et al. 2003; Wilde et al. 2002) and C3lim from *Clostridium limosum* (Vogelsgesang et al. 2008) (Fig. 2).

3 Oxocarbenium Ion Intermediate for the ADP-Ribosylation

Poly(ADP-ribose) synthase, CT, LT, and DT do not form ADP-ribosyl-enzyme intermediates, and all four enzymes mediate configuration inversion for α-glycosidic linkage (Moss et al. 1979a, b; Ferro and Oppenheimer 1978; Oppenheimer and Bodley 1981; Oppenheimer 1994). It has been suggested that the reaction proceeds via an Sn1 mechanism, despite the observed configuration inversion for the glycosidic bond of ribosyl diphthamide (Oppenheimer and Bodley 1981). Studies of substituent effects on hydrolysis of 2'-substituted nicotinamide arabinosides indicate that the mechanism likely involves the formation of an oxocarbocationic intermediate, which implies an Sn1 attack with characteristic first-order reaction kinetics (Buckley et al. 1994). In DT, the transition state shows oxocarbenium ion character, based on the kinetic isotope effect, which is similar to the solvolytic hydrolysis of NAD^+ (Berti et al. 1997). The predicted lifetime of a glucopyranosyl oxocarbenium in solution is $<10^{-12}$ s and is believed to show stability similar to that of the glucofuranosyl oxocarbenium implicated in the cleavage of the glycosylic bond of NAD^+ (Oppenheimer 1994). Therefore, transition state stabilization, either by the enzyme or by a nucleophile, is likely required for the reaction to proceed efficiently. With respect to VIP2, it was proposed the enzyme must catalyze the break of the C1'-N glycosylic bond and the formation of an oxocarbenium ion-like transition state without the formation of a strong bond to the nuclephile, as was observed during hydrolysis of NAD^+ with other ADP-ribosyltransferases (Han et al. 1999). In considering how to stabilize the oxocarbenium ion in VIP2, two possibilities were suggested: (1) interaction of the protein and the NAD^+ phosphate group could provide transition state stabilization of the oxocarbenium ion; or (2) the Glu428 (the second glutamate in EXE) Oε1 could form a hydrogen bond with the O2'hydroxyl of the nicotinamide ribose,

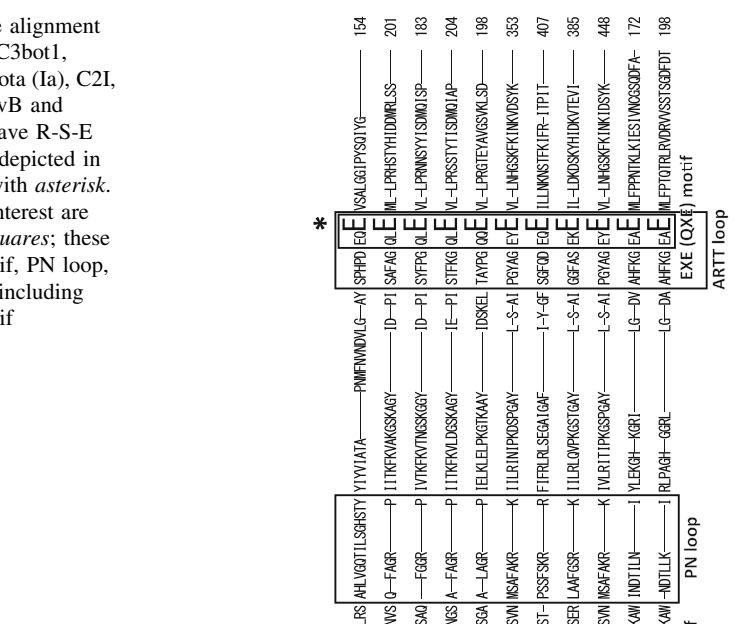

Fig. 3 Sequence alignment of ARTCs: CT, C3bot1, C3bot2, C3lim, Iota (Ia), C2I, VIP2, CDTa, SpvB and VahC. ARTCs have R-S-E motif which are depicted in large character with *asterisk*. The regions of interest are highlighted in *squares*; these include STS motif, PN loop, and ARTT loop including EXE (QXE) motif

which would increase the electronic density on the ring and stabilize the oxocarbenium ion. The NAD^+-bound VIP2 structure suggests that rate enhancement is driven more by ground-state destabilization than by transition-state stabilization. This is because the nicotinamide ring, situated at the edge of a deeper hydrophobic pocket, is a major contributor to ground-state stabilization of the substrate, which enables formation of the oxocarbenium ion.

4 Strain-Alleviation Model Based on the Structure of the Ia-Actin Complex

As mentioned, there is no direct information available on the interaction between ARTCs (C3-like or C2-like) and substrate proteins. In 2008, we succeeded in crystallizing and solving the structure of Ia in complex with actin (Fig. 4). To stabilize the complex, we added latrunculin A, a small-molecule inhibitor that prevented actin polymerization, thereby sequestering the G-actin (Bubb et al. 2002). In addition, instead of NAD^+ we used βTAD (thiazole-4-carboxamide adenine dinucleotide), a similar but non-hydrolyzable product of NAD^+ (Gebeyehu et al. 1983). These conditions made the Ia-actin complex crystal sufficiently durable to withstand X-ray analysis. The structure showed that the intermolecular interaction is via five loops: loop I (Tyr60-Tyr62), loop II (the active site loop), loop III (the loop between β9 and α10), loop IV (the phosphate-nicotinamide loop (PN loop which was defined in C3 exoenzyme (Menetrey et al. 2002)), and loop V (the ADP-ribosylating turn-turn loop (ARTT loop) containing the EXE motif) (Tsuge et al. 2008) (Fig. 4). Loops II to IV surround the NAD^+ binding cleft in the C-domain. Somewhat surprisingly, loop I, in the N-domain, was also involved in binding actin, a finding that was confirmed in a mutagenesis study (Tsuge et al. 2008).

Actin interacts with a variety of actin binding proteins, and the structures of these complexes have been reported, beginning with the high-resolution structure of the DNase I-actin complex (McLaughlin et al. 1993; Otterbein et al. 2002; Kabsch et al. 1990; Schutt et al. 1993). But the binding mode of Ia differs greatly from those used by other actin binding proteins (Tsuge et al. 2008), and we managed to use the crystal as a tool to take snapshots of the ADP-ribosylation reaction using X-ray crystallography. We first crystallized apo-Ia-actin crystals and found the ethylene glycol used as a cryoprotectant inhibited the ADP-ribosylation reaction. NAD^+ was then soaked with the apo-Ia-actin crystals under different conditions to trap the pre- and post-ADP-ribosylation structures (Tsurumura et al. 2013) (Fig. 4). These snapshots of ADP-ribosylation within the Ia-actin complex suggested the possibility that the reaction proceeds via a strain-alleviation model (Fig. 5). Briefly, positively charged Arg295 and Arg352 interact electrostatically with NAD^+ phosphate and contribute to the highly folded and strained NMN ring-like conformation. This specific conformation appears to induce an equilibrium shift toward an oxocarbenium cation. In the pre-reaction state, the ADP moiety of NAD^+ is gripped by Ia.

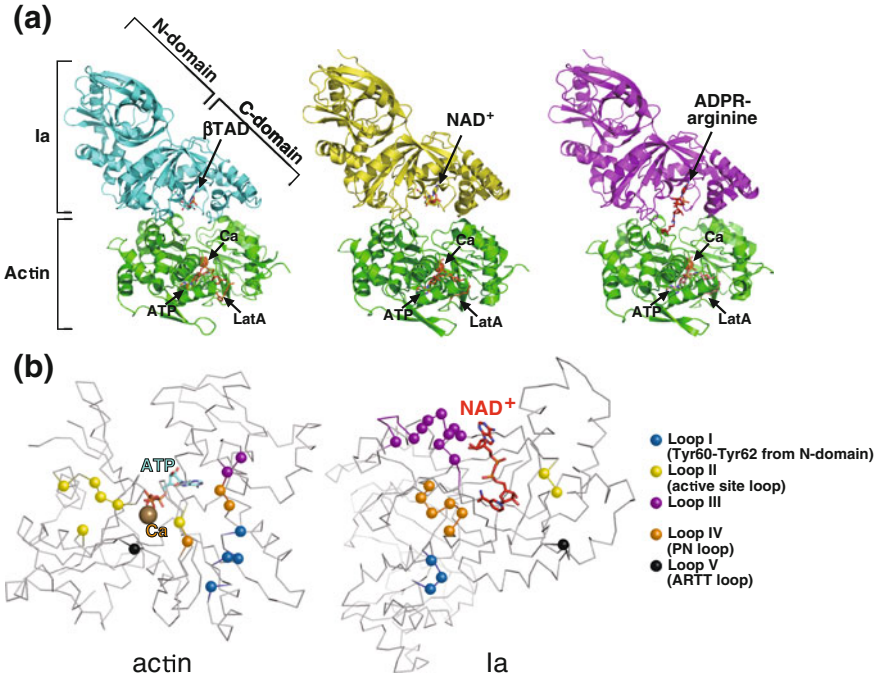

Fig. 4 Crystal structure of Ia-actin complex. **a** Crystal structures of βTAD-Ia-actin, NAD^+-Ia-actin and Ia-ADPR-actin are depicted in *cyan*, *yellow*,and *magenta*, respectively. All actin molecules are in *green*. **b** The five loops of Ia and actin that participate in binding each other are shown using the colors as described in the inset. ATP and calcium are depicted in *cyan* and *light brown*, respectively

After scission of the nicotinamide via an Sn1 reaction, the electrophile (NC1 of *N*-ribose) in the first oxocarbenium cation is still $\sim$8 Å away from Arg177, the actin acceptor amino acid. To reduce this distance, a central rotation occurs mainly via the β-phosphate of ADP-ribose, resulting in strain relief and formation of a second oxocarbenium cation, which is able to reach Arg177 of actin. This strain-alleviation model was first proposed for the βTAD complex structure (Tsuge et al. 2008) and became more plausible with additional snapshots of ADP-ribosylation (Tsurumura et al. 2013; Jank and Aktories 2013). The oxocarbenium ion intermediate would be stabilized by Tyr251 via cation-π interaction (Gallivan and Dougherty 1999). Two amino acids in the ARTT loop, Tyr375 and Glu378 (the first glutamate of EXE) move substantially in the transition from NAD^+-Ia-actin to Ia-ADPR-actin. It was proposed that Tyr375 interacts with actin and Glu378 recognizes actin Arg177 (Han et al. 2001). In fact, Tyr375 was shown to be involved with actin binding within the NAD^+-Ia-actin complex, but a direct interaction between Glu378 and actin Arg177 was not seen in either complex (Tsurumura et al. 2013). In addition, two other amino

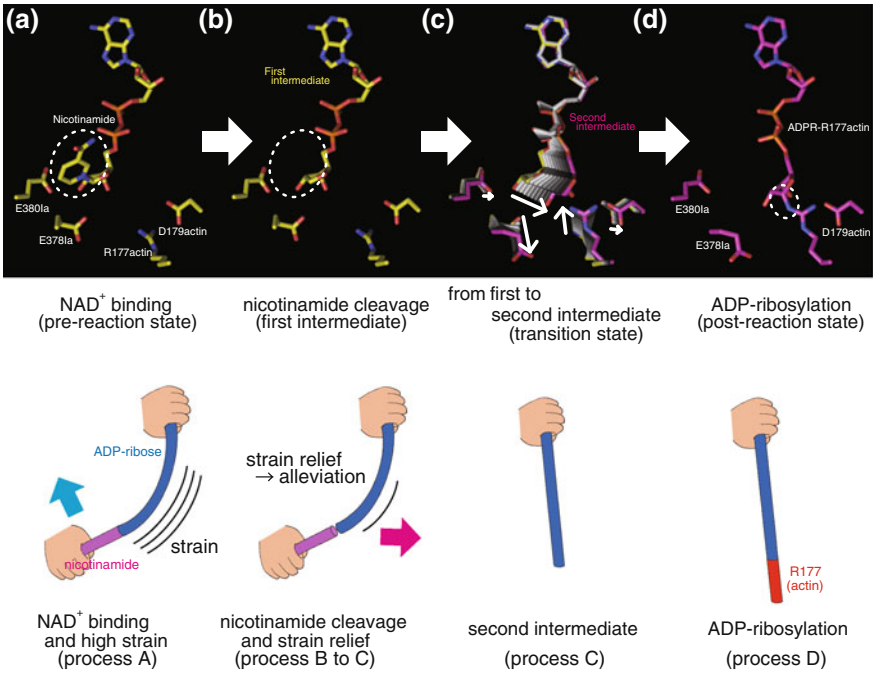

Fig. 5 Strain alleviation model of ADP-ribosylation. *Upper panels* represent the process of ADP-ribosylation and *lower panels* are cartoon representations of *upper panels*. **a** NAD^+ binding, **b** nicotinamide cleavage and first intermediate, **c** transient motion from first to second intermediate and **d** ADP-ribosylation

acids, Ser338 (the first residue in the STS motif) and Phe349, may act cooperatively to stabilize the oxocarbenium ion during the transfer, as they are situated near the nicotinamide and may be important for fixing the position of the nicotinamide. Glu380 (the second glutamate residue in the EXE motif) is important for NADase activity and interacts with the 2'hydroxyl of N-ribose. In contrast to Glu378, Glu380 remains at the same position throughout the reaction, but a more important feature is that actin Asp179 is situated beside Arg177. The electron density of Arg177 and Asp179 were clearly visible in NAD^+-Ia-actin. It will be interesting to see whether Asp179 is linked to the ART activity.

At present, there is no structural information on Rho-targeting C3-like ARTs in complex with a substrate protein, though the structure of C3 in complex with RalA, which is not a substrate of the enzyme, has been reported (Holbourn et al. 2005; Kimoto et al. 2006). Protein modeling and site-directed mutagenesis studies have been used to shed light on the structural basis for the difference in substrate specificity between ExoS and ExoT from *Pseudomonas aeruginosa*, which are similar to C3 (Sun et al. 2004). Whereas substrate recognition by ExoS is via the active site loop (ARTT motif and PN-loop), an additional region is used by ExoT. Resolution of the structure of C3-like ART in complex with Rho could provide

crucial information on the mechanism of substrate specificity. In particular, it will be important to determine whether Gln in the QXE motif recognizes Rho Asn41 within the complex.

5 Comparison of ARTC and ARTD Complexes and Reactions

DT and ExoA ADP-ribosylate diphthamide 687 of eEF2. The structure of the ExoA-eEF2 complex was reported by Jørgensen et al. in 2005 and was the first ART-substrate protein complex resolved (Jørgensen et al. 2005). The βTAD-ExoA-eEF2 complex suggested the involvement of two ExoA active-site loops, loop 1 (L1, residues 457-464) and loop 3 (L3, 546-551) in the reaction. A subsequent paper on the complex with intact NAD^+ revealed the conformational change that occurs in these loops upon binding eEF2. Mutational studies also revealed that Glu546, Arg551 and Glu553 in ExoA are crucial for catalytic activity. Glu553 forms hydrogen bonds with the 2'hydroxyl group of the nicotinamide ribose of NAD^+ and orientates the dinucleotide substrate for nucleophilic attack by the diphthamide residue. A marked conformational change in loop L1 could be seen in the NAD^+-ExoA-eEF2 complex. Glu461 in loop1 appears to be a key residue in the structure, though the D461A mutant showed full ART and NADase activities. At present, only two structures of an ART complexed with a substrate protein are available: Ia-actin and ExoA-eEF2, which are ARTC and ARTD representatives, respectively. Comparison of the NAD^+-ExoA-eEF2 and ExoA-ADPR-eEF2 complexes revealed that the diphthamide N3 nucleophilic atom remains about 10 Å away from the electrophilic C1 center of the *N*-ribose (Fig. 6). Investigators therefore proposed a transition state model in which the imidazole ring of the diphthamide residue migrates toward the nicotinamide ribose as the TMA group of the diphthamide moves between L1 of the toxin and the NAD^+ phosphates (Jørgensen et al. 2008). This kind of motion is unlikely within the Ia-actin structure because the structure of actin is virtually unchanged by ADP-ribosylation. In addition to the movement of the substrate protein observed in eEF2, the strain-alleviation model, which was proposed for the Ia-actin structure, could explain the reaction.

6 Fitting ADP-Ribosylated Actin into the Filamentous Actin Cryo-EM Structure

Actin is one the most abundant and well-conserved proteins in cells and is involved in such important cellular functions as cell motility, contractility, intracellular transport, and the control of cell shape and polarity (Dominguez 2004). Actin exists

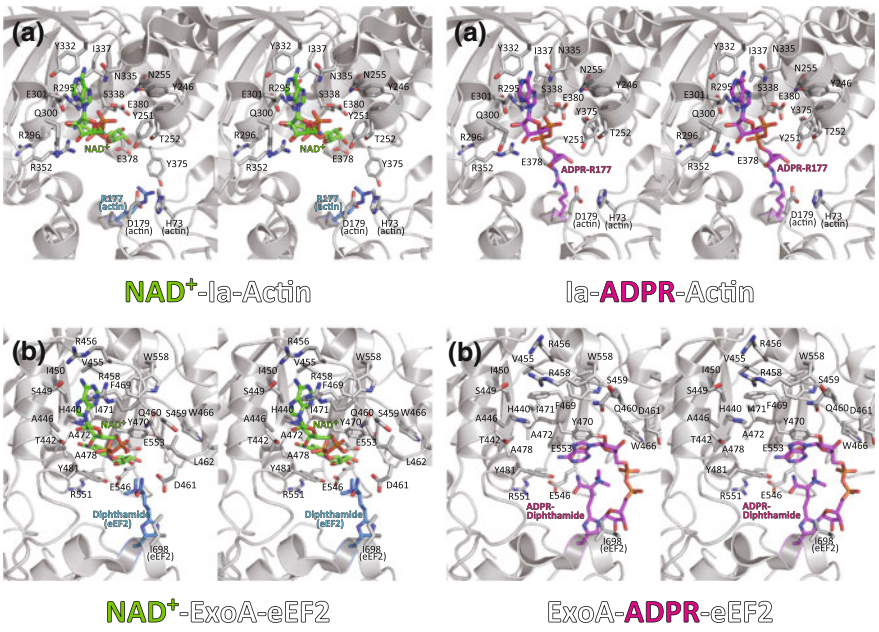

Fig. 6 Comparison of ARTC and ARTD complexes and reactions. The structure of the NAD^+-ExoA-eEF2 and ExoA-ADPR-eEF2 complexes are compared with NAD^+-Ia-actin and Ia-ADPR-actin in stereo view. NAD^+ is depicted in *green*, Arg177 of actin and diphthamide of eEF2 are depicted in *blue*. ADP-ribosylated Arg177 and diphthamide are in magenta

in two forms as the major component of the cytoskeleton, a monomeric form (G-actin) and a filamentous form (F-actin). The structures of actin after ADP-ribosylation by SpvB have been reported (Margarit et al. 2006). It is of interest whether this modification induces conformational changes in actin that are incompatible with filament formation, and whether the presence of ADPR at Arg177 causes a steric clash preventing the protein–protein interactions necessary for polymerization. The reported structure of ADPR-actin shows that ADP-ribosylation by SpvB induces no substantial conformational alterations in actin, though the ADP-ribosylation was not trapped crystallographically in the structure because of its flexibility (Margarit et al. 2006). Those investigators concluded that a model in which steric clash hinders intraprotomer contacts within the filament (the Holmes model (Holmes et al. 1990)) provides the most likely explanation for the activity of SpvB. The first visible structure of ADP-ribosylated actin, within the Ia-ADPR-actin complex, confirmed the earlier finding that actin is unchanged by ADP-ribosylation (Tsurumura et al. 2013). Recently the high-resolution structure of F-actin was revealed using cryo-electron microscopy (Murakami et al. 2010; Fujii et al. 2010). We tried fitting the ADPR-actin monomer into the filamentous actin structure using a UCSF chimera (Pintilie et al. 2010) (Fig. 7). This model also supports that ADP-ribosylation prevents actin polymerization through steric clash.

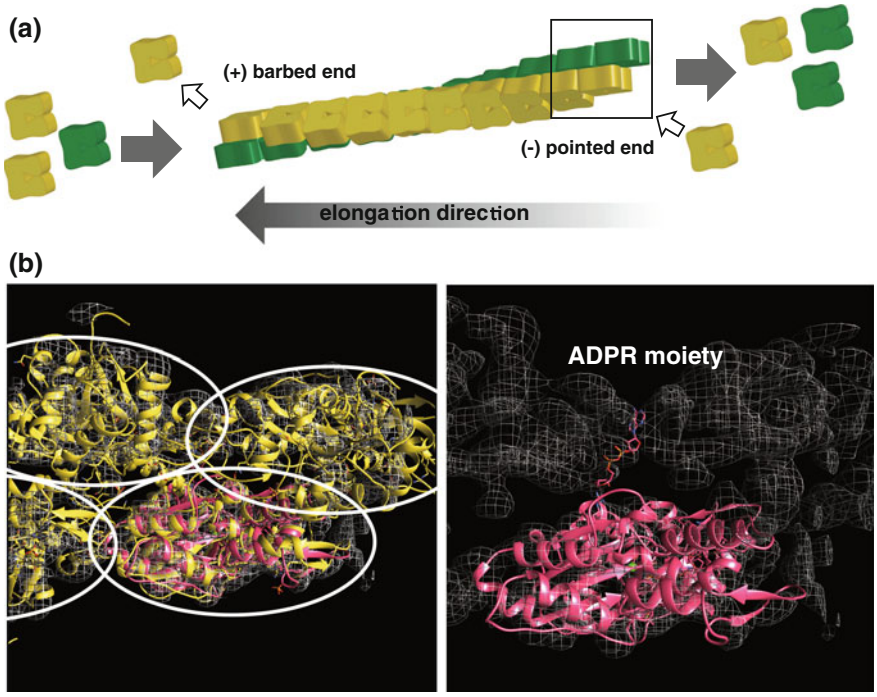

Fig. 7 Fitting of ADP-ribosylated actin into the filamentous actin structure. **a** Actin filaments undergo tread milling. Actin monomers add at the (+) barbed end and dissociate from the (−) pointed end. The *black square* represents in detail in **b**. **b** In the *left panel*, the structure of intact actin (*yellow*) and ADPR-actin (4H0T, *magenta*) were fitted into the cryo-microscopy electron density map (EMD-5168). *Right pane* Close-up view of ADPR-actin in the electron density

7 An Actin-Targeting ART Subgroup: SpvB and VahC

The SpvB protein from *Salmonella enterica* was recently identified as an actin-targeting ART (Hochmann et al. 2006). The C-terminal domain of SpvB (amino acid residues 375–591, 24.5 kDa) shares homology with other known ARTs, and it also ADP-ribosylates actin on Arg177 (Hochmann et al. 2006). Interestingly, the N-terminal domain of SpvB shares no homology with the enzymatic components of any known binary toxins, and the structure has not yet been resolved. It was recently found that VahC, a toxin from *Aeromonas hydrophila*, has similarity with SpvB (Shniffer et al. 2012). It is interesting that both SpvB and VahC lack NADase activity, whereas Ia, VIP2 and C2 show NADase activity in the absence of a substrate protein. It was suggested that the absence of an essential residue (corresponding to Phe349 in Ia) and a shorter PN loop (Region IV) accounts for the loss of NADase activity. Region IV could thus be important for the restriction against the conformation of the nicotinamide.

The structure of the SpvB C-terminal domain revealed the similarity with Ia and C2I, but it contains a unique insertion of 29 amino acids between α8 and α9 (Margarit et al. 2006). The N-terminal adaptor portion of the enzymatic component of binary toxins is critical for actin recognition in the Ia/C2I subtype, but it is absent in the SpvB/VahC subtype toxins. In the modeling of SpvB-actin, the 29-residue insertion in SpvB appeared to be important for actin binding and to compensate for the lack of the N-terminal binding region of Ia; however, the significance of this insertion is not yet been revealed experimentally (Tsuge et al. 2008; Shniffer et al. 2012). Comparison of the surface region involved in actin binding based on modeling using Ia-actin structure is also of interest (Shniffer et al. 2012) (Fig. 8). Figure 8 shows that three toxins (Ia/VIP2/SpvB), with the same substrate protein actin, seem to have similar surface electrostatic potential to recognize actin and NAD^+. These facts indicate that the three toxins recognize substrate (NAD^+) and substrate protein (actin) with the same manner. Furthermore, we consider that the three toxins possibly to have the same ADP-ribosylation mechanism as we proposed. On the other hand, whereas C3 and CT have similar surface electrostatic potential as well as Ia, they ADP-ribosylate other substrate proteins. It is still an open question whether the same ADP-ribosylation mechanism is applicable to C3 and CT. Further crystallographic studies of toxin-substrate protein complex are expected to understand ADP-ribosylation mechanism and recognition of substrate protein.

8 Structure of the Cholera Toxin-Gsα Complex

CT, LT and PT all ADP-ribosylate the α subunit of heteromeric G-proteins at a specific arginine (CT and LT) or cysteine residue (PT). These proteins are AB5-type toxins, which consist of a catalytic subunit (A) and a receptor binding and delivery subunit (B). The structures of LT and CT were reported more than two decades ago (Sixma et al. 1991; Zhang et al. 1995), though less structural information is available for the catalytic A subunit. This is because proteolytic cleavage of the A subunit and reduction of the disulfide bond separate the A1 and A2 domains of the subunit. CTA1 (A1 subunit) ADP-ribosylates Arg201 of Gsα. It contains a R-S-E motif and is thus classified as an ARTC. From a structural viewpoint, however, CTA1 differs substantially from the C2/C3/iota toxin group. By itself, CTA1 shows relatively little activity in vitro, but the affinity of CTA1 for its substrates and its enzymatic efficiency are increased through interaction with host ADP-ribosylation factor (Kahn and Gilman 1986; Noda et al. 1990). Likewise, LT also needs to be activated through interaction with an auxiliary ADP-ribosylation factor (Moss et al. 1993). The conformation of the CTA1 activation loop (residues 25–40) changes from an ordered coil to a amphipathic α-helix upon binding ARF6 (GTP) (O'Neal et al. 2005). Although the structure of the CTA1-Gsα complex is not yet known, it seems clear that resolving the structure of the CT-ARF6-Gs complex will provide a wealth of important information.

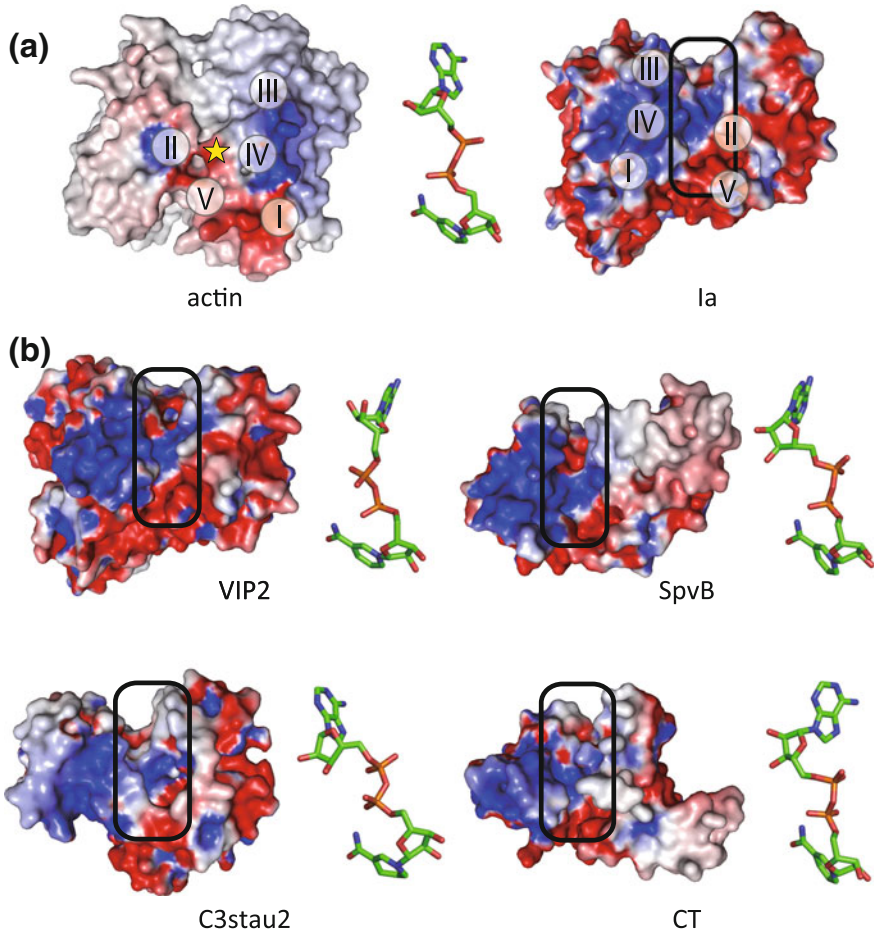

Fig. 8 Electrostatic representation of ARTC toxins and actin. The surface electrostatic potential was calculated using APBS software (Baker et al. 2001). **a** The surface electrostatic potentials of interface of Ia and actin are shown. Five interaction loops are shown in *Roman* numerals. The *black square* surrounds the NAD^+ binding site, the *yellow star* marks the position of Arg177. **b** The surface electrostatic potentials and NAD^+ conformations are shown of each ARTC toxins. The color of NAD^+ is depicted in *green*

9 Conclusion

Actin-specific and Rho-specific ARTs are well-studied classes of toxins. Recent advances in our understanding of their structures, especially the structure of the Ia-actin complex has provided important insight into target-protein recognition and the reaction mechanism of these toxins. Although the residues targeted by bacterial toxins are arginine, asparagine, cysteine and diphthamide, several other amino

acids are also known to be ADP-ribosylated (aspartic acid, glutamic acid and lysine) by mammalian ARTD (Hassa et al. 2006; Koch-Nolte et al. 2008). It is anticipated that additional information on the structures of other ARTs in complex with substrate proteins will further our understanding of substrate-amino acid recognition by these ARTs. Moreover, it will likely be possible to explain that there is a common reaction mechanism in not only bacterial ARTs but also mammalian ARTs.

Acknowledgments H.T. appreciates Masahiro Nagahama, Masataka Oda, and Jun Sakurai, who support our work on the structure of ART, and Nobuhiko Katunuma for his continuous research support. This work was supported in part by a Strategic Research Foundation Grant-aided Project for Private Universities and Grant-in-Aid for Scientific Research on Innovative Areas, MEXT/JSPS KAKENHI Grant Number: 25121733 of Japan.

References

Aktories K, Barmann M, Ohishi I, Tsuyama S, Jakobs KH, Habermann E (1986) Botulinum C2 toxin ADP-ribosylates actin. Nature 322(6077):390–392

Aktories K, Braun U, Rosener S, Just I, Hall A (1989) The rho gene product expressed in *E. coli* is a substrate of botulinum ADP-ribosyltransferase C3. Biochem Biophys Res Commun 158(1):209–213

Aktories K, Frevert J (1987) ADP-ribosylation of a 21-24 kDa eukaryotic protein(s) by C3, a novel botulinum ADP-ribosyltransferase, is regulated by guanine nucleotide. Biochem J 247(2):363–368

Aktories K, Lang AE, Schwan C, Mannherz HG (2011) Actin as target for modification by bacterial protein toxins. FEBS J 278(23):4526–4543

Baker NA, Sept D, Joseph S, Holst MJ, McCammon JA (2001) Electrostatics of nanosystems: application to microtubules and the ribosome. Proc Nat. Acad Sci USA 98(18):10037–10041

Barth H, Preiss JC, Hofmann F, Aktories K (1998) Characterization of the catalytic site of the ADP-ribosyltransferase *Clostridium botulinum* C2 toxin by site-directed mutagenesis. J Biol Chem 273(45):29506–29511

Berti PJ, Blanke SR, Schramm VL (1997) Transition state structure for the hydrolysis of NAD catalyzed by diphtheria toxin. J Am Chem Soc 119(50):12079–12088

Bokoch GM, Katada T, Northup JK, Hewlett EL, Gilman AG (1983) Identification of the predominant substrate for ADP-ribosylation by islet activating protein. J Biol Chem 258(4):2072–2075

Bubb MR, Govindasamy L, Yarmola EG, Vorobiev SM, Almo SC, Somasundaram T, Chapman MS, Agbandje-McKenna M, McKenna R (2002) Polylysine induces an antiparallel actin dimer that nucleates filament assembly: crystal structure at 3.5-Å resolution. J Biol Chem 277(23):20999–21006

Buckley N, Handlon AL, Malby D, Burlingame AL, Oppenheimer NJ (1994) J Org Chem 59:3609–3615

Cassel D, Pfeuffer T (1978) Mechanism of cholera toxin action: covalent modification of the guanyl nucleotide-binding protein of the adenylate cyclase system. Proc Nat Acad Sci USA 75(6):2669–2673

Chung DW, Collier RJ (1977) Enzymatically active peptide from the adenosine diphosphate-ribosylating toxin of *Pseudomonas aeruginosa*. Infect Immun 16(3):832–841

Domenighini M, Magagnoli C, Pizza M, Rappuoli R (1994) Common features of the NAD-binding and catalytic site of ADP-ribosylating toxins. Mol Microbiol 14(1):41–50

Domenighini M, Rappuoli R (1996) Three conserved consensus sequences identify the NAD-binding site of ADP-ribosylating enzymes, expressed by eukaryotes, bacteria and T-even bacteriophages. Mol Microbiol 21(4):667–674

Dominguez R (2004) Actin-binding proteins—a unifying hypothesis. Trends Biochem Sci 29(11):572–578

Etienne-Manneville S, Hall A (2002) Rho GTPases in cell biology. Nature 420(6916):629–635

Evans HR, Sutton JM, Holloway DE, Ayriss J, Shone CC, Acharya KR (2003) The crystal structure of C3stau2 from *Staphylococcus aureus* and its complex with NAD. J Biol Chem 278(46):45924–45930

Ferro AM, Oppenheimer NJ (1978) Structure of a poly (adenosine diphosphoribose) monomer: 2'-(5"-hosphoribosyl)-5'-adenosine monophosphate. Proc Nat Acad Sci USA 75(2):809–813

Fu ZQ, Guo M, Jeong BR, Tian F, Elthon TE, Cerny RL, Staiger D, Alfano JR (2007) A type III effector ADP-ribosylates RNA-binding proteins and quells plant immunity. Nature 447(7142):284–288

Fujii T, Iwane AH, Yanagida T, Namba K (2010) Direct visualization of secondary structures of F-actin by electron cryomicroscopy. Nature 467(7316):724–728

Gallivan JP, Dougherty DA (1999) Cation-pi interactions in structural biology. Proc Nat Acad Sci USA 96(17):9459–9464

Gebeyehu G, Marquez VE, Kelley JA, Cooney DA, Jayaram HN, Johns DG (1983) Synthesis of thiazole-4-carboxamide adenine dinucleotide. A powerful inhibitor of IMP dehydrogenase. J Med Chem 26(6):922–925

Han S, Arvai AS, Clancy SB, Tainer JA (2001) Crystal structure and novel recognition motif of rho ADP-ribosylating C3 exoenzyme from *Clostridium botulinum*: structural insights for recognition specificity and catalysis. J Mol Biol 305(1):95–107

Han S, Craig JA, Putnam CD, Carozzi NB, Tainer JA (1999) Evolution and mechanism from structures of an ADP-ribosylating toxin and NAD complex. Nat Struct Biol 6(10):932–936

Hassa PO, Haenni SS, Elser M, Hottiger MO (2006) Nuclear ADP-ribosylation reactions in mammalian cells: where are we today and where are we going? Microbiol Mol Biol Rev: MMBR 70(3):789–829

Hochmann H, Pust S, von Figura G, Aktories K, Barth H (2006) *Salmonella enterica* SpvB ADP-ribosylates actin at position arginine-177-characterization of the catalytic domain within the SpvB protein and a comparison to binary clostridial actin-ADP-ribosylating toxins. Biochemistry 45(4):1271–1277

Holbourn KP, Sutton JM, Evans HR, Shone CC, Acharya KR (2005) Molecular recognition of an ADP-ribosylating *Clostridium botulinum* C3 exoenzyme by RalA GTPase. Proc Nat Acad Sci USA 102(15):5357–5362

Holmes KC, Popp D, Gebhard W, Kabsch W (1990) Atomic model of the actin filament. Nature 347(6288):44–49

Honjo T, Nishizuka Y, Hayaishi O (1968) Diphtheria toxin-dependent adenosine diphosphate ribosylation of aminoacyl transferase II and inhibition of protein synthesis. J Biol Chem 243(12):3553–3555

Honjo T, Nishizuka Y, Kato I, Hayaishi O (1971) Adenosine diphosphate ribosylation of aminoacyl transferase II and inhibition of protein synthesis by diphtheria toxin. J Biol Chem 246(13):4251–4260

Hottiger MO, Hassa PO, Luscher B, Schuler H, Koch-Nolte F (2010) Toward a unified nomenclature for mammalian ADP-ribosyltransferases. Trends Biochem Sci 35(4):208–219

Iglewski BH, Kabat D (1975) NAD-dependent inhibition of protein synthesis by *Pseudomonas aeruginosa* toxin. Proc Nat Acad Sci USA 72(6):2284–2288

Jank T, Aktories K (2013) Strain-alleviation model of ADP-ribosylation. Proc Nat Acad Sci USA 110(11):4163–4164

Jørgensen R, Merrill AR, Yates SP, Marquez VE, Schwan AL, Boesen T, Andersen GR (2005) Exotoxin A-eEF2 complex structure indicates ADP ribosylation by ribosome mimicry. Nature 436(7053):979–984

Jørgensen R, Wang Y, Visschedyk D, Merrill AR (2008) The nature and character of the transition state for the ADP-ribosyltransferase reaction. EMBO Rep 9(8):802–809
Kabsch W, Mannherz HG, Suck D, Pai EF, Holmes KC (1990) Atomic structure of the actin:DNase I complex. Nature 347(6288):37–44
Kahn RA, Gilman AG (1986) The protein cofactor necessary for ADP-ribosylation of Gs by cholera toxin is itself a GTP binding protein. J Biol Chem 261(17):7906–7911
Katada T, Ui M (1982) ADP ribosylation of the specific membrane protein of C6 cells by islet-activating protein associated with modification of adenylate cyclase activity. J Biol Chem 257(12):7210–7216
Kimoto H, Fujii Y, Hirano S, Yokota Y, Taketo A (2006) Genetic and biochemical properties of streptococcal NAD-glycohydrolase inhibitor. J Biol Chem 281(14):9181–9189
Koch-Nolte F, Kernstock S, Mueller-Dieckmann C, Weiss MS, Haag F (2008) Mammalian ADP-ribosyltransferases and ADP-ribosylhydrolases. Front Biosci: J Virtual Libr 13:6716–6729
Lang AE, Schmidt G, Schlosser A, Hey TD, Larrinua IM, Sheets JJ, Mannherz HG, Aktories K (2010) *Photorhabdus luminescens* toxins ADP-ribosylate actin and RhoA to force actin clustering. Science 327(5969):1139–1142
Margarit SM, Davidson W, Frego L, Stebbins CE (2006) A steric antagonism of actin polymerization by a salmonella virulence protein. Structure 14(8):1219–1229
McLaughlin PJ, Gooch JT, Mannherz HG, Weeds AG (1993) Structure of gelsolin segment 1-actin complex and the mechanism of filament severing. Nature 364(6439):685–692
Menetrey J, Flatau G, Stura EA, Charbonnier JB, Gas F, Teulon JM, Le Du MH, Boquet P, Menez A (2002) NAD binding induces conformational changes in Rho ADP-ribosylating *Clostridium botulinum* C3 exoenzyme. J Biol Chem 277(34):30950–30957
Moss J, Garrison S, Oppenheimer NJ, Richardson SH (1979a) NAD-dependent ADP-ribosylation of arginine and proteins by *Escherichia coli* heat-labile enterotoxin. J Biol Chem 254(14):6270–6272
Moss J, Stanley SJ, Oppenheimer NJ (1979b) Substrate specificity and partial purification of a stereospecific NAD- and guanidine-dependent ADP-ribosyltransferase from avian erythrocytes. J Biol Chem 254(18):8891–8894
Moss J, Stanley SJ, Vaughan M, Tsuji T (1993) Interaction of ADP-ribosylation factor with *Escherichia coli* enterotoxin that contains an inactivating lysine 112 substitution. J Biol Chem 268(9):6383–6387
Murakami K, Yasunaga T, Noguchi TQ, Gomibuchi Y, Ngo KX, Uyeda TQ, Wakabayashi T (2010) Structural basis for actin assembly, activation of ATP hydrolysis, and delayed phosphate release. Cell 143(2):275–287
Nagahama M, Sakaguchi Y, Kobayashi K, Ochi S, Sakurai J (2000) Characterization of the enzymatic component of *Clostridium perfringens* iota-toxin. J Bacteriol 182(8):2096–2103
Noda M, Tsai SC, Adamik R, Moss J, Vaughan M (1990) Mechanism of cholera toxin activation by a guanine nucleotide-dependent 19 kDa protein. Biochim Biophys Acta 1034(2):195–199
O'Neal CJ, Jobling MG, Holmes RK, Hol WG (2005) Structural basis for the activation of cholera toxin by human ARF6-GTP. Science 309(5737):1093–1096
Oppenheimer NJ (1994) NAD hydrolysis: chemical and enzymatic mechanisms. Mol Cell Biochem 138(1–2):245–251
Oppenheimer NJ, Bodley JW (1981) Diphtheria toxin. Site and configuration of ADP-ribosylation of diphthamide in elongation factor 2. J Biol Chem 256(16):8579–8581
Otterbein LR, Cosio C, Graceffa P, Dominguez R (2002) Crystal structures of the vitamin D-binding protein and its complex with actin: structural basis of the actin-scavenger system. Proc Nat Acad Sci USA 99(12):8003–8008
Perelle S, Domenighini M, Popoff MR (1996) Evidence that Arg-295, Glu-378, and Glu-380 are active-site residues of the ADP-ribosyltransferase activity of iota toxin. FEBS Lett 395(2–3):191–194
Pintilie GD, Zhang J, Goddard TD, Chiu W, Gossard DC (2010) Quantitative analysis of cryo-EM density map segmentation by watershed and scale-space filtering, and fitting of structures by alignment to regions. J Struct Biol 170(3):427–438

Popoff MR, Milward FW, Bancillon B, Boquet P (1989) Purification of the *Clostridium spiroforme* binary toxin and activity of the toxin on HEp-2 cells. Infect Immun 57(8): 2462–2469

Popoff MR, Rubin EJ, Gill DM, Boquet P (1988) Actin-specific ADP-ribosyltransferase produced by a *Clostridium difficile* strain. Infect Immun 56(9):2299–2306

Schleberger C, Hochmann H, Barth H, Aktories K, Schulz GE (2006) Structure and action of the binary C2 toxin from *Clostridium botulinum*. J Mol Biol 364(4):705–715

Schutt CE, Myslik JC, Rozycki MD, Goonesekere NC, Lindberg U (1993) The structure of crystalline profilin-beta-actin. Nature 365(6449):810–816

Sekine A, Fujiwara M, Narumiya S (1989) Asparagine residue in the rho gene product is the modification site for botulinum ADP-ribosyltransferase. J Biol Chem 264(15):8602–8605

Shniffer A, Visschedyk DD, Ravulapalli R, Suarez G, Turgeon ZJ, Petrie AA, Chopra AK, Merrill AR (2012) Characterization of an actin-targeting ADP-ribosyltransferase from *Aeromonas hydrophila*. J Biol Chem 287(44):37030–37041

Sixma TK, Pronk SE, Kalk KH, Wartna ES, van Zanten BA, Witholt B, Hol WG (1991) Crystal structure of a cholera toxin-related heat-labile enterotoxin from *E. coli*. Nature 351(6325): 371–377

Sternweis PC, Robishaw JD (1984) Isolation of two proteins with high affinity for guanine nucleotides from membranes of bovine brain. J Biol Chem 259(22):13806–13813

Sun J, Maresso AW, Kim JJ, Barbieri JT (2004) How bacterial ADP-ribosylating toxins recognize substrates. Nat Struct Mol Biol 11(9):868–876

Sundriyal A, Roberts AK, Shone CC, Acharya KR (2009) Structural basis for substrate recognition in the enzymatic component of ADP-ribosyltransferase toxin CDTa from *Clostridium difficile*. J Biol Chem 284(42):28713–28719

Tsuge H, Nagahama M, Nishimura H, Hisatsune J, Sakaguchi Y, Itogawa Y, Katunuma N, Sakurai J (2003) Crystal structure and site-directed mutagenesis of enzymatic components from *Clostridium perfringens* iota-toxin. J Mol Biol 325(3):471–483

Tsuge H, Nagahama M, Oda M, Iwamoto S, Utsunomiya H, Marquez VE, Katunuma N, Nishizawa M, Sakurai J (2008) Structural basis of actin recognition and arginine ADP-ribosylation by *Clostridium perfringens* iota-toxin. Proc Nat Acad Sci USA 105(21): 7399–7404

Tsurumura T, Tsumori Y, Qiu H, Oda M, Sakurai J, Nagahama M, Tsuge H (2013) Arginine ADP-ribosylation mechanism based on structural snapshots of iota-toxin and actin complex. Proc Nat Acad Sci USA 110(11):4267–4272

Vandekerckhove J, Schering B, Barmann M, Aktories K (1987) *Clostridium perfringens* iota toxin ADP-ribosylates skeletal muscle actin in Arg-177. FEBS Lett 225(1–2):48–52

Visschedyk D, Rochon A, Tempel W, Dimov S, Park HW, Merrill AR (2012) Certhrax toxin, an anthrax-related ADP-ribosyltransferase from *Bacillus cereus*. J Biol Chem 287(49): 41089–41102

Vogelsgesang M, Stieglitz B, Herrmann C, Pautsch A, Aktories K (2008) Crystal structure of the *Clostridium limosum* C3 exoenzyme. FEBS Lett 582(7):1032–1036

Wilde C, Just I, Aktories K (2002) Structure-function analysis of the Rho-ADP-ribosylating exoenzyme C3stau2 from *Staphylococcus aureus*. Biochemistry 41(5):1539–1544

Zhang RG, Scott DL, Westbrook ML, Nance S, Spangler BD, Shipley GG, Westbrook EM (1995) The three-dimensional crystal structure of cholera toxin. J Mol Biol 251(4):563–573

Regulation of Nitrogenase by Reversible Mono-ADP-Ribosylation

Vivian R. Moure, Flavia F. Costa, Leonardo M. Cruz, Fabio O. Pedrosa, Emanuel M. Souza, Xiao-Dan Li, Fritz Winkler and Luciano F. Huergo

Abstract Posttranslational modification of proteins plays a key role in the regulation of a plethora of metabolic functions. Protein modification by mono-ADP-ribosylation was first described as a mechanism of action of bacterial toxins. Since these pioneering studies, the number of pathways regulated by ADP-ribosylation in organisms from all domains of life expanded significantly. However, in only a few cases the full regulatory ADP-ribosylation circuit is known. Here, we review the system where mono-ADP-ribosylation regulates the activity of an enzyme: the regulation of nitrogenase in bacteria. When the nitrogenase product, ammonium, becomes available, the ADP-ribosyltransferase (DraT) covalently links an ADP-ribose moiety to a specific arginine residue on nitrogenase switching-off nitrogenase activity. After ammonium exhaustion, the ADP-ribosylhydrolase (DraG) removes the modifying group, restoring nitrogenase activity. DraT and DraG activities are reversibly regulated through interaction with P_{II} signaling proteins. Bioinformatics analysis showed that DraT homologs are restricted to a few nitrogen-fixing bacteria while DraG homologs are widespread in Nature. Structural comparisons indicated that bacterial DraG is closely related to Archaea

Electronic Supplementary Material The online version of this article (DOI:10.1007/82_2014_380) contains supplementary material (Table S1 and Table S2), which is available to authorized users.

V. R. Moure · F. F. Costa · L. M. Cruz · F. O. Pedrosa · E. M. Souza · L. F. Huergo (✉)
Instituto Nacional de Ciência e Tecnologia da Fixação Biológica de Nitrogênio, Departamento de Bioquímica e Biologia Molecular, UFPR, Curitiba, PR, Brazil
e-mail: huergo@ufpr.br

X.-D. Li · F. Winkler
Biomolecular Research, Paul Scherrer Institut, CH-5232 Villigen, Switzerland

Current Topics in Microbiology and Immunology (2015) 384: 89–106
DOI: 10.1007/82_2014_380

Published Online: 17 June 2014

and mammalian ADP-ribosylhydrolases (ARH). In all available structures, the ARH active site consists of a hydrophilic cleft carrying a binuclear Mg^{2+} or Mn^{2+} cluster, which is critical for catalysis.

Contents

1 Introduction

Protein mono-ADP-ribosylation is emerging as an important posttranslational modification affecting various biological processes. In some nitrogen-fixing bacteria, the nitrogenase activity is regulated through reversible mono-ADP-ribosylation. This covalent modification is catalyzed by the mono-ADP-ribosyltransferase (DraT) and is reverted by the mono-ADP-ribosylhydrolase (DraG). Here, we focus on the current biochemical and structural knowledge on how DraT and DraG affect nitrogenase activity. After a brief review of the biochemical aspects of N_2 reduction to ammonia catalyzed by nitrogenase and its regulation by arginine mono-ADP-ribosylation, we review the properties and distribution of DraT- and DraG-related enzymes and present structural comparisons between DraG and its homologs. Finally, we introduce the current model for the reciprocal regulation of DraT and DraG in response to ammonium in nitrogen-fixing organisms.

2 Biological Nitrogen Fixation

Nitrogen is an essential element for life. The most abundant source of nitrogen in nature is dinitrogen gas (N_2), corresponding to 78 % of the atmosphere. In the N_2 form, nitrogen is chemically inert due to the strength of the triple bond,

nonpolarity, and high ionization potential. In order to be assimilated into biomolecules, N_2 needs to be reduced to ammonia (NH_3). The ability to convert N_2 into NH_3 in nature is restricted to a small group of prokaryotes known as diazotrophs (Postgate 1982). The diazotrophs encode a metalloenzyme complex–nitrogenase–which catalyzes the reduction of N_2 to NH_3 (Burgess and Lowe 1996). Biological nitrogen fixation is responsible for approximately 60 % of the total fixed N input from N_2 into the global biogeochemical nitrogen cycle. The remaining 40 % comes from the industrial synthesis of ammonia through the Haber-Bosch process (30 %) and oxidative N_2 fixation by lightning and combustion (10 %) (Fisher and Newton 2004).

3 Biochemistry of Nitrogenase

Nitrogenase enzymes comprise four different subgroups that are classified by their metal composition. The best characterized and most prevalent is the molybdenum (Mo)-dependent nitrogenase (Hu and Ribbe 2011). All Mo-nitrogenases are highly conserved in sequence, structure, and reaction mechanism. The *Azotobacter vinelandii* Mo-nitrogenase is the best-studied enzyme and is the focus of this section.

Mo-nitrogenase is composed of two functional components. The γ_2 homodimer (Mr $\approx$ 64,000 Da), named dinitrogenase reductase, NifH or Fe-protein and contains a [4Fe−4S] cluster and two nucleotide-binding sites (Fig. 1). Structural analysis shows that the dinitrogenase reductase [4Fe−4S] cluster is located symmetrically between the two γ subunits and is coordinated by the C98 and C133 residues (Georgiadis et al. 1992) (Fig. 1b). These cysteine residues are in close proximity to R101 (Fig. 1b), which is the site of reversible mono-ADP-ribosylation that will be discussed later.

The dinitrogenase reductase transfers electrons to second nitrogenase component, a $\alpha_2\beta_2$ heterotetramer (Mr $\approx$ 250,000 Da) named dinitrogenase, NifDK, or MoFe-protein that, in turn, reduces N_2 to NH_3 (Fig. 1a). Each $\alpha\beta$ dimer of the dinitrogenase contains a P cluster [8Fe−7S] at the interface between α and β subunits and an FeMo-cofactor [7Fe−9S−1Mo−C-homocitrate] within the α-subunit (Lancaster et al. 2011; Spatzal et al. 2011) (Fig. 1a). The FeMo-cofactor is the site where N_2 reduction occurs. Each $\alpha\beta$ dimer has independent catalytic activity; the $\alpha_2\beta_2$ dinitrogenase binds two γ_2 dinitrogenase reductase to form the nitrogenase complex (Fig. 1a) (Seefeldt et al. 2009).

The function of the dinitrogenase reductase is to transfer electrons to the dinitrogenase in an ATP-dependent form. In the reduced form, the Fe^{Red} protein [4Fe−4S] cluster has the oxidation state 1 + ($3Fe^{2+}$ and $1Fe^{3+}$). Two MgATP molecules bind to Fe^{Red} lowering its oxidation potential from −300 to −430 mV. Conformational changes induce a transient association between the Fe^{Red} and the dinitrogenase proteins (Seefeldt et al. 2009). The interaction between dinitrogenase reductase and dinitrogenase triggers one electron transfer within the dinitrogenase, from the P cluster to the FeMo-cofactor, reducing the active site of

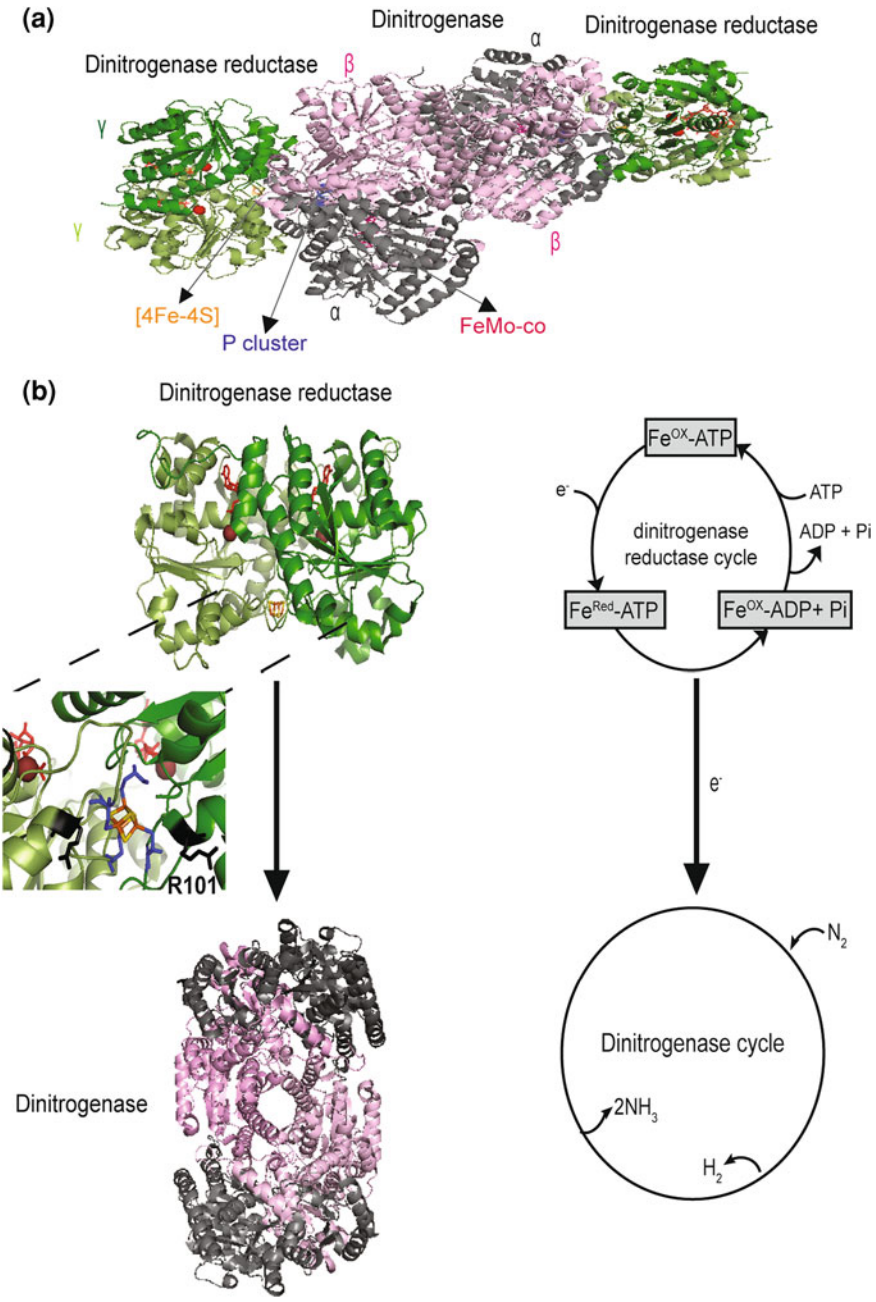
(a)
Dinitrogenase
Dinitrogenase reductase
Dinitrogenase reductase
α
β
γ
γ
β
α
[4Fe-4S]
P cluster
FeMo-co
(b)
Dinitrogenase reductase
R101
Dinitrogenase
Fe^OX-ATP
e-
ATP
dinitrogenase
reductase cycle
ADP + Pi
Fe^Red-ATP
Fe^OX-ADP+ Pi
e-
N2
Dinitrogenase cycle
2NH3
H2

◀**Fig. 1** Nitrogenase structure and catalytic cycle. **a** The structure of the *A. vinelandii* nitrogenase complex is shown illustrating the complex between two catalytic $\alpha\beta$-subunits of dinitrogenase and two dimers of dinitrogenase reductase. The γ_2 dimers of dinitrogenase reductase are shown in green and the ADP bound is shown in red. The dinitrogenase α-subunits are shown in gray and the β-subunits in *light pink*. The [4Fe−4S] cluster bridging the dinitrogenase reductase subunits, and the P cluster and FeMo−co in the dinitrogenase are indicated. **b** One dimer of the dinitrogenase reductase was rotated 90°. Inset: the dinitrogenase reductase was rotated to show the cysteine residues involved in the binding of the [4Fe−4S] cluster and the arginine 101 residues displayed as blue and black sticks, respectively. The dinitrogenase reductase cycle involves three states: reduced $[4Fe{-}4S]^{1+}$ (*Red*) and oxidized $[4Fe{-}4S]^{2+}$ (OX) with either ADP or ATP-bound. In the dinitrogenase cycle, the reduction of N_2 with the liberation of H_2 and two NH_3 molecules is represented. ADP-ribosylation of the dinitrogenase reductase R101 prevents its association with dinitrogenase blocking the enzyme activity. The nitrogenase complex structure (PDB 1N2C) and the separated dinitrogenase reductase and dinitrogenase structures (PDB 1FP6 and 1M1N) were prepared using PyMol (http://www.pymol.org)

nitrogenase. The Fe^{Red} then restores the resting state of the P cluster, becoming oxidized $[4Fe{-}4S]^{2+}$ ($2Fe^{2+}$ and $2Fe^{3+}$). The electron transfer is driven by dinitrogenase reductase ATP hydrolysis (Mayweather et al. 2012) (Fig. 1b). The oxidized MgADP-bound form of the dinitrogenase reductase dissociates from the dinitrogenase and releases two MgADP molecules to start a new reduction cycle. Eight electrons transfer events are required for the reduction of one mol of N_2 to two NH_3, consuming 16 mols of ATP (two for each electron transferred) and liberating one mol of H_2 (Hoffman et al. 2013) (Fig. 1b). The reaction stoichiometry is:

$$N_2 + 8\ e^- + 8\,H^+ + 16\ MgATP \rightarrow 2\ NH_3 + H_2 + 16\ MgADP + 16\ Pi$$

Given the high input of energy required for biological nitrogen fixation, it is not surprising that different mechanisms have evolved to control nitrogenase activity in response to the availability of alternative nitrogen sources. In this review, we will focus on the mechanism that controls nitrogenase posttranslationally through reversible mono-ADP-ribosylation. For more general reviews describing other mechanisms that regulate nitrogenase at the transcriptional and posttranslational levels see (Dixon and Kahn 2004; Huergo et al. 2012, 2013).

4 Inactivation of Nitrogenase by Reversible ADP-Ribosylation

The best-characterized mechanism of posttranslational regulation of nitrogenase occurs through reversible mono-ADP-ribosylation of one arginine residue (R101, *A. vinelandii* numbering) of the dinitrogenase reductase dimer (Pope et al. 1985). The R101 residue is solvent exposed and is in close proximity to the [4Fe−4S] cluster (Fig. 1b) (Georgiadis et al. 1992). This surface of the dinitrogenase

reductase is the docking site for the dinitrogenase (Schindelin et al. 1997) (Fig. 1a). ADP-ribosylation of dinitrogenase reductase R101 prevents its association with the dinitrogenase, inhibiting the electron transfer cycles and thereby inactivating nitrogenase (Moure et al. 2013; Murrell et al. 1988) (Fig. 1b).

Only one of the two R101 residues of the dinitrogenase reductase dimer is modified. Presumably, ADP-ribosylation of one subunit sterically blocks access of the ADP-ribosyltransferase enzyme to the second arginine site of the dinitrogenase reductase homodimer. The modification of dinitrogenase reductase can be detected in cell extracts by western blot since the ADP-ribosylated subunit has a slower migration rate than the nonmodified subunit on SDS-PAGE. Consequently, a double band pattern is observed on western blots (Kanemoto and Ludden 1984; Ludden et al. 1982).

5 The DraT and DraG Enzymes

The ADP-ribosyl-transferase that catalyzes the ADP-ribosylation of the dinitrogenase reductase is named DraT (Dinitrogenase Reductase ADP-ribosyl-Transferase). The ADP-ribosyl-hydrolase, which catalyzes the dinitrogenase reductase ADP-ribose removal is named DraG (Dinitrogenase Reductase-Activating Glycohydrolase) (Pope et al. 1985, 1986; Saari et al. 1986). These enzymes were first characterized in *Rhodospirillum rubrum* and are encoded by the *draTG* operon located upstream of the nitrogenase structural genes *nifHDK* (Liang et al. 1991). Genes sharing similarity to *draT* are restricted to bacteria and only found in diazotrophs (see Sect. 7). In stark contrast, *draG* homologs are found in all three domains of life: Bacteria, Archaea, and Eukarya (see Sect. 7). These DraG homologs share similarities at both sequence and structural levels (Huergo et al. 2012).

5.1 DraT

DraT is a 30 kDa monomer that catalyzes the transfer of ADP-ribose from NAD^+ to the R101 side chain of the dinitrogenase reductase (Lowery et al. 1986). DraT is classified as part of the cholera toxin-like ADP-ribosyl-transferases (ARTC), in which the R-S-E motif is involved in NAD^+ cosubstrate binding (Hottiger et al. 2010). However, the amino acid sequence of DraT is very different from other ARTC members. No structure of DraT has been described to date.

In contrast to the bacterial toxins, DraT can use other NAD^+ analogs such as NADP and nicotinamide mononucleotide as substrates for the modification reaction (Ponnuraj et al. 2005). However, the only known DraT ADP-ribose acceptor is the dinitrogenase reductase carrying an intact [4Fe−4S] cluster (Lowery and Ludden 1988). The ability of DraT to modify the dinitrogenase reductase is not

species specific. For instance, DraT from *R. rubrum* is able to modify the dinitrogenase reductase from other diazotrophs, including organisms that do not carry endogenous DraT/DraG such as *A. vinelandii* (Grunwald et al. 2000; Lowery and Ludden 1989; Zhang et al. 1995). This DraT cross-species reactivity toward the dinitrogenase reductase is expected given the highly conserved structure of the dinitrogenase reductase (Georgiadis et al. 1992).

5.2 DraG

DraG is a 32 kDa monomer, first purified and characterized in *R. rubrum* (Saari et al. 1984, 1986). This enzyme cleaves the N-glycosidic bond of ADP-ribosylated dinitrogenase reductase (Ljungstrom et al. 1989; Saari et al. 1984). Although DraT catalyzes the modification of only native dinitrogenase reductase, DraG is able to catalyze the removal of the ADP-ribose moiety from a number of ADP-ribosyl-arginine substrate analogs, including the denatured dinitrogenase reductase (Pope et al. 1986). ADP-ribosylated-arginine spontaneously anomerizes and is found as a mixture of the α- and β-ribosyl-guanidinum linkages. DraG activity is stereospecific acting only on α-linked ADP-ribosyl-arginine (Pope et al. 1986).

The in vitro activity of *Azospirillum brasilense* and *R. rubrum* DraG requires the presence of divalent cations, such as Mg^{2+}, Mn^{2+}, or Fe^{2+}, with Mn^{2+} being the most effective (Ljungstrom et al. 1989; Nordlund and Nóren 1984). Electron paramagnetic resonance showed that *R. rubrum* DraG has a binuclear Mn^{2+} center, which is essential for catalysis (Antharavally et al. 2001). Furthermore, crystallographic studies (see below) indicated that the presence of a binuclear metal center (composed of either Mn^{2+} or Mg^{2+}) within the active site is a common feature of all DraG homologs (Table 1).

6 Structural Relationships Among ADP-Ribosylhydrolases

The crystal structures of 10 DraG homologs, from all domains of life, have been deposited with the Protein Data Bank (PDB) (Table 1). In all cases, the overall structure is very similar, with the protein being composed of 15–19 α-helices and the active site located within a hydrophilic cleft surrounded by four internal loop regions (Li et al. 2009). The active site contains a binuclear metal center formed by two magnesium or two manganese ions octahedrally coordinated by the side chains of conserved acidic residues (Fig. 2a). The metal ions contribute to the binding of the sugar ring of ADP-ribose and also participate in the catalytic mechanism (Berthold et al. 2009).

DraG has become the archetype of arginine-specific ADP-ribosylhydrolases as it is the only enzyme of this group whose biological function is well established, its cognate substrate is known, and for which a catalytic mechanism has been

Table 1 Crystal structures of DraG homologs available in the PDB database

Organism	Protein	Ligand	Complex with	PDB code	Reference
Homo sapiens	ARH 3	Mg^{2+}	–	2FOZ	Mueller-Dieckmann et al. (2006)
	ARH 1	Mg^{2+}, ADP	–	3HFW	Kernstock et al. (2009)
Mus musculus	ARH 3	Mg^{2+}	–	2QTY	Mueller-Dieckmann et al. (2008)
R. rubrum	DraG	Mn^{2+}	–	2WOC	Berthold et al. (2009)
	DraG	Mn^{2+}, ADP-ribosyllysine	–	2WOD	Berthold et al. (2009)
	DraG	Mn^{2+}, ADP-ribose	–	2WOE	Berthold et al. (2009)
A. brasilense	DraG	Mg^{2+}	–	3G9D	Li et al. (2009)
A. brasilense	DraG	Mg^{2+}	GlnZ-ADP	305T	Rajendran et al. (2011)
M. jannaschii	ARH	Mg^{2+}	–	1T5 J	Gogos et al., unpublished
T. thermophilus	ARGH	Mg^{2+}	–	2YZV	Ebihara et al., unpublished

proposed (Berthold et al. 2009). In one of the structures of *R. rubrum* DraG, obtained in the presence of excess ADP-ribose, one DraG molecule appears to have catalyzed the reverse reaction leading to ADP-ribosylation of a lysine residue of a neighbor DraG molecule and leaving this ADP-ribosyl-lysine trapped within the DraG active site (Berthold et al. 2009). This structure supports a reaction mechanism initiated by opening the ribose ring through formation of a protonated Schiff base. After ring opening, the ribose C1' is re-positioned for nucleophilic attack by a metal activated hydroxide ion derived from water. DraG residue D97 is thought to be involved in a proton transfer event converting the hydroxylated Schiff base into the reaction products (Berthold et al. 2009).

To assess the conservation of the residues involved in the binding of metals, ADP-ribose and in catalysis, the structure of *R. rubrum* DraG was compared to the structure of its homologs (Fig. 2b and Table 2). The prokaryotic homologs are more similar to each other than they are to the mammalian ARHs. Structural comparisons using *SSM* (Krissinel and Henrick 2004) and the PDB coordinates for each protein structure showed that *A. brasilense* DraG is the most similar to *R. rubrum* DraG (Fig. 2b) with the highest *Z*-score and lowest RMSD, followed by other prokaryotic ARHs (Fig. 2b), and then by human ARH3 and 1 (Fig. 2b and Table 2). These structural similarities are also reflected in the amino acid sequence identity (Table 2).

All residues involved in metal binding are conserved among all DraG homologs, reinforcing the importance of a binuclear metal center for the activity of the mono-ADP-ribosylhydrolases. The only exception is *Methanococcus jannaschii* ARH where a metal coordination point involving T246 in *R. rubrum* DraG is substituted by S256 (Table 2 and Fig. 2b). In DraG, Mn^{2+} is the metal that

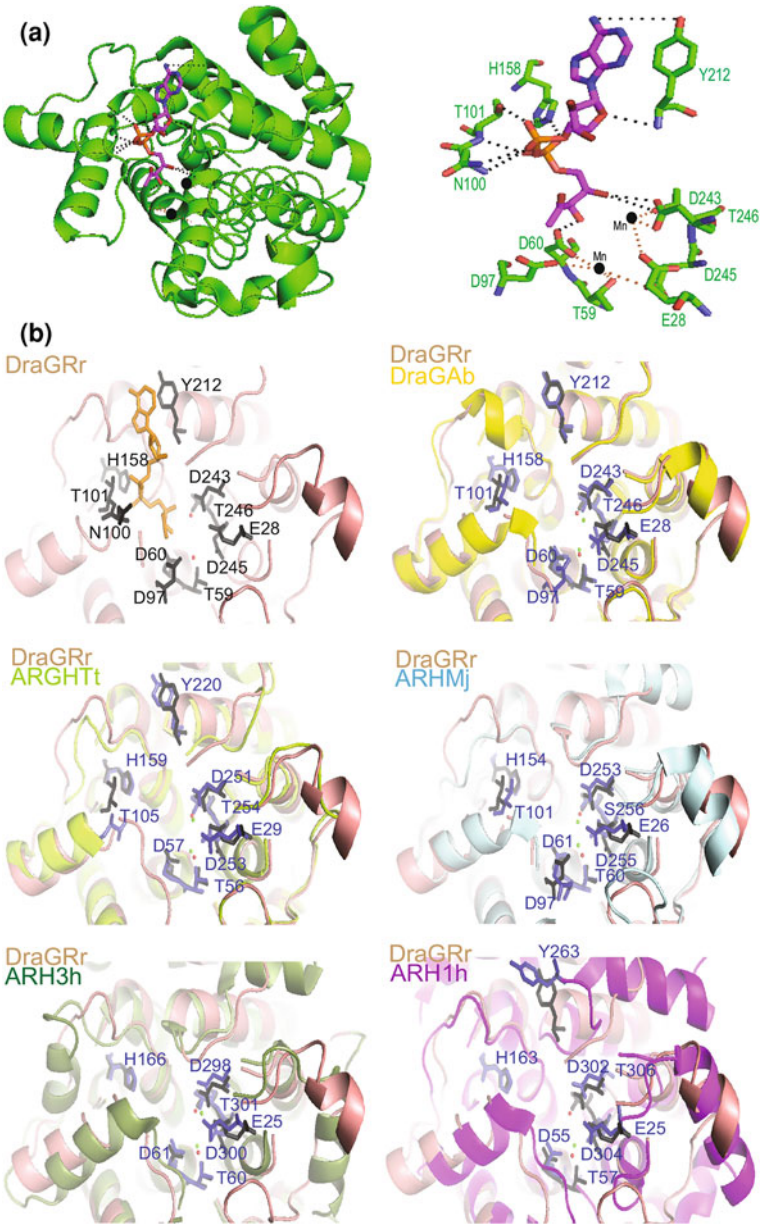
(a)
H158
Y212
T101
N100
D243
T246
Mn
D60
Mn
D97
D245
T59
E28
(b)
DraGRr
Y212
H158
D243
T101
T246
N100
E28
D60
D245
D97
T59
DraGRr
DraGAb
Y212
H158
D243
T101
T246
E28
D60
D245
D97
T59
DraGRr
ARGHTt
Y220
H159
D251
T254
T105
E29
D57
D253
T56
DraGRr
ARHMj
H154
D253
T101
S256
E26
D61
D255
T60
D97
DraGRr
ARH3h
H166
D298
T301
E25
D61
D300
T60
DraGRr
ARH1h
Y263
H163
D302
T306
E25
D55
D304
T57

◀**Fig. 2** **a** Mode of ADP-ribose binding in *Rhodospirillum rubrum* DraG (PDB 2WOD). Overall structure of *R. rubrum* DraG (*green*) with bound ADP-ribose (*magenta*) showing the details of the DraG ADP-ribose binding site. ADP-ribose is shown in *magenta* and selected DraG residues in *green*. Polar contacts between DraG residues and ADP-ribose are shown as *black dashed* lines. Interactions between DraG residues and the two Mn^{2+} ions (*black* balls) are shown in *brown dashed* lines. **b** Structural relationship between *R. rubrum* DraG and its homologs. *R. rubrum* DraG (PDB 2WOD) (DraGRr). Structural alignment between *R. rubrum* DraG and: (DraGAb) *A. brasilense* DraG (PDB 3G9D); (ARGHTt) *Thermus thermophilus* ARH (PDB 2YZV); (ARHMj) *Methanococcus jannaschii* ARH (PDB 1T5 J); (ARH3 h) human ARH 3 (PDB 2FOZ); and (ARH1 h) human ARH 1 (PDB 3HFW). The main amino acid residues participating in catalytic mechanism, metal, and ADP-ribose binding are highlighted in *black* sticks in the *R. rubrum* DraG structure, its equivalents in the other structures are shown in *dark blue* sticks. ADP-ribose is shown in *orange* sticks. Mn^{2+} and Mg^{2+} are shown as spheres in *red* and *green*, respectively. The overlapped structures were generated aligning the structures using PyMol

promotes maximum activity at lower concentrations (Ljungstrom et al. 1989; Saari et al. 1986). The preference of Mn^{2+} over Mg^{2+} apparently reflects its higher binding affinity to the DraG active site (V.R. Moure, unpublished). Based on the structures of *R. rubrum* DraG, it was postulated that the preference for Mn^{2+} is based on the longer coordination distances of this metal (Berthold et al. 2009). Historically, mammalians ARH have been tested in vitro in the presence of Mg^{2+}. It remains to be determined if the preference for Mn^{2+} over Mg^{2+} is a common feature of the whole ARH family.

Most of the residues that participate in the catalytic mechanism of *R. rubrum* DraG are conserved among other ARHs (Table 2 and Fig. 2b). The exception is D97, which seems critical for catalysis (Berthold et al. 2009). This residue is replaced by glycine in human ARH1 and ARH3 and in *Thermus thermophilus* ARH. Other differences concern residues involved in the binding of ADP-ribose. Among these, only *R. rubrum* DraG H158 is fully conserved throughout the ARH family (Table 2, Fig. 2a). While both H158 and T101 residues of *R. rubrum* DraG make important side chain contacts with the ADP-ribose di-phosphate (Berthold et al. 2009), T101 is absent in human ARH representatives (Table 2, Fig. 2a).

The lack of the critical D97 and T101 residues in human ARHs suggests that these homologs might have slightly different functions. Indeed, the preferred substrate for human ARH3 are poly-ADP-ribosylated substrates (PAR) and, apparently, ARH3 cannot remove the last remaining ADP-ribose moiety of its target substrates (Mueller-Dieckmann et al. 2006). The active site of ARH3 may have evolved to accommodate PAR substrates and cleave sugar-sugar O-glycosidic bounds. However, ARH1, which is more active toward mono-ADP-ribosylated substrates, still lacks D97 and T101, critical residues for substrate binding and catalysis. In addition to ADP-ribose cleavage, human ARH1 and ARH3 can hydrolyze O-acetyl-ADP-ribose in vitro (Kasamatsu et al. 2011; Mueller-Dieckmann et al. 2006). The interpretation of the structural particularities found within the active site of human ARH1 and ARH3 will rely on the precise identification of the physiologically relevant substrates for each of these enzymes.

Table 2 Conservation of amino acids implied in catalytic mechanism, metal ion, and ADP-ribose binding in DraG homologs and structural comparison of *R. rubrum* DraG with its homologs using the search algorithms from *SSM* (Krissinel and Henrick 2004—PDBeFOLD)

Residue function	*R. rubrum* DraG[a]	*A. brasilense* DraG	*Homo sapiens* ARH 3	*Homo sapiens* ARH 1	*M. jannaschii* ARH	*T. thermophilus* ARH
Catalysis	D97	D97	–	–	D97	*
	E28	E28	E25	E25	E26	E29
	D60	D60	D61	D55	D61	D57
Metal binding	D243	D243	D298	D302	D253	D251
	T246	T246	T301	T306	S256	T254
	D245	D245	D300	D304	D255	D253
	T59	T59	T60	T57	T60	T56
Side chain interaction with ADP-ribose	N100	–	–	–	–	*
	T101	T101	–	–	T101	T105
	H158	H158	H166	H163	H154	H159
	Y212	Y212	–	Y263	–	Y220
RMSD (Å)[b]		0.75	1.77	1.83	1.52	1.15
Z-score [b]		15.11	10.78	9.37	11.40	12.44
N° of residues	294	297	363	357	313	303
Sequence identity (%)		63	25	21	29	35

[a] The main residues involved in the catalytic mechanism, metal coordination and ADP-ribose binding were selected according to *R. rubrum* DraG structure (Berthold et al. 2009)

[b] The homologs residues were reported based on structures alignment of *R. rubrum* DraG and its homologs separately using PyMol. The RMSD and Z-score values were reported by the PDBeFOLD

– the corresponding residue is absent

* the electron density is absent in the structure

7 Distribution of DraT and DraG Homologs

In order to determine the extent of the distribution of both *draG* and *draT* genes, a BlastP search was performed using the *A. brasilense* DraT (Uniprot AZOBR_70132) and DraG (Uniprot AZOBR_70133) as queries against the protein database (August 2013).

For the DraG search, the BlastP results were filtered for sequence showing at least 20 % identity and expected value threshold of 1×10^{-3}. The use of this relatively low E-value cutoff was based on the fact that the structural comparison between *A. brasilense* DraG and human ARH3 indicated a clear evolutionary relation despite the relatively low E-values obtained in BlastP comparisons (E-value 1×10^{-3}). The result of this DraG search indicated that DraG homologs are widespread in nature being found in 1,405 organisms representing all domains of life including viruses (Table S1).

For the DraT search, the BlastP results were filtered for sequence showing at least 20 % identity and expected value threshold of 1×10^{-20}. The protein hits excluded using these cutoff parameters were clearly unrelated to DraT since there was a big gap between the E-value of the last hit considered as positive (E-value 1×10^{-24}) and the E-value of the first excluded hit (E-value 0.39). The result of this search indicated that, in stark contrast to DraG, DraT homologs are restricted to Bacteria, representing 93 different organisms, most of them belonging to α, β, γ, or δ Proteobacteria. Other bacterial classes, including Chrysiogenales, Deferribacterales, Opitutae, and Verrucomicrobiae, were also identified in this analysis (Table S2).

All the organisms containing a *draT* homolog also encoded for the minimal set of proteins required for the assembly of the nitrogenase enzyme (NifH, NifD, NifK, NifN, NifB, NifE) (dos Santos et al. 2012) and most of them contain *draG* homologs (Table S2). Given that DraT is apparently restricted to nitrogen-fixing organisms (Table S2), we speculate that the only function of DraT is to catalyze dinitrogenase reductase ADP-ribosylation. On the other hand, the extensive distribution of DraG related proteins in non-nitrogen-fixing prokaryotes (Table S1) supports that other cellular processes, apart from nitrogen fixation, might be regulated by ADP-ribosylation (Souza and Aravind 2012). The identification of novel cellular processes where ADP-ribosylation plays a role is a possible fertile ground for future studies in prokaryotes.

8 The Regulation of DraT and DraG in Bacteria

The regulation of DraT and DraG is best described in *A. brasilense* and *R. rubrum.* In these organisms, nitrogenase is switched-off by DraT-catalyzed ADP-ribosylation of dinitrogenase reductase when ammonium becomes available in the environment or when these organisms are exposed to low-energy conditions such

as anaerobiosis (in the organotrophic *A. brasilense*) or darkness (in the phototropic *R. rubrum*) (Huergo et al. 2012; Nordlund and Högbom 2013).

When ammonium is exhausted from the medium or when the oxygen (*A. brasilense*) or light (*R. rubrum*) return to optimum levels, the ADP-ribosyl group attached to dinitrogenase reductase is removed by DraG. In order to avoid a futile cycle of ADP-ribosylation, DraT and DraG activities are reciprocally regulated in response to both ammonium and energy signals.

The mechanism that regulates DraT and DraG in response to the energy signal (oxygen or light) is still elusive. In contrast, much more is known about the ammonium signaling pathway where the P_{II} signaling proteins regulate DraT and DraG reciprocally (Huergo et al. 2012). The role of P_{II} proteins in the control of DraT and DraG is best described in *A. brasilense* and only this organism will be considered here. For reviews describing the particularities found in other organisms see (Huergo et al. 2012; Nordlund and Högbom 2013).

8.1 The Role of the P_{II} Proteins

The current model in *A. brasilense* supports that DraG has a default activity which is downregulated upon interaction with P_{II}. In contrast, DraT default state is inactive; becoming active upon interaction with P_{II} (Huergo et al. 2012).

P_{II} proteins are structurally conserved homotrimeric proteins widely distributed in Archaea, Bacteria, and plants (Forchhammer 2008). The P_{II} proteins act as sensing and signaling modules. These functions rely on the ability of P_{II} to physically interact and regulate the activities of a wide range of target proteins. The P_{II}–target protein interactions are, in turn, controlled by the levels of ATP, ADP, and 2-oxoglurate (2-OG); these molecules act as allosteric modulators of P_{II} (for a review see Huergo et al. 2013). ATP and ADP bind competitively to three nucleotide-binding sites located in the lateral clefts between P_{II} subunits (Jiang and Ninfa 2007; Xu et al. 1998). Three 2-OG binding sites are located in the vicinity of the nucleotide-binding sites and the binding of 2-OG requires the preoccupancy of the P_{II} nucleotide-binding site by MgATP (Fokina et al. 2010; Gerhardt et al. 2012; da Rocha et al. 2013; Truan et al. 2010).

In *A. brasilense,* two P_{II} paralogs sharing 67 % amino acid identity, namely GlnB and GlnZ, were identified (de Zamaroczy 1998). In addition to the allosteric regulation by ATP, ADP, and 2-OG, GlnB and GlnZ are subjected to reversible uridylylation catalyzed by the bifunctional uridylyltransferase/uridylyl-removing enzyme GlnD in response to glutamine levels. This covalent modification occurs at a conserved residue (Y51) present on each of the three P_{II} monomers (Araújo et al. 2008).

Under nitrogen-fixing conditions, the intracellular glutamine is low and 2-OG is high. GlnB and GlnZ are uridylylated and bound to MgATP and 2-OG, under this particular structural state, the P_{II} proteins cannot interact with DraT and DraG (Huergo et al. 2006a, 2007, 2009). DraG and DraT keep their default status, which

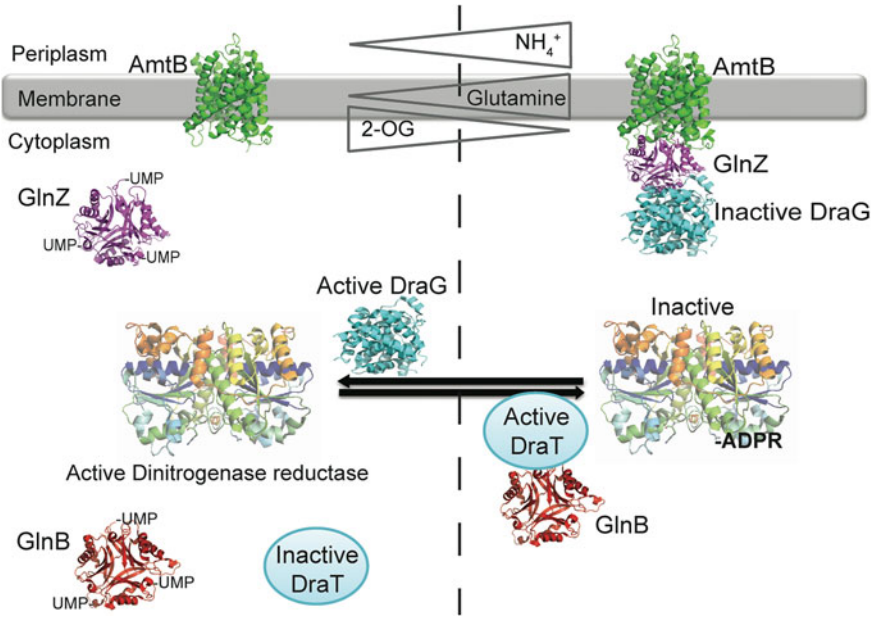

Fig. 3 Model for the regulation of DraT and DraG activities in response to ammonium in *A. brasilense*. The *left* part shows the nitrogen-fixing condition, the P_{II} proteins, GlnB and GlnZ are uridylylated and uncomplexed to DraT and DraG. DraG is active and DraT is inactive, the dinitrogenase reductase is unmodified allowing nitrogen fixation to occur. Upon ammonium shock (*right* part), GlnB and GlnZ are de-uridylylated. GlnB interacts with DraT turning the enzyme into an active form, which ADP-ribosylates the R101 of dinitrogenase reductase switching-off nitrogenase. DraG is directed to the membrane through the formation of the AmtB-GlnZ-DraG ternary complex resulting in DraG inactivation by active site steric hindrance. Adapted from Huergo et al. (2009). The protein structures were prepared from the PDB files 1FP6 (dinitrogenase reductase), 3MHY (P_{II} proteins), 3G9D (DraG) 1U77 (AmtB) using PyMol

are active and inactive, respectively. Consequently, dinitrogenase reductase remains unmodified allowing nitrogen fixation to occur.

When ammonium ions increase, the glutamine levels also increase while 2-OG decreases. GlnB and GlnZ are de-uridylylated and become bound to ADP, under this particular structural state, GlnB and GlnZ physically interact with DraT and DraG, respectively (Gerhardt et al. 2012; Huergo et al. 2006a, 2007, 2009).

The formation of the DraT-GlnB complex results in DraT conformational changes activating the ADP-ribosyltransferase and therefore promoting dinitrogenase reductase ADP-ribosylation and nitrogenase inactivation (Moure et al. 2013) (Fig. 3). Under these conditions, the DraG-GlnZ complex moves toward the cell membrane where it binds to the ammonium transporter AmtB, resulting in DraG inactivation (Gerhardt et al. 2012; Huergo et al. 2006a, b, 2009; Rajendran et al. 2011; Rodrigues et al. 2011) (Fig. 3).

The structure of the DraG-GlnZ complex has been solved. GlnZ interacts with the solvent exposed α-helix 5 on the DraG surface. This helix is also present in other DraG homologs; therefore, it is a candidate site for the docking of putative ARH regulators in other organisms (Rajendran et al. 2011).

The structure of DraG bound to GlnZ is virtually identical to that of DraG alone, precluding conformational changes as the mechanism of enzyme inactivation (Rajendran et al. 2011). Structural modeling supports that DraG is inactivated when bound to GlnZ due to steric hindrance of the DraG active site (Rajendran et al. 2011). The formation of the AmtB-GlnZ-DraG ternary complex on the membrane would enhance the affinity between GlnZ and DraG further avoiding access of the ADP-ribosylated dinitrogenase reductase substrate to the DraG active site.

9 Conclusions

The control of nitrogenase activity through reversible ADP-ribosylation is the best-described system where mono-ADP-ribosylation regulates an enzyme activity. ADP-ribosylation of the nitrogenase dinitrogenase reductase blocks the docking site between the nitrogenase components, thereby inhibiting nitrogenase activity. The enzymes responsible for the nitrogenase modification (DraT) and de-modification (DraG) have been extensively characterized.

ADP-ribosyltransferase DraT homologs are restricted to a few nitrogen-fixing organisms. DraT is expressed on a default inactive state, which is converted to an active form upon interaction with the P_{II} protein GlnB. The DraT activation probably results from conformational changes induced upon GlnB binding. Much more progress has been made with the nitrogenase ADP-ribosyl-hydrolase DraG. Several crystal structures of bacterial DraG have been determined including: a structure where a reaction intermediate was trapped inside the DraG active site; and the structure of the complex between DraG and its regulatory partner GlnZ. This wealth of data allowed a better understanding of the DraG reaction mechanism as well as its mode of regulation.

In the recent years, there has been an exponential increase in the number of key biological processes where ADP-ribosylation apparently plays a role. DraG homologs are widespread in Nature and, quite remarkably, their general structure and their active site are well conserved throughout all domains of life. The lessons learned with the bacterial DraG can help to elucidate the function, mechanism of action, and regulation of ARH homologs derived from more complex forms of life such as mammals.

Acknowledgments The authors thank the Brazilian Research Council (CNPq), CAPES, National Institute of Science and Technology of Biological Nitrogen Fixation (CNPq/INCT FBN), and Fundação Araucária for financial support.

References

Antharavally BS, Poyner RR, Zhang Y et al (2001) Effects of specific amino acid substitutions on activities of dinitrogenase reductase-activating glycohydrolase from *Rhodospirillum rubrum*. J Bacteriol 183:5743–5746

Araújo LM, Huergo LF, Invitti AL et al (2008) Different responses of the GlnB and GlnZ proteins upon in vitro uridylylation by the *Azospirillum brasilense* GlnD protein. Braz J Med Biol Res 41:289–294

Berthold CL, Wang H, Nordlund S et al (2009) Mechanism of ADP-ribosylation removal revealed by the structure and ligand complexes of the dimanganese mono-ADP-ribosylhydrolase DraG. Proc Natl Acad Sci 106:14247–14252

Burgess BK, Lowe DJ (1996) Mechanism of molybdenum nitrogenase. Chem Rev 96:2983–3012

Da Rocha RA, Weschenfelder TA, de Castilhos F et al (2013) Mathematical model of the binding of allosteric effectors to the *Escherichia coli* PII signal transduction protein GlnB. Biochemistry (Mosc) 52:2683–2693

de Souza RF, Aravind L (2012) Identification of novel components of NAD-utilizing metabolic pathways and prediction of their biochemical functions. Mol BioSyst 8:1661–1677

de Zamaroczy M (1998) Structural homologues PII and Pz of Azospirillum brasilense provide intracellular signalling for selective regulation of various nitrogen-dependent functions. Mol Microbiol 29:449–463

Dixon R, Kahn D (2004) Genetic regulation of biological nitrogen fixation. Nat Rev Microbiol 2:621–631

Dos Santos PC, Fang Z, Mason SW et al (2012) Distribution of nitrogen fixation and nitrogenase-like sequences amongst microbial genomes. BMC Genom 13:162–173

Fisher F, Newton WE (2004) Nitrogen fixation: an historical perspective. In: Smith BE, Richards RL, Newton WE (eds) Catalysts for nitrogen fixation: nitrogenases, relevant chemical models and commercial processes. Kluwer Academic, Dordrecht, pp 1–31

Fokina O, Chellamuthu V-R, Forchhammer K et al (2010) Mechanism of 2-oxoglutarate signaling by the *Synechococcus elongatus* PII signal transduction protein. Proc Natl Acad Sci 107:19760–19765

Forchhammer K (2008) PII signal transducers: novel functional and structural insights. Trends Microbiol 16:65–72

Georgiadis MM, Komiya H, Chakrabarti P et al (1992) Crystallographic structure of the nitrogenase iron protein from *Azotobacter vinelandii*. Science 257:1653–1659

Gerhardt ECM, Araujo LM, Ribeiro RR et al (2012) Influence of the ADP/ATP ratio, 2-oxoglutarate and divalent ions on *Azospirillum brasilense* PII protein signalling. Microbiology 158:1656–1663

Grunwald SK, Ryle MJ, Lanzilotta WN et al (2000) ADP-ribosylation of variants of *Azotobacter vinelandii* dinitrogenase reductase by *Rhodospirillum rubrum* dinitrogenase reductase ADP-ribosyltransferase. J Bacteriol 182:2597–2603

Hoffman BM, Lukoyanov D, Dean DR et al (2013) Nitrogenase: a draft mechanism. Accounts Chem Res 46:587–595

Hottiger MO, Hassa PO, Lüscher B et al (2010) Toward a unified nomenclature for mammalian ADP-ribosyltransferases. Trends Biochem Sci 35:208–219

Hu Y, Ribbe MW (2011) Historic overview of nitrogenase research. (Nitrogen fixation). Meth Mol Biol 766:3–7

Huergo LF, Chubatsu LS, Souza EM et al (2006a) Interactions between PII proteins and the nitrogenase regulatory enzymes DraT and DraG in *Azospirillum brasilense*. FEBS Lett 580:5232–5236

Huergo LF, Souza EM, Araujo MS et al (2006b) ADP-ribosylation of dinitrogenase reductase in *Azospirillum brasilense* is regulated by AmtB-dependent membrane sequestration of DraG. Mol Microbiol 59:326–337

Huergo LF, Merrick M, Pedrosa FO et al (2007) Ternary complex formation between AmtB, GlnZ and the nitrogenase regulatory enzyme DraG reveals a novel facet of nitrogen regulation in bacteria. Mol Microbiol 66:1523–1535

Huergo LF, Merrick M, Monteiro RA et al (2009) In vitro interactions between the PII proteins and the nitrogenase regulatory enzymes dinitrogenase reductase ADP-ribosyltransferase (DraT) and dinitrogenase reductase-activating glycohydrolase (DraG) in *Azospirillum brasilense*. J Biol Chem 284:6674–6682

Huergo LF, Pedrosa FO, Muller-Santos M et al (2012) PII signal transduction proteins: pivotal players in post-translational control of nitrogenase activity. Microbiology 158:176–190

Huergo LF, Chandra G, Merrick M (2013) P(II) signal transduction proteins: nitrogen regulation and beyond. FEMS Microbiol Rev 37:251–283

Jiang P, Ninfa AJ (2007) *Escherichia coli* PII signal transduction protein controlling nitrogen assimilation acts as a sensor of adenylate energy charge in vitro. Biochemistry (Mosc) 46: 12979–12996

Kanemoto RH, Ludden PW (1984) Effect of ammonia, darkness, and phenazine methosulfate on whole-cell nitrogenase activity and Fe protein modification in *Rhodospirillum rubrum*. J Bacteriol 158:713–720

Kasamatsu A, Nakao M, Smith BC et al (2011) Hydrolysis of O-acetyl-ADP-ribose isomers by ADP-ribosylhydrolase 3. J Biol Chem 286:21110–21117

Kernstock S, Koch-Nolte F, Mueller-Dieckmann J et al (2009) Cloning, expression, purification and crystallization as well as X-ray fluorescence and preliminary X-ray diffraction analyses of human ADP-ribosylhydrolase 1. Acta Crystallograph Sect F Struct Biol Cryst Commun 65:529–532

Krissinel E, Henrick K (2004) Secondary-structure matching (SSM), a new tool for fast protein structure alignment in three dimensions. Acta Crystallogr D Biol Crystallogr 60:2256–2268

Lancaster KM, Roemelt M, Ettenhuber P et al (2011) X-ray emission spectroscopy evidences a central carbon in the nitrogenase iron-molybdenum cofactor. Science 334:974–977

Li X-D, Huergo LF, Gasperina A et al (2009) Crystal structure of dinitrogenase reductase-activating glycohydrolase (DRAG) reveals conservation in the ADP-ribosylhydrolase fold and specific features in the ADP-ribose-binding pocket. J Mol Biol 390:737–746

Liang JH, Nielsen GM, Lies DP et al (1991) Mutations in the *draT* and *draG* genes of *Rhodospirillum rubrum* result in loss of regulation of nitrogenase by reversible ADP-ribosylation. J Bacteriol 173:6903–6909

Ljungstrom E, Yates MG, Nordlund S (1989) Purification of the activating enzyme for the Fe protein of nitrogenase from *Azospirillum brasilense*. Biochim Biophys Acta 994:210–214

Lowery RG, Ludden PW (1988) Purification and properties of dinitrogenase reductase ADP-ribosyltransferase from the photosynthetic bacterium *Rhodospirillum rubrum*. J Biol Chem 263:16714–16719

Lowery RG, Ludden PW (1989) Effect of nucleotides on the activity of dinitrogenase reductase ADP-ribosyltransferase from *Rhodospirillum rubrum*. Biochemistry (Mosc) 28:4956–4961

Lowery RG, Saari LL, Ludden PW (1986) Reversible regulation of the nitrogenase iron protein from *Rhodospirillum rubrum* by ADP-ribosylation in vitro. J Bacteriol 166:513–518

Ludden PW, Preston GG, Dowling TE (1982) Comparison of active and inactive forms of iron protein from *Rhodospirillum rubrum*. Biochem J 203:663–668

Mayweather D, Danyal K, Dean DR et al (2012) Temperature invariance of the nitrogenase electron transfer mechanism. Biochemistry (Mosc) 51:8391–8398

Moure VR, Danyal K, Yang Z-Y et al (2013) The nitrogenase regulatory enzyme dinitrogenase reductase ADP-ribosyltransferase (DraT) is activated by direct interaction with the signal transduction protein GlnB. J Bacteriol 195:279–286

Mueller-Dieckmann C, Kernstock S, Lisurek M et al (2006) The structure of human ADP-ribosylhydrolase 3 (ARH3) provides insights into the reversibility of protein ADP-ribosylation. Proc Natl Acad Sci USA 103:15026–15031

Mueller-Dieckmann C, Kernstock S, Mueller-Dieckmann J et al (2008) Structure of mouse ADP-ribosylhydrolase 3 (mARH3). Acta Crystallogr., Sect. F: Struct. Biol. Cryst. Commun 64:156–162

Murrell SA, Lowery RG, Ludden PW (1988) ADP-ribosylation of dinitrogenase reductase from *Clostridium pasteurianum* prevents its inhibition of nitrogenase from *Azotobacter vinelandii*. Biochem J 251:609–612

Nordlund S, Högbom M (2013) ADP-ribosylation, a mechanism regulating nitrogenase activity. FEBS J 280:3484–3490

Nordlund S, Noren A (1984) Dependence on divalent cations of the activation of inactive Fe-protein of nitrogenase from *Rhodospirillum rubrum*. Biochim Biophys Acta, Protein Struct Mol Enzym 791:21–27

Ponnuraj RK, Rubio LM, Grunwald SK et al (2005) NAD-, NMN-, and NADP-dependent modification of dinitrogenase reductases from *Rhodospirillum rubrum* and *Azotobacter vinelandii*. FEBS Lett 579:5751–5758

Pope MR, Murrell SA, Ludden PW (1985) Covalent modification of the iron protein of nitrogenase from *Rhodospirillum rubrum* by adenosine diphosphoribosylation of a specific arginine residue. Proc Natl Acad Sci 82:3173–3177

Pope MR, Saari LL, Ludden PW (1986) N-glycohydrolysis of adenosine diphosphoribosyl arginine linkages by dinitrogenase reductase activating glycohydrolase (activating enzyme) from *Rhodospirillum rubrum*. J Biol Chem 261:10104–10111

Postgate JR (1982) The fundamentals of nitrogen fixation. Cambridge University Press, New York, pp 1–5

Rajendran C, Gerhardt ECM, Bjelic S et al (2011) Crystal structure of the GlnZ-DraG complex reveals a different form of PII-target interaction. Proc Natl Acad Sci 108:18972–18976

Rodrigues TE, Souza VEP, Monteiro RA et al (2011) In vitro interaction between the ammonium transport protein AmtB and partially uridylylated forms of the P(II) protein GlnZ. Biochim Biophys Acta 1814:1203–1209

Saari LL, Triplett EW, Ludden PW (1984) Purification and properties of the activating enzyme for iron protein of nitrogenase from the photosynthetic bacterium *Rhodospirillum rubrum*. J Biol Chem 259:15502–15508

Saari LL, Pope M, Murrell S et al (1986) Studies on the activating enzyme for iron protein of nitrogenase from *Rhodospirillum rubrum*. J Biol Chem 261:4973–4977

Schindelin H, Kisker C, Schlessman JL et al (1997) Structure of ADP.AIF4$^-$-stabilized nitrogenase complex and its implications for signal transduction. Nature 387:370–376

Seefeldt LC, Hoffman BM, Dean DR (2009) Mechanism of Mo-dependent nitrogenase. Annu Rev Biochem 78:701–722

Spatzal T, Aksoyoglu M, Zhang L et al (2011) Evidence for interstitial carbon in nitrogenase FeMo cofactor. Science 334:940

Truan D, Huergo LF, Chubatsu LS et al (2010) A new PII protein structure identifies the 2-oxoglutarate binding site. J Mol Biol 400:531–539

Xu Y, Cheah E, Carr PD et al (1998) GlnK, a PII-homologue: structure reveals ATP binding site and indicates how the T-loops may be involved in molecular recognition. J Mol Biol 282:149–165

Zhang Y, Burris RH, Ludden PW et al (1995) Comparison studies of dinitrogenase reductase ADP-ribosyl transferase/dinitrogenase reductase activating glycohydrolase regulatory systems in *Rhodospirillum rubrum* and *Azospirillum brasilense*. J Bacteriol 177:2354–2359

ADP-Ribosylation of P2X7: A Matter of Life and Death for Regulatory T Cells and Natural Killer T Cells

Björn Rissiek, Friedrich Haag, Olivier Boyer, Friedrich Koch-Nolte and Sahil Adriouch

Abstract ADP-ribosyltransferases comprise a family of enzymes originally discovered as bacterial toxins and later characterised also in mammals. In mice, the ADP-ribosyltransferase ARTC2.2 is expressed at the surface of T lymphocytes and has been studied extensively. In the presence of extracellular NAD^+, ARTC2.2 ADP-ribosylates several cell surface target proteins and thereby regulates their function. P2X7, an ATP-gated cation channel, has been discovered as a prominent ARTC2.2 target at the surface of mouse T cells. ADP-ribosylation of P2X7 in the presence of low micromolar extracellular NAD^+ induces long-lasting P2X7 activation and triggers cell death. Regulatory T cell subsets (Tregs and NKT cells) are remarkably sensitive to NAD^+-induced cell death (NICD). Thus, liberation of endogenous NAD^+ by stressed cells is now viewed as a danger signal promoting immune responses by hindering regulatory T cells. This review will highlight the recent discoveries on the in vivo role of the ARTC2.2/P2X7 pathway triggered by the endogenous release of extracellular NAD^+, the relative sensitivity of lymphocytes subsets to this regulatory pathway and its pharmacological manipulation using camelid-derived ARTC2.2-blocking nanobodies.

B. Rissiek · F. Haag · F. Koch-Nolte
Institute of Immunology, University Medical Center, Hamburg-Eppendorf, Germany

B. Rissiek
Department of Neurology, University Medical Center, Hamburg-Eppendorf, Germany

O. Boyer · S. Adriouch
National Institute of Health and Medical Research (INSERM), U905 Rouen, France

O. Boyer · S. Adriouch
Institute for Research and Innovation in Biomedicine (IRIB), Normandy University, Rouen, France

O. Boyer
Laboratory of Immunology, Rouen University Hospital, Rouen, France

S. Adriouch (✉)
Institute for Research and Innovation in Biomedicine (IRIB), Rouen University, Normandy, France
e-mail: sahil.adriouch@univ-rouen.fr

Current Topics in Microbiology and Immunology (2015) 384: 107–126
DOI: 10.1007/82_2014_420

Published Online: 22 July 2014

Abbreviations

αGalCer	Alpha-galactosylceramide
ADPR	Adenosine diphosphate ribose
ART	Mono-ADP-ribosyl transferase
ATP	Adenosine triphosphate
cADPR	Cyclic ADP-ribose
CDR3	Complementarity determining region 3
ConA	Concanavalin A
DC	Dendritic cell
E-NPP	Ecto-nucleotide pyrophosphatase/phosphodiesterases
mAb	Monoclonal antibody
NAD^+	Nicotinamide adenine dinucleotide
NA	Nicotinamide
NICD	NAD^+-induced cell death
NKT	Natural killer T cell
NOD	Non-obese-diabetic
PARP	Poly-ADP-ribose polymerase
PS	Phosphatidylserine
TACE	TNFα-converting enzyme
TCR	T cell receptor
Treg	Regulatory T cell
WT	Wild-type

Contents

1 Introduction

ADP-ribosyltransferases (ARTs) comprise a family of proteins originally discovered as bacterial toxins, including diphtheria toxin of *Corynebacterium diphtheria,* cholera toxin of *Vibrio chloerae* and the C2/C3 botulinum toxins of *Clostridium botulinum*. These enzymes catalyse a post-translational modification of target proteins by covalently attaching the ADP-ribose moiety of nicotinamide adenine dinucleotide (NAD^+) to specific amino acid residues on target proteins (Honjo et al. 1968).

Toxin-related ARTs have also been discovered in and cloned from mammals. On the basis of structural features, mammalian ARTs have been divided into four groups: (i) the mammalian poly-ADP-ribose polymerases (PARPs); (ii) an NAD^+-dependent tRNA 2'-phosphotransferase (TpT); (iii) NEURL4-like ARTs (De Souza and Aravind 2012), and (iv) the extracellular membrane-associated ADP-ribosyltransferases (ecto-ARTs). The members of the first three groups fall within the diphtheria-toxin-related ARTD family in the newly proposed unified nomenclature, whereas ecto-ARTs correspond to C2/C3-toxin-related ARTC proteins (Hottiger et al. 2010). In the latter group, ARTC1–ARTC4 are expressed as GPI-anchored ecto-enzymes whereas ARTC5 is secreted as a soluble protein (Koch-Nolte et al. 2006). An arginine-specific ADP-ribosylation activity has been confirmed for human and mouse ARTC1, for the two isoforms of mouse ARTC2, and for human and mouse ARTC5 (Glowacki et al. 2002). In this review, we will focus only on the ARTC2 proteins expressed as ecto-enzymes on the surface of mouse immune cells and on their crucial regulatory function on the activity, survival, phenotype and homeostasis of these cells in situations where extracellular NAD^+ is liberated from endogenous sources.

2 Endogenous Sources of Extracellular NAD^+

An important question when examining the biological function of ecto-ARTs is the endogenous source of extracellular NAD^+ in normal and pathophysiological situations. The concentration of extracellular NAD^+ in serum has been reported to range between 0.1 and 0.3 μM, while intracellular NAD^+ concentrations are much higher at 400–500 μM. This concentration range of NAD^+ in serum is approximately five fold lower than that required in vitro to observe ARTC2.2-mediated effects (Davies et al. 1999; Haag et al. 2007). Several studies have, however, demonstrated that NAD^+ can be released from intracellular sources (Scheuplein et al. 2009). Release of NAD^+ into the extracellular space is observed under

conditions where cells are stressed by various means (e.g., mechanical shear forces, oxidative stress) and, obviously, in conditions where cells are dying (Haag et al. 2007; Scheuplein et al. 2009; Seman et al. 2004). In this line, we found that acute inflammation is associated with the liberation of significant amounts of NAD^+ (1–10 μM range) into the extracellular milieu (Adriouch et al. 2007). Interestingly, NAD^+ liberated into the inflammatory site can diffuse to some extent and reach local draining lymph nodes where it induces measurable ARTC2.2-dependent effects on the phenotype and on the function of T lymphocytes (Adriouch et al. 2007). This is compatible with the relatively long half-life of extracellular NAD^+ as compared to ATP in biological contexts (15 min vs. only a few seconds in plasma) (Scheuplein et al. 2009; Burnstock 2006; Burnstock and Kennedy 2011).

3 Degradation of Extracellular NAD^+ by CD38 and Other NAD^+-Catabolising Ecto-enzymes

Enzymes that can hydrolyse extracellular NAD^+ involve three known families of ecto-enzymes: (i) NAD^+-glycohydrolases/ADP-ribose cyclases (CD38 and CD157), (ii) ecto-nucleotide pyrophosphatases/phosphodiesterases (E-NPPs) such as PC-1 (CD203) and (iii) the 5'-ecto-nucleotidase CD73, which is reported to directly degrade NAD^+ (Haag et al. 2007; Garavaglia et al. 2012). Some members of the ART family, e.g. rat ARTC2 and mouse ARTC5 also exhibit potent NADase activity (Haag et al. 1995; Weng et al. 1999). These enzymes, by degrading extracellular NAD^+, directly compete with the NAD^+-dependent arginine-ADP-ribosylation activity of ecto-ARTs. We and others found that the half-life of NAD^+ in biological fluids is considerably increased in $CD38^{-/-}$ mice, suggesting that CD38 plays a major role in the hydrolysis of NAD^+ in vivo (Adriouch et al. 2007; Cockayne et al. 1998). Indeed, CD38 expressed predominantly by B lymphocytes competes with ARTC2.2 expressed on T lymphocytes for the consumption of extracellular NAD^+ and significantly limits the amount of ADP-ribosylation on the surface of T lymphocytes in normal conditions (Krebs et al. 2005). Hence, upon its release into the extracellular space by stressed cells, at sites of inflammation or upon cell injury, extracellular NAD^+ can either be used by ecto-ARTs to covalently modify specific target proteins by ADP-ribosylation or be degraded into smaller metabolites. These metabolites, in turn, can stimulate specific receptors (for instance adenosine can stimulate P1 receptors and regulates several physiological functions) or be internalised into cells by equilibrative or concentrative nucleoside transporters and finally be recycled by the nucleotide salvage pathway (Seman et al. 2004; Deterre et al. 1996). Hence, the net biological effect of extracellular NAD^+ depends on the amount of NAD^+ released into the extracellular space, the quality and quantity of specific receptors/enzymes expressed by surrounding cells, and on the activities of the catabolising-enzymes (Haag et al. 2007; Koch-Nolte and Ziegler 2013). Such a balance between local production of a signalling molecule that is normally absent from the extracellular space and its

rapid degradation/consumption is characteristic of the class of molecules that mediates "danger signals" and that can alert immune cells (Matzinger 2002). We have previously proposed that extracellular NAD^+, by regulating immune functions through ARTC2.2, can be regarded as a genuine member of this family of signalling molecules (Adriouch et al. 2012).

4 Expression of ARTC Enzymes in Mouse and Human Tissues

Genes encoding ARTC proteins display similar structural organisation in mouse and human. They are composed of 4 to 14 exons with a large central exon encoding the NAD^+ binding catalytic domain (Glowacki et al. 2002). Three amino acids in this domain located around the catalytic site in the folded protein form a R–S–E triad motif involved in mono-ADP-ribosyltransferase activity (Hottiger et al. 2010; Glowacki et al. 2002; Stilla et al. 2011). Mouse and human ARTC3 and ARTC4 lack this motif suggesting that they might have lost or deviated from their presumable original enzymatic activity. The last 3' exon of ARTC1-ARTC4 codes for a GPI anchor signal sequence compatible with their attachment to the cell membrane by a glycosyl-phosphatidylinositol linker. Human and mouse ART5 lack this sequence and are rather produced as secreted proteins (Hottiger et al. 2010; Glowacki et al. 2001, 2002).

Four human (ARTC1, 3, 4, 5) and six mouse (ARTC1, 2.1, 2.2, 3, 4, 5) ARTC genes have been characterised. Their expression at the mRNA level has been analysed by RT-PCR and northern blot from human and mouse tissues. For both species, ARTC3 and ARTC4 expression is found in several tissues including the hematopoietic system. The other genes display a more restricted expression with ARTC1 mainly expressed in skeletal and cardiac muscles and ARTC5 in testis. The gene that would code for ARTC2 in human and chimpanzee corresponds to a pseudogene, inactivated during evolution by three premature stop codons (Haag et al. 1994). Whether human ARTC1 can partially compensate for this defect and/or can participate in the modulation of immune cell function, akin to mouse ARTC2.1 and ARTC2.2 (see below), is presently not clear. This could, however, very well be the case at least in human neutrophils where ARTC1 expression was demonstrated by northern blot and by staining with specific antibodies (Paone et al. 2002). Indeed, the human anti-microbial peptide HNP-1 produced by activated neutrophils was previously demonstrated to be a substrate of ARTC1 in vitro. Interestingly, ADP-ribosylated HNP-1 was also detected in the bronchoalveolar lavages from cigarette smokers and was suggested to modulate its ability to recruit immune cells (Paone et al. 2002).

In mouse, two related genes presumably originated from a recent gene duplication event have been characterised. They code for ARTC2.1 and ARTC2.2 enzymes that share less than 85 % amino acid sequence identity. This suggests that their structures and functions have considerably diverged. Regarding their

expression, ARTC2.1 is expressed in T cells and macrophage while ARTC2.2 is only detected in T cells (Glowacki et al. 2002; Hong et al. 2009). Also, while expression of ARTC2.1 is up-regulated on the surface of macrophages upon activation by lipopolysaccharide, IFN-β or IFN-γ, ARTC2.2 is rather down-regulated on activated T cells (Hong et al. 2007, 2009; Kahl et al. 2000). Both enzymes display arginine-specific ADP-ribosyltransferase enzymatic activity and show similar target specificities. Yet, ARTC2.1 is active only in the presence of reducing agents (Hong et al. 2007; Hara et al. 1999). This has been ascribed to the presence of an additional disulfide bridge, absent from all other known ARTs, that restrains its enzymatic activity. Subsequently, while ARTC2.2 is constantly active, ARTC2.1 activity is limited in vivo to environments as inflammatory sites where thiol donors, akin to glutathione, and thiol oxidoreductases may accumulate (Hong et al. 2007, 2009).

5 ARTC2.2 Mediated ADP-Ribosylation of P2X7

ARTC2.2 catalyses the ADP-ribosylation of several T cell surface proteins including LFA-1, CD8, and the purinergic P2X7 receptor (Nemoto et al. 1996; Okamoto et al. 1998; Seman et al. 2003; Lischke et al. 2013). In the case of P2X7, the functional consequences of ADP-ribosylation have been well studied on lymphocytes. P2X7 is a ligand-gated ion channel that is normally activated by the non-covalent binding of the soluble ATP ligand. As ADP-ribosylation covalently attaches an ADP-ribose moiety, structurally related to ATP, onto the P2X7 protein, we investigated whether this may mimic ATP binding. We indeed demonstrated that ADP-ribosylation represents an alternative pathway to trigger P2X7 activation on T lymphocytes in the presence of extracellular NAD^+ (Seman et al. 2003). Co-expression of P2X7 and ARTC2.2 on the surface of mouse T cells renders these cells sensitive to low micromolar concentrations of extracellular NAD^+ by a mechanism that involves ARTC2.2-dependent ADP-ribosylation of P2X7 and its consequent triggering. Gating of the P2X7 ion-channel by ADP-ribosylation depends mechanistically on ADP-ribosylation of the arginine residue at position 125 (R125), which we hypothesised to be located in the vicinity of the ATP binding site (Adriouch et al. 2008; Schwarz et al. 2009). Three-dimensional modelling of the P2X7-trimer structure based on the recently solved structure of the related P2X4-trimer from zebrafish confirmed this assertion and remarkably predicted R125 to be located on a prominent mound just above the ATP-binding crevice (Hattori and Gouaux 2012; Laing et al. 2011; Browne et al. 2010; Young 2010; Jiang et al. 2013).

Interestingly, a new splice variant of P2X7, designated P2X7(k), has been recently characterised in rodents (Nicke et al. 2009). This variant differs from the classical P2X7(a) owing to the usage of an alternative exon 1. The P2X7 protein expressed by this variant harbours a distinct cytosolic N-terminus and first trans-membrane region. In functional tests, P2X7(k) receptor displays 10-fold higher

sensitivity to ATP and a slower deactivation time upon agonist removal (Nicke et al. 2009; Xu et al. 2012). Importantly, expression of P2X7(a) and P2X7(k) governs cell sensitivity not only to ATP, but also to NAD^+-induced P2X7 activation. Indeed, while both variants can be ADP-ribosylated in cells cotransfected with ARTC2.1 or ARTC2.2, only P2X7(k) can be activated by ADP-ribosylation (Xu et al. 2012; Schwarz et al. 2012). Given the preferential expression of P2X7(k) by T cells, these findings explain their unique sensitivity to extracellular ATP and NAD^+ as compared to others cells (Schwarz et al. 2012). For comparison, macrophages which preferentially express the P2X7(a) variant only respond to millimolar concentrations of ATP and do not respond at all to NAD^+, even in conditions where ADP-ribosylation of P2X7 can be demonstrated (Hong et al. 2009).

6 Molecular and Cellular Consequences of P2X7 ADP-Ribosylation in Mouse T Cells

Incubation of mouse T lymphocytes with either high concentrations of ATP (100–500 μM) or with low concentrations of NAD^+ (3–30 μM) induces comparable biochemical and cellular features that are characteristic of P2X7 activation (Scheuplein et al. 2009; Seman et al. 2003; Schwarz et al. 2009). These events include influx of Ca^{2+}/Na^+ and efflux of K^+ ions, shedding of cell surface proteins such as CD27 (Moon et al. 2006) and CD62L (Gu et al. 1998), externalisation of phosphatidylserine (PS), cell shrinkage (Taylor et al. 2008) and ultimately cell death when P2X7 is activated for a prolonged time (Fig. 1). Interestingly, while high concentrations of extracellular ATP have to be maintained for more than 30 min to induce T cells to die in vitro, a brief exposition with low micromolar NAD^+ concentrations is sufficient to durably ADP-ribosylate P2X7 and to irreversibly induce cell death (Seman et al. 2003). These observations suggest that induction of T cell death by extracellular NAD^+ is likely to occur in vivo in various pathophysiological situations. We termed this new immune regulatory pathway NAD^+-induced cell death (NICD) (Seman et al. 2003).

7 T Cell Subsets Differ in Their Sensitivity to Extracellular NAD^+

7.1 Naive T Cells Are Sensitive to NICD and Activated Effector T Cells Are Resistant

Naïve $CD4^+$ and $CD8^+$ T cells constitutively express ARTC2.2 and P2X7 although at slightly different levels. P2X7 is expressed at a higher level on naive $CD4^+$ T cells as compared to naive $CD8^+$ cells, whereas the reverse is true for ARTC2.2.

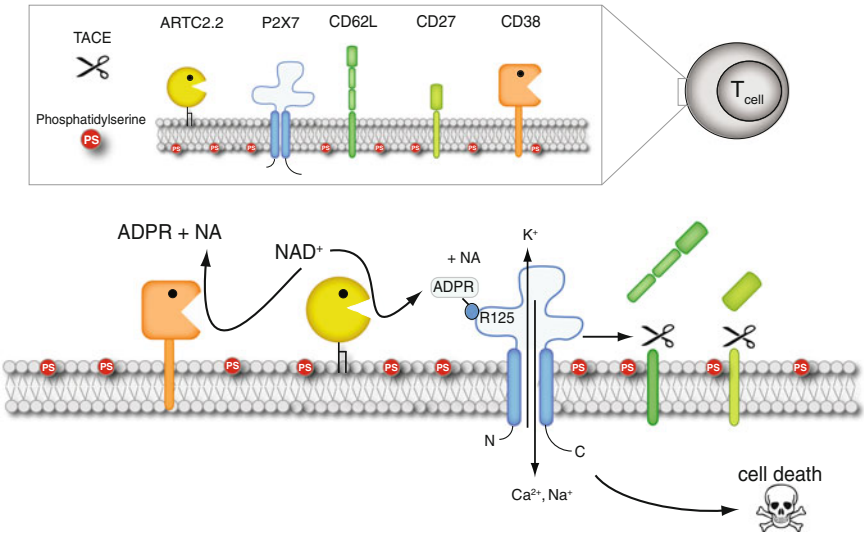

Fig. 1 ARTC2.2 ADP-ribosylates P2X7 on the surface of T cells. The ARTC2.2 ecto-enzyme catalyses the covalent linkage of the adenosine diphosphate ribose (ADPR) group from nicotinamide adenine dinucleotide (NAD^+) onto arginine residue 125 (R125) of P2X7. This posttranslational modification induces P2X7 channel opening, influx of Ca^{2+} and Na^+, efflux of K^+, externalisation of phosphatidylserine (PS), proteolytic shedding of cell surface proteins (CD27, CD62L) by TNFα-converting enzyme (TACE) and ultimately cell death. CD38 limits the activity of ecto-ARTs by degrading the common NAD^+ substrate to ADPR and nicotinamide (NA)

In unimmunised mice, $CD4^+$ T cells were more sensitive to NICD than their $CD8^+$ counterparts, suggesting that expression of P2X7 rather than of ARTC2.2 is the factor limiting NICD on naive T cells (Adriouch et al. 2007).

Contrary to naive T cells, activated T cells become resistant to NICD (Nemoto et al. 1996; Adriouch et al. 2001). This was correlated with metalloprotease-dependent proteolytic cleavage of ARTC2.2 from the cell surface upon activation of the T cell receptor (TCR) or upon PMA-based polyclonal stimulation (Kahl et al. 2000). Consistently, T cells surviving NAD^+ treatment in vivo display a $CD44^{high}$ $CD62L^{low}$ phenotype characteristic of activated/memory T cell and express lower levels of ARTC2.2 and of P2X7 at their surface (Adriouch et al. 2007). Further, as mentioned earlier, the activity of ART enzymes can be limited by the activity of the CD38 ecto-NAD^+-glycohydrolase (Krebs et al. 2005). In mice, activated T cells express CD38 on their surface, which further contributes to their resistance to NICD (Krebs et al. 2005; Adriouch et al. 2001) .

Compared to conventional T cells, regulatory T cells (Tregs), natural killer T (NKT) cells, and intestinal $CD8^+$ T cells display higher sensitivity to extracellular ATP and NAD^+ (Aswad and Dennert 2006; Aswad et al. 2005; Kawamura et al. 2005, 2006; Heiss et al. 2008; Hubert et al. 2010; Scheuplein et al. 2010;

Rissiek et al. 2013). In the following section, we will summarise the functional consequences of ARTC2.2-mediated P2X7 ADP-ribosylation on Tregs and NKT cells. For intestinal $CD8^+$ T cells, it has been suggested that their higher expression of ARTC2.2 and P2X7 is related to their exposition to retinoic acid in the intestinal environment (Heiss et al. 2008). Their higher sensitivity to extracellular ATP or NAD^+ may physiologically regulate their function in the intestinal tract possibly to avoid overwhelming cytotoxicity during infections.

7.2 Tregs and NKT Cells Are Highly Sensitive to Extracellular NAD^+

7.2.1 Phenotype and Function of Tregs Are Altered in Vitro by extracellular NAD^+

$CD4^+$ $Foxp3^+$ Tregs represent a subset of T cells that play a major role in the regulation of immune responses and in the prevention of autoimmune diseases. Their sensitivity to extracellular NAD^+ has been precisely studied ex vivo using DEREG mice in which live $CD4^+Foxp3^+$ T cells can be identified by their eGFP fluorescence (Lahl et al. 2007). Tregs from the DEREG mice responded to extracellular NAD^+ by exposing phosphatidylserine at their cell surface upon addition of as low as 1 μM NAD^+ and as early as 2 min after incubation with NAD^+. Side-by-side comparison showed that Tregs are indeed much more sensitive to NAD^+-induced phosphatidylserine exposure and to NAD^+-induced shedding of CD62L and CD27 than conventional $CD4^+$ T cells (Hubert et al. 2010). Notably, 0.5 μM NAD^+ was enough to inhibit their function in classical in vitro suppression assays. Later studies revealed that the higher sensitivity of Tregs to extracellular NAD^+ and ATP is not only linked to their high global expression of P2X7 at their surface, but also to their predominant expression of the more sensitive P2X7(k) splice variant (Schwarz et al. 2012).

7.2.2 Survival of Tregs and NKT Cells in Vivo Is Regulated by Extracellular NAD^+

Induction of NICD in Tregs and in NKT cells by extracellular NAD^+ is strictly dependent on the ARTC2.2/P2X7 pathway (Kawamura et al. 2006; Hubert et al. 2010; Scheuplein et al. 2010; Rissiek et al. 2013). Similarly, the total numbers of Tregs in peripheral lymph nodes under steady-state conditions is influenced by the ARTC2.2/P2X7 pathway and by CD38 NAD^+-glycohydrolase. Indeed, peripheral lymph nodes of wild-type mice exhibit significantly less Tregs as compared to $P2X7^{-/-}$ mice and, conversely, significantly more Tregs as compared to $CD38^{-/-}$ mice (Hubert et al. 2010). This demonstrates that sufficient amounts of extracellular

NAD^+ are released in vivo in normal physiological situations to trigger NICD. These findings were also verified for NKT cells (Scheuplein et al. 2010).

7.2.3 Regulation of Tregs and NKT Cells by Extracellular NAD^+ in Pathophysiological Situations

Interestingly, by regulating the number and function of Tregs and NKT cells, the ARTC2.2/P2X7 pathway (and its regulation by CD38) influences disease outcome in animal models of autoimmune diseases and cancer. For instance, lower numbers of Tregs and NKT cells in $CD38^{-/-}$ mice have been linked to accelerated onset of diabetes in the non-obese-diabetic (NOD) mice model (Chen et al. 2006). Indeed, $CD38^{-/-}$ NOD mice showed an earlier onset of disease that could be attributed to the enhanced activation of the ARTC2.2/P2X7 axis, resulting in reduced numbers of Tregs and diabetes-protective iNKT cells in the pancreatic lymph node (Scheuplein et al. 2010). Involvement of ARTC2.2 in this model was corroborated by the observations that its genetic deletion or its durable pharmacological blockade with an inhibitory nanobody-Fc fusion protein resulted in a delayed onset of disease in $CD38^{-/-}$ NOD mice (Chen et al. 2006; Scheuplein et al. 2010). Again, these data suggest that sufficient amounts of NAD^+ are liberated in pathophysiological situations in vivo to influence the homeostasis of Tregs and NKT cells, and highlight the importance of the ARTC2.2/P2X7 axis in this regulation. In the tumour models described below, the high sensitivity of Tregs and NKT cells to extracellular NAD^+ has been used to manipulate these subsets in vivo by intravenous injections of NAD^+.

7.2.4 In Vivo Manipulation of Regulatory T Cells Expressing ARTC2.2 and P2X7 by NAD^+ Injection

The higher expression of P2X7 on some T cell subsets expressing ARTC2.2, like Tregs and NKT cells, has brought forward the idea that NAD^+ could be used in vivo to selectively manipulate the number and/or function of these subsets. NAD^+ has been used in vivo in several mouse models to selectively deplete Tregs or NKT cells and to study the role of the ARTC2.2/P2X7 pathway in various pathophysiological situations (Adriouch et al. 2007; Aswad et al. 2005; Kawamura et al. 2006; Hubert et al. 2010). Intravenous injection of 10 mg NAD^+ into $CD38^{-/-}$ mice or 60 mg into wild-type mice led to a 80 % reduction of Tregs in spleen and peripheral lymph nodes (Hubert et al. 2010). Pharmacological manipulation of Tregs by the natural compound NAD^+ showed beneficial effects in several tumour models. Indeed, injection of NAD^+ into wild-type mice one day prior to syngeneic tumour implantation led, depending on the tumour model, either to complete tumour rejection or to significant inhibition of tumour growth and, in all situations, to stimulation of a *bona fide* $CD8^+$ cytotoxic T cell anti-tumour

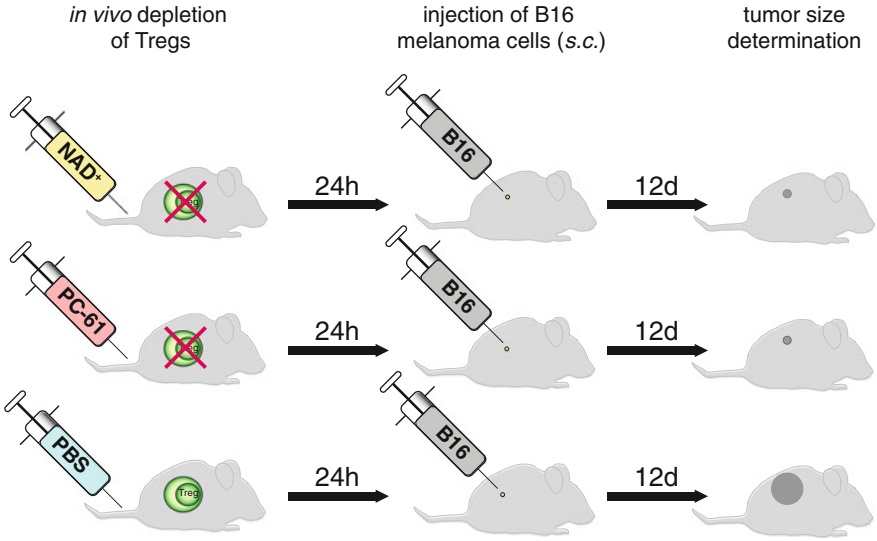

Fig. 2 Intravenous injection of NAD^+ induces depletion of Tregs and promotes anti-tumour responses. Injection of NAD^+ or anti-CD25 antibody (PC-61) similarly affects the number or function of peripheral Tregs. This favours the natural emergence of a cytotoxic anti-tumour immune response and significantly reduces tumour progression as illustrated here upon subcutaneous transfer of the aggressive B16 tumour model 24h post-treatment (Hubert et al. 2010)

response (Hubert et al. 2010) (Fig. 2). Manipulation of Tregs using NAD^+ was at least as effective as classical anti-CD25 antibody treatment to block Tregs and to elicit an anti-tumour response in vivo. In DEREG mice, which express a diphtheria toxin receptor under control of the *Foxp3* promoter, treatment with NAD^+ led to a comparable level of Treg depletion as a single injection of diphtheria toxin (Hubert et al. 2010; Klages et al. 2010). Interestingly, as with other T cell subsets, activated Tregs appeared to be more resistant to NAD^+ (Hubert et al. 2010). Not surprisingly therefore, Tregs surviving NAD^+ treatment in vivo displayed an activated/memory $CD44^{high}CD62L^{low}$ phenotype. Again, their resistance correlates with their lower expression of ARTC2.2 and P2X7 as compared to naive Tregs.

On the side of NKT cells, injection of NAD^+ has been shown to deplete liver NKT cells and to protect animals from concanavalin A- (ConA-) induced autoimmune liver inflammation (Kawamura et al. 2006). Interestingly, the sensitivity of liver NKT cells to NAD^+ also depends on their activation status. If injected prior to ConA, NAD^+ induced a rapid depletion of naïve NKT cells in the liver and inhibited ConA-induced liver damage. Conversely, when NAD^+ was injected 3h after injection of the mitogen ConA, liver damage was instead enhanced. Taking into consideration that ARTC2.2 is cleaved upon mitogenic stimulation of conventional T cells (Kahl et al. 2000), it is tempting to speculate that resistance of NKT cells to NICD in this experimental situation is due to proteolytic cleavage of ARTC2.2 upon the activation of NKT cells by ConA in vivo.

8 Liberation of Endogenous NAD^+ During Cell Preparation Ex Vivo Influences the Phenotype and Function of Cells Expressing ARTC2.2 and P2X7

Low micromolar concentrations of extracellular NAD^+ suffice to kill Tregs and NKT cells by NICD. As endogenous NAD^+ can readily be released into the extracellular compartment from stressed cells, the question arises as to whether this can also occur ex vivo during cell preparation and affect the phenotype and/or function of cells expressing ARTC2.2 and P2X7. We reported that routine preparation of primary lymphocytes from spleen and peripheral lymph nodes is sufficient to release NAD^+ and to ADP-ribosylate P2X7 on a fraction of T cells (Scheuplein et al. 2009). It is worth noting that ADP-ribosylation of P2X7 by the ARTC2.2 enzyme occurs even when cells are prepared at 4° C. As P2X7 function is inhibited at low temperature, this induces a covalent but "silent" modification of P2X7 that becomes perceptible upon incubation at 37° C. Returning the cells back to 37° C triggers gating of P2X7, shedding of CD27/CD62L, externalisation of phosphatidylserine and finally cell death (Fig. 3). Not surprisingly, cell subsets known to be highly sensitive to extracellular NAD^+, such as Tregs and liver NKT cells, are particularly affected by this ARTC2.2-dependent deleterious effect. In routine cell preparations, as many as 50 % of splenic Tregs and more than 80 % of liver NKT cells are visibly affected by this phenomenon upon incubation at 37° C (Rissiek et al. 2013). ARTC2.2-dependent ADP-ribosylation during cell preparation affects the phenotype and function of cells in multiple ways and can interfere with numerous downstream applications. For instance, wild-type (WT) Tregs show weaker suppressive functions in vitro as compared to $ARTC2^{-/-}$ or $P2X7^{-/-}$ Tregs (Hubert et al. 2010; Rissiek et al. 2013). Similarly, ADP-ribosylation of P2X7 during preparation of liver NKT cells from WT mice inhibits αGalCer-mediated cell expansion and IFNγ production as compared to liver NKT cells prepared from $ARTC2^{-/-}$ and $P2X7^{-/-}$ animals (Rissiek et al. 2013). From these data, it has become evident that the release of NAD^+ during cell preparation can significantly impact the phenotype and function or Tregs and liver NKT cells analysed ex vivo. Furthermore, they imply that much caution should be taken when interpreting such data, particularly when CD62L, CD27 expression or phosphatidylserine exposure are analysed. These results also illustrate a unique situation where the brief release of endogenous NAD^+ ex vivo during mechanical dissociation and cell manipulation durably affects sensitive T cell subsets by covalent modification of the P2X7.

On T cell subsets expressing lower levels of P2X7 and displaying a lower sensitivity to NICD, liberation of NAD^+ during cell preparation can also affect cell phenotype and function albeit at a lower degree. Apart from P2X7, the ARTC2.2 enzyme can ADP-ribosylate numerous other cell surface proteins involved in T cell functions such as LFA-1 or CD8. ADP-ribosylation of LFA-1 at the surface of $CD8^+$ CTL clones inhibits cell adhesion and LFA-1-associated signalling events (Nemoto et al. 1996; Okamoto et al. 1998). ADP-ribosylation of CD8α was

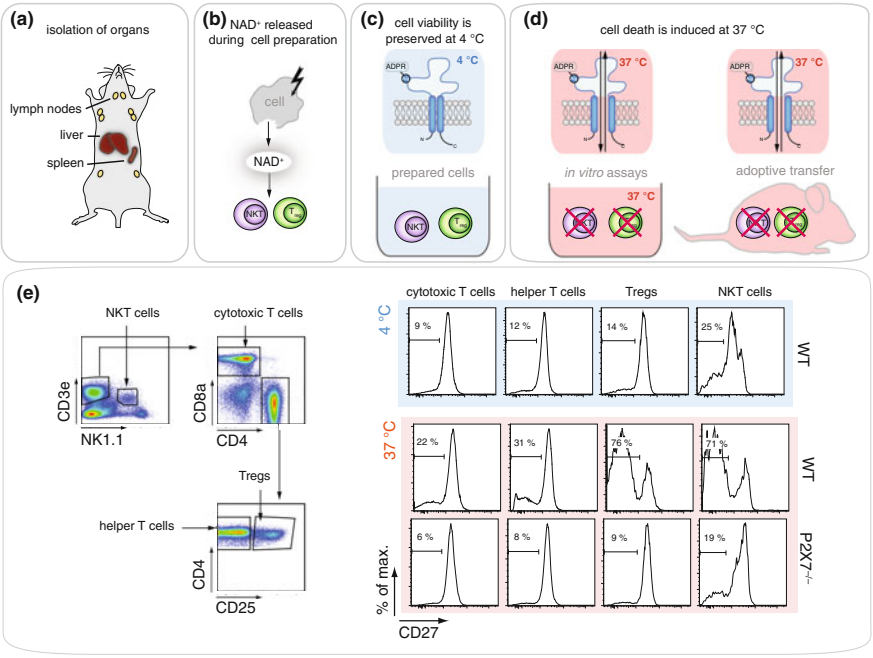

Fig. 3 NAD^+ released during cell preparation affects the survival and phenotype of Tregs and NKT cells. After the isolation of spleen, peripheral lymph nodes and liver from donor mice (**a**), mechanical cell dissociation leads to mechanical stress, cell damage and the release of endogenous NAD^+ (**b**). Extracellular NAD^+ is then used by ARTC2.2 to ADP-ribosylate P2X7 even at 4 °C (**c**). Returning the cells to 37 °C during in vitro assays or after adoptive transfer into recipient mice induces gating of P2X7 and NICD in Tregs and NKT cells (**d**). T cell subpopulations respond differently to extracellular NAD^+ (**e**). Splenic T cell subpopulations from WT or P2X7$^{-/-}$ C57BL/6 mice were distinguished by flow cytometry using cell surface markers: cytotoxic T cells ($CD3^+CD8^+$), T helper cells ($CD3^+CD4^+CD25^-$), Tregs ($CD3^+CD4^+CD25^+$), NKT cells ($CD3^+NK1.1^+$). Cells were incubated at 37 °C or kept at 4 °C. NAD^+-mediated gating of P2X7 was monitored by the loss of CD27 from the cell surface of the respective T cell subpopulation

suggested to inhibit p56lck downstream events (Okamoto et al. 1998; Wang et al. 1996). More recently, it has been shown that CD8β is also ADP-ribosylated at the surface of $CD8^+$ T cells, and that this happens during cell preparation ex vivo (Lischke et al. 2013). The consequences of CD8β ADP-ribosylation include modification of the epitopes recognised by some antibodies, inhibition of MHC-tetramer binding by TCR transgenic $CD8^+$ T cells, and inhibition of their cytotoxic activity.

9 Camelid-Derived Nanobodies Represent New Pharmacological Tools to Manipulate the ARTC2.2/P2X7 Pathway

ARTC2.2 and/or P2X7 blocking agents would represent valuable pharmacological tools in vivo, to further study the role of the ARTC2.2/P2X7 pathway on the regulation of immune cells and its implication in pathophysiology. In fundamental research, such agents may also help to preserve the viability and function of Tregs and NKT cells during cell preparation ex vivo that can seriously bias results interpretation.

9.1 ARTC2.2-Blocking Nanobodies Protect Tregs and NKT Cells from the Deleterious Effects of NAD^+ Released During Cell Preparation

Nanobodies are single-domain antibodies derived from camelid antibodies lacking the classical antibody light-chain (Hamers-Casterman et al. 1993). Nanobodies display remarkable properties: they are highly stable at high temperatures and during pH shift, are easily produced as recombinant proteins, and have the ability to form long protrusions that can bind inside active site crevices of enzymes. Indeed, their complementarity determining region 3 (CDR3) can form a finger-like extension that can reach cryptic epitopes that are normally inaccessible to conventional antibodies (Wesolowski et al. 2009). Several blocking nanobodies directed against mammalian and bacterial toxin ADP-ribosyltransferases have been recently described (Menzel et al. 2013). The blocking nanobody s+16a potently and specifically inhibits ARTC2.2 and prevents ARTC2.2-catalysed ADP-ribosylation of P2X7 (Fig. 4a). Notably, even in presence of high concentrations of extracellular NAD^+ in vitro, s+16a completely prevents ARTC2.2/P2X7-dependent T cell death.

A further advantage of nanobodies is their small size, which confers a rapid distribution and penetration into tissues in vivo. Consistently, intravenous injection of 50 μg of s+16a 15 min prior to mouse sacrifice was sufficient to completely inhibit ARTC2.2 activity at the surface of T cells harvested from peripheral lymph nodes and spleen (Koch-Nolte et al. 2007). The nanobody s+16a can therefore be used to protect NAD^+-sensitive Tregs and NKT cells from the deleterious effects of NAD^+ released during cell preparation. Tregs prepared from mice injected with s+16a before sacrifice displayed a higher suppressive capacity in vitro, retained a $CD62L^{high}$ phenotype and a better capacity to survive in vivo when adoptively transferred into recipient mice than Tregs prepared from control mice (Hubert et al. 2010; Rissiek et al. 2013) (Fig. 4b). Similarly, injection of s+16a protected liver NKT cells from NAD^+ released during cell preparation and allowed better

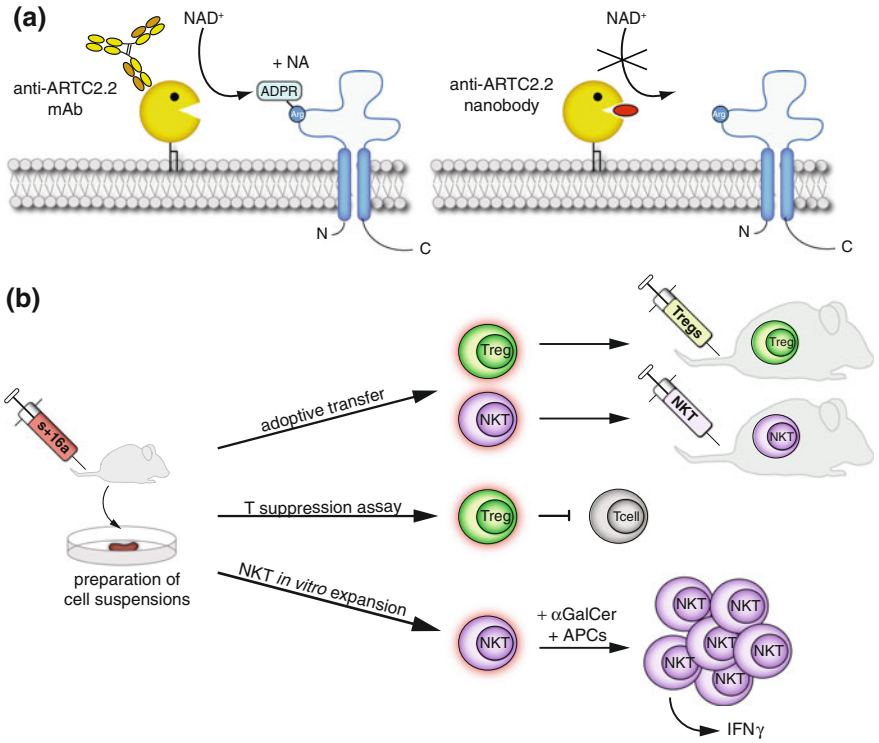

Fig. 4 Blockade of ARTC2.2 during cell preparation by camelid-derived nanobodies preserves the function of Tregs and NKT cells. Conventional monoclonal antibodies (mAbs) typically recognise flat epitopes on the surface of their target antigens and can usually not access molecular cavities. In contrast, nanobodies derived from camelid heavy chain antibodies can bind inside catalytic sites and crevices and can block enzymatic function. The nanobody s+16a, depicted in red inside the catalytic site of its ARTC2.2 target, can prevent ADP-ribosylation of P2X7 (**a**). Injection of s+16a into mice 15 min prior to organ collection protects highly sensitive Tregs and NKT cells from ADP-ribosylation during cell preparation and preserves the suppressive function of Tregs in vitro, promotes the expansion and function of NKT cells in vitro, and preserves Tregs and NKT cells from loss after adoptive transfer into recipient mice (**b**)

expansion of these cells ex vivo, higher levels of αGalCer-induced IFNγ secretion and more efficient survival of these cells upon adoptive transfer into recipient mice (Rissiek et al. 2013) (Fig. 4b).

9.2 ARTC2.2-Blocking Nanobodies can be Used to Manipulate Tregs and NKT Cells in Vivo

Given that NAD^+ is released in pathophysiological conditions and can affect the function and survival of Tregs and NKT cells in vivo, pharmacological inhibition of the ARTC2.2/P2X7 pathway in vivo could represent a new way to preserve

these subsets. As mentioned above, the onset of diabetes is accelerated in $CD38^{-/-}$ NOD mice concordant with a reduction in the number of Tregs and diabetes-protective iNKT cells (Scheuplein et al. 2010; Chen et al. 2006). This finding, showing that amplification of the ARTC2.2/P2X7 pathway by genetic ablation of CD38 accelerates the spontaneous T-cell mediated autoimmune diabetes of NOD mice, provided the basis for an illustration of the therapeutic potential of pharmacological blockade of ARTC2.2 in vivo. Indeed, weekly injection of s+16aFc (s+16a nanobody fused to murine IgG1 to increase its half-life in vivo) for 4 weeks provided long-term in vivo inhibition of ARTC2.2 activity and restored iNKT cell numbers. This treatment protected from diabetes when mice were co-injected with alpha-galactosylceramide (αGalCer) to stimulate regulatory iNKT cells (Scheuplein et al. 2010). Long-term treatment with s+16a also improved the suppressive capacity of Tregs and allowed accumulation of Tregs into the pancreatic lymph nodes of mice challenged with αGalCer. Thus, nanobodies directed against ARTC2.2, and possibly also future nanobodies directed against P2X7, represent valuable tools to manipulate the ARTC2.2/P2X7 pathway in vivo. These tools will help to further elucidate the role of this pathway in various pathophysiological models and may open new therapeutic options for inflammatory diseases.

10 Conclusions

Endogenous NAD^+ can be released from intracellular sources into the extracellular milieu in different situations including mechanical shear forces, oxidative stress, tissue injury, or inflammation, and represents a genuine danger signal that can potentiate the immune response by dampening Treg subsets. This concept has been illustrated in two animal models so far. A single intravenous injection of NAD^+ selectively depletes 80 % of the peripheral $CD4^+Foxp3^+$ Tregs and consequently promotes a spontaneous *bona fide* cytotoxic T cell response against implanted tumours. Genetic deletion of CD38 in NOD mice resulted in increased availability of extracellular NAD^+ and an ARTC2.2-dependent acceleration of diabetes onset by reducing the number and function of Tregs and regulatory iNKT cells. Taken together, these data suggest that the ARTC2.2/P2X7 pathway indeed plays an important role in the fine modulation of the balance between effector and Treg subsets. Therefore, the development of pharmacological agents targeting this pathway could be of significant interest to manipulate immune responses in various pathophysiological situations. Proof-of-principle experiments have established that injection of camelid-derived nanobodies blocking the enzymatic activity of ARTC2.2 can indeed be used ex vivo as well as in vivo to preserve the viability, function and phenotype of Treg and NKT cells that are highly sensitive to extracellular NAD^+. Nanobodies targeting ARTC2.2 and P2X7 will be useful in future studies to decipher the role of ARTC2.2 and P2X7 in other pathophysiological models and may provide new biotherapeutics for modulating immune responses.

Acknowledgments The authors would like to thank Inserm, Association Française contre les Myopathies (AFM), Normandy University and the Deutsche Forschungsgemeinschaft (DFG) for their financial supports.

References

Adriouch S, Ohlrogge W, Haag F, Koch-Nolte F, Seman M (2001) Rapid induction of naive T cell apoptosis by ecto-nicotinamide adenine dinucleotide: requirement for mono(ADP-ribosyl)transferase 2 and a downstream effector. J Immunol 167(1):196–203

Adriouch S, Hubert S, Pechberty S, Koch-Nolte F, Haag F, Seman M (2007) NAD+ released during inflammation participates in T cell homeostasis by inducing ART2-mediated death of naive T cells in vivo. J Immunol 179(1):186–194

Adriouch S, Bannas P, Schwarz N, Fliegert R, Guse AH, Seman M, Haag F, Koch-Nolte F (2008) ADP-ribosylation at R125 gates the P2X7 ion channel by presenting a covalent ligand to its nucleotide binding site. FASEB J 22(3):861–869

Adriouch S, Haag F, Boyer O, Seman M, Koch-Nolte F (2012) Extracellular NAD(+): a danger signal hindering regulatory T cells. Microbes Infect 14(14):1284–1292

Aswad F, Dennert G (2006) P2X7 receptor expression levels determine lethal effects of a purine based danger signal in T lymphocytes. Cell Immunol 243(1):58–65

Aswad F, Kawamura H, Dennert G (2005) High sensitivity of CD4+CD25+ regulatory T cells to extracellular metabolites nicotinamide adenine dinucleotide and ATP: a role for P2X7 receptors. J Immunol 175(5):3075–3083

Browne LE, Jiang LH, North RA (2010) New structure enlivens interest in P2X receptors. Trends Pharmacol Sci 31(5):229–237

Burnstock G (2006) Pathophysiology and therapeutic potential of purinergic signaling. Pharmacol Rev 58(1):58–86

Burnstock G, Kennedy C (2011) P2X receptors in health and disease. Adv Pharmacol 61:333–372

Chen J, Chen YG, Reifsnyder PC, Schott WH, Lee CH, Osborne M, Scheuplein F, Haag F, Koch-Nolte F, Serreze DV, Leiter EH (2006) Targeted disruption of CD38 accelerates autoimmune diabetes in NOD/Lt mice by enhancing autoimmunity in an ADP-ribosyltransferase 2-dependent fashion. J Immunol 176(8):4590–4599

Cockayne DA, Muchamuel T, Grimaldi JC, Muller-Steffner H, Randall TD, Lund FE, Murray R, Schuber F, Howard MC (1998) Mice deficient for the ecto-nicotinamide adenine dinucleotide glycohydrolase CD38 exhibit altered humoral immune responses. Blood 92(4):1324–1333

Davies CA, Perrett D, Zhang Z, Nielsen BR, Blake DR, Winyard PG (1999) Simultaneous analysis of nitrite, nitrate and the nicotinamide nucleotides by capillary electrophoresis: application to biochemical studies and human extracellular fluids. Electrophoresis 20(10):2111–2117

De Souza RF, Aravind L (2012) Identification of novel components of NAD-utilizing metabolic pathways and prediction of their biochemical functions. Mol Biosyst 8(6):1661–1677

Deterre P, Gelman L, Gary-Gouy H, Arrieumerlou C, Berthelier V, Tixier JM, Ktorza S, Goding J, Schmitt C, Bismuth G (1996) Coordinated regulation in human T cells of nucleotide-hydrolyzing ecto-enzymatic activities, including CD38 and PC-1. Possible role in the recycling of nicotinamide adenine dinucleotide metabolites. J Immunol 157(4):1381–1388

Garavaglia S, Bruzzone S, Cassani C, Canella L, Allegrone G, Sturla L, Mannino E, Millo E, De Flora A, Rizzi M (2012) The high-resolution crystal structure of periplasmic Haemophilus influenzae NAD nucleotidase reveals a novel enzymatic function of human CD73 related to NAD metabolism. Biochem J 441(1):131–141

Glowacki G, Braren R, Cetkovic-Cvrlje M, Leiter EH, Haag F, Koch-Nolte F (2001) Structure, chromosomal localization, and expression of the gene for mouse ecto-mono(ADP-ribosyl)transferase ART5. Gene 275(2):267–277

Glowacki G, Braren R, Firner K, Nissen M, Kuhl M, Reche P, Bazan F, Cetkovic-Cvrlje M, Leiter E, Haag F, Koch-Nolte F (2002) The family of toxin-related ecto-ADP-ribosyltransferases in humans and the mouse. Protein Sci 11(7):1657–1670

Gu B, Bendall LJ, Wiley JS (1998) Adenosine triphosphate-induced shedding of CD23 and L-selectin (CD62L) from lymphocytes is mediated by the same receptor but different metalloproteases. Blood 92(3):946–951

Haag F, Koch-Nolte F, Kuhl M, Lorenzen S, Thiele HG (1994) Premature stop codons inactivate the RT6 genes of the human and chimpanzee species. J Mol Biol 243(3):537–546

Haag F, Andresen V, Karsten S, Koch-Nolte F, Thiele H (1995) Both allelic forms of the rat T cell differentiation marker RT6 display nicotinamide adenine dinucleotide (NAD)-glycohydrolase activity, yet only RT6.2 is capable of automodification upon incubation with NAD. Eur J Immunol 25(8):2355–2361

Haag F, Adriouch S, Brass A, Jung C, Moller S, Scheuplein F, Bannas P, Seman M, Koch-Nolte F (2007) Extracellular NAD and ATP: partners in immune cell modulation. Purinergic Signal 3(1–2):71–81

Hamers-Casterman C, Atarhouch T, Muyldermans S, Robinson G, Hamers C, Songa EB, Bendahman N, Hamers R (1993) Naturally occurring antibodies devoid of light chains. Nature 363(6428):446–448

Hara N, Badruzzaman M, Sugae T, Shimoyama M, Tsuchiya M (1999) Mouse Rt6.1 is a thiol-dependent arginine-specific ADP-ribosyltransferase. Eur J Biochem 259(1–2):289–294

Hattori M, Gouaux E (2012) Molecular mechanism of ATP binding and ion channel activation in P2X receptors. Nature 485(7397):207–212

Heiss K, Janner N, Mahnss B, Schumacher V, Koch-Nolte F, Haag F, Mittrucker HW (2008) High sensitivity of intestinal CD8+ T cells to nucleotides indicates P2X7 as a regulator for intestinal T cell responses. J Immunol 181(6):3861–3869

Hong S, Brass A, Seman M, Haag F, Koch-Nolte F, Dubyak GR (2007) Lipopolysaccharide, IFN-gamma, and IFN-beta induce expression of the thiol-sensitive ART2.1 Ecto-ADP-ribosyltransferase in murine macrophages. J Immunol 179(9):6215–6227

Hong S, Brass A, Seman M, Haag F, Koch-Nolte F, Dubyak GR (2009a) Basal and inducible expression of the thiol-sensitive ART2.1 ecto-ADP-ribosyltransferase in myeloid and lymphoid leukocytes. Purinergic Signal 5(3):369–383

Hong S, Schwarz N, Brass A, Seman M, Haag F, Koch-Nolte F, Schilling WP, Dubyak GR (2009b) Differential regulation of P2X7 receptor activation by extracellular nicotinamide adenine dinucleotide and ecto-ADP-ribosyltransferases in murine macrophages and T cells. J Immunol 183(1):578–592

Honjo T, Nishizuka Y, Hayaishi O (1968) Diphtheria toxin-dependent adenosine diphosphate ribosylation of aminoacyl transferase II and inhibition of protein synthesis. J Biol Chem 243(12):3553–3555

Hottiger MO, Hassa PO, Luscher B, Schuler H, Koch-Nolte F (2010) Toward a unified nomenclature for mammalian ADP-ribosyltransferases. Trends Biochem Sci 35(4):208–219

Hubert S, Rissiek B, Klages K, Huehn J, Sparwasser T, Haag F, Koch-Nolte F, Boyer O, Seman M, Adriouch S (2010) Extracellular NAD+ shapes the Foxp3+ regulatory T cell compartment through the ART2-P2X7 pathway. J Exp Med 207(12):2561–2568

Jiang LH, Baldwin JM, Roger S, Baldwin SA (2013) Insights into the molecular mechanisms underlying mammalian P2X7 receptor functions and contributions in diseases, revealed by structural modeling and single nucleotide polymorphisms. Front Pharmacol 4:55

Kahl S, Nissen M, Girisch R, Duffy T, Leiter EH, Haag F, Koch-Nolte F (2000) Metalloprotease-mediated shedding of enzymatically active mouse ecto-ADP-ribosyltransferase ART2.2 upon T cell activation. J Immunol 165(8):4463–4469

Kawamura H, Aswad F, Minagawa M, Malone K, Kaslow H, Koch-Nolte F, Schott WH, Leiter EH, Dennert G (2005) P2X7 receptor-dependent and -independent T cell death is induced by nicotinamide adenine dinucleotide. J Immunol 174(4):1971–1979

Kawamura H, Aswad F, Minagawa M, Govindarajan S, Dennert G (2006) P2X7 receptors regulate NKT cells in autoimmune hepatitis. J Immunol 176(4):2152–2160

Klages K, Mayer CT, Lahl K, Loddenkemper C, Teng MW, Ngiow SF, Smyth MJ, Hamann A, Huehn J, Sparwasser T (2010) Selective depletion of Foxp3+ regulatory T cells improves effective therapeutic vaccination against established melanoma. Cancer Res 70(20):7788–7799

Koch-Nolte F, Ziegler M (2013) Physiology of ADP-ribosylation. FEBS J 280(15):3483

Koch-Nolte F, Adriouch S, Bannas P, Krebs C, Scheuplein F, Seman M, Haag F (2006) ADP-ribosylation of membrane proteins: unveiling the secrets of a crucial regulatory mechanism in mammalian cells. Ann Med 38(3):188–199

Koch-Nolte F, Reyelt J, Schossow B, Schwarz N, Scheuplein F, Rothenburg S, Haag F, Alzogaray V, Cauerhff A, Goldbaum FA (2007) Single domain antibodies from llama effectively and specifically block T cell ecto-ADP-ribosyltransferase ART2.2 in vivo. FASEB J 21(13):3490–3498

Krebs C, Adriouch S, Braasch F, Koestner W, Leiter EH, Seman M, Lund FE, Oppenheimer N, Haag F, Koch-Nolte F (2005) CD38 controls ADP-ribosyltransferase-2-catalyzed ADP-ribosylation of T cell surface proteins. J Immunol 174(6):3298–3305

Lahl K, Loddenkemper C, Drouin C, Freyer J, Arnason J, Eberl G, Hamann A, Wagner H, Huehn J, Sparwasser T (2007) Selective depletion of Foxp3+ regulatory T cells induces a scurfy-like disease. J Exp Med 204(1):57–63

Laing S, Unger M, Koch-Nolte F, Haag F (2011) ADP-ribosylation of arginine. Amino Acids 41(2):257–269

Lischke T, Schumacher V, Wesolowski J, Hurwitz R, Haag F, Koch-Nolte F, Mittrucker HW (2013) CD8-beta ADP-ribosylation affects CD8(+) T-cell function. Eur J Immunol 43(7):1828–1838

Matzinger P (2002) The danger model: a renewed sense of self. Science 296(5566):301–305

Menzel S, Rissiek B, Haag F, Goldbaum FA, Koch-Nolte F (2013) The art of blocking ADP-ribosyltransferases (ARTs): nanobodies as experimental and therapeutic tools to block mammalian and toxin ARTs. FEBS J 280(15):3543–3550

Moon H, Na HY, Chong KH, Kim TJ (2006) P2X7 receptor-dependent ATP-induced shedding of CD27 in mouse lymphocytes. Immunol Lett 102(1):98–105

Nemoto E, Yu Y, Dennert G (1996a) Cell surface ADP-ribosyltransferase regulates lymphocyte function-associated molecule-1 (LFA-1) function in T cells. J Immunol 157(8):3341–3349

Nemoto E, Stohlman S, Dennert G (1996b) Release of a glycosylphosphatidylinositol-anchored ADP-ribosyltransferase from cytotoxic T cells upon activation. J Immunol 156(1):85–92

Nicke A, Kuan YH, Masin M, Rettinger J, Marquez-Klaka B, Bender O, Gorecki DC, Murrell-Lagnado RD, Soto F (2009) A functional P2X7 splice variant with an alternative transmembrane domain 1 escapes gene inactivation in P2X7 knock-out mice. J Biol Chem 284(38):25813–25822

Okamoto S, Azhipa O, Yu Y, Russo E, Dennert G (1998) Expression of ADP-ribosyltransferase on normal T lymphocytes and effects of nicotinamide adenine dinucleotide on their function. J Immunol 160(9):4190–4198

Paone G, Wada A, Stevens LA, Matin A, Hirayama T, Levine RL, Moss J (2002) ADP ribosylation of human neutrophil peptide-1 regulates its biological properties. Proc Natl Acad Sci U S A 99(12):8231–8235

Rissiek B, Danquah W, Haag F, Koch-Nolte F (2013) Technical advance: a new cell preparation strategy that greatly improves the yield of vital and functional Tregs and NKT cells. J Leukoc Biol (in press)

Scheuplein F, Schwarz N, Adriouch S, Krebs C, Bannas P, Rissiek B, Seman M, Haag F, Koch-Nolte F (2009) NAD+ and ATP released from injured cells induce P2X7-dependent shedding of CD62L and externalization of phosphatidylserine by murine T cells. J Immunol 182(5):2898–2908

Scheuplein F, Rissiek B, Driver JP, Chen YG, Koch-Nolte F, Serreze DV (2010) A recombinant heavy chain antibody approach blocks ART2 mediated deletion of an iNKT cell population that upon activation inhibits autoimmune diabetes. J Autoimmun 34(2):145–154

Schwarz N, Fliegert R, Adriouch S, Seman M, Guse AH, Haag F, Koch-Nolte F (2009) Activation of the P2X7 ion channel by soluble and covalently bound ligands. Purinergic Signal 5(2):139–149

Schwarz N, Drouot L, Nicke A, Fliegert R, Boyer O, Guse AH, Haag F, Adriouch S, Koch-Nolte F (2012) Alternative splicing of the N-terminal cytosolic and transmembrane domains of P2X7 controls gating of the ion channel by ADP-ribosylation. PLoS ONE 7(7):e41269

Seman M, Adriouch S, Scheuplein F, Krebs C, Freese D, Glowacki G, Deterre P, Haag F, Koch-Nolte F (2003) NAD-induced T cell death: ADP-ribosylation of cell surface proteins by ART2 activates the cytolytic P2X7 purinoceptor. Immunity 19(4):571–582

Seman M, Adriouch S, Haag F, Koch-Nolte F (2004) Ecto-ADP-ribosyltransferases (ARTs): emerging actors in cell communication and signaling. Curr Med Chem 11(7):857–872

Stilla A, Di Paola S, Dani N, Krebs C, Arrizza A, Corda D, Haag F, Koch-Nolte F, Di Girolamo M (2011) Characterisation of a novel glycosylphosphatidylinositol-anchored mono-ADP-ribosyltransferase isoform in ovary cells. Eur J Cell Biol 90(8):665–677

Taylor SR, Gonzalez-Begne M, Dewhurst S, Chimini G, Higgins CF, Melvin JE, Elliott JI (2008) Sequential shrinkage and swelling underlie P2X7-stimulated lymphocyte phosphatidylserine exposure and death. J Immunol 180(1):300–308

Wang J, Nemoto E, Dennert G (1996) Regulation of CTL by ecto-nictinamide adenine dinucleotide (NAD) involves ADP-ribosylation of a p56lck-associated protein. J Immunol 156(8):2819–2827

Weng B, Thompson WC, Kim HJ, Levine RL, Moss J (1999) Modification of the ADP-ribosyltransferase and NAD glycohydrolase activities of a mammalian transferase (ADP-ribosyltransferase 5) by auto-ADP-ribosylation. J Biol Chem 274(45):31797–31803

Wesolowski J, Alzogaray V, Reyelt J, Unger M, Juarez K, Urrutia M, Cauerhff A, Danquah W, Rissiek B, Scheuplein F, Schwarz N, Adriouch S, Boyer O, Seman M, Licea A, Serreze DV, Goldbaum FA, Haag F, Koch-Nolte F (2009) Single domain antibodies: promising experimental and therapeutic tools in infection and immunity. Med Microbiol Immunol 198(3):157–174

Xu XJ, Boumechache M, Robinson LE, Marschall V, Gorecki DC, Masin M, Murrell-Lagnado RD (2012) Splice variants of the P2X7 receptor reveal differential agonist dependence and functional coupling with pannexin-1. J Cell Sci 125(Pt 16):3776–3789

Young MT (2010) P2X receptors: dawn of the post-structure era. Trends Biochem Sci 35(2):83–90

Pierisins and CARP-1: ADP-Ribosylation of DNA by ARTCs in Butterflies and Shellfish

Tsuyoshi Nakano, Azusa Takahashi-Nakaguchi, Masafumi Yamamoto and Masahiko Watanabe

Abstract The cabbage butterfly, *Pieris rapae*, and related species possess a previously unknown ADP-ribosylating toxin, guanine specific ADP-ribosyltransferase. This enzyme toxin, known as pierisin, consists of enzymatic N-terminal domain and receptor-binding C-terminal domain, or typical AB-toxin structure. Pierisin efficiently transfers an ADP-ribosyl moiety to the N^2 position of the guanine base of dsDNA. Receptors for pierisin are suggested to be the neutral glycosphingolipids, globotriaosylceramide (Gb3), and globotetraosylceramide (Gb4). This DNA-modifying toxin exhibits strong cytotoxicity and induces apoptosis in various human cell lines, which can be blocked by Bcl-2. Pierisin also produces detrimental effects on the eggs and larvae of the non-habitual parasitoids. In contrast, a natural parasitoid of the cabbage butterfly, *Cotesia glomerata*, was resistant to this toxin. The physiological role of pierisin in the butterfly is suggested to be a defense factor against parasitization by wasps. Other type of DNA ADP-ribosyltransferase is present in certain kinds of edible clams. For example, the

T. Nakano (✉)
Division of Cancer Development System, National Cancer Center Research Institute, 5-1-1 Tsukiji, Chuo-ku, Tokyo 104-0045, Japan
e-mail: Nakano.Tsuyoshi@sysmex.co.jp

Present Address:
T. Nakano
Central Research Laboratories, Sysmex Corporation, 4-4-4 Takatsukadai, Nishi-ku, Kobe 651-2271, Japan

A. Takahashi-Nakaguchi
Medical Mycology Research Center, Chiba University, 1-8-1 Inohana, Chuo-ku, Chiba 260-8673, Japan

M. Yamamoto
Laboratory Animal Research Department, Central Institute for Experimental Animals, 3-25-12 Tonomachi, Kawasaki-ku, Kawasaki 210-0821, Japan

M. Watanabe
School of Pharmacy, Shujitsu University, 1-6-1 Nishigawara, Naka-ku, Okayama 703-8516, Japan

Current Topics in Microbiology and Immunology (2015) 384: 127–149
DOI: 10.1007/82_2014_416

Published Online: 18 July 2014

CARP-1 protein found in *Meretrix lamarckii* consists of an enzymatic domain without a possible receptor-binding domain. Pierisin and CARP-1 are almost fully non-homologous at the amino acid sequence level, but other ADP-ribosyltransferases homologous to pierisin are present in different biological species such as eubacterium *Streptomyces*. Possible diverse physiological roles of the DNA ADP-ribosyltransferases are discussed.

Abbreviations

dsDNA	Double-strand DNA
Gb3	Globotriaosylceramide
Gb4	Globotetraosylceramide
GADPRT	*N*-glycosidic cholera toxin-like-ADP-ribosyltransferase catalyzing mono-ADP-ribosylation

Contents

1 Introduction

ADP-ribosyltransferase activity is observed in a variety of prokaryotes and eukaryotes (Corda and Di Girolamo 2003). For example, cholera and pertussis toxins transfer the ADP-ribose moiety from NAD^+ to specific arginine or cysteine residues of the α-subunit of G proteins, respectively, while diphtheria toxin transfers this moiety to the diphthamide residue of elongation factor 2. ART1 and ART2 modify the arginine residues of human neutrophil peptide-1 and the cytolytic $P2X_7$ receptor, respectively (Corda and Di Girolamo 2002; Stevens et al. 2009; Scheuplein et al. 2009). In general, each ADP-ribosyltransferase exhibits significant substrate specificity for its acceptor molecule, and most acceptors are known to be proteins.

In 1996, we identified a potent cytotoxic substance in the cabbage butterfly, *Pieris rapae* (Koyama et al. 1996). Subsequent cDNA sequencing demonstrated that this substance was a protein, denoted pierisin, and was an ADP-ribosylating toxin (Watanabe et al. 1999). After some unsuccessful attempts to find target molecules of pierisin, we finally identified an acceptor that was not predicted, the guanine base of DNA (Takamura-Enya et al. 2001). This kind of DNA-modifying toxin exists only in some Pierid butterflies among a variety of examined Lepidopteran insects. However, certain prokaryotic organisms have also been found to harbor a guanine specific ADP-ribosyltransferase that is homologous to the pierisins (Koyama et al. 1996; Matsumoto et al. 2008; Yamamoto et al. 2009; Nakano et al. 2013). We additionally characterized another kind of DNA ADP-ribosyltransferase in shellfish (Nakano et al. 2006) with virtually no sequence similarities with pierisin. This review focuses on these intriguing enzymes.

2 ADP-Ribosylation of DNA by Pierisins

2.1 Identification of NAD^+:DNA ADP-Ribosyltransferases

In 1996, we found cytotoxic activity in protein extracts of cabbage butterfly pupae (*Pieris rapae*, possibly *Pieris rapae crucivora*, which inhabit Japan; Koyama et al. 1996), and subsequently purified this toxin and named it pierisin (Watanabe et al. 1998). Since the deduced amino acid sequence of pierisin shows 30 % homology with the mosquitocidal ADP-ribosylating toxin from *Bacillus sphaericus* SSII-I (MTX) (Watanabe et al. 1999), the pierisins were predicted to be ADP-ribosylating toxins. Mono ADP-ribosyltransferases target nitrogen-or sulfate-atoms in specific amino acid residues of their target proteins. Bacterial ADP-ribosyltransferases mainly target key regulator proteins, whereas vertebrate mono ADP-ribosyltransferases (ARTs) target defensins and T-cell $P2X_7$ receptors, although the physiological targets for some ARTs are still under investigation (Hottiger et al. 2010, and references therein). In our laboratory, we first screened for ADP-ribosylated acceptors through autoradiography analysis of SDS-PAGE resolved HeLa-cell extracts incubated with pierisin-1 in the presence of β-[*adenylate*-^{32}P] NAD^+ ([^{32}P]NAD^+). However, we could not detect any incorporation of radioactivity in the proteins. The autoradiogram instead revealed a smear fraction above 100 kDa, which could be digested with DNase, suggesting that the major target of pierisin is double-strand DNA (dsDNA).

Our examination of the incorporation of ADP-ribose into dsDNA and oligo DNA in the presence of pierisin-1 and NAD^+ suggested that the acceptor was guanine. The structure of the product from a reaction of pierisin-1, calf thymus DNA, and NAD^+ was identified as N^2-(α-ADP-D-ribos-1-yl)-2′-deoxyguanosine and its β form (Fig. 1; Takamura-Enya et al. 2001). Pierisin-2, purified from large white butterfly *Pieris brassicae* (Matsushima-Hibiya et al. 2000), produces the

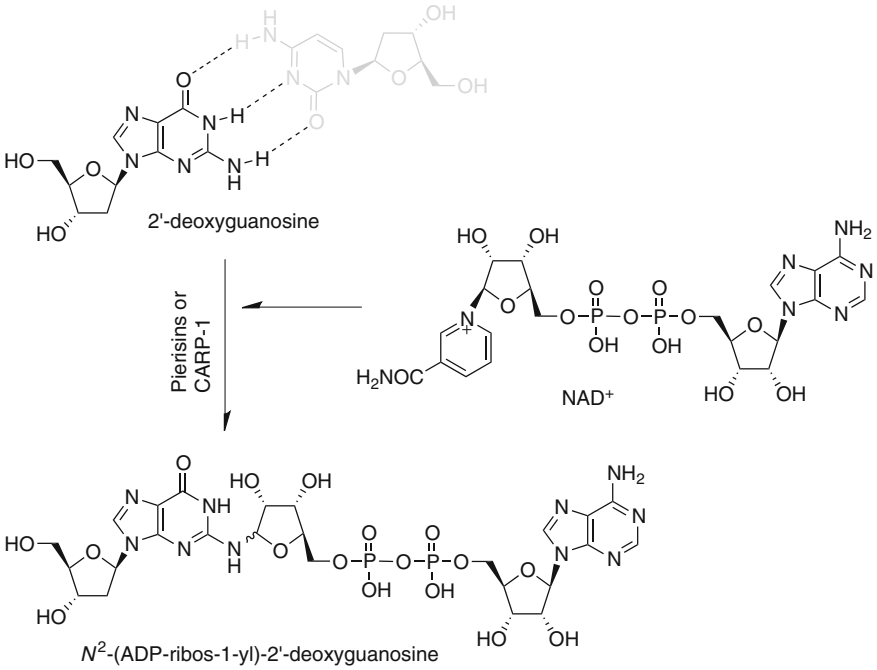

Fig. 1 Mono (ADP-ribosyl)ation of the N^2 amino group of 2′-deoxyguanosine residues in DNA by pierisin-1 in the presence of NAD^+

same product by incubation with NAD^+ and dsDNA (Takamura-Enya et al. 2004). In addition, in vitro translated pierisin homologues cloned from *Pieris melete* and *Aporia crataegi*, (pierisin-3 and -4, respectively) also target dsDNA (Yamamoto et al. 2009). Moreover, Orth et al. have reported that in vitro translated Pierisin-1b, cloned from the *Pieris rapae* species from the United Kingdom (possibly *Pieris rapae rapae*), incorporates radioactivity into oligo(dG) in the presence of $[^{32}P]NAD^+$ (Orth et al. 2011).

The ratio of the recovered α- and β-form of N^2-(ADP-ribos-1-yl)-2′-deoxyguanosine, anomerized at C1′ of ADP-ribose, was found to be 1:1, but only a single isomer is formed through the initial reaction with pierisin-2 (Takamura-Enya et al. 2004) and both isoforms easily anomerize in aqueous solution (Takamura-Enya et al. 2004; Nakano et al. 2013). We have thus proposed two possible reaction routes. One is the SN1 reaction involving an exclusive one-sided attack on the N^2 of dG via an oxocarbenium intermediate of ADP-ribose; the other is the SN2 reaction involving a direct back-attack of the N^2 of dG at the C1′ of ADP-ribose (Takamura-Enya, et al. 2004).

We could not determine the precise reaction route of the pierisins due to the lack of three-dimensional structural analysis of these proteins co-crystallized with DNA and NAD^+. However, the crystal structure of MTX revealed three characteristic conserved motifs in a cholera toxin-like reaction center: an arginine on the

β1 strand, serine-threonine-serine at the β2 strand, and a glutamic acid at the head of the β8 strand (Reinert et al. 2006). Since the secondary structure prediction for pierisin-1 matches the determined secondary structure of MTX, and the three motifs listed above are also conserved in pierisin-1 (Carpusca et al. 2006), the pierisins could be classified as an *N*-glycosidic cholera toxin-like-ADP-ribosyltransferases catalyzing mono-ADP-ribosylation (short systematic name: GADPRT) [EC 2.4.2.30.1.X.1.2] with the systematic name NAD^+:mono-ADP-D-ribosyl-DNA(guanine-N^2)-ADP-D-ribosyltransferase in accordance with the new extended EC numbering system proposed by Hottiger et al. (2010).

2.2 Kinetics of Pierisin-1

The deduced amino acid sequence of pierisin-1 indicates that this enzyme is a typical AB-toxin comprising an N-terminal ADP-ribosyltransferase activity domain and a C-terminal receptor-binding domain. Since these two domains are separated by a furin-recognition sequence (R227-D-Q-R-S-G-R-S234), pierisin would be activated by cleavage after its introduction to target cells (Kanazawa et al. 2001). Indeed, pierisin is cleaved at Arg233-Ser234 by trypsin (Watanabe et al. 1999). Neither the in vitro translated N-terminal nor C-terminal regions of pierisin alone show cytotoxicity but co-treatment of both, or electroporation of the N-terminal but not the C-terminal domain alone produces cytotoxicity, indicating that the N-terminal domain is the toxic-activity domain (Kanazawa et al. 2001). In addition, replacement of glutamic acid 165 on pierisin with aspartic acid causes a loss of activity, further suggesting that the activity domain of this enzyme is an ADP-ribosyltransferase (Watanabe et al. 1999). Meanwhile, mutation of a possible sugar-recognition motif in the C-terminus of pierisin results in a reduction of cytotoxicity, indicating that the receptor-binding domain is in this region (Matsushima-Hibiya et al. 2003). Since we could not construct an expression vector for pierisin-1 in *Escherichia coli* without any mutations, possibly due to the toxicity of basal-level pierisin-1, we determined the kinetics of this enzyme using both purified protein and an in vitro synthesized activity domain in a rabbit reticulocyte lysate. ADP-ribosyltransferase activity was determined by counting Cherenkov rays from trichloroacetic acid-precipitated substrate DNA after incubation with pierisin-1 and [^{32}P]NAD^+ (Watanabe et al. 2004a).

The activity of trypsin-cleaved pierisin-1, which still contains both the activity domain and receptor-binding domain (pierisin-1^{1-850}/trypsin), is somewhat lower than that of pierisin-1^{1-233}, and the optimum conditions for these products differ slightly. No major differences were observed in terms of substrate preference in the presence or absence of the binding domain, but the activity of pierisin-1^{1-850}/trypsin is suppressed at pH 7 and below, or at 20 °C and below. Intact pierisin-1^{1-850} without exposure to trypsin did not show activity. These observations suggest that the binding domain masks the reaction center and acts as a suppressor of the activity domain. Both pierisins are enzymatically active for more than 24 h

at 37 °C, and they ADP-ribosylate about 50 % of the guanine residues in dsDNA. Lineweaver-Burk plot analysis revealed that pierisin-1^{1-233} ADP-ribosylates dsDNA at a maximum turnover rate of 55 s^{-1}, and pierisin-1^{1-850}/trypsin does so with a maximum turnover rate of 25 s^{-1}. The turnover rates for single-strand DNA in this experiment were almost half of those of dsDNA, and that of tRNA was around 1–3 %. The K_m values of pierisin-1^{1-233} and pierisin-1^{1-850}/trypsin for NAD^+ were estimated at 0.17 and 0.18 mM, respectively.

On the other hand, the receptor-binding domain of the pierisins comprises four subdomains that show homology to the lectin domains of the ricin B-chain (smart00458). Thus, the pierisins were predicted to bind glycosylated receptors on the cell surface. To test this hypothesis, we purified pierisin-binding receptors from lipid fractions of HeLa cells and identified globotriaosylceramide (Gb3) and globotetraosylceramide (Gb4). We further confirmed the decrease in the binding activity of pierisin-1 to Gb3 and Gb4 with the introduction of mutations in the QXW motifs, which are critical for the structural organization and function of the ricin B-chain. QXW motifs are conserved in 11 of the 12 subdomains in the pierisin receptor-binding domain, and replacement of one tryptophan with a glycine causes a marked reduction in cytotoxicity. Mouse myeloma MEB4 cells lack Gb3 and Gb4 and are resistant to pierisin-1, but pretreatment of these cells with these receptors sensitizes them to pierisin-1 (Matsushima-Hibiya et al. 2003).

2.3 Distribution of the Pierisins

Pierisin was first described as a cytotoxic factor by Koyama et al. who screened for cytotoxic activity in extracts of pupa and adults of 20 kinds of Lepidopteran insects (butterflies and moths) against the human gastric carcinoma TMK-1 cell line. Extracts from three butterfly species of the family Pieridae (*Pieris rapae*, *Pieris brassicae* and *Pieris napi*) showed cytotoxicity in this analysis (Koyama et al. 1996). At that time, the cytotoxic factor was specific to the genus *Pieris*, and was termed pierisin. We subsequently demonstrated that pierisin is a DNA ADP-ribosylating protein and causes apoptosis (Watanabe et al. 1998; Takamura-Enya et al. 2001). In another report on the toxic effects of Lepidopteran insects, Marsh and Rothschild tested the toxicity of about 53 species of both aposematic and cryptic Lepidoptera in mice (Marsh and Rothschild 1974). In that study, toxicity was observed in some insects, but no relationship with pierisin was fully elucidated.

We have now revealed the distribution of pierisin-like proteins in the family Pieridae and detected pierisin-like activity in extracts from 13 species including the subtribes Pierina (*Pieris rapae*, *Pieris canidia*, *Pieris napi*, *Pieris melete*, *Pieris brassicae*, *Pontia daplidice*, and *Talbotia naganum*), Aporiina (*Aporia gigantea*, *Aporia crataegi*, *Aporia hippia*, and *Delias pasithoe*), and Appiadina (*Appias nero* and *Appias paulina,* except for *Appias lyncida*) in the subfamily

Pierinae of the family Pieridae. This activity was not found in three species of butterflies in the subfamily Pierinae or in four species of butterflies in the subfamily Coliadinae, the family Pieridae (Fig. 2a) (Matsumoto et al. 2008). Interestingly, the family Pieridae is divided into two types by the morphology of the pupal stage (Braby et al. 2006). This classification of pupal morphology corresponds with the distribution of pierisin-like activity, except for that in *Appias lyncida*. Thirty-three species of butterfly with Pierisin-like activity are classified as Type II (Fig. 2b). It is presumed that Type II species acquired the pierisin-like proteins when they emerged from Type I during the evolution of the family Pieridae.

Pierisins have now been purified from four kinds of butterflies, *Pieris rapae* (pierisin-1), *Pieris brassicae* (pierisin-2), *Pieris melete* (pierisin-3) and *Aporia crataei* (pierisin-4) (Watanabe et al. 1998; Matsushima-Hibiya et al. 2000; Yamamoto et al. 2009). When incubated with calf thymus DNA and NAD^+, pierisin-1 and -2 form N^2-(ADP-ribos-1-yl)-2′-deoxyguanosine. In vitro synthesized pierisin-3 and -4 also exhibit this DNA ADP-ribosylating activity. The cDNAs of the corresponding genes were also cloned from these butterflies and showed that pierisin-1, -2 and -3 each encode an 850 amino acid protein. On the other hand, the pierisin-4 gene encodes an 858 amino acid protein. The deduced amino acid sequences of these proteins indicate that pierisin-2 is 91 % similar to pierisin-1, whereas pierisin-3 is 93 % and pierisin-4 is 64 % similar. In addition, cDNA cloning of pierisin-1b was also reported from *Pieris rapae* species collected in Europe (Orth et al. 2011). Pierisin-1b is an 849 amino acid protein with a 91 % identity to pierisin-1. Because the subtribes Pierina and Aporiina are separated phylogenetically, a relatively low amino acid identity between the pierisins in Pierina and pierisin-4 is clearly evident.

An important question that emerges from these studies is why only some butterfly species express pierisins. Recently, de Souza and Aravind (2012) termed five novel superfamilies of peptide domains that have potential to associate with NAD-metabolism, and proposed the spreading of utility during gene transfer between bacteria and archaeo-eukaryotes. We speculate in this regard that the pierisin gene has been horizontally transferred from some bacteria to butterflies. As a basis for this prediction, gram-positive bacteria, *Bacillus sphaericus* SSII-1 and *Paenibacillus larvae*, have the homologous proteins, MTX and Plx1, respectively (Thanabalu et al. 1991; Fünfhaus et al. 2013). However, there have been no reports that MTX or Plx1 have DNA ADP-ribosylating activity. It is not known yet whether pierisin acquired ADP-ribosylating activity against DNA during the evolutionary process in butterfly or from a specific bacterium with this activity. Yamamoto et al. have demonstrated that the pierisin-1 gene is located in the genome of *Pieris rapae*. In addition, nucleotide sequence analysis of pierisin-1 has provided new evidence that the pierisin-1 gene is derived from bacteria. The pierisin-1 gene consists of two exons, a 0.1-kb exon 1 and 3.9-kb exon 2, and a 2.3-kb intron (Yamamoto et al. 2011). The domains of the eukaryotic proteins strongly correlate with the exons during the exon-shuffling evolution. However,

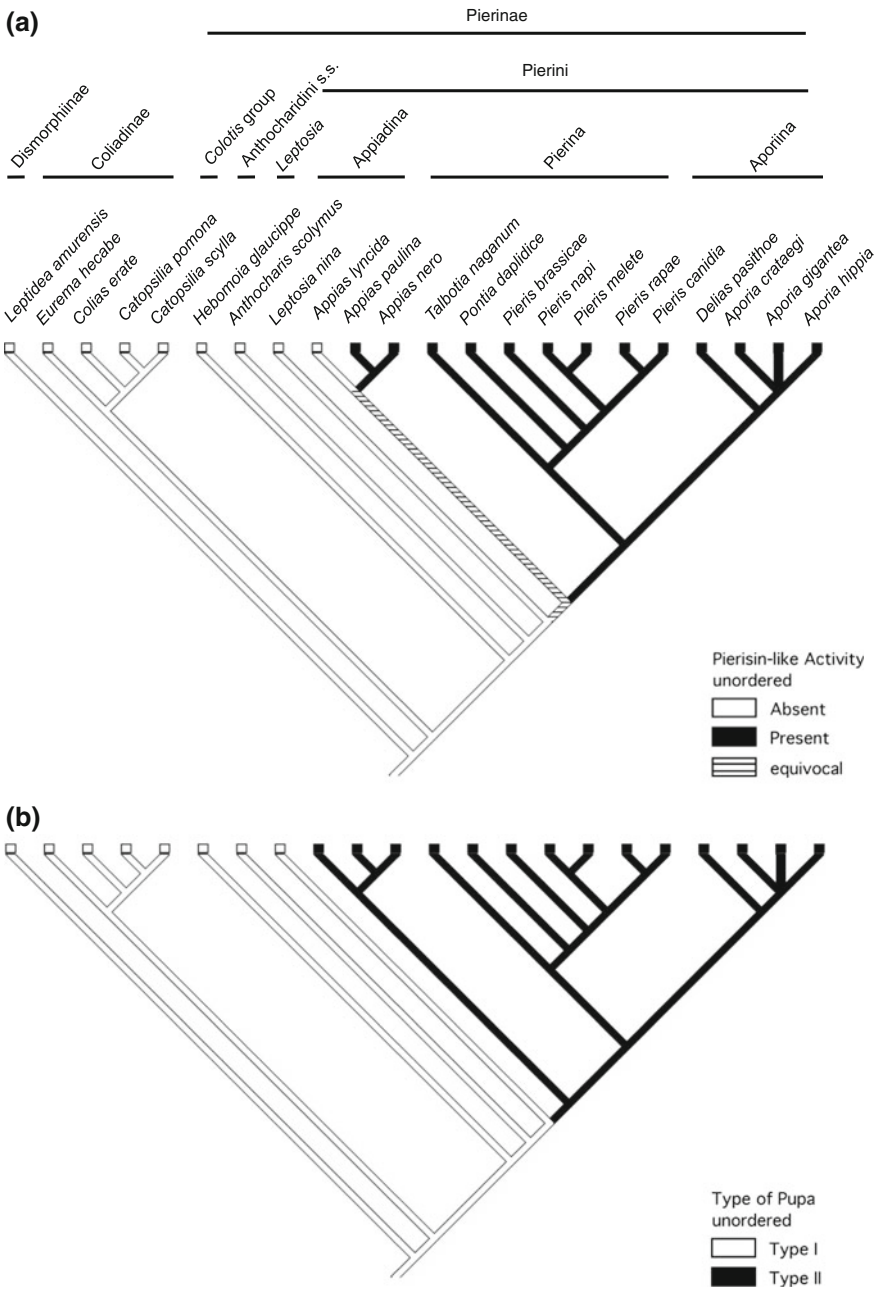

Fig. 2 Most-parsimonious reconstruction analysis of the plesiomorphy of (**a**) pierisin-like activity and **b** pupal morphology in 22 butterfly species from the family Pieridae. The phylogenic tree were created by reference to Braby et al. (2006) (Modified from Odagiri (2009)

intron-1 divides the activity domain and no intron exists between the border of the activity and receptor-binding domain of pierisin-1. de Souza and Aravind also proposed that some ADP-ribosylating toxins develop potential to specialized substrates, which are difficult to resist during gene transfer (2012). A DNA ADP-ribosylating toxin produced by bacteria could be the ancestor of pierisins, which had been transferred with self-protection mechanism against DNA modification.

Further analysis of the evolution of pierisins in butterflies has been performed by Odagiri (Odagiri 2009), with a phylogenetic analysis tool MacClade (Maddison and Maddison 2005). In that study, the author carried out Most-Parsimonious Reconstruction analysis of plesiomorphy in major host plants, from a genealogical tree of 22 species from the family Pieridae, based on the fact that many host plants of the tribe Pierini are highly toxic. According to these analyses, several host shifts occurred in the family Pieridae, and it is possible that pierisin-like activity was acquired in two subtribes between Pierina (*Pieris rapae*, *Pieris canidia*, *Pieris napi*, *Pieris melete*, *Pieris brassicae*, *Pontia daplidice*, and *Talbotia naganum*), Aporiina (*Aporia gigantea*, *Aporia crataegi*, *Aporia hippia*, and *Delias pasithoe*), and in one subgroup Catophaga (*Appias nero* and *Appias paulina* of subtribe Appiadina). The other hypothesis is that Appias lyncida lost pierisin gene, which was acquired once in Pierini. The relationship with pierisins and the host plant is not yet known, but a relationship between host plants and bacteria might be closely related to the distribution and original source of the pierisins.

2.4 Physiological Roles of the Pierisins

Insects have very numerous and very different types of predators ranging from vertebrates to viruses, and have developed specific defense systems accordingly. The cabbage butterfly *Pieris rapae* whips using its head and regurgitates digestive juice against formidable predators such as birds, spiders, and parasitic wasps (Higginson et al. 2011). Defensive lipids from the glandular hairs of *Pieris rapae* larvae are also deterrents against an important natural enemy, the ant (Smedley et al. 2002). In the same manner as common insects, *Pieris rapae* develop "cellular immunity" mediated by macrophage-like cells and "humoral immunity" involving antimicrobial peptides and melanization against microorganisms, which invade the body. The body fluids of some insects, including *Pieris rapae*, also show cytotoxicity against mammalian cells (Marsh and Rothschild 1974; Koyama et al.1996). In the larval stages of *Pieris rapae*, pierisin-1 protein is mainly produced in the fat body, and released into the body fluid (the fat body is the insect equivalent of the liver. Its main functions are to transport nutrient substrates to utilization sites and deliver metabolic waste to the excretory system; see Gilbert and Chino 1974). The cytotoxic potency of pierisin-1 varies among different mammalian cell lines, with measured IC_{50} values ranging from 0.043 to 270 ng/ml for the 13 samples examined thus far (Kono et al. 1999; Matsushima-Hibiya et al. 2000; Kanazawa et al. 2001).

Most mammalian cells exhibit apoptotic cell death when treated with pierisin-1. Activation of caspase-2, -3, and -6 is observed in pierisin-treated HeLa cells. This apoptotic response is suppressed by transfection with the *bcl-2* gene or by treatment with a caspase-3 inhibitor. Hence, pierisin-1-induced apoptosis is mediated primarily via a mitochondrial pathway involving Bcl-2 and caspases (Kanazawa et al. 2002).

The strong cytotoxicity of pierisin-1 is effective as a protective agent against microbes and parasitoids. Our latest study findings suggest pierisin-1 transcript levels increase after parasitization by parasitic wasps and bacterial injection of *Pieris rapae* larvae, with the activated 27 kDa pierisin-1 enzyme domain also appearing following parasitization (Fig. 3a). Moreover, culture studies have shown that pierisin-1 causes cellular damage to the eggs and larvae of parasitic wasps (*Cotesia plutellae*, *Cotesia kariyai*, *Glyptapanteles pallipes*, which usually cannot parasitize and survive in *Pieris rapae,* Fig. 3b, c; Takahashi-Nakaguchi et al. 2013). Based on these data, we speculate that pierisin-1 has an important role as a defense factor in *Pieris rapae*. The fat body and hemocytes play an important role in the insect immune system by producing antimicrobial peptides or various enzymes for melanization in response to infectious bacteria (Ferrandon et al. 2007). Pierisin-1 is also expressed in the fat body and in hemocytes (Fig. 3e). Pierisin-1 induction may be regulated by important overlapping genes for other fundamental components of the insect immune system.

Interestingly, eggs and larvae of *Cotesia glomerata* the dominant gregarious parasitic wasp of *Pieris rapae*, were found in our recent study to be resistant to pierisin-1 (Takahashi-Nakaguchi et al. 2013). The cytotoxic activity of pierisin-1 is dependent on whether DNA contact has been made. The inner cells of *Cotesia glomerata* are sensitive to pierisin-1, but *Cotesia glomerata* has muciform special structures on its surface to block pierisin-1 penetration (Fig. 3c, d). Furthermore, *Cotesia glomerata* parasitization does not induce the additional expression and activation of pierisin-1. It is well known that parasitic wasps inhibit the host immune system via the co-injection of a cocktail of maternal secretions into the host hemocoel, including venom, calyx fluid, and polydnaviruses. These substances may also inhibit pierisin-1 expression and activation. It is possible that *Cotesia glomerata* has acquired evolutionary tolerance to pierisin-1 by inhibiting its penetration of the egg shells and the surface layers of its larvae.

Another possibility is that pierisin-1 could also be involved in metamorphosis in *Pieris rapae*. The pierisin-1 protein levels increase by about 100-fold from the first to fifth instar larvae, and then gradually decrease by over 90 % during the pupal stage (Watanabe et al. 2004b). During pupation in Lepidopteran insects, the larval mid-gut, silk gland, larval epidermis, and some fat bodies are removed by apoptosis and undergo remodeling to form adult organs (Fig. 4; Wigglesworth 1972; Uwo et al. 2002). A role of pierisin-1 may be to induce the apoptotic removal of larval cells during the metamorphosis of *Pieris rapae*.

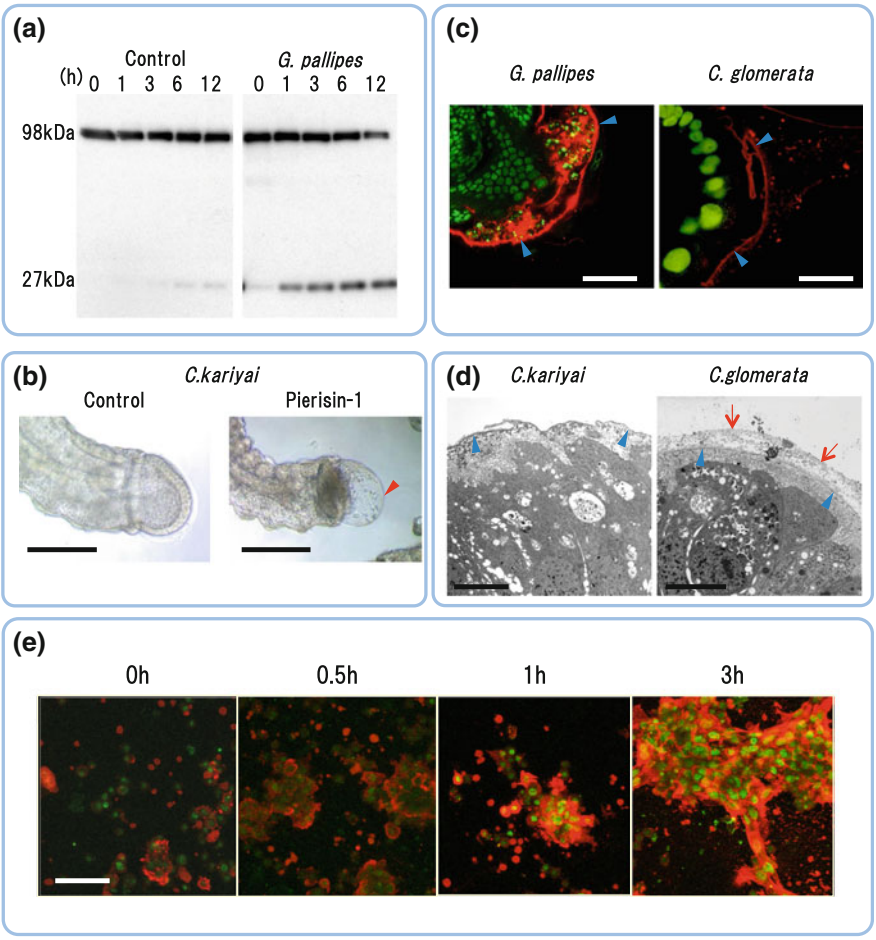

Fig. 3 **a** Activation of pierisin-1 in body fluid of *Pieris rapae* following incubation with parasitic wasp eggs. Western blotting analysis of pierisin-1 protein in the hemolymph 1–12 h after co-incubation with (*right panel*) or without (*left panel*) eggs of *Glyptapanteles pallipes*. Amounts of full-length pierisin-1 (98 kDa) and activated 27-kDa N-terminal fragments of pierisin-1 were detected on these immunoblots. **b** Morphological analysis of pierisin-treated *Cotesia kariyai* larva. Apoptosis-like damage was observed at the caudal vesicle cells of *Cotesia kariyai* larva (*arrowhead*) following pierisin-1 treatment. Wasp larvae were treated with pierisin-1 at 10 mg/ml in the medium, and representative microscope images are shown. The anterior is on the *left*. *Horizontal bars* represent 100 μm. c Prevention of incorporation of pierisin-1 in *Cotesia glomerata* larvae. Pierisin-1 is incorporated into the caudal vesicle cells of the nonpermissive wasp (*G. pallipes*; *left panel*). However, in the case of *Cotesia glomerata*, HiLyte dye-labeled pierisin-1 was observed on the exterior of the surface layer of the caudal vesicle, but not inside the cells (*right panel*). Each stage of parasitoids was cultured with HiLyte dye-labeled pierisin-1 (*red*) for 24 h, and then labeled with STYO-16 live-cell nucleic acid stain (*green*); *arrowheads* outer membrane of caudal vesicle of wasp larvae. *Horizontal bars* represent 50 μm. **d** Transmission electron microscope (TEM) analysis of caudal vesicle of wasp larvae. *Cotesia glomerata* has an additional layer *outside* the outer membrane (*right panel*), but *Cotesia kariyai*

◀ do not have additional layer (*left panel*). *Arrowheads* outer membrane, *arrows* additional layer of the *Cotesia glomerata* caudal vesicle. *Horizontal bars* represent 1 μm. (Modified from Takahashi-Nakaguchi et al. (2013). Copyright: Takahashi-Nakaguchi et al.) **e** Localization of pierisin-1 in immunologically activated hemocytes. Hemocytes of *Pieris rapae* are immunologically activated on glass slides. Pierisin-1 mRNA is expressed and pierisin-1 proteins accumulate in these cells. *Red* anti pierisin-1 antibody (Cy3), *green* nuclear staining (SYTO-16). *Horizontal bars* represent 100 μm

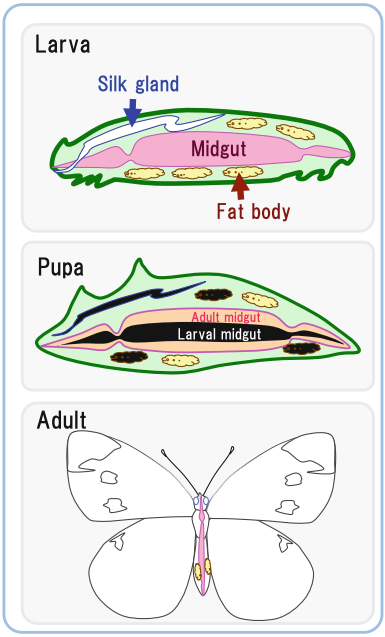

Fig. 4 Pierisin-1 is mainly produced in the fat body of *Pieris rapae* and released into the body fluid. During the pre-pupa stage, pierisin-1 penetrates some organs, including the silk gland, larval mid-gut, and a part of the fat body (*painted black*), and is removed at the pupal stage

3 ADP-Ribosylation of DNA by Shellfish (Bivalve) Enzymes

3.1 Screening for NAD^+:DNA ADP-Ribosyltransferases

To analyze the distribution of DNA ADP-ribosyltransferase activity independently of homology or cytotoxicity assays, we developed a simple and sensitive screening system. Radioluminography (a sensitive autoradiography system with imaging plates) analysis of Thin-layer chromatography-separated dsDNA hydrolysate incubated with crude samples and activator trypsin in the presence of [^{32}P]NAD^+, enables the activity detection of 1 picogram of pierisin-1 in 50 μg of proteins in the crude extract. The initial wide-range screening targeted 100 species including insects (especially butterflies and moths), common experimental animals (mice, starfish, planaria, tunicates, sea urchin, earthworms, *Caenohabditis elegans*), and edible marine animals (shellfish and other fish species). During this screening, we

found that protein extracts of edible clams (bivalves), such as clams (*Meretrix lamarckii*, *Ruditapes phillipinarum*, *Corbicula japonica*, *Spisula sacharinensis*), rasor clams (*Solen strictus*), mussels (*Mytilus galloprovincialis*), and oysters (*Crassostrea gigas*), contain DNA ADP-ribosyltransferase activity. Hard clams, which are believed to be relatively newer bivalves than oysters, contained higher activity per protein (Nakano et al. 2006), and both marine and brackishwater species were also found to contain this ADP-ribosylating activity. Gastropods, however, contained only a small level of ADP-ribosylating activity, and we could not detect this activity in cepharopods (Nakano et al. 2006).

3.2 *Purification and cDNA Cloning of CARP-1 from the Hard Clam* Meretrix lamarckii

All soft tissues of *Meretrix lamarckii* contain DNA ADP-ribosylating activity, and the foot muscle, dymiarian, and branches contain relatively higher activity than the gills, mantle, or digestive glands that are exposed to the external environment. The purified enzyme responsible, named CARP-1, also ADP-ribosylates guanine residues on dsDNA. CARP-1 modifies about 50 % of the guanines in dsDNA, although we could not determine its precise enzymatic properties. No part of the CARP-1 protein shows BLAST-detectable homology with any other characterized proteins, toxins, secretion motifs, or receptor-binding domains. CARP-1 shows homology only with some genome-project derived hypothetical proteins from oysters and bacteria (Fig. 5a, b). The substitution of E128, but not E127, on CARP-1 for aspartic acid results in a >90 % loss of ADP-ribosylation activity, and both the LYRVLR and STT motifs in this protein exist upstream of glutamic acid (Nakano et al. 2006). These observations suggest that as with the pierisins, CARP-1 could be classified as an *N*-glycosidic cholera toxin-like-ADP-ribosyltransferase catalyzing mono-ADP-ribosylation (short systematic name: GADPRT) [EC 2.4.2.30.1.X.1.2] with the systematic name NAD^+:mono-ADP-D-ribosyl-DNA(guanine-N^2)-ADP-D-ribosyltransferase according to the new extended EC numbering system proposed by Hottiger et al. (2010).

3.2.1 Possible Physiological Roles of CARP-1

We studied shellfish DNA ADP-ribosyltransferases for two principal reasons. The first is the biological importance of these animals. Molluscs are one of the most ancient animals to be traceable by fossils and are distributed in many different environments, from the sides of hydrothermal vents in deep sea locations to brackish water areas, coastal lagoons, and fresh water lakes and rivers. The second reason concerns human health implications. Molluscs are widely consumed by humans and often cause algae-induced food poisoning, although they are rarely

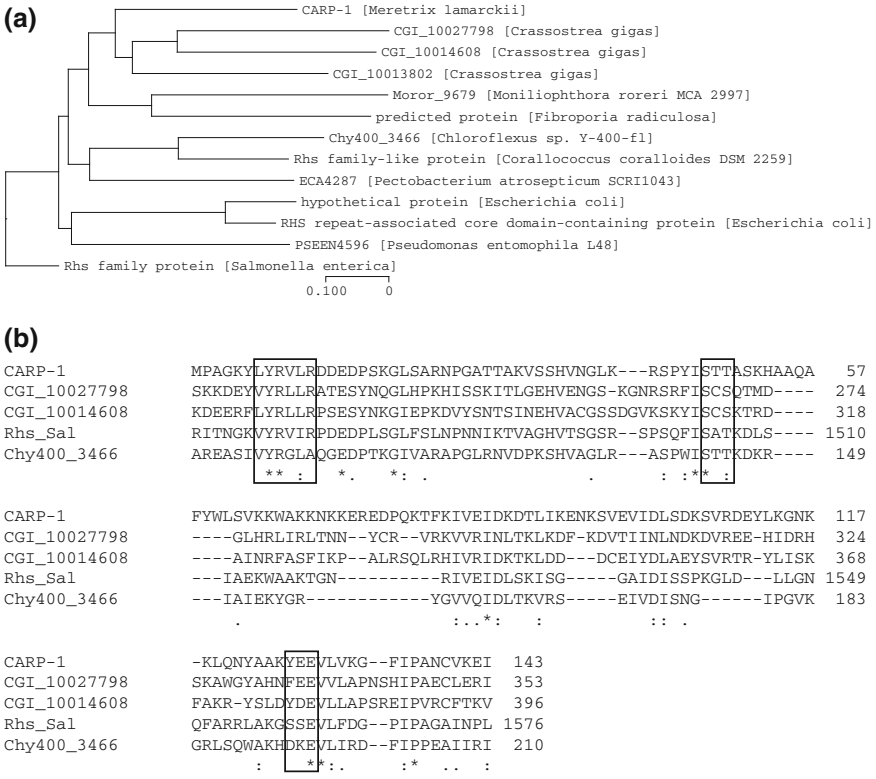

Fig. 5 **a** Dendrogram for amino acid sequences having homology to CARP-1. Sequences were chosen from the international nucleotide sequence databases using the BLASTp program (Altschul et al. 1990) (expect value <1.0), and similarities were calculated by ClustalW program (Thompson et al. 1994). The scale represents the number of substitutions per site. The tree was drawn using DendroMaker for Macintosh software ver. 4.1 (Imanishi 1998). **b** Alignment for amino acid sequences having homology to CARP-1. Rhs_Sal, Rhs family protein from *Salmonella enterica*. Accession numbers in the International nucleotide sequence databases for these sequences are as follows; CARP-1, BAF03560; CGI_10027798, EKC40156; CGI_10014608, CGI_10014608; Rhs_Sal, WP_023221539; Chy400_3466, YP_002571167. The conserved arginine, Ser–Thr–Ser/Thr motif, and glutamic acid residues are *boxed*. Conserved amino acids are marked by *colons*, completely conserved amino acids are marked by *asterisks*

eaten in raw form. We have previously documented our concerns that DNA ADP-ribosyltransferases might be the causative agent for food poisoning in molluscs.

Since sequence analysis has demonstrated that CARP-1 lacks binding domains, this shellfish enzyme may not in fact be harmful to humans. In addition, CARP-1 showed no cytotoxic activity against 10 human cancer cell lines, unless introduced by electroporation, supporting the contention that CARP-1 itself lacks the binding domains to enter mammalian cells (Nakano et al. 2006). Thus, the working hypothesis regarding the human health concerns of eating certain shellfish

containing CARP-1 could be refuted on these grounds. We have now three hypotheses regarding the physiological role of CARP-1, although we have not yet tested these experimentally:

(1) CARP-1 exerts toxic effects as a defense response to invading organisms.

CARP-1 requires additional factors to act as a toxin such as *Clostridium difficule* C2-toxin-like pore-forming subunits, or the *Salmonella enterica* SpvB-like entry system.

(2) CARP-1 is a regulator of the NAD^+ concentration.

Some parasites (Kita et al. 2002), and microenvironments in human cancer (Hirayama et al. 2009) are suggested to synthesize ATPs from fumarate by reversing a part of the TCA cycle under anaerobic condition (fumarate respiration). Bivalves are also suggested to synthesize ATPs by reversing a part of the TCA cycle under anaerobic conditions. This results in the accumulation of succinate and NAD^+(Grieshaber et al. 1994; de Zwaan et al. 1991; Ortmann and Grieshaber 2003). CARP-1 may regulate this pathway by decreasing excess amounts of NAD^+.

(3) CARP-1 forms part of the innate immune response to DNA viruses.

Bivalves are filter-feeders and feed on plankton and bacteria in sea water. This means that bivalves would need to have a self-defense mechanism against viral- and bacterial-infections. In the case of mammalian cells, cytosolic dsDNA, i.e., infected viral DNA, upregulates the innate immune system (Koyama et al. 2010; Civril et al. 2013; Gao et al. 2013). Cytosolic CARP-1 may, therefore, modify viral dsDNA, resulting in a failure of integration, or ADP-ribosylated DNA (or its degraded nucleotides) may induce innate immunity.

4 Homologues of the Pierisins and CARP-1

The sequencing and cloning of pierisin-1 was accomplished in 1999 and the deduced amino acid sequence of pierisin-1 showed a 32 % identity with mosquitocidal toxin (MTX) (Watanabe et al. 1999; Carpusca et al. 2006). It is well known that cholera toxin-like ADP-ribosyltransferase has three highly conserved regions, an arginine residue (Region I) that is thought to maintain the structure of the reaction pocket, the Ser–Thr–Thr/Ser motif (Region II), which is considered to enable a β-strand-α-helix structure to form, and the glutamic acid residue (Region III) that serves as an NAD-binding site (Masignani et al. 2000; Domenighini and Rappuoli 1996). These conserved regions and their surrounding amino acid sequences are similar between pierisin-1 and MTX. However, there is no evidence at present that MTX has DNA ADP-ribosylating activity. Moreover, the C-terminal regions of pierisin-1 and MTX consist of ricin B-chain-like domains including QXW motifs. These domains of pierisin-1 possess receptor-binding ability, and are

responsible for incorporating it into cells (Matsushima-Hibiya et al. 2003). These features are common in all pierisins. Recently, a pierisin-like sequence was found in the genome of *Paenibacillus larvae*, a gram-positive bacterial pathogen that causes American foulbrood in the honey bee (Fünfhaus et al. 2013). *Paenibacillus larvae* toxin (Plx1) consists of 975 amino acids and harbors three conserved regions and QXW motifs. Plx1 shows a 35 % amino acid identity with pierisin-1, but it has not been revealed whether Plx1 has DNA ADP-ribosylating activity. MTX and Plx1 contain an N-terminal signal sequence that is not present on the pierisins (Fig. 6a).

The activity domain of the pierisins shares homology with SCO5461, comprising an N-terminal secretion domain and a C-terminal activity domain, in *Streptomyces coelicolor* (Pallen et al. 2001; Fig. 6a, b). SCO5461 orthologues are distributed in many *Streptomyces* spp. strains and *Streptosporangium roseum*, and an imperfect ORF remains in *Streptomyces avermitilis* (Szirák et al. 2012; Nakano et al. 2013). Contrary to pierisins, MTX, and Plx1, which shows toxicity (Shiga et al. 2006; Takahashi-Nakaguchi et al. 2013; Thanabalu et al. 1991; Schirmer et al. 2002; Fünfhaus et al. 2013), physiological roles for SCO5461 might not be toxin due to the lack of receptor-binding domains. Szirák et al. (2012) have reported the possible ADP-ribosylation of a 65-kDa endogenous protein by SCO5461, and that a disruption of the *SCO5461* gene affects sporulation and antibiotic production depending on the culture conditions. This deficiency is rescued by co-cultivation with a wild-type strain (Szirák et al. 2012). Moreover, we have found that SCO5461 ADP-ribosylates guanine residues of nucleosides and mononucleotides, such as guanosine, deoxyguanosine, cyclic GMP, rather than dsDNA, in vitro. We have also detected SCO5461 in culture medium, but in contrast, Widdick et al. (2006) have reported the existence of SCO5461 in the membrane fraction. It may be possible that SCO5461 targets guanine-containing messenger molecules, such as ppGpp and cyclic di-GMP, which regulate quorum sensing and virulence (Srivastava and Waters 2012; Krasteva et al. 2012).

On the other hand, no part of the CARP-1 protein shows detectable homology with any characterized proteins nor any conserved domains. The genome project for the oyster *Crassostrea gigas*, a species which contains CARP-1-like DNA ADP-ribosylating activity (see Sect. 3), revealed that hypothetical CGI_10027798 and CGI_10014608 proteins show around 30 % homology to the ADP-ribosylating motifs of CARP-1. Interestingly, some Rhs family-like proteins such as *Salmonella enterica* show homology with CARP-1 in their uncharacterized domains, but not in Rhs-domains (Fig. 5b). Deep genome sequence analysis predicts that some proteins, which contain newly predicted ART domains, contain Rhs/YD-repeats or proline-/glycine-rich region at their N-terminus (de Souza and Aravind 2012). It is possible that the origin of CARP-1 would be the acquired bacterial ADP-ribosylating toxins that later lost the Rhs domain.

Amino acid sequences for mammalian ecto-ARTs and poly(ADP-ribose)polymerases share less similarity with toxic ADP-ribosyltransferases, although they share the typical folding in three-dimensional structure (Domenighini and Rappuoli 1996). Genes for these enzymes might be originated bacterial NAD-metabolizing

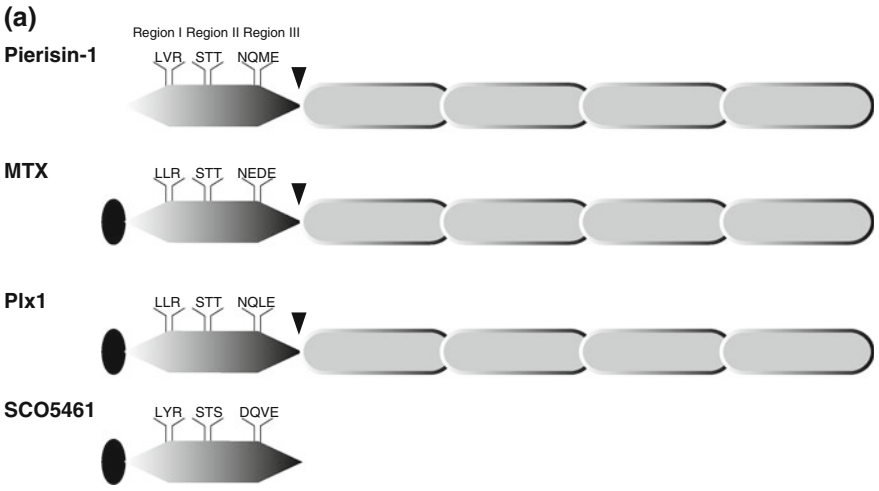

(b)

```
Pierisin-1      rrqrlvrwdrrppneifldgf-vpivtrenp-dwe--etdlygfakn------nhpsifv 113
Pierisin-4      RRQRLVRWDRRPPNEIFLNGF-VPIVTNENP-DWS--QTDLYNFAKS------NVPSIFV 119
MTX             NEHRLLRWDRRPPNDIFLNGF-IPRVTNQNLSPVE--DTHLLNYLRT------NSPSIFV 141
Plx1            ERQRLLRWDRRPPNEILINGF-VPQVINADP-SLE--ETNLFRYVKS------NTKSIFV 144
SCO5461         TCGTLYRSDSRGPQVVFEEGF-HAKDVQNGQ-------YDVEKYVLV------NQPSPYV 120
ctx_A           NDDKLYRADSRPPDEIKQSGGLMPRGQSEYFDRGTQMNINLYDHARGTQTGFVRHDDGYV 78
                    * * * * *: :  .*                    .:  .         .  . :*

Pierisin-1      sttktqrn---kkk--yvwtprnanrgivyqye-iyapggvdvndsfsd-aspwpnqmev 166
Pierisin-4      STTKTQFKK--NGK--YVWTPRSANRGIVYQYE-IYAPGGLDVNESLSE-QSPWPNQMEV 173
MTX             STTRARYNN--LGLEITPWTPHSANNNIIYRYE-IFAPGGIDINASFSRNHNPFPNEDEI 198
Plx1            STTKTKYKN---GKRYQPWSPRTRDNGIVYQYE-IFAPGGVDVNRSFGE-QSPWPNQLEV 199
SCO5461         STSYDHD-------LYKTWYK------SGYNYY-VDAPGGIDVNKTIGD-THKWADQVEV 165
ctx_A           STSISLRSAHLVGQ--TIL----SGHSTYYIYVIATAPNMFNVNDVLGA-YSPHPDEQEV 131
                **:                              * *    **  .::*  :.       :: *:

Pierisin-1      afpggiqniyirsarelhngriqriw 192
Pierisin-4      AFPGGIQNVYIRSARELHDGRVQRIW 199
MTX             TFPGGIRPEFIRSTYEYHNGEIVRIW 224
Plx1            AFPGGIRPEFIRSVRELQNGRIQRIW 225
SCO5461         AFPGGIQRKYIIGVCPVDRQTKTEIM 191
ctx_A           SALGGIPYSQIYGWYRVHFGVLDEQL 157
                :  ***    * .    .    .
```

Fig. 6 **a** Schematic representations of the primary structure of Pierisins, MTX, Plx1, and SCO5461 homologues. *Arrowheads* indicate protease-recognition sites. *Black ovals* secretion signals, *hexagons* activity domains, *shaded ovals,* lectin domains of ricin B-chain-like domains. **b** Alignment of the deduced amino acid sequence of the activity domains of pierisins, MTX, Plx1, SCO5461, compared with the other R-S-E type cholera toxin. ctx_A, the A subunit of cholera toxin. Accession numbers in the International Nucleotide Sequence Databases for these sequences are as follows; pierisin-1, Q9U8Q4; pierisin-4, BAH96563; MTX, AAA22601; Plx1, AGJ74029; SCO5461, CAB76015; the A subunit of cholera toxin, CAA24995. The conserved arginine, Ser–Thr–Ser/Thr motif, and glutamic acid residues are *boxed*. Conserved amino acids are marked by *colons*, completely conserved amino acids are marked by *asterisks*

enzymes, not toxins. Contrary to these proteins, ancestor of pierisins would be so toxic ADP-ribosyltransferases that could be distributed within the limited taxa of butterflies. There are no reports for ARTDs that could target bases of nucleic acids.

5 Significance of DNA ADP-Ribosylation and Future Perspectives

ADP-ribosylation is widely known to be a post-translational modification reaction to a variety of specific residues from proteins. Our investigation of cytotoxic potential in Pierid butterflies such as *Pieris rapae* led to the discovery of a new and unforeseen enzymatic reaction, DNA ADP-ribosylation at the N^2 position of guanine (Takamura-Enya et al. 2001). Subsequent screening for this unique ADP-ribosylation activity yielded the finding of another guanine specific ADP-ribosyltransferase in a variety of shellfish species (Nakano et al. 2006). Surprisingly, the DNA ADP-ribosyltransferase identified in the shellfish *Meretrix lamarckii* is almost completely nonhomologous, except for some ATRC motifs, to the pierisins enzyme in the butterfly. Hence, at least two different evolutional processes would have needed to occur to acquire the DNA modification activity in these species. As we have mentioned above, *Streptomyces* spp. also expresses a guanine ADP-ribosyltransferase, which is homologous to the pierisins in butterfly (Nakano et al. 2013). In addition, ordinary homology searches have demonstrated the presence of a number of proteins in different species homologous to those in butterflies and shellfishes, although some of them may not be expressed nor have DNA-modification potential. However, evidence for the presence of DNA ADP-ribosyltransferases in a variety of living organisms is accumulating.

DNA is responsible for all biol ogical activity in living organisms and for the transmission of hereditary characteristics from parents to offspring. Hence, enzymatic DNA modifications carry great biological significance. A number of modification reactions for nucleic acids have been identified, but most of these events are known to be specific biological processes or reactions, e.g., synthesis of modified bases composed of tRNA, and modification of specific sequences in restriction-modification systems (Grosjean 2009). The DNA ADP-ribosyltransferases transfer ADP-ribose to the guanine bases of dsDNA in a nonselective manner to produce a "DNA adduct", and this property confers cytotoxic or even genotoxic potential on these enzymes. Cytotoxic substances are common in nature, and a diverse array of cytotoxins are produced by many virulent bacteria and even by some multicellular organisms (Lubran 1988; Shogomori and Kobayashi 2008; Natori 2010). The pierisins are an example of AB-toxins that also show strong cytotoxicity (Kono et al. 1999; Kanazawa et al. 2001). In fact, we have speculated that these butterfly toxins are defense factors against certain kinds of parasitic wasps (Takahashi-Nakaguchi et al. 2013). When we focus on biological genotoxic substances, however, there are few types of these, including the DNA ADP-ribosyltransferases so

far reported. Cytolethal distending toxins were the first bacterial genotoxins described (Elwell and Dreyfus 2000; Lara-Tejero and Galan 2000; Guerra et al. 2011; Gargi et al. 2012). These toxins present in several gram-negative bacteria, display DNase activity and induce G2/M arrest in mammalian cells. In addition, cytolethal distending toxins may also play a role in human malignancy, although this may be indirectly through an alteration of cellular signaling and immune response pathways rather than direct mutations induction by DNA cleavage. The guanine specific ADP-ribosyltransferases found in Pierid butterflies and shellfishes also can be classified as potent biological genotoxins. Furthermore, they possess unique features that produce bulky DNA adducts in a manner similar to chemical carcinogens. Indeed ADP-ribose adducts cause replication arrest of a variety of polymerases and are repaired by the nucleotide excision repair system (Shiotani et al. 2005, 2006). In addition, the pierisins induces cell cycle arrest through the ATR and ATM pathways and gene mutations in culture cells (Totsuka et al. 2003; Shiotani et al. 2006). These findings demonstrate that the adduct-based DNA damage caused by a DNA ADP-ribosyltransferase is indistinguishable from that caused by chemical carcinogens. However, the involvement of DNA-modification enzymes in genetic alterations in living organisms remains to be elucidated. It is theoretically possible that the pierisins are incorporated in the gut cells of the predators of butterfly larvae and induce mutations. A more interesting hypothesis may be that the organisms harboring the modification enzymes show accelerated evolution due to mutation. It is also likely, however, that the modified DNA or RNA in this context triggers a signal transduction or immune response instead of mutation, as discussed on the previous section on shellfishes. These enzymes have the capacity to initiate a defense response to all foreign organisms since DNA is common to all living organisms. It will be of interest to identify new species that express DNA ADP-ribosyltransferases and further elucidate the biological significance of the DNA modifications that are caused by these enzymes.

Acknowledgments The authors thank Dr. Ken-Ichi Odagiri for giving us a copy of phylogenic tree drawing.

References

Altschul SF, Gish W, Miller W, Myers EW, Lipman DJ (1990) Basic local alignment search tool. J Mol Biol 215:403–410

Braby M, Viar R, Pierce N (2006) Molecular phylogeny and systematics of the Pieridae (Lepidoptera: Papilionoidea): higher classification and biogeography. Zool J Linnean Soc 147:239–275

Carpusca I, Jank T, Aktories K (2006) *Bacillus sphaericus* mosquitocidal toxin (MTX) and pierisin: the enigmatic offspring from the family of ADP-ribosyltransferases. Mol Microbiol 62:621–630

Civril F, Deimling T, de Oliveira Mann CC, Ablasser A, Moldt M, Witte G, Hornung V, Hopfner KP (2013) Structural mechanism of cytosolic DNA sensing by cGAS. Nature 498:332–337

Corda D, Di Girolamo M (2002) Mono-ADP-ribosylation: a tool for modulating immune response and cell signaling. Sci STKE 2002:PE53

Corda D, Di Girolamo M (2003) Functional aspects of protein mono-ADP-ribosylation. EMBO J 22:1953–1958

Domenighini M, Rappuoli R (1996) Three conserved consensus sequences identify the 462 NAD-binding site of ADP-ribosylating enzymes, expressed by eukaryotes, bacteria 463 and T-even bacteriophages. Mol Microbiol 21:667–674

Elwell CA, Dreyfus LA (2000) DNase I homologous residues in CdtB are critical for cytolethal distending toxin-mediated cell cycle arrest. Mol Microbiol 37:952–963

Ferrandon D, Imler JL, Hetru C, Hoffmann JA (2007) The Drosophila systemic immune response: sensing and signalling during bacterial and fungal infections. Nat Rev Immunol 7:862–874

Fünfhaus A, Poppinga L, Genersch E (2013) Identification and characterization of two novel toxins expressed by the lethal honey bee pathogen *Paenibacillus larvae*, the causative agent of American foulbrood. Environ Microbiol 15:2951–2965

Gao D, Wo J, Wo Y-T, Du F, Aroh C, Yan N, Sun L, Chen Z (2013) Cyclic GMP-AMP synthase is an innate immune sensor of HIV and other retroviruses. Science 341:903–906

Gargi A, Reno M, Blanke SR (2012) Bacterial toxin modulation of the eukaryotic cell cycle: are all cytolethal distending toxins created equally? Front Cell Infect Microbiol 2:Article 124

Gilbert LI, Chino H (1974) Transport of lipids in insects. J Lipid Res 15:439–456

Grieshaber MK, Hardewig I, Kreutzer U, Pörtner H-O (1994) Physiological and metabolic responses to hypoxia in invertebrates. Rev Physiol Biochem Pharmacol 125:43–147

Grosjean H (ed) (2009) DNA and RNA modification enzymes: structure, mechanism, function and evolution. Landes Biosciences, Austin

Guerra L, Cortes-Bratti X, Guidi R, Frisan T (2011) The biology of the cytolethal distending toxins. Toxins 3:172–190

Higginson AD, Delf J, Ruxton GD, Speed MP (2011) Growth and reproductive costs of larval defence in the aposematic lepidopteran *Pieris brassicae*. J Anim Ecol 80:384–392

Hirayama A, Kami K, Sugimoto M, Sugawara M, Toki N, Onozuka H, Kinoshita T, Saito N, Ochiai A, Tomita M, Esumi H, Soga T (2009) Quantitative metabolome profiling of colon and stomach cancer microenvironment by capillary electrophoresis time-of-flight mass spectrometry. Cancer Res 69:4918–4925

Hottiger MO, Hassa PO, Lüscher B, Schüler H, Koch-Nolte F (2010) Toward a unified nomenclature for mammalian ADP-ribosyltransferases. Trends Biochem Sci 35:208–219

Imanishi T (1998) DendroMaker for Macintosh for unrooted trees. Version 4.1. http://www.cib.nig.ac.jp/dda/timanish/dendromaker/home.html (archived in: http://web.archive.org/web/20120810103811/, http://www.cib.nig.ac.jp/dda/timanish/dendromaker/home.html)

Kanazawa T, Watanabe M, Matsushima-Hibiya Y, Kono T, Tanaka N, Koyama K, Sugimura T, Wakabayashi K (2001) Distinct roles for the N- and C-terminal regions in the cytotoxicity of pierisin-1 a putative ADP-ribosylating toxin from cabbage butterfly, against mammalian cells. Proc Natl Acad Sci USA 98:2226–2231

Kanazawa T, Kono T, Watanabe M, Matsushima-Hibiya Y, Nakano T, Koyama K, Tanaka N, Sugimura T, Wakabayashi K (2002) Bcl-2 blocks apoptosis caused by pierisin-1, a guanine-specific ADP-ribosylating toxin from the cabbage butterfly. Biochem Biophys Res Commun 296:20–25

Kita K, Hirawake H, Miyadera H, Amino H, Takeo S (2002) Role of complex II in anaerobic respiration of the parasite mitochondria from *Ascaris suum* and *Plasmodium falciparum*. Biochim Biophys Acta 1553:123–139

Kono T, Watanabe M, Koyama K, Kishimoto T, Fukushima S, Sugimura T, Wakabayashi K (1999) Cytotoxic activity of pierisin, from the cabbage butterfly, *Pieris rapae*, in various human cancer cell lines. Cancer Lett 137:75–81

Koyama K, Wakabayashi K, Masutani M, Koiwai K, Watanabe M, Yamazaki S, Kono T, Miki K, Sugimura T (1996) Presence in *Pieris rapae* of cytotoxic activity against human carcinoma cells. Jpn J Cancer Res 87:1259–1262

Koyama S, Akira S, Ishii KJ (2010) Immune recognition of nucleic acids and their metabolites. In: Kikuchi Y, Rykova EY (eds) Extracellular nucleic acids. Springer, Heiderberg, pp 209–227
Krasteva PV, Giglio KM, Sondermann H (2012) Sensing the messenger: the diverse ways that bacteria signal through c-di-GMP. Protein Sci 21:929–948
Lara-Tejero M, Galan JE (2000) A bacterial toxin that controls cell cycle progression as a deoxyribonuclease I-like protein. Science 290:354–357
Lubran MM (1988) Bacterial toxins. Ann Clin Lab Sci 18:58–71
Maddison DR, Maddison WP (2005) MacClade 4: analysis of phylogeny and character evolution. http://macclade.org
Marsh N, Rothschild M (1974) Aposematic and cryptic Lepidoptera tested on the mouse. J Zool Lond 174:89–122
Masignani V, Pizza M, Rappuoli R (2000) Common features of ADP-ribosyltransferase. In: Aktories K, Just I (eds) Bacterial protein toxins, vol 145. Springer, Berlin, pp 21–44
Matsumoto Y, Nakano T, Yamamoto M, Matsushima-Hibiya Y, Odagiri K, Yata O, Koyama K, Sugimura T, Wakabayashi K (2008) Distribution of cytotoxic and DNA ADP-ribosylating activity in crude extracts from butterflies among the family Pieridae. Proc Natl Acad Sci USA 105:2516–2520
Matsushima-Hibiya Y, Watanabe M, Hidari KI, Miyamoto D, Suzuki Y, Kasama T, Kanazawa T, Koyama K, Sugimura T, Wakabayashi K (2003) Identification of glycosphingolipid receptors for pierisin-1, a guanine-specific ADP-ribosylating toxin from the cabbage butterfly. J Biol Chem 278:9972–9978
Matsushima-Hibiya Y, Watanabe M, Kono T, Kanazawa T, Koyama K, Sugimura T, Wakabayashi K (2000) Purification and cloning of pierisin-2, an apoptosis-inducing protein from the cabbage butterfly, *Pieris brassicae*. Eur J Biochem 267:5742–5750
Nakano T, Matsushima-Hibiya Y, Yamamoto M, Enomoto S, Matsumoto Y, Totsuka Y, Watanabe M, Sugimura T, Wakabayashi K (2006) Purification and molecular cloning of a DNA ADP-ribosylating protein, CARP-1, from the edible clam *Meretrix lamarckii*. Proc Natl Acad Sci USA 103:13652–13657
Nakano T, Matsushima-Hibiya Y, Yamamoto M, Takahashi-Nakaguchi A, Fukuda H, Ono M, Takamura-Enya T, Kinashi H, Totsuka Y (2013) ADP-ribosylation of guanosine by SCO5461 protein secreted from *Streptomyces coelicolor*. Toxicon 63:55–63
Natori S (2010) Molecules participating in insect immunity of *Sarcophaga peregrina*. Proc Jpn Acad Ser B 86:927–938
Odagiri K (2009) Distribution of pierisin-like activities in the genus *Appias*. Insect Nat 44:20–23
Orth JH, Schorch B, Boundy S, Ffrench-Constant R, Kubick S, Aktories K (2011) Cell-free synthesis and characterization of a novel cytotoxic pierisin-like protein from the cabbage butterfly *Pieris rapae*. Toxicon 57:199–207
Ortmann C, Grieshaber MK (2003) Energy metabolism and valve closure behaviour in the Asian clam *Corbicula fluminea*. J Exp Biol 206:4167–4178
Pallen MJ, Lam AC, Loman NJ, McBride A (2001) An abundance of bacterial ADP-ribosyltransferases: implications for the origin of exotoxins and their human homologues. Trends Microbiol 9:302–307
Reinert DJ, Carpusca I, Aktories K, Schulz GE (2006) Structure of the mosquitocidal toxin from *Bacillus sphaericus*. J Mol Biol 357:1226–1236
Scheuplein F, Schwarz N, Adriouch S, Krebs C, Bannas P, Rissiek B, Seman M, Haag F, Koch-Nolte F (2009) NAD^+ and ATP released from injured cells induce $P2X_7$-dependent shedding of CD62L and externalization of phosphatidylserine by murine T cells. J Immunol 182:2898–2908
Shiga A, Kakamu S, Sugiyama Y, Shibata M, Makino E, Enomoto M (2006) Acute toxicity of pierisin-1, a cytotoxic protein from *Pieris rapae*, in mouse and rat. J Toxicol Sci 31:123–137
Shiotani B, Watanabe M, Totsuka Y, Sugimura T, Wakabayashi K (2005) Involvement of nucleotide excision repair (NER) system in repair of mono ADP-ribosylated dG adducts produced by pierisin-1, a cytotoxic protein from cabbage butterfly. Mutat Res 572:150–155

Shiotani B, Kobayashi M, Watanabe M, Yamamoto K, Sugimura T, Wakabayashi K (2006) Involvement of the ATR- and ATM-dependent checkpoint responses in cell cycle arrest evoked by pierisin-1. Mol Cancer Res 4:125–133

Schirmer J, Wieden HJ, Rodnina MV, Aktories K (2002) Inactivation of the elongation factor Tu by mosquitocidal toxin-catalyzed mono-ADP-ribosylation. Appl Environ Microbiol 68:4894–4899

Shogomori H, Kobayashi T (2008) Lysenin: a sphingomyelin specific pore-forming toxin. Biochim Biophys Acta 1780:612–618

Smedley SR, Schroeder FC, Weibel DB, Meinwald J, Lafleur KA, Renwick JA, Rutowski R, Eisner T (2002) Mayolenes: labile defensive lipids from the glandular hairs of a caterpillar (*Pieris rapae*). Proc Natl Acad Sci USA 99:6822–6827

de Souza RF, Aravind L (2012) Identification of novel components of NAD-utilizing metabolic pathways and prediction of their biochemical functions. Mol BioSyst 8:1661–1677

Srivastava D, Waters CM (2012) A tangled web: regulatory connections between quorum sensing and cyclic di-GMP. J Bacteriol 149:4485–4493

Stevens LA, Levine RL, Gochuico BR, Moss J (2009) ADP-ribosylation of human defensin HNP-1 results in the replacement of the modified arginine with the noncoded amino acid ornithine. Proc Natl Acad Sci USA 106:19796–19800

Szirák K, Keserű J, Biró S, Schmelczer I, Barabás G, Penyige A (2012) Disruption of *SCO5461* gene coding for a mono-ADP-ribosyltransferase enzyme produces a conditional pleiotropic phenotype affecting morphological differentiation and antibiotic production in *Streptomyces coelicolor*. J Microbiol 50:409–418

Takahashi-Nakaguchi A, Matsumoto Y, Yamamoto M, Iwabuchi K, Totsuka Y, Sugimura T, Wakabayashi K (2013) Demonstration of cytotoxicity against wasps by pierisin-1: a possible defense factor in the cabbage white butterfly. PLoS One 8:e60539

Takamura-Enya T, Watanabe M, Totsuka Y, Kanazawa T, Matsushima-Hibiya Y, Koyama K, Sugimura T, Wakabayashi K (2001) Mono(ADP-ribosyl)ation of 2′-deoxyguanosine residue in DNA by an apoptosis-inducing protein, pierisin-1, from cabbage butterfly. Proc Natl Acad Sci USA 98:12414–12419

Takamura-Enya T, Watanabe M, Koyama K, Sugimura T, Wakabayashi K (2004) Mono(ADP-ribosyl)ation of the N^2 amino groups of guanine residues in DNA by pierisin-2, from the cabbage butterfly, *Pieris brassicae*. Biochem Biophys Res Commun 323:579–582

Thanabalu T, Hindley J, Jackson-Yap J, Berry C (1991) Cloning, sequencing, and expression of a gene encoding a 100-kilodalton mosquitocidal toxin from *Bacillus sphaericus* SSII-1. J Bacteriol 173:2776–2785

Thompson JD, Higgins DG, Gibson TJ (1994) CLUSTAL W: improving the sensitivity of progressive multiple sequence alignment through sequence weighting, position-specific gap penalties and weight matrix choice. Nucleic Acids Res 22:4673–4680

Totsuka Y, Kawanishi M, Nishigaki R, Matsukawa K, Yagi T, Takamura-Enya T, Watanabe M, Sugimura T, Wakabayashi K (2003) Analysis of *HPRT* and *supF* mutations caused by pierisin-1, a guanine specific ADP-ribosylating toxin derived from the cabbage butterfly. Chem Res Toxicol 16:945–952

Uwo MF, Ui-Tei K, Park P, Takeda M (2002) Replacement of midgut epithelium in the greater wax moth, *Galleria mellonella*, during larval–pupal moult. Cell Tissue Res 308:319–331

Watanabe M, Kono T, Koyama K, Sugimura T, Wakabayashi K (1998) Purification of pierisin, an inducer of apoptosis in human gastric carcinoma cells, from cabbage butterfly, *Pieris rapae*. Jpn J Cancer Res 89:556–561

Watanabe M, Kono T, Matsushima-Hibiya Y, Kanazawa T, Nishisaka N, Kishimoto T, Koyama K, Sugimura T, Wakabayashi K (1999) Molecular cloning of an apoptosis-inducing protein, pierisin, from cabbage butterfly: possible involvement of ADP-ribosylation in its activity. Proc Natl Acad Sci USA 96:10608–10613

Watanabe M, Enomoto S, Takamura-Enya T, Nakano T, Koyama K, Sugimura T, Wakabayashi K (2004a) Enzymatic properties of pierisin-1 and Its N-terminal domain, a guanine-specific ADP-ribosyltransferase from the cabbage butterfly. J Biochem 135:471–477

Watanabe M, Nakano T, Shiotani B, Matsushima-Hibiya Y, Kiuchi M, Yukuhiro F, Kanazawa T, Koyama K, Sugimura T, Wakabayashi K (2004b) Developmental stage-specific expression and tissue distribution of pierisin-1, a guanine-specific ADP-ribosylating toxin, in *Pieris rapae*. Comp Biochem Physiol A Mol Integr Physiol 139:125–131

Widdick DA, Dilks K, Chandra G, Bottrill A, Naldrett M, Pohlschroder M, Palmer T (2006) The twin-arginine translocation pathway is a major route of protein export in *Streptomyces coelicolor*. Proc Natl Acad Sci USA 103:17927–17932

Wigglesworth VB (1972) Digestion and nutrition. In The principles of insect physiology. Chapman and Hall, London, pp 476–552

Yamamoto M, Nakano T, Matshshima-Hibiya Y, Totsuka Y, Takahashi-Nakaguchi A, Matsumoto Y, Sugimura T, Wakabayashi K (2009) Molecular cloninig of apoptosis-inducing pierisin-like proteins, from two species of white butterfly, *Pieris melete* and *Aporia crataegi*. Comp Biochem Physiol B 154:326–333

Yamamoto M, Takahashi-Nakaguchi A, Matsushima-Hibiya Y, Nakano T, Totsuka Y, Imanishi S, Mitsuhashi J, Watanabe M, Nakagama H, Sugimura T, Wakabayashi K (2011) Nucleotide sequence and chromosomal localization of the gene for pierisin-1, a DNA ADP-ribosylating protein, in the cabbage butterfly *Pieris rapae*. Genetica 139:1251–1258

de Zwaan A, Cortesi P, van den ThiHart G, Roos J, Storey KB (1991) Differential sensitivities to hypoxia by two anoxia-tolerant marine molluscs: a biochemical analysis. Mar Biol 111:343–351

Part III
ADP-Ribosylation by ARTDs (H-Y-E ARTs)

Comparative Structural Analysis of the Putative Mono-ADP-Ribosyltransferases of the ARTD/PARP Family

Ana Filipa Pinto and Herwig Schüler

Abstract The existence and significance of endogenous cytosolic and nuclear mono-ADP-ribosylation has been a matter of debate. Today, evidence suggests that the human enzymes that catalyze the reaction have been rounded up. Moreover, substrate proteins and specific functions for mono-ADP-ribosyltransferases are beginning to be defined. Reader domains that specifically recognize mono-ADP-ribosylated target proteins and erasers that remove the mono-ADP-ribosyl mark have been identified. Here, we review the contribution of crystal structures to our understanding of the putative mono-ADP-ribosyltransferases with Diphtheria toxin and ARTD1/PARP1 homology.

Abbreviations

ARTC	ADP-ribosyltransferases with Clostridium toxin homology
ARTD	ADP-ribosyltransferases with Diphtheria toxin homology
DT	Diphtheria toxin
ExoA	Exotoxin A
mARTD	Mono-ADP-ribosylating ARTD enzymes
PARP	Poly-ADP-ribose polymerase

Contents

A. F. Pinto · H. Schüler (✉)
Department of Medical Biochemistry and Biophysics, Karolinska Institutet, S-17177 Stockholm, Sweden
e-mail: herwig.schuler@ki.se

Current Topics in Microbiology and Immunology (2015) 384: 153–166
DOI: 10.1007/82_2014_417

Published Online: 12 July 2014

1 Introduction

Enzymatic protein ADP-ribosylation as a posttranslational modification is characterized by the transfer of ADP-ribose from the co-substrate NAD^+ to a specific target protein, and often involves formation of a poly-ADP-ribose (PAR) chain, generating poly-ADP-ribosylated target proteins. As other signaling processes, intracellular ADP-ribosylation is highly dynamic and involves the actions of dedicated writers (members of the Diphtheria toxin (DT) related ADP-ribosyltransferases, or ARTD, formerly called PARP family), readers (Kalisch et al. 2012), and erasers (Barkauskaite et al. 2013). Mono-ADP-ribosylation, the transfer of a single ADP-ribose unit, is a hallmark of several classes of bacterial toxins, but recently this activity has also been attributed to a subset of the ARTD/PARP family members, eukaryotic intracellular enzymes formerly thought to catalyze PARylation (Kleine et al. 2008; Hottiger et al. 2010). Specific mono-ADP-ribosylation reader and eraser domains have also been identified (Feijs et al. 2013a, b). Clostridium toxin related ADP-ribosyltransferases (ARTC) have mono-ADP-ribosyltransferase activity; apart from bacterial toxins, this class contains extracellular and membrane-associated proteins (Koch-Nolte et al. 2008).

There is still only limited functional information on the putative mono-ADP-ribosyltransferases of the ARTD family (the "mARTDs"). Classification into mono- and poly-ADP-ribosyltransferases relies partially on biochemical analyses, and mainly on sequence comparison and the observation by Kleine et al. (2008) that a subset of family members carry a small hydrophobic residue instead of glutamate in the 4th position of the uniting H-Y-Y-E motif (described in detail in Sect. 3.1). Meanwhile, crystal structures of six members of this subfamily have been solved in our laboratory (Andersson et al. 2012; Karlberg et al. 2012; Wahlberg et al. 2012; unpublished results). Here, we summarize what we have learned from those crystal structures. For the sake of simplicity within this text, we will use the term "mARTD" for those family members which lack a glutamate in the position corresponding to E988 of human ARTD1/PARP1, even if the catalytic activities of these enzymes have not been sufficiently characterized, and despite the fact that the function of this glutamate is yet incompletely understood. Thus, we focus here on family members ARTD7-17 (PARP6-16; Hottiger et al. 2010).

As other ARTD/PARP proteins, the mARTD enzymes are multidomain proteins; they combine the ADP-ribosyltransferase domains with two types of ADP-ribose binding modules (macrodomains in ARTD7-9, and WWE domains in ARTD8 and ARTD11-14; He et al. 2012; Karlberg et al. 2013), CCCH-type zinc-finger domains

(ARTD12, -13) as well as protein-protein interaction domains. The macrodomain-containing ARTD7-9 (also known as B-agressive lymphoma proteins BAL1-3) are overexpressed in diffuse large B-cell lymphoma and are implicated in the regulation of gene transcription (Aguiar et al. 2005; Barbarulo et al. 2013; Cho et al. 2009; Mehrotra et al. 2011). The WWE domain containing ARTD14 is a transcriptional repressor of the aryl hydrocarbon receptor (Macpherson et al. 2013). Zinc finger containing mARTDs 12 and −13 have been associated with regulation of stress granules and viral immunity (Atasheva et al. 2012; Gao et al. 2002; Leung et al. 2011). ARTD10 is a component in the NF-κB signaling pathway by directly modifying NEMO (Verheugd et al. 2013). ARTD15, the only membrane anchored family member, modifies karyopherin β1 (Di Paola et al. 2012) as well as PERK and IRE1α, two key kinases in the unfolded protein response (Jwa and Chang 2012). Finally, mARTDs are implicated in cytoskeletal regulation and cell cycle control (Vyas et al. 2013). For a more comprehensive review of mARTD biological functions, see Feijs et al. (2013a) and Kaufmann et al. 2014.

2 Structural Homology Within the mARTD Transferase Domains

Revelation of the crystal structures of DT (Bell and Eisenberg 1996) and ARTD1/PARP1 (Ruf et al. 1996) represented a major increment in understanding ADP-ribosylation. The crystal structures confirmed an evolutionary relationship that was not fully accepted based solely on sequence comparisons. Although an additional α-helical subdomain is present, the catalytic fragment of ARTD1 preserves the core structure of the toxin, with two central β-sheets surrounded by α-helices, and the NAD^+ binding crevice at the interface of the two slightly staggered β-sheets (Fig. 1a, b). This core structure is present also in the tankyrase and mARTD subfamilies (Fig. 1c, d) as well as in the ARTC enzymes.

Superimposition of the available mARTD structures illustrates their similarity (Fig. 1e): Despite considerable variation in length and sequence of loop regions (Fig. 2), and despite crystallization with a number of different symmetries, all structures align with a root mean square deviation (RMSD) in backbone atom positions of below 2 Å (Fig. 1f). This analysis also illustrates that presence of additional domains, such as the α-helical subdomain of ARTD15 (Karlberg et al. 2012), does not necessarily induce a different conformation of the transferase domains: Despite their evolutionary distance (Otto et al. 2005), the transferase domains of ARTD15 and −7 align to only 0.4 Å.

Sequence relationships within the ARTD genes have been extensively analyzed by Otto and coworkers and their sequence alignment has provided a gold standard for defining the functional transferase domain (Otto et al. 2005). With the crystal structures of several mARTD structures at hand, we asked whether structure-based sequence alignments could further improve the identification of homologous

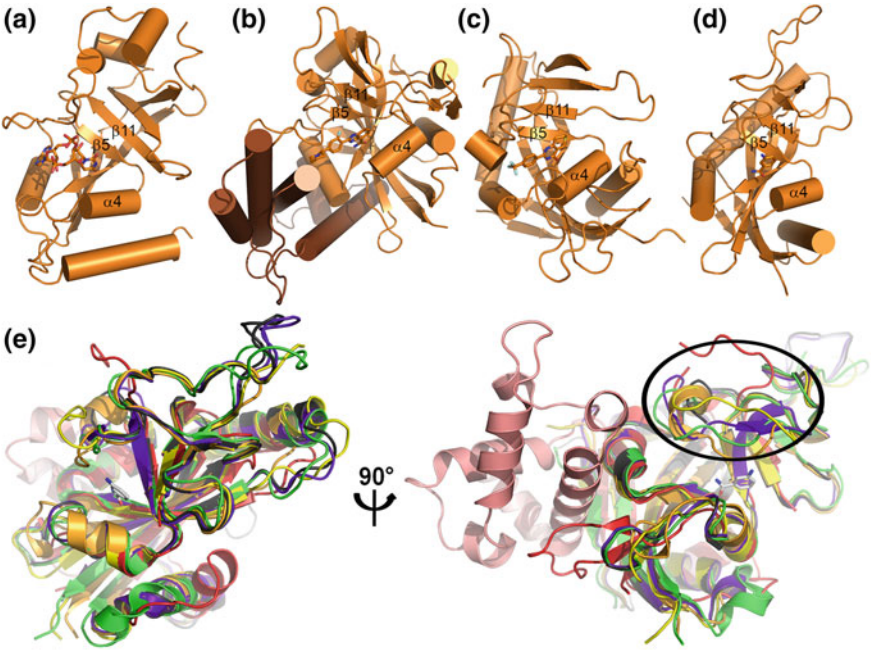

(f)

Transferase	PDB entry (chain)	3BLJ (B)	3SE2 (C)	3HKV	2PQF	2X5Y	4F0E	3L3M	3KR8	1TOX
ARTD7/PARP15	3BLJ (B)		1.1 (185)	1.7 (184)	1.8 (183)	1.6 (169)	0.4 (198)	2.6 (163)	2.0 (167)	3.1 (101)
ARTD8/PARP14	3SE2 (C)	29.8		1.8 (186)	1.6 (181)	1.7 (169)	1.1 (184)	2.5 (161)	2.0 (167)	3.4 (104)
ARTD10/PARP10	3HKV	27.7	28		1.8 (189)	1.8 (179)	1.7 (183)	2.4 (163)	2.3 (171)	3.1 (102)
ARTD12/PARP12	2PQF	27.6	27.2	25.8		1.4 (167)	1.8 (182	2.3 (165)	2.1 (165)	3.5 (108)
ARTD13/PARP13	2X5Y	24.8	24.6	24.1	26.4		1.6 (168)	2.5 (164)	2.1 (159)	3.1 (99)
ARTD15/PARP16	4F0E:B	34.8	29.1	26.9	27	24.2		2.5 (161)	2.1 (167)	3.2 (101)
ARTD1/PARP1	3L3M	17.8	17.4	18.1	19	18.3	17.5		2.3 (170)	n/a
ARTD6/TNKS2	3KR8	20	20.2	20.4	20.4	19.6	19.9	18.9		3.0 (106)
DT	1TOX	5.7	6	5.9	6.3	6	5.8	<2	6.2	

Fig. 1 Structural conservation within ARTD family ADP-ribosyltransferase domains. **a–d** Overall structures of Diphtheria toxin (**a**; PDB entry 1TOX, Bell and Eisenberg 1996) and, as representatives for each ARTD subfamily, ARTD1/PARP1 (**b** 3L3M, Penning et al. 2010), ARTD6/TNKS2 (**c** 3KR8, Karlberg et al. 2010), and ARTD10/PARP10 (**d** 3HKV). Selected secondary structural elements are indicated with the symbols identifying the corresponding elements of ARTD7 in Fig. 2. These and all following structure images were generated using PyMOL (The PyMOL Molecular Graphics System, Version 1.2; Schrödinger, LLC). **e** Superimposition of one representative crystal structure each of the mARTD transferase domains (ARTD7, *gray* ARTD8, *purpleblue* ARTD10, *green* ARTD12, *yellow* ARTD13, *orange* ARTD15, *red* with its α-helical domain in pale *red*). Ligand 3-aminobenzamide of ARTD7 is shown to indicate the active site pockets, and the position of the D-loops is *circled*. PDB entries are those listed in panel f below. **f** Similarity matrix showing pairwise 3D similarities among mARTD transferase domains and representatives for each ARTD subfamily, calculated by the DALI server (Holm and Rosenström 2010). The *lower left* sector lists the DALI Z-scores, and the *upper right* sector lists the RMSD of backbone atomic positions (in Å) and, in parentheses, the number of residues over which these were computed

positions, and of domain borders in the uncharacterized family members. The result shows that this might be the case: Our structure-based alignment (Fig. 2) likely makes a more precise prediction of homologous positions in particular at the N-termini, where conserved "marker positions" are scarce. However, the structure-based alignment is nearly identical with the sequence alignment of Otto et al. (2005) for the C-terminal half of the transferase domains (roughly starting at $\beta 3$). Importantly though, transferase domains cannot be regarded in isolation from their domain context within the proteins, of which ARTD15 is a reminder (Karlberg et al. 2012). It is possible that transferase domains (isolated from their putative regulatory domains) of the yet uncharacterized mARTDs are not meaningful targets for biochemical analysis, as is the case for ARTD1-4 and ARTD15.

3 Structural Features of the Active Sites

To understand ARTD enzymatic activities, it is important to understand the functions of residues surrounding the active site. Here, we will summarize what mARTD crystal structures have contributed in this context so far.

3.1 The H-Y-Y-E Motif

It was recognized early on that ARTD1/PARP1 shared sequence similarity with DT-class ADP-ribosylating toxins, in particular in key positions involved in NAD^+ co-substrate binding (Domenighini et al. 1991). These positions included a histidine, two aromatic residues, and two glutamic acids, separated in the sequences. Marsischky et al. (1995) analyzed two of the corresponding residues in ARTD1 by mutagenesis and found that a conserved histidine was needed for NAD^+ binding, as in DT (Blanke et al. 1994). A conserved glutamate side chain was critical for activity in several bacterial toxins (summarized by Marsischky et al. 1995). Surprisingly, the corresponding glutamate of ARTD1 was needed for PAR chain elongation but not for ADP-ribosyl transfer *per se*. Crystal structures and mutagenesis confirmed a key role for the H-Y-Y-E motif residues in NAD^+ binding and PAR chain elongation in ARTD1 (Ruf et al. 1996, 1998; Fig. 3). Subsequently, the structural roles of these residues have been confirmed with crystal structures of ten other ARTD family members, including mARTDs (Fig. 3). The histidine side chain forms a hydrogen bond with the N-ribose, whereas the tyrosine side chains stack with the N-ribose and the nicotinamide moiety. ARTD9 and ADRT13, the only two family members that do not share the H-Y-Y-E motif, are generally regarded as catalytically inactive.

The last position of the H-Y-Y-E motif deviates from the sequence consensus in the mARTD enzymes. Sequence comparisons and a model of the transferase

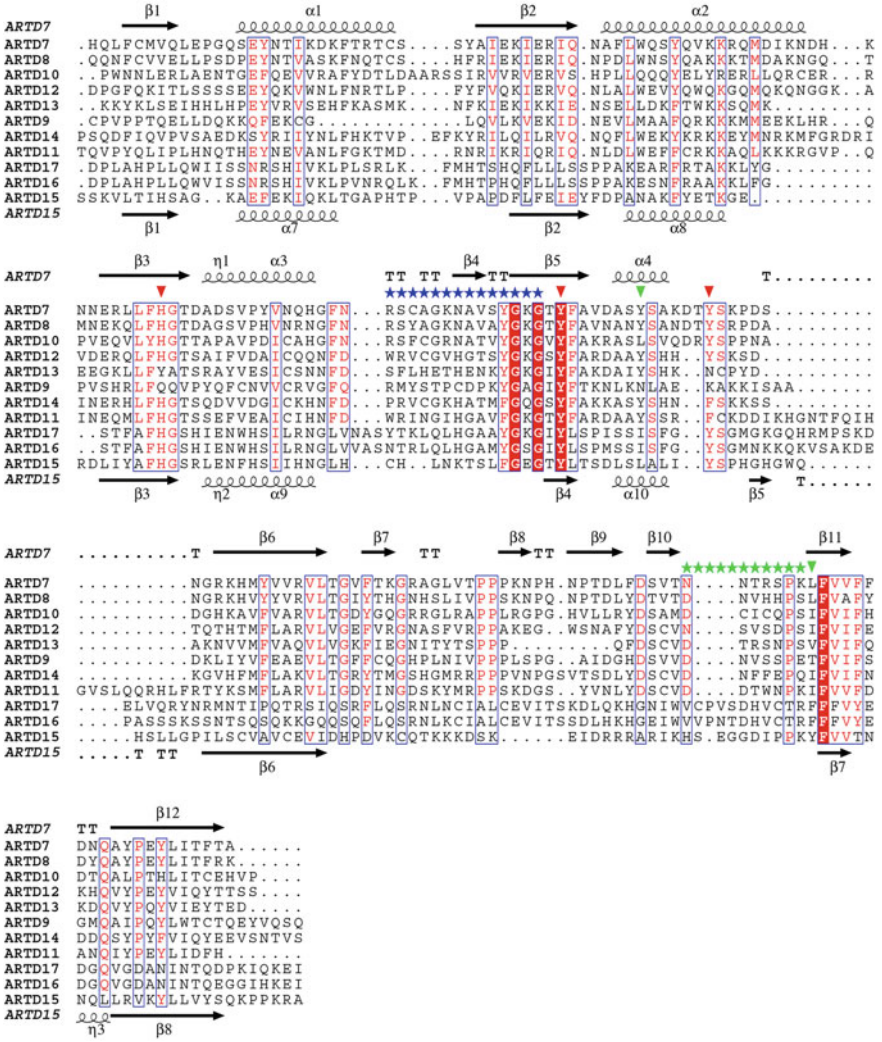

Fig. 2 Structure-based sequence alignment of mARTD ADP-ribosyltransferase domains. An alignment of sequences for which crystal structures were available (see Fig. 1f) was created using the PROMALS3D server (Pei et al. 2008) based on both sequence homology and the positions of secondary structural elements. Next, the sequences of the mARTD proteins for which no structural information was available were aligned to the PROMALS3D output using ClustalW (Chenna et al. 2003). The resulting alignment was truncated at the consensus N- and C-terminal borders of the transferase domains (based on crystal structures). Finally, the alignment was stained for sequence similarity and the secondary structural elements for ARTD7 and -15 were added using ESPript (Gouet et al. 1999). The respective positions of the D- and A-loops are indicated by blue and green stars above the alignment. *Red arrowheads* indicate the positions (H-Y-Y/F) involved in NAD^+ binding. *Green arrowheads* indicate the positions corresponding to catalytic ARTD1 residues K903 (in α4) and E988

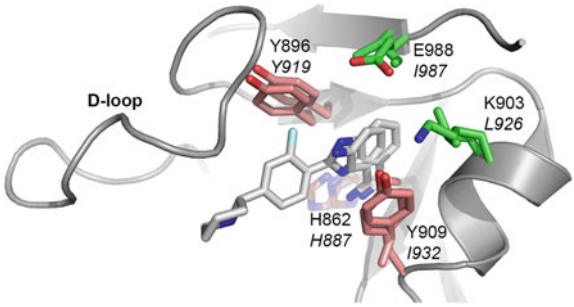

Fig. 3 Positioning of H-Y-Y-E motif residues in the active sites of ARTD1 and ARTD10. The structures of the ARTD1 and ARTD10 transferase domains (PDB entries 3L3M and 3HKV) were aligned and selected side chains were shown as sticks on top of selected secondary structural elements of ARTD1. Side chains involved in NAD^+ binding are shown with salmon-colored carbons; side chains involved in PAR chain elongation are shown with green carbons. An ARTD1 bound benzamidazole derivative and ARTD10 bound 3-aminobenzamide are also shown. Residue numbering refers to human ARTD1 and, below in italics, human ARTD10

domain of ARTD10 based on the crystal structure of ARTD12 led Kleine et al. (2008) to note that the glutamate was replaced by a small hydrophobic residue in all family members outside the ARTD1-4 and tankyrase subfamilies. Since then, it has been verified by X-ray crystallography for six mARTDs that the positioning of this small hydrophobic side chain in the active site resembles that of ARTD1 E988 (Table 1 and Fig. 3). Apparently, a glutamate is essential for stabilizing a reaction intermediate when a hydrogen bond donor is posed for nucleophilic attack (such as a target arginine in the toxins, or a growing PAR chain in ARTD1). Other residues lining the active sites might make similar contributions. Notable in this context is the side chain variation in the position corresponding to K903 of ARTD1 (Fig. 3). Mutation of this lysine had similar effects as mutation of E988, suggesting the side chain is involved in PAR chain elongation (Ruf et al. 1998; Carter O'Connell et al. 2014). A lysine in this position is conserved in ARTD1-3 and the tankyrases, but not in any other ARTD family member. Thus, as we do not know the ARTD substrate residues, and do not fully understand the role of E988 and other side chains in the chemistries of different ADP-ribosylation reactions, presence or absence of the glutamate should not be the *bona fide* discriminator between poly- and mono-ADP-ribosylating enzymes, and it appears that the mARTDs get by without these side chains for transfer of single ADP-ribose units.

As for the small hydrophobic side chains that line the active site in mARTDs, these observations can be viewed in light of the model for substrate-assisted catalysis suggested by Kleine et al. (2008), according to which the substrate protein would need to contribute a catalytic side chain together with the side chain being modified. We can speculate that small hydrophobic side chains, such as I987 of ARTD10, might generate an environment to accurately guide the positioning of catalytic and substrate residues by their aliphatic segments.

Table 1 Available crystal structures of ARTD family ADP-ribosyltransferase domains with an apparent lack of PAR chain elongation activity

PDB code	Protein	Ligand	Ligand MW	Resolution (Å)	References
3BLJ	ARTD7/PARP15	–		2.2	
3GEY	ARTD7/PARP15	PJ-34	295.34	2.2	
4F0E	ARTD7/PARP15	STO1102[a]	284.34	2.4	Andersson et al. (2012)
3GOY	ARTD8/PARP14	3-AB[b]	136.15	2.8	Wahlberg et al. (2012)
3SE2	ARTD8/PARP14	6(5H)-Phe[c]	195.22	2.3	Wahlberg et al. (2012)
3SMI	ARTD8/PARP14	cpd 98[d]	288.33	2.4	Wahlberg et al. (2012)
3SMJ	ARTD8/PARP14	cpd 145[e]	206.26	1.5	Wahlberg et al. (2012)
4F1L	ARTD8/PARP14	U16(z)[f]	234.21	1.9	Andersson et al. (2012)
4F1Q	ARTD8/PARP14	U16(e)[g]	234.21	2.8	Andersson et al. (2012)
3HKV	ARTD10/PARP10	3-AB[b]	136.15	2.1	
2PQF	ARTD12/PARP12	3-AB[b]	137.14	2.2	
2X5Y	ARTD13/PARP13	–		1.05	
4F0D	ARTD15/PARP16	3-AB[b]	136.15	2.7	Karlberg et al. (2012)

[a] 8-methyl-2-[(pyrimidin-2-ylsulfanyl)methyl]quinazolin- 4(1H)-one
[b] 3-aminobenzamide
[c] 6(5H)-phenanthridinone (in chains A and B)
[d] 2-[(5-amino-1H-1,2,4-triazol-3-yl)sulfanylmethyl]-8-methyl-1H-quinazolin-4-one (PubChem T5867921)
[e] 2-methyl-3,5,6,7-tetrahydro-4H-cyclopenta[4,5]thieno[2,3- d]pyrimidin-4-one (ChemDiv 3909-7439)
[f, g] (2Z/E)-4-[(3-carbamoylphenyl)amino]-4-oxobut-2-enoic acid (Z- and E-isomers, respectively)

3.2 The Donor Loop (Loop 1)

The donor loop (D-loop), or loop 1, has crucial functions in protein substrate recognition and catalysis in the DT-class ADP-ribosylating bacterial toxins. Its role is possibly best documented in exotoxin A (ExoA) from *Pseudomonas aeroginosa*Pseudomonas aeroginosa, and its host target protein, eukaryotic elongation factor-2 (eEF2). Crystal structures of the toxin-protein substrate complex are available at different stages along the ADP-ribosyl transfer reaction, and with several dinucleotide analogs (Jørgensen et al. 2005, 2008). These studies documented a large scale rearrangement of loop 1 of ExoA during the activity cycle, bringing a critical aspartic carboxyl into the vicinity of the diphthamide substrate (Fig. 4a). Together with analysis of site-directed mutants, evidence suggests that side chains in loop 1, as well as a second structural element with critical residues (loop 3), are necessary for correct positioning of the substrate protein side chain and the dinucleotide, and stabilization and protection of the reactive intermediate

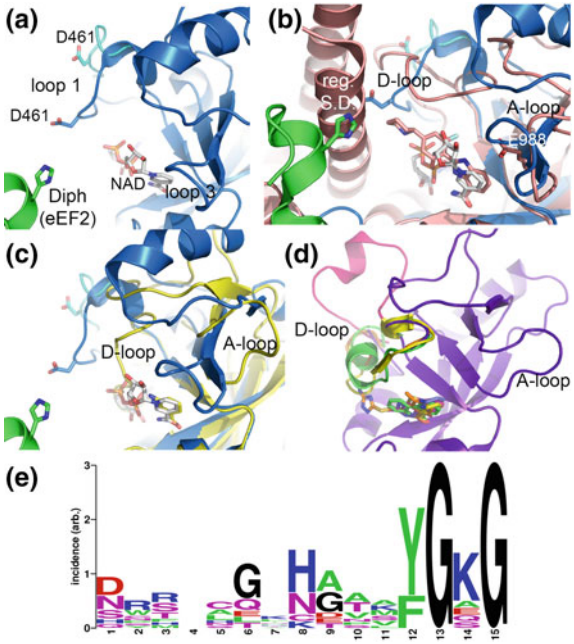

Fig. 4 Structural plasticity and sequence variability in the mARTD D-loops. **a** Structure of ExoA (*blue*) in complex with its protein target, eEF2 (*green*) with loop 1 and critical side chain D461 approaching the eEF2 diphthamide (PDB entry 3B78). The conformation of loop 1 in the dinucleotide free complex (1ZM3) is shown in *light blue* (Jørgensen et al. 2008). **b** The same structures, superimposed with the ARTD1 structure (salmon; 3L3M). The α-helical regulatory subdomain, D-loop, and the catalytic side chain E988 in the A-loop of ARTD1 are indicated. **c** The same structures as in panel a, superimposed with the ARTD10 structure (*yellow* 3HKV). The D- and A-loops are indicated. **d** The structures of ARTD8/PARP14 sequence N1617-G1631 as well as the respective ligands in five individual crystal structures are shown superimposed onto the ARTD8–3-aminobenzamide complex (*purple* PDB entry 3GOY). D-loop residues S1619-V1626 are missing in the electron density in this structure, indicating loop disorder. In a second complex with 3-AB the D-loop folds over the ligand pocket, featuring a short *β*-turn-*β* motif (*yellow* chains C and D of the asymmetric unit in PDB entry 3SE2). The complex with the small ligand U16(z) is nearly identical (not shown; 4F1L). In the complex with 6(5H)-phenanthridinone, the D-loop folds over the ligand pocket, but the *β*-turn-*β* motif is replaced by an α-helical segment R1618-N1624 (green; chains A and B of the asymmetric unit in PDB entry 3SE2). The complex with the elongated ligand cpd 98 (Wahlberg et al. 2012) lacks electron density for G1622-N1624, but the position of A1625 shows the C-terminal end of the D-loop over the ligand pocket (*orange* 3SMI). The complex with U16(e) is nearly identical (not shown; 4F1Q; Andersson et al. 2012). Finally, the D-loop in the complex with cpd 145 (Wahlberg et al. 2012) is engaged in a crystal contact and folds out of the ligand pocket (*magenta* 3SMJ). This crystallographic artifact does not influence the structure of the overall transferase domain, which aligns with 3SE2 to an RMSD of 1.1 Å over 188 residues. **e** D-loop sequences for all mARTD transferases (see Fig. 2) were extracted and their degree of conservation illustrated using WebLogo (Crooks et al 2004)

in the transfer reaction. As discussed in detail by Jørgensen et al. (2008), a large body of literature favors a similar mechanism in all DT-class toxins. Nonconservation of critical side chains is thought to reflect the different chemistries of the different target side chains, and the need for exact positioning of the side chains and dinucleotide over the course of the transfer reaction.

Despite overall low sequence similarity and domain arrangements, the active sites of ARTD-family transferase domains align fairly well with ExoA (Fig. 4b). When superimposing the ARTD1 and ExoA structures with the nicotinamide moiety and its closest secondary structural elements as guidelines, the D-loop and acceptor loop (A-loop) of ARTD1 are in positions corresponding to ExoA loops 1 and 3. The H-Y-Y-E motif glutamate of critical importance for PAR chain elongation is at the C-terminal end of the A-loop, in a position near the important residues for catalysis in loop 3 of ExoA. Given these structural similarities, it is not unreasonable to assume that as they share a common ancestor, the DT-class toxins and the ARTD proteins also share a common general enzymatic mechanism.

Interestingly, the D-loop of ARTD1 is in an open position reflecting the inactive state of the toxin; and its mobility is constricted by two structural features: placement of the α-helical regulatory subdomain (Fig. 4b), and a salt cluster formed by the ε-amide of K893 with backbone oxygens in the center region of the loop. All crystal structures of ARTD1-3 are highly similar in these two features; and despite a large number of different ligands in crystal complexes, the D-loop has not been observed in a conformation resembling more an active ExoA loop 1. Thus, ARTD1-3 crystal structures likely reflect the inactive enzymes.

The situation is quite different in the tankyrases and the mARTDs, which all lack the α-helical subdomain. Superimposition of ExoA and ARTD10 shows that the D-loop of ARTD10 is in a conformation that would clash with the major part of the dinucleotide, and the A-loop is folded away from the active site (Fig. 4c). However, crystal structures indicate that the D-loops of mARTDs and tankyrases are flexible. The conformation of the tankyrase D-loop is variable depending on the ligand in the active site, and is not fully resolved in several crystal structures (Wahlberg et al. 2012). ARTD8 represents the best showcase of a flexible D-loop: in six crystal structures with different ligands in the active site, the D-loop can be found in a variety of conformations (Fig. 4d). Conversely, the A-loop, with essential residues for catalytic activity (Kleine et al 2008), is found folded away from the active site in all mARTD structures.

Notably, the D-loop is one of the regions of high sequence variability within the ARTD family (Otto et al. 2005). Only the C-terminus of the loop shows a high degree of sequence conservation, with a G-X-G triad in which the glycines are strictly conserved and the intermediate position is preferentially occupied by lysine (Fig. 4e). A notable difference between ARTD1-3 and mARTD D-loop regions is the absence of proline residues in the latter. Together, conserved glycines and absence of prolines indicate an evolutionary requirement for loop flexibility in the mARTDs.

Thus, crystal structures of mARTD transferase domains show either floppy or putative inactive D-loop conformations and folded away A-loops. Together,

comparison with DT-class toxin structure and mechanism suggest there is space and flexibility for the mARTD transferase domains to dock onto their substrates to form a functioning dinucleotide cleft and a reactive center at the interface. Sequence variability in the D- and A-loops likely reflects the various substrates and reaction chemistries among different mARTDs.

3.3 Implications for Pharmacology

Inarguably, selective inhibitors are important research tools for probing the functions of individual enzymes in complex reactant mixtures or in cells and organisms. Two decades of PARP inhibitor development have provided us with a large set of compounds, with synthetic protocols established and partial characterization accomplished. Several of these inhibit mARTs (Wahlberg et al. 2012), although the most potent compounds are still rather small and do not live up to the full potential of compound-enzyme interactions (Table 1). The discussion above illustrates how active site variability among mARTD family members can be built upon in the development of selective mARTD inhibitors. Similar approaches have already yielded selective inhibitors of tankyrases (Lehtiö et al. 2013). *In silico* methods such as virtual library screening and docking procedures can provide starting points for medicinal chemistry programs (Andersson et al. 2012). Here, mARTD crystal structures form the essential templates, and they can serve as cornerstones in selecting scaffold modifications that achieve selective interactions with unique side chains. Nevertheless, X-ray crystallography must be combined with solution studies and successful development of selective inhibitors will also require a better understanding of mARTD enzymology.

4 Outlook

Partially owing to a number of enzyme structures, the mARTD research branch has grown out of its cradle. Yet, much groundwork remains before the field can fly. We need to better define mARTD substrate proteins and their sites of ADP-ribosylation. We need to define enzyme-substrate pairs that are amenable to structural and solution studies. We need systematic analyses of individual mARTD enzymes in order to address mARTD activity and regulation at high resolution. Finally, we need to generate a set of tools, including selective inhibitors, antibodies, cell lines, and animal and disease models in order to probe new in vitro findings in a relevant context.

Structural biology of ADP-ribosyltransferases—FAQ

- *If mARTDs have automodification activity, why do we not see the ADP-ribosylated site in crystal structures?* Incorporation of macromolecules into a crystal lattice requires a substantial uniform population of molecules. A covalent modification that does not disturb the crystal contacts must still be present at a substantial frequency in order to be visible in the electron density. Since none of the mARTD crystal structures show signs of ADP-ribosylation, we speculate that mARTD enzymes might be somewhat site-promiscuous and automodification might lead to subpopulations that do not crystallize in the same lattice as the unmodified population, or do not resolve.
- *Why is there no crystal structure of an ARTD in complex with NAD^+?* ADP-ribosyltransferases use NAD^+ as co-substrate; they are "designed" to retain nicotinamide and bind the ADP-ribosyl moiety only loosely, so that it can be passed on to the substrate. This is achieved by a snug nicotinamide binding pocket, and an ADP-ribosyl binding site that likely only forms in the enzyme-substrate complex. A loosely bound, partially disordered ADP-ribosyl conformation might explain why no ARTD-NAD^+ complex structure has been reported. In fact, we have solved crystal structures of several ARTD family members in the presence of different nonhydrolyzable NAD^+ analogs. In each case, we could resolve an occupied nicotinamide pocket, but not the remainder of the compounds (unpublished results).
- *Do PARP inhibitors block the active sites of other NAD^+-metabolizing enzymes?* By contrast to ARTDs, enzymes that use NAD^+ as cofactor often bind NAD^+ tightly in a well-defined pocket. In many instances, the nicotinamide moiety is part of the cofactor function (such as electron transfer), and is exposed to solvent or to the substrate binding site. Historically, PARP inhibitors have been designed to mimic nicotinamide and then grow into the pocket that is defined by the variable D-loop on one face. Therefore, the risk of inhibiting a broad range of NAD^+-binding enzymes is low, while the risk of inhibiting other nicotinamide retaining enzymes (including ARTC-class transferases) is more substantial. Thus, PARP inhibitor specificities will need to be confirmed for these enzymes.

Acknowledgments The majority of available mARTD crystal structures have been solved through funding by the Structural Genomics Consortium (www.thesgc.org). We wish to thank Torun Ekblad, Tobias Karlberg, Mirjam Klepsch, Ann-Gerd Thorsell, Patricia Verheugd, and Johan Weigelt for discussions, as well as Martin Moche (Protein Science Facility at Karolinska Institutet) and members of the Structural Genomics Consortium for their roles in solving mARTD

crystal structures. Work in the laboratory is funded by the Swedish Foundation for Strategic Research, the Swedish Research Council, the Swedish Cancer Society, and the IngaBritt och Arne Lundbergs Research Foundation.

References

Andersson CD, Karlberg T, Ekblad T et al (2012) Discovery of ligands for ADP-ribosyltransferases via docking-based virtual screening. J Med Chem 55(17):7706–7718

Aguiar RC, Takeyama K, He C et al (2005) B-aggressive lymphoma family proteins have unique domains that modulate transcription and exhibit poly(ADP-ribose) polymerase activity. J Biol Chem 280(40):33756–33765

Atasheva S, Akhrymuk M, Frolova EI et al (2012) New PARP gene with an anti-alphavirus function. J Virol 86(15):8147–8160

Barbarulo A, Iansante V, Chaidos A et al (2013) Poly(ADP-ribose) polymerase family member 14 (PARP14) is a novel effector of the JNK2-dependent pro-survival signal in multiple myeloma. Oncogene 32(36):4231–4242

Barkauskaite E, Jankevicius G, Ladurner AG et al (2013) The recognition and removal of cellular poly(ADP-ribose) signals. FEBS J 280(15):3491–3507

Bell CE, Eisenberg D (1996) Crystal structure of diphtheria toxin bound to nicotinamide adenine dinucleotide. Biochemistry 35(4):1137–1149

Blanke SR, Huang K, Wilson BA (1994) Active-site mutations of the diphtheria toxin catalytic domain: role of histidine-21 in nicotinamide adenine dinucleotide binding and ADP-ribosylation of elongation factor 2. Biochemistry 33(17):5155–5161

Carter O'Connell I, Jin H, Morgan RK, David LL, Cohen MS (2014) Engineering the substrate specificity of ADP-ribosyltransferases for identifying direct protein targets. J Am Chem Soc 136(14):5201–5204

Chenna R, Sugawara H, Koike T et al (2003) Multiple sequence alignment with the Clustal series of programs. Nucl Acids Res 31(13):3497–3500

Cho SH, Goenka S, Henttinen T et al (2009) PARP-14, a member of the B-aggressive lymphoma family, transduces survival signals in primary B cells. Blood 113(11):2416–2425

Crooks GE, Hon G, Chandonia JM et al (2004) WebLogo: a sequence logo generator. Genome Res 14:1188–1190

Di Paola S, Micaroni M, Di Tullio G et al (2012) PARP16/ARTD15 is a novel endoplasmic-reticulum-associated mono-ADP-ribosyltransferase that interacts with, and modifies karyopherin-ß1. PLoS One 7(6):e37352

Domenighini M, Montecucco C, Ripka WC et al (1991) Computer modelling of the NAD binding site of ADP-ribosylating toxins: active-site structure and mechanism of NAD binding. Mol Microbiol 5(1):23–31

Feijs KL, Verheugd P, Lüscher B (2013a) Expanding functions of intracellular resident mono-ADP-ribosylation in cell physiology. FEBS J 280(15):3519–3529

Feijs KL, Verheugd P, Forst AH et al (2013b) Macrodomain-containing proteins: regulating new intracellular functions of mono(ADP-ribosyl)ation. Nat Rev Mol Cell Biol 14(7):443–451

Gao G, Guo X, Goff SP (2002) Inhibition of retroviral RNA production by ZAP, a CCCH-type zinc finger protein. Science 297(5587):1703–1706

Gouet P, Courcelle E, Stuart DI et al (1999) ESPript: multiple sequence alignments in PostScript. Bioinformatics 15:305–308

He F, Tsuda K, Takahashi M et al (2012) Structural insight into the interaction of ADP-ribose with the PARP WWE domains. FEBS Lett 586(21):3858–3864

Holm L, Rosenström P (2010) Dali server: conservation mapping in 3D. Nucl Acids Res 38:W545–W549

Hottiger MO, Hassa PO, Lüscher B et al (2010) Toward a unified nomenclature for mammalian ADP-ribosyltransferases. Trends Biochem Sci 35(4):208–219
Jørgensen R, Merrill AR, Yates SP et al (2005) Exotoxin A-eEF2 complex structure indicates ADP ribosylation by ribosome mimicry. Nature 436(7053):979–984
Jørgensen R, Wang Y, Visschedyk D et al (2008) The nature and character of the transition state for the ADP-ribosyltransferase reaction. EMBO Rep 9(8):802–809
Jwa M, Chang P (2012) PARP16 is a tail-anchored endoplasmic reticulum protein required for the PERK- and IRE1α-mediated unfolded protein response. Nat Cell Biol 14(11):1223–1230
Kalisch T, Amé JC, Dantzer F et al (2012) New readers and interpretations of poly(ADP-ribosyl)ation. Trends Biochem Sci 37(9):381–390
Karlberg T, Markova N, Johansson I et al (2010) Structural basis for the interaction between tankyrase-2 and a potent Wnt-signaling inhibitor. J Med Chem 53(14):5352–5355
Karlberg T, Thorsell AG, Kallas Å et al (2012) Crystal structure of human ADP-ribose transferase ARTD15/PARP16 reveals a novel putative regulatory domain. J Biol Chem 287(29):24077–24081
Karlberg T, Langelier MF, Pascal JM et al (2013) Structural biology of the writers, readers, and erasers in mono- and poly(ADP-ribose) mediated signaling. Mol Aspects Med 34(6): 1088–1108
Kaufmann M, Feijs KL, Lüscher B (2014) Function and Regulation of the Mono-ADP-Ribosyltransferase ARTD10. Curr Top Microbiol Immunol [Epub ahead of print]
Kleine H, Poreba E, Lesniewicz K et al (2008) Substrate-assisted catalysis by PARP10 limits its activity to mono-ADP-ribosylation. Mol Cell 32(1):57–69
Koch-Nolte F, Kernstock S, Mueller-Dieckmann C et al (2008) Mammalian ADP-ribosyltransferases and ADP-ribosylhydrolases. Front Biosci 13:6716–6729
Lehtiö L, Chi NW, Krauss S (2013) Tankyrases as drug targets. FEBS J 280(15):3576–3593
Leung AK, Vyas S, Rood JE et al (2011) Poly(ADP-ribose) regulates stress responses and microRNA activity in the cytoplasm. Mol Cell 42(4):489–499
MacPherson L, Tamblyn L, Rajendra S et al (2013) 2,3,7,8-Tetrachlorodibenzo-p-dioxin poly(ADP-ribose) polymerase (TiPARP, ARTD14) is a mono-ADP-ribosyltransferase and repressor of aryl hydrocarbon receptor transactivation. Nucleic Acids Res 41(3):1604–1621
Marsischky GT, Wilson BA, Collier RJ (1995) Role of glutamic acid 988 of human poly-ADP-ribose polymerase in polymer formation. Evidence for active site similarities to the ADP-ribosylating toxins. J Biol Chem 270(7):3247–3254
Mehrotra P, Riley JP, Patel R et al (2011) PARP-14 functions as a transcriptional switch for Stat6-dependent gene activation. J Biol Chem 286(3):1767–1776
Otto H, Reche PA, Bazan F et al (2005) In silico characterization of the family of PARP-like poly(ADP-ribosyl)transferases (pARTs). BMC Genomics 6:139
Pei J, Kim BH, Grishin NV (2008) PROMALS3D: a tool for multiple protein sequence and structure alignments. Nucl Acids Res 36(7):2295–2300
Penning TD, Zhu GD, Gong J et al (2010) Optimization of phenyl-substituted benzimidazole carboxamide poly(ADP-ribose) polymerase inhibitors: identification of (S)-2-(2-fluoro-4-(pyrrolidin-2-yl)phenyl)-1H-benzimidazole-4-carboxamide (A-66492), a highly potent and efficacious inhibitor. J Med Chem 53:3142–3153
Ruf A, Mennissier de Murcia J et al (1996) Structure of the catalytic fragment of poly(AD-ribose) polymerase from chicken. Proc Natl Acad Sci USA 93(15):7481–7485
Ruf A, Rolli V, de Murcia G et al (1998) The mechanism of the elongation and branching reaction of poly(ADP-ribose) polymerase as derived from crystal structures and mutagenesis. J Mol Biol 278(1):57–65
Verheugd P, Forst AH, Milke L et al (2013) Regulation of NF-κB signalling by the mono-ADP-ribosyltransferase ARTD10. Nat Commun 4:1683
Vyas S, Chesarone-Cataldo M, Todorova T (2013) A systematic analysis of the PARP protein family identifies new functions critical for cell physiology. Nat Commun 4:2240
Wahlberg E, Karlberg T, Kouznetsova E et al (2012) Nat Biotech 30(3): 283–288

Function and Regulation of the Mono-ADP-Ribosyltransferase ARTD10

Max Kaufmann, Karla L. H. Feijs and Bernhard Lüscher

Abstract The transfer of ADP-ribose from NAD^+ to a substrate by ADP-ribosyltransferases, ADP-ribosylation, is a multifunctional posttranslational modification. While many studies have addressed the function of poly-ADP-ribosylation, for example, in DNA repair, signaling, and gene transcription, little is known about the role of mono-ADP-ribosylation. Recent work describing the mono-ADP-ribosyltransferase ARTD10/PARP10 suggests that this enzyme affects apoptosis, NF-κB signaling, and DNA damage repair, at least in part dependent on its activity as mono-ADP-ribosyltransferase. Moreover, the macrodomain-containing proteins MacroD1, MacroD2, and TARG1/C6orf130 were recently characterized as hydrolases, which remove mono-ADP-ribosylation thus providing evidence that this modification is reversible. In this review, we discuss these novel findings and their broader implications for cell behavior. We suggest functions of ARTD10 in immunity, metabolism, and cancer biology.

Abbreviations

ADAR	Adenosine deaminases acting on RNA
APOB	Apolipoprotein B
ARTC	ADP-ribosyltransferases Cholera toxin-like
ARTD	ADP-ribosyltransferase Diphtheria toxin-like
GSK3β	Glycogen synthase kinase 3β
IFN	Interferon
MEFs	Mouse embryo fibroblasts
NES	Nuclear export sequence

M. Kaufmann · K. L. H. Feijs · B. Lüscher (✉)
Institute of Biochemistry and Molecular Biology, RWTH Aachen University, Pauwelsstraße 30, 52074 Aachen, Germany
e-mail: Luescher@rwth-aachen.de

K. L. H. Feijs
Sir William Dunn School of Pathology, University of Oxford, South Parks Road, Oxford OX1 3RE, UK

Current Topics in Microbiology and Immunology (2015) 384: 167–188
DOI: 10.1007/82_2014_379

Published Online: 1 June 2014

NLS	Nuclear localization sequence
PIP	PCNA-interacting peptide
PTM	Posttranslational modification
RRM	RNA recognition motif
SNP	Single nucleotide polymorphism
UIM	Ubiquitin interaction motif

Contents

1 Introduction

Controlling the activities of proteins transiently and independently of gene transcription is fundamental for the regulation of numerous cellular processes. This is achieved by modulating the function of proteins by posttranslational modifications (PTMs). A large number of PTMs exist, including phosphorylation, glycosylation, and ubiquitination, which can affect, for example, the subcellular localization, the catalytic activity, or the half-life of the modified protein. ADP-ribosylation is a PTM, where ADP-ribose is linked to proteins either as a monomer—called mono-ADP-ribosylation—or where chains of multiple ADP-ribose units are formed, which is referred to as poly-ADP-ribosylation. The addition of a single ADP-ribose moiety introduces negative charges to the modified substrate and thus is thought to affect protein function. Poly-ADP-ribosylation creates linear or branched ADP-ribose chains, which serve as scaffolds for other proteins to interact with. For instance, DNA repair proteins and transcriptional cofactors and cofactor

complexes have been shown to be recruited by poly-ADP-ribose (De Vos et al. 2012; Gibson and Kraus 2012; Kleine and Luscher 2009; Schreiber et al. 2006). The length of the polymers suggests that multiple proteins may bind simultaneously and thus poly-ADP-ribose may promote the assembly of large protein complexes. Poly-ADP-ribosylation may also directly affect protein function, for example the automodification of ARTD1 in response to DNA damage inhibits eventually DNA binding (D'Amours et al. 1999; Kraus 2008). Currently 22 ADP-ribosyltransferases have been described in humans. These proteins can be subdivided into two families according to their homology to bacterial toxins, which also resulted in the suggestion for an updated nomenclature (Hottiger et al. 2010). The ADP-ribosyltransferases of the ARTC family are found at the cell membrane and ADP-ribosylate arginine residues (Laing et al. 2011). The residues involved in NAD^+ binding and catalysis, Arg-Ser-Glu, are also present in certain toxins such as cholera toxin, hence the name ADP-ribosyltransferases Cholera toxin-like. Intracellular mono-ADP-ribosylation and poly-ADP-ribosylation are catalyzed by the ADP-ribosyltransferase Diphtheria toxin-like family (ARTDs), also referred to as the PARP family (Fig. 1), which have a distinct amino acid motif, His-Tyr-Glu, compared to ARTCs that is key to execute ADP-ribosylation (Hottiger et al. 2010). The ARTD family can be further subdivided into proteins with iterative mono-ADP-ribosyltransferase activity and thus capable to form ADP-ribose polymers, proteins with single mono-ADP-ribosyltransferase activity, and inactive family members (Hottiger et al. 2010). These three subfamilies are characterized with distinct alterations in the amino acid motif. In particular the replacement of the catalytically relevant Glu distinguishes polymer-forming enzymes from mono-ADP-ribosyltransferases (Fig. 1). The distinction between mono- and poly-ADP-ribosylation is further emphasized by the existence of both mono-ADP-ribose- and poly-ADP-ribose-specific reader domains and hydrolases, which recognize and reverse these modifications (Barkauskaite et al. 2013; Feijs et al. 2013a).

ARTD1/PARP1 is the best-characterized poly-ADP-ribosyltransferase. It reacts to different forms of cellular stress by its influence on DNA repair, gene transcription, chromatin remodeling, and signal transduction mechanisms, thereby contributing to, for example, an inflammatory response and the survival or death of cells (De Vos et al. 2012; Krishnakumar and Kraus 2010; Luo and Kraus 2012; Messner and Hottiger 2011). ADP-ribosylation of proteins was recognized 50 years ago and a distinction was made between mono-ADP-ribosylation and poly-ADP-ribosylation in cells soon after (Hassa et al. 2006). However, the mono-ADP-ribosyltransferases investigated were predominantly bacterial toxins and extracellular enzymes, while it remained unclear whether intracellular mono-ADP-ribosyltransferases exist (Deng and Barbieri 2008; Di Girolamo et al. 2005). ARTD10/PARP10 was the first intracellular ARTD, which was identified as a bona fide mono-ADP-ribosyltransferase, defining a new subfamily of ADP-ribosyltransferases with nine members (Hottiger et al. 2010; Kleine et al. 2008). The functional characterization of these enzymes is still rather preliminary compared with at least some of the poly-ADP-ribosylating enzymes. However, the last

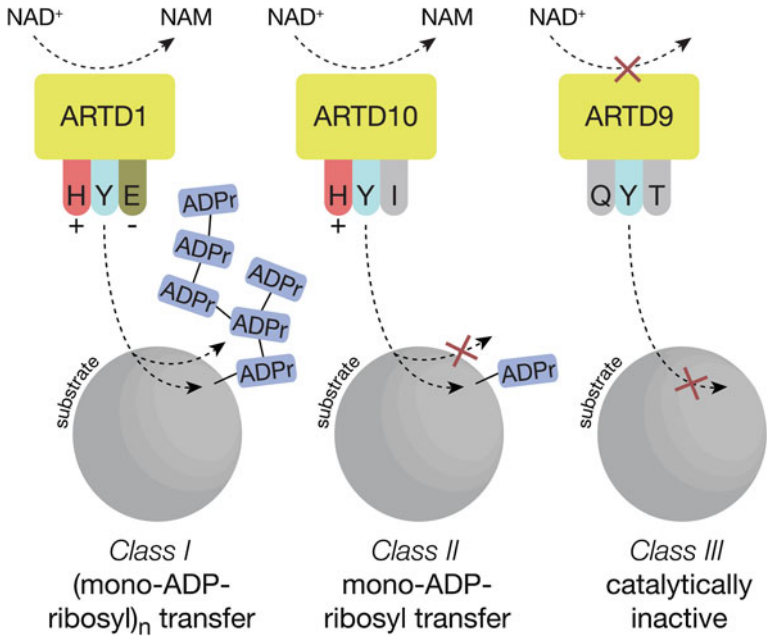

Fig. 1 Summary of the catalytic activities of intracellular ADP-ribosyltransferase (ARTD) family members. ADP-ribosylation involves the transfer of ADP-ribose from NAD^+ to a substrate and release of nicotinamide (NAM). The ARTD family enzymes are subdivided according to differences in their catalytic activity. The activity of poly-ADP-ribosyltransferases such as ARTD1 depends on three critical amino acid residues (His-Tyr-Glu) in the active center/cofactor binding site, two of which (His and Tyr) are important to interact with NAD^+, while the glutamate stabilizes an oxacarbenium intermediate during catalysis. These amino acids, which are referred to as the catalytic motif, are not conserved in all ARTDs. As a consequence the catalytic activities are changed. Hence three different subfamilies of ARTDs have been proposed. Class I ARTDs are poly-ADP-ribosyltransferases with the original motif HYE. In class II ARTDs, including ARTD10, the acidic glutamate is replaced by I/L/T/V/Y, which results in restriction to mono-ADP-ribosylation. This class of enzymes uses substrate-assisted catalysis to modify substrates, i.e., a glutamate of the substrate activates NAD^+ but is subsequently modified and cannot be reused for a second reaction. In the third class also the basic histidine residue is replaced with an uncharged amino acid and these enzymes lose the ability to bind NAD^+ rendering them catalytically inactive

couple of years have seen the beginning of the elucidation of pathways and processes that are affected by mono-ADP-ribosyltransferases (Feijs et al. 2013c). Here we summarize these findings and discuss broader implications of these observations with an outlook towards a potential role of ARTD10 in immunity, metabolism, and cancer biology. Moreover, we highlight open questions that need to be addressed to understand mono-ADP-ribosylation in more general terms.

2 Mechanism of Mono-ADP-Ribosylation by ARTD10

ARTDs catalyze the addition of ADP-ribose to proteins by consuming the co-factor NAD^+ and releasing nicotinamid (Fig. 1). The catalytic domain of ARTD10 was identified in a homology search for ADP-ribosyltransferase domains based on the catalytic domain of ARTD1 (Ame et al. 2004; Otto et al. 2005). Later, key differences in catalytic residues were recognized in ARTD10 (Kleine et al. 2008). The catalytic motif His-Tyr-Glu is altered to His-Tyr-Ile in ARTD10, resulting in the ability to transfer only a single ADP-ribose to a substrate (Fig. 1). Mutating the glutamate of the catalytic motif in ARTD1 prevents the formation of polymers, supporting the essential role of this residue for poly-ADP-ribosylation activity, whereas ARTD10 does not acquire the capacity to form polymers when the glutamate is restored (Kleine et al. 2008; Marsischky et al. 1995). The catalytic glutamate in ARTD1 stabilizes the oxacarbenium ion transition state of NAD^+, whereas in the model of the reaction catalyzed by ARTD10, a glutamate of a substrate takes over this function. However, unlike the catalytic glutamate in ARTD1, the glutamate of the substrate is subsequently ADP-ribosylated and as a result this modified residue is no longer available for a second round of catalysis. Thus, this mechanism—referred to as substrate-assisted catalysis—limits the activity of ARTD10 and the other subfamily members, ARTD7-8, ARTD11-12 and ARTD14-17 to mono-ADP-ribosylation (Kleine et al. 2008). Based on this model and chemical analysis of the reaction products it was proposed that ARTD10 selectively modifies acidic amino acids. More recent evidence suggests that ARTD family members may also be capable of modifying lysine residues (Altmeyer et al. 2009; Messner et al. 2010). These findings initiated a more general discussion about the specificity of different ARTDs which still continues, and led us to reevaluate the acceptor amino acids of ARTD10. An ARTD10 mutant, in which all lysines were exchanged to arginines, is still efficiently trans-automodified, indicating that lysines are at least not the exclusive acceptor sites (Rosenthal et al. 2013). With the evidence presently available we would argue that ARTD10 modifies acid amino acids, as it is unclear how this enzyme would be able of modifying both acidic side chains and lysines in the same catalytic center.

3 The Structure of ARTD10

The family of ARTDs was defined based on homology of the catalytic domains of these enzymes (Ame et al. 2004; Otto et al. 2005). The different ARTDs possess a great variety of additional domains and motifs besides the catalytic domain, which is thought to reflect the broad range of functions they carry out (Ame et al. 2004; Hottiger et al. 2010). Human ARTD10 contains 1025 amino acids, which approximate to an apparent molecular size of 150 kDa on SDS-PAGE. Less than 20% of the sequence contributes to the defining catalytic domain at the very

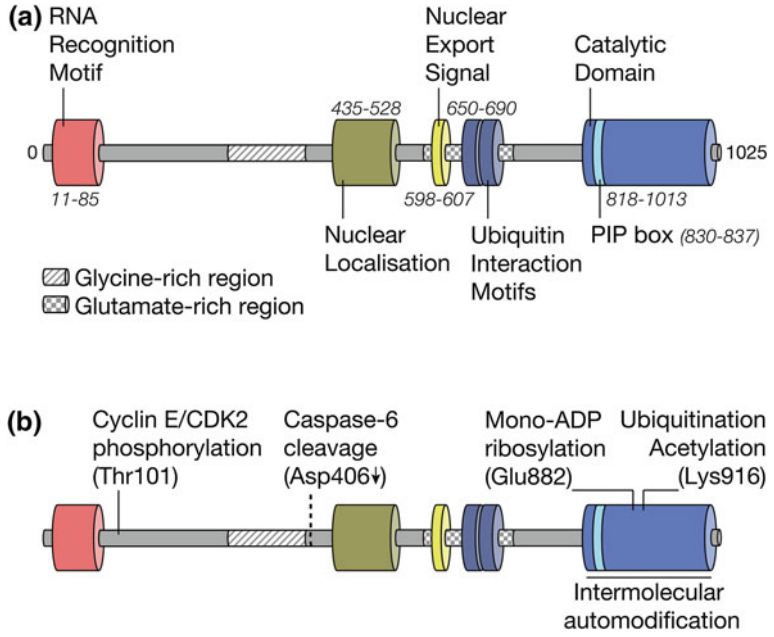

Fig. 2 Domains and structural motifs of ARTD10. **a**. The following domains and motifs are indicated: an RNA recognition motif (amino acids 11–85), a glycine-rich region (281–399), a caspase-6 cleavage site (C-terminal of Asp406), a nuclear localization region (435–528), a glutamate-rich region (588–697), a nuclear export signal (598–607), two ubiquitin interaction motifs (650–667 and 673–690), and a catalytic domain (818–1013), which contains a PCNA-interaction peptide motif (PIP box, amino acids 830–837). **b**. The known posttranslational modifications are indicated: Thr101 is phosphorylated by Cyclin E/CDK2; caspase-6 cleaves ARTD10 C-terminal of Asp406 during apoptosis; the catalytic domain is the major automodification region with Glu882 being one of the mono-ADP-ribosylation sites; Lys916 is both acetylated and ubiquitinated

C-terminus (Fig. 2a) (Yu et al. 2005), which is sufficient to mono-ADP-ribosylate ARTD10 substrates in vitro, comparable to the full-length protein (Kleine et al. 2008; Yu et al. 2005). ARTD10 furthermore contains several other domains and motifs, including an RNA recognition motif (RRM), two functional ubiquitin interaction motifs (UIM), sequences capable to promote nuclear targeting as well as nuclear export, and a small motif that mediates interaction with PCNA (Fig. 2a) (Kleine et al. 2008, 2012; Nicolae et al. 2014; Verheugd et al. 2013; Yu et al. 2005). It is conceivable that some of these domains orient ARTD10-mediated mono-ADP-ribosylation toward specific substrates in different compartments, guided for instance by the interaction with poly-ubiquitin (Herzog et al. 2013; Verheugd et al. 2013). ARTD10 hence seems suited to participate in a wide set of processes in cells.

4 Regulation of ARTD10

At present, little is known about the regulation of ARTD10. Several PTMs can be found on ARTD10, suggesting that multiple signaling pathways control it. The transferase domain of ARTD10 is mono-ADP-ribosylated by intermolecular automodification, presumably on multiple sites (Kleine et al. 2008; Yu et al. 2005). The only modification site that has been mapped to date is a glutamate (Glu882) (Fig. 2b). The mutation of Glu882 has no effect on catalytic activity and only a partial effect on automodification, in agreement with multiple ADP-ribosylation sites in ARTD10 (Kleine et al. 2008). Furthermore, two independent mass spectrometry approaches have suggested that ubiquitination of ARTD10 occurs at Lys916 in cells (Fig. 2b) (Hornbeck et al. 2012; Wagner et al. 2011). This represents a PTM, which might affect catalytic activity, as an ARTD10-K916I mutant yields a strongly reduced automodification signal (Yu et al. 2005). Intriguingly, another study found the same residue to be acetylated in cells (Choudhary et al. 2009). Competing ubiquitination and acetylation have been previously recognized as rivaling modulators of protein function and half-life (Caron et al. 2005; Li et al. 2012; Vervoorts et al. 2003; Yang and Seto 2008). ARTD10 activity could thus be regulated by ubiquitin ligases and acetyltransferases. Interestingly, K916 has only been introduced during primate evolution, while a highly conserved glutamine is present at the same site in lower species, including mice (Kim and Hahn 2012). Glutamines are commonly accepted as imperfect mimics of acetylated lysines (Fujimoto et al. 2012; Kamieniarz and Schneider 2009). Hence acetylation of K916 may preserve while ubiquitination of this residue may interfere with ARTD10 catalytic activity.

ARTD10 is also phosphorylated at multiple sites (our own unpublished findings), thus providing potential opportunities for regulation. In one report, Thr101 was identified as a phosphorylation site of cyclin-dependent kinases (Chou et al. 2006). The work performed in vitro suggested that phosphorylation at Thr101 enhances ARTD10 catalytic activity. We have also identified this phosphorylation site, but were unable to measure phosphorylation-dependent effects on catalytic activity (Fig. 2b). In summary the available evidence indicates that various enzymes modify ARTD10. Future work will have to address the pathways that potentially converge onto ARTD10 and to define the molecular consequences of different PTMs on the functions of ARTD10.

5 ARTD10 Shuttles Between the Cytoplasm and the Nucleus

ARTD10 substrates and interaction partners are situated both in the nucleus (e.g., c-MYC, RAN, and histones) and in the cytoplasm (e.g., GSK3β, NEMO/IKKγ, p62/SQSTM1, and PCNA) (Feijs et al. 2013b; Forst et al. 2013; Kleine et al.

2012; Nicolae et al. 2014; Verheugd et al. 2013; Yu et al. 2005). Under steady-state conditions in proliferating cells, little nuclear ARTD10 is detectable because of a strong nuclear export sequence (NES) that causes rapid export from the nucleus (Fig. 2a) (Kleine et al. 2012). Even when the NES is mutated or the CRM1-dependent export is inhibited by leptomycin B (Kudo et al. 1999), only an equal distribution is achieved rather than nuclear accumulation. Hence additional mechanisms must exist that retain ARTD10 in the cytoplasm (Kleine et al. 2012). ARTD10 could potentially be bound to a cytoplasmic protein or to a scaffold like poly-ubiquitin. Indeed, organization of ARTD10 into cytoplasmic bodies (Kleine et al. 2012; Vyas et al. 2013), associated with the autophagy adaptor p62 (Johansen and Lamark 2011; Nezis and Stenmark 2012) and ubiquitin, has been described (Kleine et al. 2012). The exchange of proteins in these bodies is swift and therefore does not seem to limit dynamic redistribution of ARTD10. ARTD10 might also be exported by a nuclear export pathway, which involves an exportin other than CRM1. Alternative routes have been established for proteins such as actin or 14-3-3σ (Mingot et al. 2004; Stuven et al. 2003). This would not change the dependence on a gradient of the nuclear GTP-binding protein RAN, as all known exportins form a ternary complex with their cargo and RAN-GTP in the nucleus, complexes that disintegrate in the cytoplasm after GTP hydrolysis (Guttler and Gorlich 2011). ARTD10 specifically mono-ADP-ribosylates the GTP-bound form of RAN, while RAN-GDP is not modified (Forst et al. 2013). Presently, it is not clear whether mono-ADP-ribosylation influences RAN function.

The nuclear uptake of ARTD10 relies on a conserved central region, which functions as a nuclear localization sequence (NLS) (Fig. 2a). However this domain does not contain a recognizable classical NLS and resembles no formerly described motif (Kleine et al. 2012). This ARTD10 domain can drive nuclear translocation when fused to EGFP-β-Gal, but unlike a classical NLS only a partial nuclear accumulation was observed. This suggests that this unconventional NLS may use a pathway that is not very efficient or that this domain has additional functions such as interacting with cytosolic factors and thus preventing efficient nuclear import. The intricacy of ARTD10 localization indicates that cells can regulate the subcellular distribution of ARTD10, although it is unclear how this is achieved. An interesting but purely speculative mechanism can be based on a study that finds ARTD10 mRNA specifically altered in blood cells by adenosine deaminases acting on RNA (ADARs) (He et al. 2011). These enzymes deaminate adenosines to inosines, which are recognized as guanosines by the translational machinery. In the case of ARTD10 this results in an amino acid substitution within the NLS region; the highly conserved Ser507 is exchanged by a glycine, which might affect the activity of the unconventional NLS of ARTD10. Together these findings demonstrate that ARTD10 is localized to both the nuclear and cytoplasmic compartments. Together with the known substrates and interaction partners highlighted above, it is highly likely that ARTD10 has functions in both compartments as described in more detail below. Moreover functions associated with the transport between nuclear and cytosolic compartments may also be conceivable for ARTD10.

6 Signaling Pathways Regulated by ARTD10

Different possibilities exist as to how mono-ADP-ribosylation could influence target proteins; in analogy to other PTMs, effects on protein function and on interactions with other macromolecules are likely. Recent evidence supports both, i.e., ADP-ribose can function as allosteric regulator of enzyme activity and as docking site for distinct proteins (Feijs et al. 2013a, b; Forst et al. 2013). A reader domain of mono-ADP-ribosylated proteins was identified, indicating that mono-ADP-ribosylation promotes defined protein-protein interactions (Forst et al. 2013). This reader is a macrodomain, a highly conserved structure which is closely associated with ADP-ribosylation and ADP-ribose metabolism (for a more extensive summary of the currently known macrodomain-containing proteins and their functions see (Feijs et al. 2013a)). Two macrodomains in ARTD8 are capable to selectively interact with ARTD10-dependent mono-ADP-ribosylated substrates (Forst et al. 2013; Verheugd et al. 2013). It is noteworthy that ARTD8 functions also as mono-ADP-ribosyltransferase, which makes multistep mono-ADP-ribosylation events on proteins conceivable.

Apart from recognition of mono-ADP-ribosylation by specific protein domains, ARTD10-mediated modification of proteins can regulate substrate function directly, as exemplified by glycogen synthase kinase 3β (GSK3β). GSK3β is a well-investigated enzyme with established functions in WNT signaling, apoptosis, metabolism, neuronal development, immunity, and tumorigenesis (Beurel and Jope 2006; Beurel et al. 2010; Hur and Zhou 2010; Mills et al. 2011; Wu and Pan 2010). ARTD10 is able to mono-ADP-ribosylate GSK3β in vitro leading to a reduction of GSK3β kinase activity. This inhibition could not be overcome by increasing substrate concentration, implying that mono-ADP-ribosylation functions as an allosteric inhibitor of GSK3β.

Mono-ADP-ribosylation is currently not reliably measurable in cells due to a lack of suitable antibodies and mass spectrometry methods. To analyze GSK3β, its kinase activity was used as a surrogate parameter to evaluate ARTD10 activity in cells. Immunoprecipitated GSK3β showed reduced catalytic activity when co-expressed with ARTD10, while overexpression of the catalytically inactive mutant ARTD10-G888W or knockdown of the endogenous ARTD10 significantly enhanced it, implying that modification of GSK3β indeed takes places in cells (Feijs et al. 2013b).

Recent findings indicate that mono-ADP-ribosylation is a reversible PTM (Jankevicius et al. 2013; Rosenthal et al. 2013; Sharifi et al. 2013). The enzymes capable of removing mono-ADP-ribose from protein substrates are MacroD1, MacroD2, and C6orf130/TARG1, which all contain a catalytically active macrodomain able to reverse ARTD10-dependent mono-ADP-ribosylation. Whether they can revert mono-ADP-ribosylation catalyzed by other mono-ARTDs needs to be determined. Moreover, MacroD2 was found to de-mono-ADP-ribosylate GSK3β, thereby restoring its catalytic activity (Rosenthal et al. 2013). This in vitro finding renders GSK3β modification by ARTD10 reversible, as would be expected

from a mechanism that regulates signaling cascades. In cells, activation of GSK3β was also observed when MacroD2 was over-expressed, resulting together with the above summarized experiments in a strong case for endogenous mono-ADP-ribosylation of GSK3β and the functional relevance of this modification (Feijs et al. 2013b; Rosenthal et al. 2013). The precise understanding of the regulation of ARTD10-mediated mono-ADP-ribosylation and the antagonizing hydrolases will be important to identify the cellular contexts in which ARTD10's activity is physiologically relevant.

One pathway ARTD10 was postulated to interfere with is NF-κB signaling (Verheugd et al. 2013). The UIMs of ARTD10 were identified as interaction motifs for K63-linked poly-ubiquitin, which is an important PTM within the NF-κB signal transduction pathway as well as in other signaling networks (Grabbe et al. 2011). E3 ubiquitin ligases such as TRAF6 synthesize scaffolds of K63-linked poly-ubiquitin upon a number of stimuli, including inflammatory cytokines, which are essential to promote NF-κB translocation into the nucleus to enable transcription of its target genes (Fig. 3) (DiDonato et al. 2012; Oeckinghaus et al. 2011). ARTD10 functions as a repressor of an NF-κB reporter gene construct and chromatin embedded NF-κB target genes (Verheugd et al. 2013). This repression depends on the catalytic activity and the K63-linked poly-ubiquitin binding capability of ARTD10, as demonstrated by using the nonrepressive double mutant ARTD10-G888W-ΔUIM, which lacks catalytic and K63-linked poly-ubiquitin binding activity. These findings suggest that in response to specific signals ARTD10 is recruited to K63-linked poly-ubiquitin scaffolds, resulting in mono-ADP-ribosylation of proteins in the vicinity of these scaffolds (Fig. 3). However, the abolishment of either ubiquitin binding or catalytic activity alone did not reduce ARTD10's inhibitory potential towards NF-κB. One possible explanation for this observation might relate to the fact that the mutants were over-expressed. It is imaginable that abundant ARTD10-G888W can compete for K63-linked poly-ubiquitin binding with factors essential for signal propagation, such as NEMO. Moreover, abundant ARTD10-ΔUIM may suffice to mono-ADP-ribosylate substrates in the pathway without the need of induced proximity. Both would result in the observed inhibitory effect. A role of ARTD10 in the NF-κB pathway was corroborated with ARTD10 knockdown experiments. These resulted in enhanced NF-κB signaling, suggesting that ARTD10 indeed downregulates this pathway in cells. Additionally, overexpression of ARTD10 leads to a specific decrease of the K63-linked poly-ubiquitination of NEMO, an integral part of the IKK complex, which controls the NF-κB transcription factor (Fig. 3). NEMO serves as an adaptor of the complex to K63-linked poly-ubiquitin and is itself K63-poly-ubiquitinated, both features that are essential for NF-κB signal propagation (Chen 2012; Skaug et al. 2009). As NEMO is a substrate of ARTD10 in vitro and in cells (Verheugd et al. 2013), it will be interesting to see how its mono-ADP-ribosylation might interfere with its K63-linked poly-ubiquitination and how this relates to abortion of the signaling process.

Participation in signaling events so far is the area with the most substantial evidence for an involvement of ARTD10. Direct alteration of kinase activity as

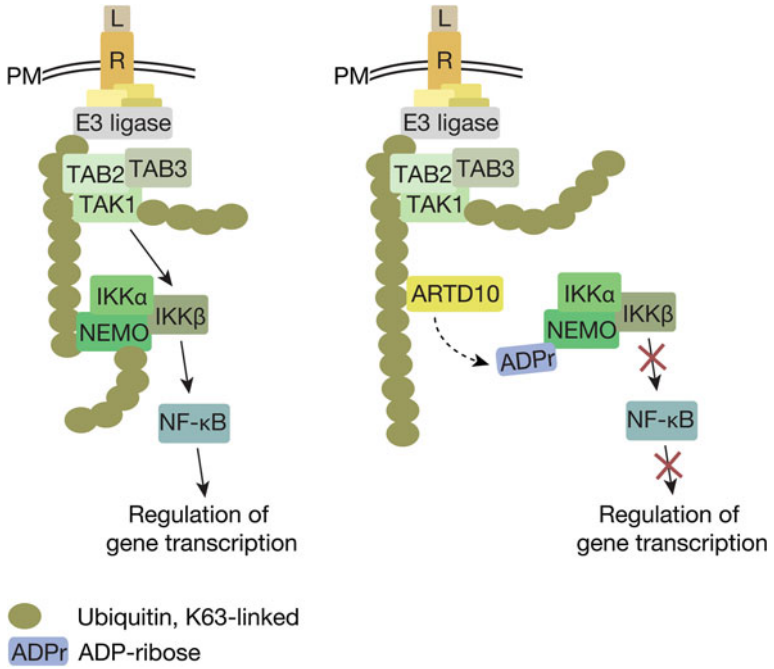

Fig. 3 ARTD10 regulates NF-κB signaling. A simplified version of the NF-κB signal transduction pathway is shown. In response to extracellular cues ubiquitin E3 ligases are activated that synthesize K63-linked poly-ubiquitin. These serve as scaffold for kinase complexes, including the TAK1 and the IKK complexes. The local vicinity allows TAK1 to phosphorylate and activate IKKβ. This kinase then modifies IκB, which results in its degradation and the subsequent activation of NF-κB transcription factors (left scheme). ARTD10 interferes with the activation of NF-κB by interacting with K63-linked poly-ubiquitin and by mono-ADP-ribosylating NEMO. This prevents poly-ubiquitination of NEMO, while enhancing it on the E3 ligase TRAF6 and on TAK1

demonstrated for GSK3β indicates an intervention of ARTD10 in intracellular communication by phosphorylation, while the results from studying the NF-κB pathway suggest that ARTD10 can both read as well as interfere with K63-poly-ubiquitination of proteins. Together these results suggest that mono-ADP-ribosylation participates in crosstalk with other PTMs, including ubiquitination and phosphorylation.

7 A Role for ARTD10 in Transcription?

Different ARTDs such as ARTD1, ARTD8, and ARTD14 are involved in transcriptional regulation (Feijs et al. 2013c; Kraus 2008). There are only initial hints for a role of ARTD10 in transcription. ARTD10 was discovered in a search for

binding partners of the oncogenic transcription factor MYC (Yu et al. 2005). Bimolecular fluorescence complementation later revealed that the MYC-ARTD10 interaction takes place in the nucleus (Kleine et al. 2012), but it has not been resolved whether the interaction occurs on DNA. Currently, the known functional relevance of the ARTD10 interaction with MYC is limited to co-transformation assays of rat embryo fibroblasts, in which ARTD10 acts as a suppressor of the transforming activity of MYC with HA-RAS (Yu et al. 2005). However, MYC is not a substrate of ARTD10, leaving it currently unknown whether ARTD10 controls MYC directly. Possible nuclear ARTD10 substrates that might influence transcription, such as histones, can be mono-ADP-ribosylated in vitro but it remains to be determined whether ARTD10 also modifies these proteins in cells (Yu et al. 2005). It is worth noting that there is substantial evidence that core histones are both mono- and poly-ADP-ribosylated in cells (Hassa et al. 2006). Nevertheless, a precise role of ARTD10 in transcription remains undefined at present.

8 ARTD10 Stimulates Apoptosis

HeLa cells with inducible expression of ARTD10 or the catalytically inactive point mutant ARTD10-G888W have been used to characterize the influence of mono-ADP-ribosylation by ARTD10 on cell proliferation (Herzog et al. 2013). In these cells ARTD10 reduces proliferation and induces apoptosis, dependent on its catalytic activity. Additionally ARTD10 knockdown in U2OS cells leads to decreased apoptosis in response to DNA damaging treatments. Together these findings provide evidence for a pro-apoptotic function of endogenous ARTD10. Moreover, early during apoptosis ARTD10 itself is processed by caspase-6 (Fig. 2b), which reduces its pro-apoptotic potential (Herzog et al. 2013). Expression of the corresponding cleavage products did not result in cell death, even though the C-terminal fragment remained catalytically active. Further experiments revealed that indeed a physical connection between the transferase domain of ARTD10 and the N-terminal RRM is needed to stimulate any significant degree of apoptosis, although the exact mechanism remains to be clarified.

What might be the role of the RRM for ARTD10-induced apoptosis? RRMs function in many different processes that regulate and are dependent on RNA and have also been described more recently to mediate protein-protein interactions (Maris et al. 2005). A potential answer to why ARTD10's RRM might be important could therefore be a dependence of ARTD10 on its RRM to interact with certain substrates, either directly or mediated by RNA. Truncation of the RRM also results in a loss of the formation of p62-associated ARTD10 bodies in the cytoplasm (Kleine et al. 2012). These structures are not identical with well-studied RNA-containing particles like stress granules or P-bodies. The p62 bodies, which are also positive for ubiquitin, have been implicated as signaling hubs that regulate apoptosis and autophagy (Johansen and Lamark 2011; Kleine et al. 2012; Nezis and Stenmark 2012).

Why is ARTD10, which promotes apoptosis, a target of caspases? Once apoptosis is proceeding, protein biosynthesis is rapidly down-regulated (Clemens et al. 2000). Accordingly, RNA binding and processing proteins such as splicing factors become major targets of caspases, resulting in impeding of mRNA maturation and transport to the cytoplasm (Thiede et al. 2001; Thomas and Lieberman 2013). Based on the findings that ARTD10 shuttles between nuclear and cytoplasmic compartments and the presence of an RRM, we speculate that ARTD10 might be part of a regulatory network that integrates the control of RNA processing with programmed cell death.

If ARTD10 stimulates apoptosis through mono-ADP-ribosylation, which substrates could contribute to such a function? Interestingly, the ARTD10 target GSK3β has been thoroughly investigated as an alternate regulator of apoptosis with the capability to stimulate the intrinsic pathway, while inhibiting the extrinsic pathway (Beurel and Jope 2006). *GSK3*β knockout mice die of massive hepatic apoptosis during development, while *GSK3*$\alpha^{-/-}$ mice are vital (Gomez-Sintes et al. 2011; Hoeflich et al. 2000). It has been suggested that the GSK3β-dependent activation of the NF-κB survival response is at least in part responsible for the observed effect (Hoeflich et al. 2000). As ARTD10 negatively regulates GSK3β by mono-ADP-ribosylation and represses NF-κB signaling by targeting NEMO, the inhibition of both GSK3β and NEMO might link ARTD10 to apoptosis (Feijs et al. 2013b; Verheugd et al. 2013). Additional ARTD10 interaction partners and substrates might contribute to the pro-apoptotic phenotype. The nuclear transport protein RAN, which is an ARTD10 substrate (Forst et al. 2013), has been suggested to prevent the nuclear import of NF-κB early during apoptosis to enhance apoptotic progression (Wong et al. 2009). As mentioned above, cytosolic p62-ubiquitin bodies are implicated as signal organizing centers during apoptosis. They can either recruit TRAF6 to subsequently activate NF-κB by auto-K63-poly-ubiquitination or aggregate ubiquitinated caspase-8, which promotes its activation and subsequent stimulation of apoptosis (Moscat and Diaz-Meco 2009), suggesting that the ARTD10 interaction partner p62 participates in controlling cell survival. Together these findings offer additional entry points for ARTD10 in the control of apoptosis that are in need of evaluation.

9 DNA Repair

One of the key activities of ARTD1 is its function in DNA repair processes. ARTD1 recognizes damaged DNA through its Zn-fingers, resulting in the allosteric activation of its catalytic domain (Langelier and Pascal 2013). Subsequently, ADP-ribose polymers are synthesized on ARTD1 itself as well as other proteins, including core histones (De Vos et al. 2012). These polymers act as scaffolds to recruit DNA repair proteins through ADP-ribose polymer binding domains (Kleine and Luscher 2009). ARTD2/PARP2 and ARTD3/PARP3 are two additional family members that are involved in DNA repair processes (De Vos et al. 2012). Thus poly-ADP-ribosylation plays a major role in different DNA repair pathways. Little is known about the role of

mono-ADP-ribosylation in DNA repair. A very recent study identified PCNA, which is associated with a large number of processes associated with genomic stability (Groth et al. 2007; Moldovan et al. 2007), as an interaction partner of ARTD10. It possesses a PCNA-interacting peptide (PIP) box near the N-terminal end of the catalytic domain (Fig. 2a) (Nicolae et al. 2014). The PIP box is found in several proteins known to interact with PCNA and thus is important to control and integrate PCNA activities (Moldovan et al. 2007). Indeed ARTD10 interacts through its PIP box with PCNA, an interaction that seems to be required to promote genomic stability and tolerance to DNA damage (Nicolae et al. 2014). ARTD10 is also important for PCNA-dependent translesion DNA synthesis and associated mutagenesis, requiring an active catalytic domain. The interaction of ARTD10 with PCNA is further promoted by the UIMs, which enhance the interaction with ubiquitinated PCNA. Together these findings support the notion that in addition to poly-ADP-ribosylation also mono-ADP-ribosylation participates in DNA repair processes. It will be of interest to determine whether and if how these two types of ADP-ribosylation reactions collaborate.

10 Clues Toward Additional Biological Functions of ARTD10

Presently our understanding of ARTD10 resembles a patchwork of promising suggestions yet little substantial evidence. To further evaluate potential functions of ARTD10, it is worth to consider the information that is available connecting ARTD10 with distinct cellular and organismal processes. In the following, we summarize the preliminary indications of interaction of ARTD10 with the immune system, metabolism, and with cancer.

10.1 ARTD10 Levels Differ Between Tissues

In the initial report on ARTD10, tissue-specific expression was analyzed by northern blotting of human samples (Yu et al. 2005). *ARTD10* mRNA was detected in all tested tissue samples with increased expression in thymus and spleen when compared to *actin* mRNA. This indicated enhanced expression of ARTD10 in cells of the immune system. Indeed ARTD10 protein levels are elevated in cell lines originating from the hematopoietic system (Yu et al. 2005). Information from publicly available human expression datasets largely confirms these results (Fig. 4). Also array data from mice and rats are available, which include a broader set of tissue samples (Fig. 4). Besides expression in thymus and spleen, high levels of *ARTD10* are found in other tissues in these studies, including adipose tissue, the Langerhans islets of the pancreas, the adrenal glands, the small intestine, the liver, and the kidneys. Low expression of *ARTD10* in the brain was

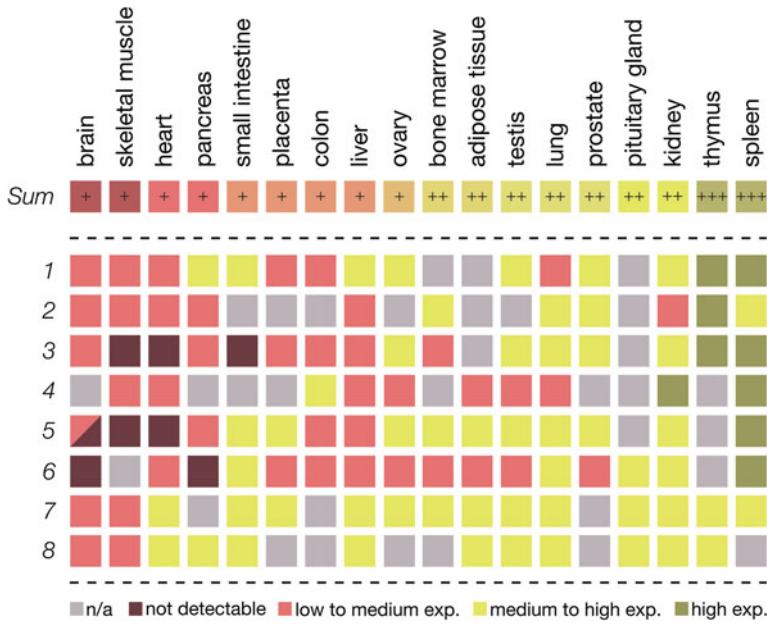

Fig. 4 Relative ARTD10 expression in different tissues. The heat map visualizes mRNA expression data from eight different studies, including one study focused on human ARTD10 (*1*, (Yu et al. 2005), three genome-wide human expression data sets (*2*, (Yanai et al. 2005), http://www.ebi.ac.uk/gxa/, E-GEOD-803; *3*, (Liu et al. 2008); *4*, (Krupp et al. 2012)), RNA expression data from the Human Protein Atlas (*5*, http://www.proteinatlas.org), and three genome-wide mouse expression data sets (*6*, (Su et al. 2002); *7*, (Thorrez et al. 2008), http://www.ebi.ac.uk/gxa/, E-GEOD-9954; *8*, (Thorrez et al. 2011), http://www.ebi.ac.uk/gxa/, E-GEOD-24940). ARTD10 expression in a given tissue was judged as not detectable, low, intermediate, or high compared to ARTD10 expression in other tissues within a given study. In the top row these results are combined to give a general impression in which organs ARTD10 is expressed preferentially. Tissues that were not studied are indicated as not applicable (n/a)

measured in multiple studies, with the pronounced exception of the pituitary gland (Hindmarch et al. 2006; Hovatta et al. 2007), a tissue that shows among the highest expression levels. Importantly this is not limited to the adenohypophysis, which is not of neuronal origin, but was also measured in the neurohypophysis (Hindmarch et al. 2006). Thus ARTD10 expression is predicted to be widespread (Fig. 4).

10.2 ARTD10 is Upregulated in Response to Inflammatory Stimuli

ARTD10, together with certain other ARTDs, belongs to a group of genes, which are upregulated in sooty mangabeys and rhesus macaques in response to infection with simian immunodeficiency virus (Bosinger et al. 2009). The enhanced expression was measured on day 7 and 10 after infection, which coincided with a

general activation of interferon (IFN) response genes as well as pro-apoptotic and cell cycle regulating genes. In other studies, the response of monocytes to phagocytosed live *borrelia burgdorferi* was investigated compared to toll-like receptor activation by *borrelia* lysates. Two studies demonstrated a dose-dependent induction of apoptosis upon *borrelia* phagocytosis, but not by *borrelia* lysates, in accordance with activation of IFN production and upregulation of a gene set including *ARTD10* (Cruz et al. 2008; Salazar et al. 2009). Furthermore, a noncytopathic variant of the Venezuelan equine encephalitis virus (an alphavirus), which is cleared from wild-type mouse embryo fibroblasts (MEFs) but not from MEFs lacking IFNα/β receptors, appears to regulate *ARTD10* expression (Atasheva et al. 2012). *ARTD10* and *ARTD12* expression are up-regulated upon infection with the virus or IFNβ treatment after 24 h, whereas no effect was observed after infection in type I IFN receptor negative MEFs, suggesting that the stimulation of the IFN response triggered *ARTD10* expression. Moreover, ARTD10 as well as other ARTD family members appear to function as strong inhibitors of protein biosynthesis and inhibit alphavirus replication (Atasheva et al. 2014). *ARTD10* is also one of 46 genes, which display high expression after IFNα treatment of a liver cell line (Mahmoud et al. 2011). In support an *ARTD10* promoter-reporter gene construct is readily responsive to infection with the Newcastle disease virus, a strong inducer of type I IFNs. ChIP-seq analysis for IRF1 binding sites, a downstream effector of IFNα, revealed that this transcription factor binds to the *ARTD10* promoter (Shi et al. 2011). Finally, one study presented evidence for a downregulation of *ARTD10* upon ectopic expression of the influenza protein NS1 (Yu et al. 2011), which may be an indirect effect as NS1 is known to inhibit type I IFN production (Hale et al. 2008). Although these studies rely largely on the analysis of RNA, together these findings strongly implicate ARTD10 in anti-viral response.

10.3 ARTD10 Might be Involved in Lipid Metabolism

ARTD10 has been identified as a locus associated with lipid traits in a large meta-analysis summarizing 46 genome-wide association studies (Teslovich et al. 2010). Using a sample of >100,000 individuals of European ancestry 95 loci were identified to be significantly associated with plasma lipids, with 22 being associated with changes in LDL cholesterol levels in the blood. Among these, the lead single nucleotide polymorphism (SNP) rs11136341 is associated with increased LDL and total cholesterol. This SNP maps to the beginning of the *Plectin1* gene and is roughly 5000 base pairs downstream of the *ARTD10* gene, consistent with the known overlap of the two genes (Fuchs et al. 2009; Lesniewicz et al. 2005). The potential relevance of ARTD10 was addressed using knockdown studies, which revealed that this resulted in a substantial decrease in apolipoprotein B (APOB) secretion of liver cells (Shen et al. 2012). The *APOB* gene was also described as one of 22 loci associated with a lead SNP of increased LDL levels (Teslovich et al. 2010). APOB is the primary lipoprotein of chylomicrons and LDL

particles, its overexpression is associated with high LDL and low HDL blood levels and it is regarded as a risk factor of atherosclerosis (Benn 2009; McCormick et al. 1996). Here, it may also be of note that macrophages treated with oxidized LDL show a significant downregulation of ARTD10 expression determined by mass spectrometry (Kang et al. 2009). Further experimentation will be required to firmly establish ARTD10 in the control of lipid metabolism.

10.4 ARTD10 in Tumor Biology?

Could ARTD10 also be relevant for tumor cells, similar to other ARTDs that have been implicated in tumorigenesis (Feijs et al. 2013c; Scarpa et al. 2013)? Some observations are in support of such a hypothesis. ARTD10 expression varies considerably in different tumor cell lines and its overexpression inhibits transformation of rat embryo fibroblasts (Yu et al. 2005). The *ARTD10* gene is also located in the same part of chromosome 8 as its oncogenic interaction partner *MYC* (8q24), which could result in simultaneous deregulation by chromosomal aberrations. Thus far ARTD10 expression in tumors has not been analyzed systematically. However one study exists, which noticed a tenfold *ARTD10* downregulation in a set of 86 samples of gastric cancer compared to normal gastric tissue (Wong et al. 2009). As ARTD10 displays anti-proliferative and pro-apoptotic properties at least in some tumor cell lines, it may function as a tumor suppressor, a hypothesis that is in need of verification.

11 Conclusions and Outlook

The expression data summarized here provide indications about the cell types and tissues in which ARTD10 may be relevant. The preferential expression of ARTD10 in the thymus and in the spleen together with its induction upon inflammatory or immunogenic stimuli suggests a role in innate immunity (Fig. 5), an area where other ARTDs have been established (Welsby et al. 2012). Expression in adipose tissue, liver, and pancreas together with data that link ARTD10 to lipoproteins may point to a role in metabolism (Fig. 5). Studies addressing roles of ARTD10 in NF-κB signaling, apoptosis, and DNA damage also indicate that this protein fulfills multiple tasks (Fig. 5), perhaps regulated by extracellular cues such as IFNα. The mechanisms through which ARTD10 functions remain largely unclear but might become better understood once for example more target proteins are identified. However, the recent identification of mono-ADP-ribosylhydrolases indicates that mono-ADP-ribosylation is a reversible PTM and the direct regulation of GSK3β underlines that it can have profound effects on the activities of substrate proteins.

An effective way to expand and deepen our knowledge of mono-ADP-ribosylation in general and mono-ADP-ribosylation by ARTD10 in particular will be

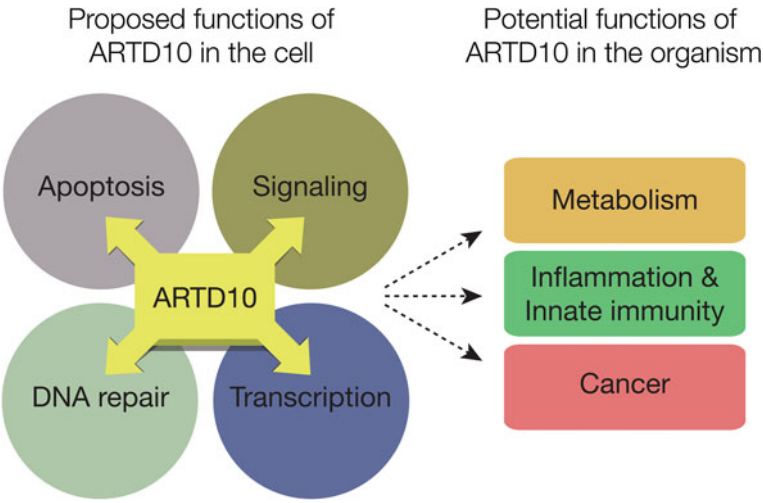

Fig. 5 Potential involvement of ARTD10 in cellular and organismal processes. Biochemical studies have implicated ARTD10 in different aspects of cell physiology such as apoptosis, signaling, transcription and DNA repair. At the organismal level, these ARTD10-mediated cellular functions may be the underlying mechanisms to modulate processes such as metabolism, innate immunity, and cancer (for more discussion see the main text)

the development of more elaborate tools to study mono-ADP-ribosylation in cells. For example the development of antibodies that specifically recognize mono-ADP-ribosylated proteins would allow analyzing the distribution, the dynamics, and the consequences of mono-ADP-ribosylation. Immediate applications of such tools would be to address the regulation of ARTD10, defining in vivo substrates and ultimately to understand the functional consequences of this PTM.

Although we have begun to understand basic characteristics of ARTD10 and recent findings have shed light on some of its biological properties, many questions remain open. We imagine that the studies addressing these will provide novel insight into the role of ARTD10 and mono-ADP-ribosylation in different fundamental processes, including inflammation and immunity and tumorigenesis. As ARTD1/PARP1 inhibitors are successfully entering clinical application (Rouleau et al. 2010), it is likely that other ARTD enzymes, including ARTD10, will serve as targets for therapeutic applications. Studying these enzymes thus provides opportunities to expand our knowledge on basic physiological processes and to translate this information into improving human health.

Acknowledgments We thank Andrew Jefferson for editing the manuscript. The work in our laboratory was supported by a Mildred Scheel Stipend of the German Cancer Aid (to MK), the START program of the Medical School of the RWTH Aachen University, and by the Deutsche Forschungsgemeinschaft DFG (to BL).

References

Altmeyer M, Messner S, Hassa PO et al (2009) Molecular mechanism of poly(ADP-ribosyl)ation by PARP1 and identification of lysine residues as ADP-ribose acceptor sites. Nucleic acids research 37:3723–3738

Ame JC, Spenlehauer C, de Murcia G (2004) The PARP superfamily. Bioessays 26:882–893

Atasheva S, Akhrymuk M, Frolova EI et al (2012) New PARP gene with an anti-alphavirus function. J Virol 86:8147–8160

Atasheva S, Frolova EI, Frolov I (2014) Interferon-stimulated poly(ADP-Ribose) polymerases are potent inhibitors of cellular translation and virus replication. J Virol 88:2116–2130

Barkauskaite E, Jankevicius G, Ladurner AG et al (2013) The recognition and removal of cellular poly(ADP-ribose) signals. FEBS J 280:3491–3507

Benn M (2009) Apolipoprotein B levels, APOB alleles, and risk of ischemic cardiovascular disease in the general population, a review. Atherosclerosis 206:17–30

Beurel E, Jope RS (2006) The paradoxical pro- and anti-apoptotic actions of GSK3 in the intrinsic and extrinsic apoptosis signaling pathways. Prog Neurobiol 79:173–189

Beurel E, Michalek SM, Jope RS (2010) Innate and adaptive immune responses regulated by glycogen synthase kinase-3 (GSK3). Trends in immunology 31:24–31

Bosinger SE, Li Q, Gordon SN et al (2009) Global genomic analysis reveals rapid control of a robust innate response in SIV-infected sooty mangabeys. The Journal of clinical investigation 119:3556–3572

Caron C, Boyault C, Khochbin S (2005) Regulatory cross-talk between lysine acetylation and ubiquitination: role in the control of protein stability. Bioessays 27:408–415

Chen ZJ (2012) Ubiquitination in signaling to and activation of IKK. Immunological reviews 246:95–106

Chou HY, Chou HT, Lee SC (2006) CDK-dependent activation of poly(ADP-ribose) polymerase member 10 (PARP10). J Biol Chem 281:15201–15207

Choudhary C, Kumar C, Gnad F et al (2009) Lysine acetylation targets protein complexes and co-regulates major cellular functions. Science 325:834–840

Clemens MJ, Bushell M, Jeffrey IW et al (2000) Translation initiation factor modifications and the regulation of protein synthesis in apoptotic cells. Cell Death Differ 7:603–615

Cruz AR, Moore MW, La Vake CJ et al (2008) Phagocytosis of Borrelia burgdorferi, the Lyme disease spirochete, potentiates innate immune activation and induces apoptosis in human monocytes. Infect Immun 76:56–70

D'Amours D, Desnoyers S, D'Silva I et al (1999) Poly(ADP-ribosyl)ation reactions in the regulation of nuclear functions. Biochem J 342 (Pt 2):249–268

De Vos M, Schreiber V, Dantzer F (2012) The diverse roles and clinical relevance of PARPs in DNA damage repair: current state of the art. Biochem Pharmacol 84:137–146

Deng Q, Barbieri JT (2008) Molecular mechanisms of the cytotoxicity of ADP-ribosylating toxins. Annu Rev Microbiol 62:271–288

Di Girolamo M, Dani N, Stilla A et al (2005) Physiological relevance of the endogenous mono(ADP-ribosyl)ation of cellular proteins. Febs J 272:4565–4575

DiDonato JA, Mercurio F, Karin M (2012) NF-kappaB and the link between inflammation and cancer. Immunol Rev 246:379–400

Feijs KL, Forst AH, Verheugd P et al (2013a) Macrodomain-containing proteins: regulating new intracellular functions of mono(ADP-ribosyl)ation. Nat Rev Mol Cell Biol 14:443–451

Feijs KL, Kleine H, Braczynski A et al (2013b) ARTD10 substrate identification on protein microarrays: regulation of GSK3beta by mono-ADP-ribosylation. Cell Commun Signal 11:5

Feijs KL, Verheugd P, Luscher B (2013c) Expanding functions of intracellular resident mono-ADP-ribosylation in cell physiology. FEBS J 280:3519–3529

Forst AH, Karlberg T, Herzog N et al (2013) Recognition of mono-ADP-ribosylated ARTD10 substrates by ARTD8 macrodomains. Structure 21:462–475

Fuchs P, Zorer M, Reipert S et al (2009) Targeted inactivation of a developmentally regulated neural plectin isoform (plectin 1c) in mice leads to reduced motor nerve conduction velocity. J Biol Chem 284:26502–26509
Fujimoto H, Higuchi M, Koike M et al (2012) A possible overestimation of the effect of acetylation on lysine residues in KQ mutant analysis. J Comput Chem 33:239–246
Gibson BA, Kraus WL (2012) New insights into the molecular and cellular functions of poly(ADP-ribose) and PARPs. Nat Rev Mol Cell Biol 13:411–424
Gomez-Sintes R, Hernandez F, Lucas JJ et al (2011) GSK-3 Mouse Models to Study Neuronal Apoptosis and Neurodegeneration. Front Mol Neurosci 4:45
Grabbe C, Husnjak K, Dikic I (2011) The spatial and temporal organization of ubiquitin networks. Nat Rev Mol Cell Biol 12:295–307
Groth A, Rocha W, Verreault A et al (2007) Chromatin challenges during DNA replication and repair. Cell 128:721–733
Guttler T, Gorlich D (2011) Ran-dependent nuclear export mediators: a structural perspective. EMBO J 30:3457–3474
Hale BG, Randall RE, Ortin J et al (2008) The multifunctional NS1 protein of influenza A viruses. J Gen Virol 89:2359–2376
Hassa PO, Haenni SS, Elser M et al (2006) Nuclear ADP-ribosylation reactions in mammalian cells: where are we today and where are we going? Microbiol Mol Biol Rev 70:789–829
He T, Wang Q, Feng G et al (2011) Computational detection and functional analysis of human tissue-specific A-to-I RNA editing. PLoS ONE 6:e18129
Herzog N, Hartkamp JD, Verheugd P et al (2013) Caspase-dependent cleavage of the mono-ADP-ribosyltransferase ARTD10 interferes with its pro-apoptotic function. FEBS J 280:1330–1343
Hindmarch C, Yao S, Beighton G et al (2006) A comprehensive description of the transcriptome of the hypothalamoneurohypophyseal system in euhydrated and dehydrated rats. Proc Natl Acad Sci U S A 103:1609–1614
Hoeflich KP, Luo J, Rubie EA et al (2000) Requirement for glycogen synthase kinase-3beta in cell survival and NF-kappaB activation. Nature 406:86–90
Hornbeck PV, Kornhauser JM, Tkachev S et al (2012) PhosphoSitePlus: a comprehensive resource for investigating the structure and function of experimentally determined post-translational modifications in man and mouse. Nucleic Acids Res 40:D261–D270
Hottiger MO, Hassa PO, Luscher B et al (2010) Toward a unified nomenclature for mammalian ADP-ribosyltransferases. Trends Biochem Sci 35:208–219
Hovatta I, Zapala MA, Broide RS et al (2007) DNA variation and brain region-specific expression profiles exhibit different relationships between inbred mouse strains: implications for eQTL mapping studies. Genome Biol 8:R25
Hur EM, Zhou FQ (2010) GSK3 signalling in neural development. Nat Rev Neurosci 11:539–551
Jankevicius G, Hassler M, Golia B et al (2013) A family of macrodomain proteins reverses cellular mono-ADP-ribosylation. Nature structural & molecular biology 20:508–514
Johansen T, Lamark T (2011) Selective autophagy mediated by autophagic adapter proteins. Autophagy 7:279–296
Kamieniarz K, Schneider R (2009) Tools to tackle protein acetylation. Chem Biol 16:1027–1029
Kang JH, Ryu HS, Kim HT et al (2009) Proteomic analysis of human macrophages exposed to hypochlorite-oxidized low-density lipoprotein. Biochim Biophys Acta 1794:446–458
Kim DS, Hahn Y (2012) Gains of ubiquitylation sites in highly conserved proteins in the human lineage. BMC Bioinformatics 13:306
Kleine H, Herrmann A, Lamark T et al (2012) Dynamic subcellular localization of the mono-ADP-ribosyltransferase ARTD10 and interaction with the ubiquitin receptor p62. Cell Commun Signal 10:28
Kleine H, Luscher B (2009) Learning how to read ADP-ribosylation. Cell 139:17–19
Kleine H, Poreba E, Lesniewicz K et al (2008) Substrate-assisted catalysis by PARP10 limits its activity to mono-ADP-ribosylation. Mol Cell 32:57–69
Kraus WL (2008) Transcriptional control by PARP-1: chromatin modulation, enhancer-binding, coregulation, and insulation. Curr Opin Cell Biol 20:294–302

Krishnakumar R, Kraus WL (2010) The PARP side of the nucleus: molecular actions, physiological outcomes, and clinical targets. Mol Cell 39:8–24

Krupp M, Marquardt JU, Sahin U et al (2012) RNA-Seq Atlas—a reference database for gene expression profiling in normal tissue by next-generation sequencing. Bioinformatics 28:1184–1185

Kudo N, Matsumori N, Taoka H et al (1999) Leptomycin B inactivates CRM1/exportin 1 by covalent modification at a cysteine residue in the central conserved region. Proc Natl Acad Sci U S A 96:9112–9117

Laing S, Unger M, Koch-Nolte F et al (2011) ADP-ribosylation of arginine. Amino Acids 41:257–269

Langelier MF, Pascal JM (2013) PARP-1 mechanism for coupling DNA damage detection to poly(ADP-ribose) synthesis. Curr Opin Struct Biol 23:134–143

Lesniewicz K, Luscher-Firzlaff J, Poreba E et al (2005) Overlap of the gene encoding the novel poly(ADP-ribose) polymerase Parp10 with the plectin 1 gene and common use of exon sequences. Genomics 86:38–46

Li H, Wittwer T, Weber A et al (2012) Regulation of NF-kappaB activity by competition between RelA acetylation and ubiquitination. Oncogene 31:611–623

Liu X, Yu X, Zack DJ et al (2008) TiGER: a database for tissue-specific gene expression and regulation. BMC Bioinformatics 9:271

Luo X, Kraus WL (2012) On PAR with PARP: cellular stress signaling through poly(ADP-ribose) and PARP-1. Genes Dev 26:417–432

Mahmoud L, Al-Saif M, Amer HM et al (2011) Green fluorescent protein reporter system with transcriptional sequence heterogeneity for monitoring the interferon response. Journal of virology 85:9268–9275

Maris C, Dominguez C, Allain FH (2005) The RNA recognition motif, a plastic RNA-binding platform to regulate post-transcriptional gene expression. The FEBS journal 272:2118–2131

Marsischky GT, Wilson BA, Collier RJ (1995) Role of glutamic acid 988 of human poly-ADP-ribose polymerase in polymer formation. Evidence for active site similarities to the ADP-ribosylating toxins. J Biol Chem 270:3247–3254

McCormick SP, Ng JK, Veniant M et al (1996) Transgenic mice that overexpress mouse apolipoprotein B. Evidence that the DNA sequences controlling intestinal expression of the apolipoprotein B gene are distant from the structural gene. J Biol Chem 271:11963–11970

Messner S, Altmeyer M, Zhao H et al (2010) PARP1 ADP-ribosylates lysine residues of the core histone tails. Nucleic Acids Res 38:6350–6362

Messner S, Hottiger MO (2011) Histone ADP-ribosylation in DNA repair, replication and transcription. Trends Cell Biol 21:534–542

Mills CN, Nowsheen S, Bonner JA et al (2011) Emerging roles of glycogen synthase kinase 3 in the treatment of brain tumors. Front Mol Neurosci 4:47

Mingot JM, Bohnsack MT, Jakle U et al (2004) Exportin 7 defines a novel general nuclear export pathway. EMBO J 23:3227–36

Moldovan GL, Pfander B, Jentsch S (2007) PCNA, the maestro of the replication fork. Cell 129:665–679

Moscat J, Diaz-Meco MT (2009) p62 at the crossroads of autophagy, apoptosis, and cancer. Cell 137:1001–1004

Nezis IP, Stenmark H (2012) p62 at the interface of autophagy, oxidative stress signaling, and cancer. Antioxid Redox Signal 17:786–793

Nicolae CM, Aho ER, Vlahos AH et al (2014) The ADP-ribosyltransferase PARP10/ARTD10 interacts with Proliferating Cell Nuclear Antigen (PCNA) and is required for DNA damage tolerance. J Biol Chem

Oeckinghaus A, Hayden MS, Ghosh S (2011) Crosstalk in NF-kappaB signaling pathways. Nat Immunol 12:695–708

Otto H, Reche PA, Bazan F et al (2005) In silico characterization of the family of PARP-like poly(ADP-ribosyl)transferases (pARTs). BMC Genomics 6:139

Rosenthal F, Feijs KL, Frugier E et al (2013) Macrodomain-containing proteins are new mono-ADP-ribosylhydrolases. Nat Struct Mol Biol 20:502–507

Rouleau M, Patel A, Hendzel MJ et al (2010) PARP inhibition: PARP1 and beyond. Nature reviews. Cancer 10:293–301
Salazar JC, Duhnam-Ems S, La Vake C et al (2009) Activation of human monocytes by live Borrelia burgdorferi generates TLR2-dependent and -independent responses which include induction of IFN-beta. PLoS pathogens 5:e1000444
Scarpa ES, Fabrizio G, Di Girolamo M (2013) A role of intracellular mono-ADP-ribosylation in cancer biology. FEBS J 280:3551–3562
Schreiber V, Dantzer F, Ame JC et al (2006) Poly(ADP-ribose): novel functions for an old molecule. Nat Rev Mol Cell Biol 7:517–528
Sharifi R, Morra R, Denise Appel C et al (2013) Deficiency of terminal ADP-ribose protein glycohydrolase TARG1/C6orf130 in neurodegenerative disease. The EMBO journal
Shen X, Wang W, Wang L et al (2012) Identification of genes affecting apolipoprotein B secretion following siRNA-mediated gene knockdown in primary human hepatocytes. Atherosclerosis 222:154–157
Shi L, Perin JC, Leipzig J et al (2011) Genome-wide analysis of interferon regulatory factor I binding in primary human monocytes. Gene 487:21–28
Skaug B, Jiang X, Chen ZJ (2009) The role of ubiquitin in NF-kappaB regulatory pathways. Annu Rev Biochem 78:769–796
Stuven T, Hartmann E, Gorlich D (2003) Exportin 6: a novel nuclear export receptor that is specific for profilin.actin complexes. EMBO J 22:5928–5940
Su AI, Cooke MP, Ching KA et al (2002) Large-scale analysis of the human and mouse transcriptomes. Proc Natl Acad Sci USA 99:4465–4470
Teslovich TM, Musunuru K, Smith AV et al (2010) Biological, clinical and population relevance of 95 loci for blood lipids. Nature 466:707–713
Thiede B, Dimmler C, Siejak F et al (2001) Predominant identification of RNA-binding proteins in Fas-induced apoptosis by proteome analysis. J Biol Chem 276:26044–26050
Thomas MP, Lieberman J (2013) Live or let die: posttranscriptional gene regulation in cell stress and cell death. Immunol Rev 253:237–252
Thorrez L, Laudadio I, Van Deun K et al (2011) Tissue-specific disallowance of housekeeping genes: the other face of cell differentiation. Genome Res 21:95–105
Thorrez L, Van Deun K, Tranchevent LC et al (2008) Using ribosomal protein genes as reference: a tale of caution. PLoS ONE 3:e1854
Verheugd P, Forst AH, Milke L et al (2013) Regulation of NF-kappaB signalling by the mono-ADP-ribosyltransferase ARTD10. Nature communications 4:1683
Vervoorts J, Luscher-Firzlaff JM, Rottmann S et al (2003) Stimulation of c-MYC transcriptional activity and acetylation by recruitment of the cofactor CBP. EMBO Rep 4:484–490
Vyas S, Chesarone-Cataldo M, Todorova T et al (2013) A systematic analysis of the PARP protein family identifies new functions critical for cell physiology. Nature communications 4:2240
Wagner SA, Beli P, Weinert BT et al (2011) A proteome-wide, quantitative survey of in vivo ubiquitylation sites reveals widespread regulatory roles. Mol Cell Proteomics 10:M111 013284
Welsby I, Hutin D, Leo O (2012) Complex roles of members of the ADP-ribosyl transferase super family in immune defences: looking beyond PARP1. Biochem Pharmacol 84:11–20
Wong CH, Chan H, Ho CY et al (2009) Apoptotic histone modification inhibits nuclear transport by regulating RCC1. Nat Cell Biol 11:36–45
Wu D, Pan W (2010) GSK3: a multifaceted kinase in Wnt signaling. Trends in biochemical sciences 35:161–168
Yanai I, Benjamin H, Shmoish M et al (2005) Genome-wide midrange transcription profiles reveal expression level relationships in human tissue specification. Bioinformatics 21:650–659
Yang XJ, Seto E (2008) Lysine acetylation: codified crosstalk with other posttranslational modifications. Mol Cell 31:449–461
Yu M, Schreek S, Cerni C et al (2005) PARP-10, a novel Myc-interacting protein with poly(ADP-ribose) polymerase activity, inhibits transformation. Oncogene 24:1982–1993
Yu M, Zhang C, Yang Y et al (2011) The interaction between the PARP10 protein and the NS1 protein of H5N1 AIV and its effect on virus replication. Virology journal 8:546

Regulation of Nucleocytoplasmic Transport by ADP-Ribosylation: The Emerging Role of Karyopherin-β1 Mono-ADP-Ribosylation by ARTD15

Maria Di Girolamo

Abstract Post-translational modifications of a cellular protein by mono- and poly-ADP-ribosylation involve the cleavage of NAD^+, with the release of its nicotinamide moiety. This is accompanied by the transfer of a single (mono-) or several (poly-) ADP-ribose molecules from NAD^+ to a specific amino-acid residue of the protein. Recent reports have shed new light on the correlation between NAD^+-dependent ADP-ribosylation reactions and the endoplasmic reticulum, in addition to the well-documented roles of these reactions in the nucleus and mitochondria. We have demonstrated that ARTD15/PARP16 is a novel mono-ADP-ribosyltransferase with a new intracellular location, as it is associated with the endoplasmic reticulum. The endoplasmic reticulum, which is a membranous network of interconnected tubules and cisternae, is responsible for specialised cellular functions, including protein folding and protein transport. Maintenance of specialised cellular functions requires the correct flow of information between separate organelles that is made possible through the nucleocytoplasmic trafficking of proteins. ARTD15 appears to have a role in nucleocytoplasmic shuttling, through karyopherin-β1 mono-ADP-ribosylation. This is in line with the emerging role of ADP-ribosylation in the regulation of intracellular trafficking of cellular proteins. Indeed, other ‚ADP-ribosyltransferases like ARTD1/PARP1, have been reported to regulate nucleocytoplasmic trafficking of crucial proteins, including p53 and NF-κB, and as a consequence, to modulate the subcellular localisation of these proteins under both physiological and pathological conditions.

Abbreviations

ART	ADP-ribosyltransferase
ARH	ADP-ribosylhydrolase
ARTC	Clostridia-toxin-like ART
ARTD	Diphtheria-toxin-like ART

M. Di Girolamo (✉)
G-Protein-Mediated Signalling Laboratory, Fondazione Mario Negri Sud,
Via Nazionale 8/A, 66030, S. Maria Imbaro (CH), Italy
e-mail: mdigirolamo@negrisud.it

Current Topics in Microbiology and Immunology (2015) 384: 189–209
DOI: 10.1007/82_2014_421

Published Online: 19 July 2014

CoaSt6	Collaborator of Stat6
ERAD	Endoplasmic-reticulum-associated degradation
GAP	Guanine-nucleotide activating proteins
GEF	Guanine-nucleotide exchange factors
GPI	Glycosylphosphatidylinositol
GSK	Glycogen synthase kinase
hnRNP	Heterogeneous nuclear ribonucleoprotein
Kapα	Karyopherin-α
Kapβ1	Karyopherin-β1
IL	Interleukin
IRE1	Inositol-requiring 1
NEMO	Nuclear factor (NF)-κB essential modulator
NES	Nuclear export signal
NLS	Nuclear localization signal
NPC	Nuclear pore complex
NTF2	Nuclear transport factor 2
PAR(P)	Poly-ADP-ribose (polymerase)
PARG	Poly-ADP-ribose glycohydrolase
PERK	Double-stranded RNA-dependent protein kinase (PKR)-like endoplasmic reticulum kinase
RanBP	Ran-binding protein
RCC1	Regulator of chromosome condensation 1
RRM	RNA recognition motif
Stat	Signal transducer and activator of transcription
UPR	Unfolded protein response

Contents

1 Introduction

In eukaryotic cells, specific specialised cellular functions occur in distinct sub-cellular organelles, such as the nucleus and the endoplasmic reticulum. Maintenance of cell homeostasis and the complex regulation of cellular functions, including gene expression and signal transduction, require the correct flow of information between separate organelles. This is made possible through the trafficking of molecules and proteins between the nucleus and the cytoplasm, a process that is known as nucleocytoplasmic transport (reviewed in (Conti and Izaurralde 2001; Fahrenkrog and Aebi 2003; Gorlich and Kutay 1999; Stewart 2007). Proteins that shuttle between the nuclear and cytoplasmic compartments are involved in diverse biological functions, including transport of RNA, cell-cycle control, and transcription (Macara 2001; Mattaj and Englmeier 1998; Michael 2000).

The nuclear envelope, which mediates the traffic into and out of the nucleus, is a distinct region of the endoplasmic reticulum that separates these two cellular compartments, both spatially and functionally. The nuclear envelope is constituted of two planar membranes that are separated by the perinuclear space, which is continuous with the lumen of the endoplasmic reticulum (Webster et al. 2009). Thus, the inner membrane of the nuclear envelope faces the nucleoplasm, while the outer membrane faces the cytoplasm. The inner and outer membranes of the nuclear envelope are connected at the nuclear pores, through which nucleocytoplasmic transport of RNA and proteins occurs. The transport of proteins, which is required to allow a protein to exert its effects in a specific sub-cellular compartment or organelle, is subject to multiple levels of regulation and is mediated by co-translational and post-translational protein modifications (Rapoport 2007; Schnell and Hebert 2003; Wickner and Schekman 2005).

Among these post-translational modifications, ADP-ribosylation,ADP-ribosylation is emerging as a regulator of the cellular transport system under physiological and pathological conditions. Post-translational modifications of proteins by mono- and poly-ADP-ribosylation consists of the transfer of a single (mono) or several (poly) ADP-ribose molecules from NAD^+ to a specific amino-acid residue of the target protein (Dani et al. 2013; Di Girolamo et al. 2005; Hassa and Hottiger 2008; Koch-Nolte et al. 2008). The role of the ADP-ribosyltransferase ARTD1/PARP1 in nucleocytoplasmic transport has been demonstrated by its poly-ADP-ribosylation of the tumour suppressor p53, which results in p53 accumulation in the nucleus (Kanai et al. 2007).

More recently, we demonstrated that ARTD15/PARP16 is localised at the endoplasmic reticulum and catalyses mono-ADP-ribosylation of a protein that has a key role in nucleocytoplasmic transport (Di Girolamo et al. 2014; Di Paola et al. 2012). This thus introduces a novel element into the regulatory mechanisms of nucleocytoplasmic shuttling.

2 Nucleocytoplasmic Transport

2.1 The Nuclear-Pore Complex

The nuclear pore comprises the nuclear-pore complex (NPC), which is a complex of ~30 different proteins that are known as nucleoporins. The first structure of the NPC was revealed by electron microscopy analysis in 1954 (Gall 1954). The three-dimensional architecture and protein composition of the NPC has been comprehensively described in yeast (Alber et al. 2007), and more recently, the organisation of the NPC has been described in *Xenopus* oocytes and rat (Loschberger et al. 2012) and human (Maimon et al. 2012) liver cells.

The details regarding the organisation of both the cytoplasmic and nucleoplasmic nucleoporin filaments have also been revealed recently (Aitchison and Rout 2012). These studies identified ~30 nucleoporins, with their classification into three different groups, passing from the outer to the inner side of the NPC: (i) the pore-membrane nucleoporins, which are transmembrane proteins that can anchor the NPC to the nuclear envelope; (ii) the structural nucleoporins, which are very stable and hold together all of the nucleoporins, as the pore-membrane nucleoporins and the phenylalanine-glycine (FG)-nucleoporins, thus contributing to the overall NPC structure; and (iii) the highly dynamic FG-nucleoporins, which are characterised by multiple FG motifs, such as GLFG (glycine-leucine-FG) and FXFG (phenylalanine-any-FG), which themselves interact with transport carriers during active translocation through the NPC (Stewart 2007). Indeed, these nucleoporins bind cargo proteins that are associated with specific carriers, which provide the translocation through the NPCs; in line with this concept, recent data have indicated that the different nucleoporins are not interchangeable. An important role in cargo transport is attributed to the nucleoporin fibres that extend from the central body of the cell into the cytoplasm, where they form eight long filaments, and also into the nucleus, where they form a basket-like structure, with the eight long filaments distally connected by a ring structure (Aitchison and Rout 2012).

2.2 Carriers and Cargo

While NPCs are freely permeable to small molecules, metabolites and ions, the transport of macromolecules greater than approximately 40 kDa in size is mediated by soluble nuclear transport carriers that cycle between the cytoplasm and the nucleus (reviewed in Refs. Fried and Kutay 2003; Pante and Kann 2002; Strambio-De-Castillia et al. 2010; Suntharalingam and Wente 2003; Terry et al. 2007). Most of these carriers belong to the karyopherin family of proteins. The karyopherins that are involved in the transport of proteins from the cytoplasm into the nucleus are called the importins, while those involved in the transport of proteins out of the

nucleus are called the exportins (Conti and Izaurralde 2001; Gorlich and Kutay 1999). The site of interaction with the karyopherins on the cargo protein has been identified only in a limited number of cases; it is generally accepted that the cargo proteins are characterised by the presence of a short amino-acid sequence that represents a transport signal: the nuclear localisation sequence (NLS) is recognised for nuclear import of proteins, while the nuclear export sequence (NES) is the signal for nuclear export. The NLSs were first identified in the SV40 large T antigen and the *Xenopus* protein nucleoplasmin, and these consist of either a single stretch of basic amino acids (P*KKKRK*V) or of two short stretches of basic amino acids separated by a linker of 10–12 unconserved amino acids (*KR*PAATKKA-GQA*KKKK*LDK) (Kalderon et al. 1984; Lanford and Butel 1984; Robbins et al. 1991). Other signals that can mediate nuclear import include the M9 sequence from heterogeneous nuclear ribonucleoprotein (hnRNP) A1 protein (hnRNP A1), and the KNS sequence from the hnRNP K protein. Both the M9 and KNS sequences function as NLS and NES and confer bi-directional transport across the nuclear envelope (Michael et al. 1997; Siomi and Dreyfuss 1995). The leucine-rich NESs were first identified in HIV1 Rev (Fischer et al. 1995) and cAMP-dependent protein kinase inhibitor (Wen et al., 1995), and these have a consensus sequence motif of Φ-X_{2-3}-Φ-X_{2-3}-Φ-X-Φ (Φ = L, I, V, F, M; X = any amino acid; (Kutay and Guttinger 2005; la Cour et al. 2004)). Both NLSs and NESs are specifically recognised by the karyopherins (Friedrich et al. 2006). The karyopherin–cargo complex docks to the NPC by binding to the nucleoporins, and it then translocates through the NPC, thus reaching its final destination. This will be either the nucleoplasm or the cytoplasm, where its cargo is released. In the regulation of karyopherin-mediated transport, the small GTPase Ran and its guanine-nucleotide state have a fundamental role, as well as regulators of the guanine-nucleotide state of Ran, which include the guanine-nucleotide exchange factors (GEFs), which catalyse the formation of Ran-GTP, and the GTPase-activating proteins (GAPs), which catalyse the hydrolysis of Ran-GTP to Ran-GDP. The nucleocytoplasmic shuttle of cellular proteins is controlled by the asymmetric distribution of Ran, which is controlled, in turn, by cellular segregation of specific Ran-GEFs and Ran-GAPs. Indeed, Ran-GTP in the nucleus is at a higher concentration than in the cytoplasm; conversely, Ran-GDP in the cytoplasm is at a higher concentration than in the nucleus. This thus establishes opposite gradients for Ran-GTP and Ran-GDP. These gradients are due to the nuclear localisation of Ran-GEF named regulator of chromosome condensation 1 (RCC1), which is strictly associated with chromatin (Bischoff and Ponstingl 1991), and to the cytoplasmic localisation of Ran-binding protein (RanBP) and Ran GTPase activating-protein 1 (Ran-GAP1), which catalyse Ran-GTP hydrolysis to its GDP-bound form (Bischoff et al. 1994).

2.3 The Role of Karyoperin-β1 in Nucleocytoplasmic Transport, and Beyond

Karyopherin-β1 (Kapβ1) is an importin (also known as importin-β or p97) and is a member of the karyopherin-β superfamily. There are 19 known human karyopherins-β, the molecular weights of which range from 90 to 150 kDa; these karyopherins have low sequence identity and they are all characterised by helical HEAT repeats. Different domains have been identified in the Kapβ1 protein: a carboxyterminal region that contains an importin-binding domain; a central region that contains binding sites for FG-nucleoporins; and an aminoterminal domain that binds Ran-GTP and that partially overlaps with the nucleoporin-binding region (Ben-Efraim and Gerace 2001).

In the classical shuttling of proteins with a NLS through the NPC, Kapβ1 uses karyopherin-α (Kapα) as an adaptor to recognize and bind cargo; specifically, Kapβs binds directly to Kapα through its importin-binding domain; Kapα in turn binds to the NLS of target proteins, leading to the formation of a tri-molecular complex (Goldfarb et al. 2004). This complex tethers to, and passes through, the NPC through the binding of Kapβ1 to the nucleoporins (Fig. 1). Once in the nucleoplasm, Ran-GTP binds to the amino-terminus of Kapβ1, which results in release of the cargo. This cargo is thus ready to function in the nucleoplasm, while Kapβ1 and Kapα are exported back to the cytosol, to re-initiate a new import cycle, through separate Ran-GTP–dependent events (for reviews, see Hetzer et al. 2002; Quimby and Dasso 2003; Weis 2003): Ran-GTP interacts directly with Kapβ1 and indirectly, via exportin-2, with Kapα (Fig. 1).

In the cytosol, Ran-GTP is released from the importins, and its rebinding is prevented by Ran-GAP–mediated hydrolysis of the phosphate bond which generates Ran-GDP, which does not bind to the importins. The classical export of proteins from the nucleus begins with CRM1 (also known as exportin-1), which can only bind cargo proteins that contain NESs in the presence of Ran-GTP (Ciciarello et al. 2007; Clarke and Zhang 2008; Kalab and Heald 2008). Once these proteins are complexed together, translocation to the cytoplasm can take place, where Ran-GAP and RanBP1 generate Ran-GDP, and results in the dissociation of CRM1 from its cargo. Finally, Ran-GDP is shuttled back to the nucleus via the cytosolic protein nuclear transport factor 2 (NTF2) (Moore and Blobel 1994a, b; Paschal and Gerace 1995). NTF2 binds directly to Ran-GDP, which can then interact more efficiently with the NPC, allowing the complex to translocate into the nucleus (Ribbeck et al. 1998). In the nucleus, Ran-GDP dissociates from NTF2, which is believed to be due to the high concentration of GTP there, for which NTF2 has low affinity (Paschal et al. 1996; Ribbeck et al. 1998), and to the activity of RCC1 (Bischoff and Ponstingl 1991). Therefore, the asymmetric distribution of the Ran effectors, and consequently of the GTP-bound and GDP-bound Ran, provides the directionality to this nucleocytoplasmic transport (reviewed by Kalab and Heald 2008; Poon and Jans 2005; Rensen et al. 2008).

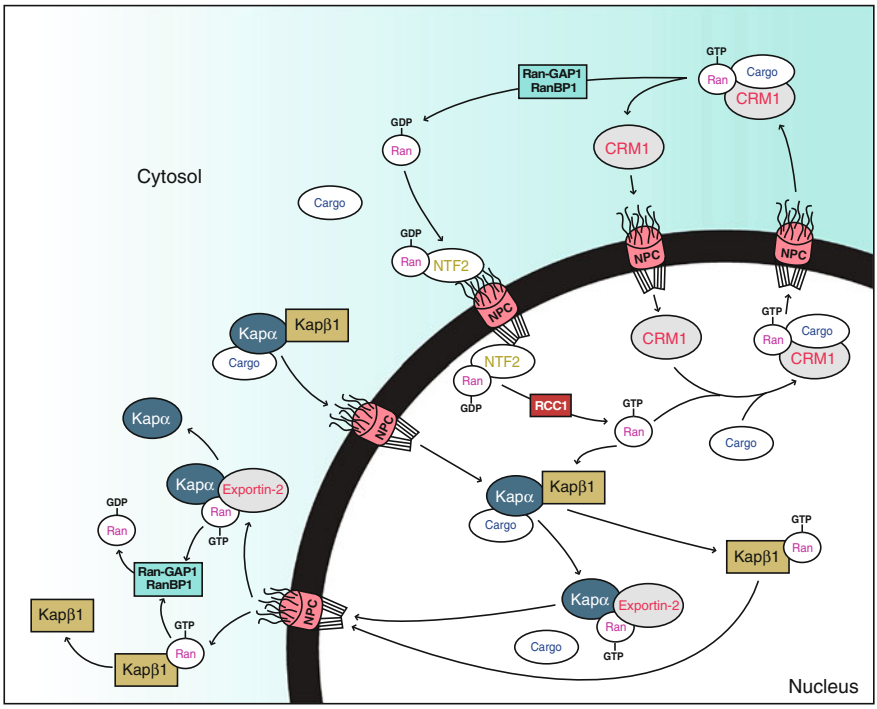

Fig. 1 Schematic representation of the karyopherin-mediated nucleocytoplasmic shuttling of proteins. The karyopherin–cargo complex translocates through the NPC, thus reaching either the nucleus or the cytosol, where its cargo is released. RCC1 forms Ran-GTP in the nucleus, while RanBP1 and Ran-GAP1 generate Ran-GDP in the cytoplasm, thus establishing the Ran gradient. The import of cargo with a NLS through the NPC is mediated by Kapβ1, which binds to Kapα, which in turn binds to the cargo, leading to the formation of a tri-molecular complex that enters the nucleus (see text for details). In the nucleus, Ran-GTP interacts directly with Kapβ1, and via exportin-2 with Kapα, which are exported into the cytosol, to re-initiate a new import cycle. The export of a cargo with a NES through the NPC is mediated by CRM1, which binds cargo in the presence of Ran-GTP. In the cytosol Ran-GAP and RanBP1 generate Ran-GDP, resulting in the dissociation of CRM1 from its cargo. Finally, Ran-GDP is shuttled back into the nucleus via NTF2 (see text for details)

Although Kapβ1 commonly uses Kapαs as adaptors to recognize and bind cargo, Kapβ1 can bind to cargo directly. Moreover, the physiological relevance of Kapβ1 has been strengthened, as in addition to its crucial role in nuclear import, Kapβ1 is also involved in mitosis (Ciciarello et al. 2007; Clarke and Zhang 2008; Kalab and Heald 2008).

In human cells, Kapβ1 interacts with mitotic microtubules and accumulates at spindle poles (Ciciarello et al. 2004), where a Ran-GTP fraction also co-localises (Tedeschi et al. 2007). Ciciariello and colleagues (Ciciarello et al. 2004) showed that moderate overexpression of Kapβ1 induces multipolar spindle formation by inhibiting NLS-containing mitotic factors; then Ran-GTP binding to Kapβ1 releases

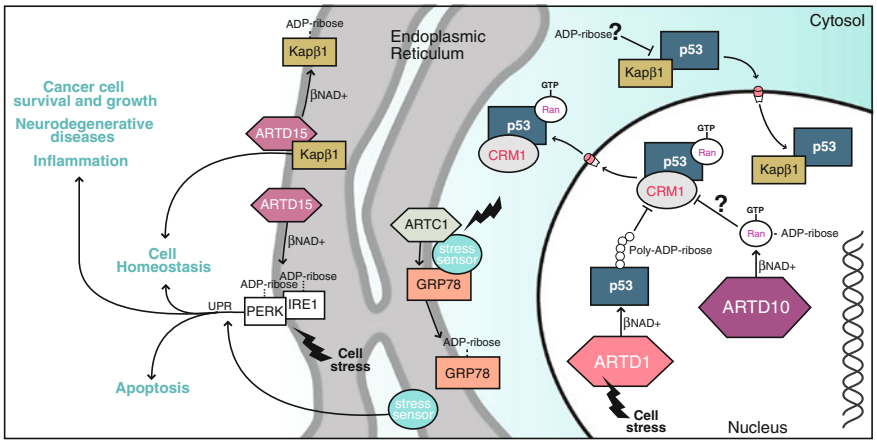

Fig. 2 The role of the ADP-ribosylating enzymes in nucleocytoplasmic transport. The nuclear import of P53 through the NPC is mediated by Kapβ1, with the nuclear export of p53 carried out by CRM1. The nuclear sequestration of p53 as a consequence of ARTD1-mediated poly-ADP-ribosylation is shown. Moreover, the possible role of ARTD10 and of ARTD15 in nucleocytoplasmic shuttling is also shown. ARTD15-dependent ADP-ribosylation of additional targets and the possible functional meaning of these reactions in response to different cellular stress are also shown (see text for details)

these factors, thus restoring spindle pole integrity. Of note, Kapβ1 also contributes to the regulation of Ran-GAP1 localisation at kinetochores. Specifically, Kapβ1 negatively regulates kinetochore-driven microtubule nucleation by inhibiting factors such as the major Ran-dependent spindle organiser, TPX2 (Tulu et al. 2006). The importin-binding carboxyterminal region of Kapβ1 can inhibit mitotic spindle pole formation, while the nucleoporin-binding site domain can regulate dynamic microtubule functions and interactions with kinetochores.

3 The ADP-Ribosylation Cycle

Transport of proteins is required to allow proteins to carry out their functions in their specific sub-cellular compartment or organelle, and this process is subject to multiple levels of regulation that rely on information encoded within protein sequences and that occur through co-translational and post-translational modifications. Among the post-translational modifications that have been reported to affect protein trafficking under physiological and pathological conditions, such as phosphorylation, ubiquitination and methylation, ADP-ribosyaltion also has an emerging role (Fig. 2).

3.1 ADP-Ribosylating Enzymes

ADP-ribosylation is a post-translational modification that is catalysed by enzymes found in organisms ranging from prokaryotes to mammals, and that promotes the transfer of one (mono) or several (poly) units of ADP-ribose from NAD^+ to a specific amino acid of a target protein, thus profoundly altering its functional properties (Corda and Di Girolamo 2003; Di Girolamo et al. 2005; Hassa and Hottiger 2008; Seman et al. 2004).

In mammals, endogenous ADP-ribosylation occurs through two main families of ARTs: the ARTCs (clostridia-toxin-like ARTs) and the ARTDs (diphtheria-toxin-like ARTs) (Hottiger et al. 2010).

The founding, and most extensively studied, member of the ARTD family is PARP1, which is also known as ARTD1. ARTD1/PARP1 and other five members of the ARTD family (ARTD2-6) are typical poly-ADP-ribosylpolymerases that can synthesise linear or branched polymers of ADP-ribose (poly-ADP-ribose) molecules linked together via an *O*-glycosidic ribose–ribose bond and are transferred onto various protein targets, mainly in the nucleus (D'Amours et al. 1999; Schreiber et al. 2006). In addition to the covalent binding of the poly-ADP-ribose polymer to cellular proteins, a non-covalent interaction with poly-ADP-ribose has been reported (Malanga and Althaus 2011), which leads to the consideration of poly-ADP-ribose as a signalling molecule that has roles in different cellular responses, including intracellular trafficking.

ARTD1/PARP1 and ARTD2/PARP2 can be directly activated by DNA damage, with the consequent synthesis of poly-ADP-ribose, which in turn recruits the proteins involved in DNA repair, and also those involved in chromatin remodelling and transcriptional regulation. The role of ARTD1/PARP1 in cellular responses to genotoxic and oxidative stress has thus been widely recognised and studied, with some PARP inhibitors under evaluation in clinical trials as anti-cancer therapeutics (Curtin 2012; Miwa and Masutani 2007; Peralta-Leal et al. 2009). A crucial role for ARTD1 in nucleocytoplasmic transport is also emerging, and this depends on its poly-ADP-ribosylation of the tumour suppressor p53, which thus inhibits the p53 interaction with the exportin CRM1, which in turn, results in the accumulation of p53 in the nucleus (see below).

In human, 17 members of the ARTD family have been identified, as characterised by a conserved ART domain, and these are classified as poly-ADP-ribose synthesising, mono-ADP-ribose synthesising, or enzymatically inactive, on the basis of the presence of an intact or modified histidine–tyrosine–glutamate (H-Y-E) triad within this PARP domain. While ARTD1-6 are typical poly-ADP-ribosylpolymerases, the other members have lost the conserved glutamate residue of the H-Y-E triad, which is crucial for polymer elongation, and so they are either inactive or only active as mono-ARTs (Ame et al. 2004; Otto et al. 2005).

The mono-ADP-ribosylation reaction consists of the transfer of a single ADP-ribose moiety to a specific amino-acid residue of various cellular proteins. This reaction is catalysed by members of both the ARTC and ARTD families. The ARTC

family of ecto-ARTs includes four human subtypes (ARTC1, 3, 4, 5) that are either glycosylphosphatidylinositol (GPI)-anchored or are secreted enzymes. ARTC1 has been reported to inhibit T-lymphocyte functions, including their cytolytic activity and proliferation, by ADP-ribosylating arginines of cell surface proteins, like the T-cell co-receptors (Koch-Nolte et al. 2006, 2008).

In addition to the active ARTC family members, some ARTDs have been reported to act as cellular mono-ARTs, including ARTD8/PARP14, ARTD10/PARP10 and ARTD15/PARP16. ARTD10 was the first ARTD to be characterised as a mono-ART; it was isolated as a partner of the oncoprotein c-Myc, and an inhibitor of cell proliferation (Yu et al. 2005). ARTD10 appears to also have a role in the Wnt/β-catenin signalling pathway, as it has been reported to catalyse mono-ADP-ribosylation of glycogen synthase kinase 3 (GSK3), and thus to reduce the GSK3 kinase activity (Feijs et al. 2013). GSK3 is known to phosphorylate β-catenin, and thus to induce proteasomal degradation of β-catenin (Wu and Pan 2010). Interestingly, nuclear factor (NF)-κB essential modulator (NEMO) can also be mono-ADP-ribosylated by ARTD10, thus inhibiting the NF-κB signalling pathway (Verheugd et al. 2013).

Mono-ART activities have also been demonstrated for ARTD8/PARP14 and ARTD15/PARP16. ARTD8, which was identified as a 'signal transducer and activator of transcription' (Stat)6-interacting protein, is also known as collaborator of Stat6 (CoaSt6) and it is associated with aggressiveness of B-cell lymphomas of the diffuse large B-cell lymphoma family (Cho et al. 2011). ARTD8 catalyses ADP-ribosylation of p100 (Goenka et al. 2007), a protein that interacts with RNA polymerase II, and functions as a bridging factor between Stat6 and the transcription machinery (Yang et al. 2002) and of the HDAC2 and HDAC3 histones deacetylases. In the presence of IL4, the ART activity of ARTD8 is activated, and HDAC2 and HDAC3 are ADP-ribosylated and released from their promoters, thus inducing efficient binding of Stat6 and the consequent transcription [84]. Thus, ARTD8 regulates interleukin (IL)4- and Stat6-dependent transcription, which induces IL4-responsive genes (Goenka et al. 2007). More recently, we demonstrated that ARTD15 is also a mono-ART that is localised at the endoplasmic reticulum and that catalyses ADP-ribosylation of Kapβ1 (Di Paola et al. 2012). There are six additional ARTD proteins for which mono-ART activity has been detected; however, their biological roles have not yet been defined, as nothing is known about ARTD7, ARTD11 and ARTD16, and limited studies are available for ARTD17, ARTD14 and ARTD12.

3.2 Deribosylating Enzymes

Both mono- and poly-ADP-ribosylation are reversible reactions. The hydrolysis of mono-ADP-ribose of arginine residues is catalysed by ADP-ribosylarginine hydrolase, ARH1. The hydrolysis of poly-ADP-ribose chains is catalysed by poly-ADP-ribose glycohydrolase (PARG) and by the structurally unrelated

glycohydrolase ARH3. PARG and ARH3 do not, however, cleave the terminal ADP-ribose off the poly-ADP-ribose chains, which is directly linked to the protein (Slade et al. 2011).

More recently, the enzymatic activity responsible for this reaction has been shown to be a function of certain macro-domain-containing proteins, including MACROD1, MACROD2 and TARG1 (Rosenthal et al. 2013). These domains can reverse the mono-ADP-ribosylation that occurs on Glu and Lys, and thus they can reverse the mono-ADP-ribosylation that is catalysed by the ARTD enzymes, but not the arginine-specific mono-ADP-ribosylation catalysed by the ARTC enzymes, which is instead reversed by ARH1.

4 The Role of the ADP-Ribosylating Enzymes in Nucleocytoplasmic Transport

In recent years, a role for ADP-ribosylating enzymes in nucleocytoplasmic transport of cargo proteins has been revealed. While there are well defined examples to indicate that, through its catalysis of poly-ADP-ribosylation of specific targets, ARTD1 can regulate their nucleocytoplasmic trafficking, the role of mono-ADP-ribosylation in this process is only now emerging. This include the identification of an ARTD that contains a NES, which is ARTD10, and another ARTD that has been demonstrated to interact with and modify Kapβ1, a carrier that is crucial for protein import into the nucleus.

4.1 ARTD1 in Nucleocytoplasmic Transport

For ARTD1, a role in nucleocytoplasmic transport has been established. The roles of poly-ADP-ribosylation catalysed by ARTD1 in the maintenance of DNA integrity, in gene transcription, and in physiological processes that include cell division, survival and death, have been studied for 40 years now. However, in recent years, a role for this post-translational modification in nucleocytoplasmic transport of cargo proteins has also been revealed, which in at least two cases results in their nuclear accumulation.

One of these cargo proteins that has its localisation regulated by ARTD1-mediated ADP-ribosylation is p53, which is a crucial tumour suppressor and a regulator of the cell cycle. P53 is known to suppress cancer through its double role as an inducer of cell-cycle arrest and of apoptosis programmes in response to different cellular stress. Indeed, p53 can activate DNA damage repair mechanisms following DNA damage, initiate apoptosis when the DNA damage cannot be repaired, and hold the cell at the G1/S cell-cycle checkpoint if DNA damage is recognized (Brady and Attardi 2010). Thus, p53 is involved in the same pathway as ARTD1.

P53 normally shuttles between the nucleus and the cytoplasm in a cell-cycle-dependent manner (David-Pfeuty et al. 1996; Komarova et al. 1997; Shaulsky et al. 1990).

Following its synthesis, p53 can translocate from the cytosol through the nuclear pores and into the nucleus through the association of the importin complex with the NLS of p53. The nuclear export of p53 is then carried out by CRM1 (Stommel et al. 1999). This regulation of p53 nuclear localisation is thus controlled by the NLS and NES transport signals and by its post-translational modification (Vandromme et al. 1996), which includes phosphorylation and, importantly, ADP-ribosylation. It is known that in response to cellular stress, p53 is retained in the nucleus via a 'NES-masking' mechanism: p53 forms homotetramers, which 'hides' its NES and thus prevents its interaction with the exportin CRM1 (Stommel et al. 1999).

Of note, the p53 interaction with the exportin CRM1 can also be blocked as a consequence of ARTD1-mediated poly-ADP-ribosylation, which has been reported to occur on residues E255, D256 and E268 of p53 (Kanai et al. 2007). Upon various stress conditions that induce DNA damage, and consequently ARTD1 activation, p53 is poly-ADP-ribosylated, which prevents it from interacting with the nuclear export receptor CRM1 (Kanai et al. 2007) inhibiting its nuclear export. This modification, therefore, provides a means by which p53 levels can accumulate in the nucleus following stress.

Another cargo that has its localisation regulated by ARTD1 activation is NF-κB. The NF-κBs are a family of dimeric transcription factors that are formed by combinations of members of the Rel protein family, among which one of the most studied is the p65–p50 dimer. All of the NF-κBs are characterised by the presence of a Rel homology domain, which is responsible for the formation of dimers and is important for DNA binding. NF-κB can be activated by a variety of stimuli, which include inflammatory cytokines and other proinflammatory products, like bacterial or viral products, and oxidative or genotoxic stress (Hadian and Krappmann 2011; Miyamoto 2011; Oeckinghaus and Ghosh 2009). In the absence of stimuli, the DNA binding of the NF-κB dimers is prevented by their association with members of the IκB family (Baltimore 2011; Oeckinghaus and Ghosh 2009), which thus retain the complex in the cytosol. Upon cell stimulation, the activation of the IKK kinases (a family of kinases that includes NEMO, which is also referred to as IKK) leads to degradation of the NF-κB inhibitor, IκB, and to the consequent NF-κB activation. P65 NF-κB has a NLS that is masked by IκB binding to the p65–p50 dimer, thereby resulting in the cytoplasmic localisation of the NF-κB–IκB complex. When the IKK kinases are activated, the free NF-κB dimers are translocated into the nucleus, where they can then initiate transcription (Baltimore 2011; Oeckinghaus and Ghosh 2009).

Post-translational modifications can regulate NF-κB activation, which include mainly phosphorylation and ubiquitylation. ARTD1-mediated poly-ADP-ribosylation of p65 has also been reported (Kameoka et al. 2000), and more recently it was shown that p65 NF-κB poly-ADP-ribosylation decreases its interaction with CRM1 in vitro, which suggests that p65 NF-κB ADP-ribosylation might be a

critical determinant for its nuclear retention under certain stimulation conditions (Zerfaoui et al. 2010). Both p53 and NF-κB are heavily involved in normal physiology and human disease, and p53 mislocalisation is involved in a large number of neoplasms, thus highlighting the importance of the correct cellular localisation of this cargo for the correct functioning of cells.

4.2 ARTD10 in Nucleocytoplasmic Transport

It is intriguing that the NF-κB regulatory subunit NEMO is ADP-ribosylated by another member of the ARTD family, the mono-ART, ARTD10. In addition to the PARP domain, the ARTD10 structure is characterised by other domains (Yu et al. 2005): an RNA recognition motif (RRM), a glycine-rich domain, and a glutamic acid (Glu)-rich region. The Glu-rich region contains two ubiquitin interaction motifs and, importantly, a leucine-rich NES sequence (amino-acids 598–607). ARTD10 is predominantly cytosolic under basal conditions, and it can shuttle between the cytoplasmic and nuclear compartments. When its NES sequence was mutated, by replacing three leucine residues with alanines, the exit of ARTD10 from the nucleus was inhibited.

The nuclear export of ARTD10 requires CRM1, as ARTD10 accumulation in the nucleus is observed as a consequence of treatment with leptomycin B (a CRM1 inhibitor that specifically inhibits nuclear export; (Kudo et al. 1998)). Whether auto- or hetero-modifications of ARTD10 regulate its interaction with CRM1 remains to be investigated, similar to ADP-ribosylated p53 and NF-κB, which cannot then interact with CRM1 and, as a consequence, cannot be exported to the cytosol. However, ARTD10 appears not to have a NLS, and thus it is not clear what mediates its nuclear import. In this respect, the ubiquitin-interaction-motif sequences of ARTD10 might be involved. Indeed, although ubiquitination generally modulates protein function by inducing proteasome-dependent degradation, it can also regulate nucleocytoplasmic trafficking by directly promoting the nuclear import and export of modified substrates (Polo et al. 2003; Shcherbik and Haines, 2004).

The presence of a NES and of an RRM within ARTD10 leads to the speculation that it also has a role in nucleocytoplasmic transport of RNA cargo. It has been reported that export to the cytoplasm of two classes of RNA, mRNA and ribosomal subunits, might not be mediated by any member of the RNA transporters (reviewed by Nakielny and Dreyfuss 1999). mRNA export factors include the hnRNP shuttling proteins, which introduces the concept that RNA-binding proteins hold the key to mRNA export. The RRM of ARTD10 is highly homologous to the RRM of the mRNA nuclear exporter hnRNP A1; however, it remains to be experimentally defined whether ARTD10 is invoved in the nuclear export of RNA.

In addition, Yu and colleagues (Yu et al. 2005) have also proposed a role for ARTD10 together with c-Myc in rRNA processing and transport, based on the previously reported role of c-Myc in the control of rRNA gene transcription

(Poortinga et al. 2004). Despite these indications, it remains to be established whether ARTD10 is involved in the regulation of nucleocytoplasmic transport of RNAs and whether this transport occurs through its RNA-recognition motif.

4.3 Mono-ADP-Ribosylation of Karyopherin-β1 by ARTD15, a New Player in Nucleocytoplasmic Transport

We provided the first demonstration that ARTD15/PARP16 is a novel ART with a new intracellular localisation (Di Paola et al. 2012). ARTD15 is the only known ARTD family member with a putative carboxyterminal transmembrane domain, and we showed that ARTD15 associates with the membranes of the nuclear envelope and of the endoplasmic reticulum, using immunofluorescence and electron microscopy (Di Paola et al. 2012). Thus ARTD15 is a ubiquitous protein and the first ART known to be associated with the endoplasmic reticulum. Moreover, we analysed the orientation of ARTD15 according to a trypsin-protease-protection assay, and this revealed that ARTD15 is a single-pass transmembrane protein with its aminoterminal region (amino-acids 1–280) positioned towards the cytoplasm, and its very short carboxyterminal tail (amino-acids 300–322) facing the lumen of the endoplasmic reticulum.

ARTD15 catalyses both auto- and hetero-modifications by the transfer of a single ADP-ribose moiety onto itself or onto Kapβ1, which we also identified as a molecular partner of ARTD15 (Di Paola et al. 2012). Here, the hetero-modification is largely the preferred reaction. In summary, we showed that the endoplasmic-reticulum-resident ARTD15 catalyses the mono-ADP-ribosylation of Kapβ1. Although the precise Kapβ1 modification site remains to be identified, we showed that this mono-ADP-ribosylation of Kapβ1 is inhibited by PJ34, a well-characterised inhibitor of ARTD1 (Yates et al. 2005), and that it is not reversed by ARH1, which hydrolyses the ADP-ribose–arginine bond, or by ARH3, which catalyses the hydrolysis of poly-ADP-ribose and *O*-acetyl-ADP-ribose. PJ34 has been described to act on the NAD^+-binding pocket of ARTD1, and thus it can also affect other ARTDs that have a similar NAD^+-binding pocket structure, independent of whether the reaction being catalysed is mono- or poly-ADP-ribosylation. The identification of the specific Kapβ1 residue or the domain of Kapβ1 that is modified by ARTD15 might be instrumental in the definition of the functional meaning of this ARTD15–Kapβ1 interaction.

In this respect, ARTD15 appears to be the only ARTD family member with a carboxyterminal transmembrane domain and an aminoterminal cytosolic catalytic domain, an orientation that is shared with other known tail-anchored proteins (Kalbfleisch et al. 2007). Several important protein families are tail-anchored proteins, including the SNAREs, which mediate vesicle tethering during intracellular transport, and the apoptotic regulator Bcl-2. The role of the tail anchor varies from protein to protein. In the case of the SNAREs, for example, it is crucial for membrane fusion, while for the Bcl-2 family, the tail anchor targets these

proteins to the mitochondrial outer membrane for the control of the release of apoptotic factors from the inter-membrane space (Borgese and Fasana 2011). The role of the ARTD15 tail anchor remains to be elucidated, as well as its role in Kapβ1 function.

In our studies, immunofluorescence analysis revealed that Kapβ1 co-localises with ARTD15 at the endoplasmic reticulum and the nuclear envelope, and we have suggested that ARTD15 is a new player in the control of nuclear transport, together with the karyopherins (Di Paola et al. 2012). Two mechanisms have been described to date for the control of the karyopherins: attenuation of protein expression, and protein sequestration. Mono-ADP-ribosylation of Kapβ1 by ARTD15 might be a further level of control of Kapβ1-mediated nuclear transport. In a similar way to the previously reported poly-ADP-ribosylation of cargo proteins, mono-ADP-ribosylation of Kapβ1 can inhibit its carrier function, thus affecting the nuclear import of those proteins that require Kapβ1 to translocate across the nuclear pore complex (Fig. 2).

5 Mislocalisation of Proteins in Human Disease

Subcellular localisation is essential for correct protein function, as it determines the access of proteins to their interacting partners. Aberrantly localised proteins have been linked to a variety of human diseases, such as Alzheimer's disease, and various types of cancers. Mislocalisation of G-protein-coupled receptors has been linked to retinitis pigmentosa when it involves rhodopsin (Hollingsworth and Gross, 2012), and to nephrogenic diabetes insipidus when it involves vasopressin receptor (Tsukaguchi et al. 1995). Also, familial hypercholesterolaemia appears to be due to defects in the trafficking or localisation of the LDL receptor (Hobbs et al. 1990), and cystic fibrosis has been linked to mislocalisation of the CTFR protein (Welsh and Smith 1993). Mislocalisation of the cell-cycle inhibitor p21WAF-1 to the cytoplasm leads to tumour progression (Keeshan et al. 2003). Similarly, mislocalisation of p53 suppresses its activity as it cannot localise to the nucleus (Fabbro and Henderson 2003). Thus, while mutations in p53 have been documented in over half of all human tumours, the malfunction of wild-type p53 due to cytoplasmic mislocalisation has been described in various solid tumours, including breast and hepatocellular carcinomas, glioblastomas, and others (Fabbro and Henderson 2003). Cytoplasmic sequestration of wild-type p53 has been reported in the vast majority (96 %) of undifferentiated neuroblastomas (Moll et al. 1995), and more recently, also in a patient with therapy-related resistant acute myeloid leukemia (Prokocimer and Peller 2012). Thus, p53 cytoplasmic sequestration represents a general mechanism for its inactivation that is found also in tumours that were previously not believed to be affected by p53 alterations (Moll et al. 1995).

In addition, it has been shown that in breast cancer cells, the reduced nuclear accumulation of p53 is not a consequence of its increased nuclear export; instead, the association of p53 with Kapβ1, which is essential for p53 nuclear import, was

significantly impaired (Poon and Jans 2005). Thus, this impaired association with importin might represent a novel mechanism for the cytoplasmic sequestration of p53 that affects its nuclear transport, thus rendering cells functionally deficient in p53. It is therefore intuitive that the re-localisation of mislocalised components to their optimal subcellular sites might contribute to the development of novel cancer therapies. For instance, the optimal location of the tumour suppressor p53 for promoting cell arrest and apoptosis appears to be the nucleus, while nuclear NF-κB would be better localised to the cytoplasm. Thus, the mechanisms of nuclear translocation of endogenous signalling components like p53 and NF-κB might serve as targets for pharmacological intervention.

6 ADP-Ribosylating Enzymes as Drug Targets

The use of post-translational modifications to regulate protein transport might represent additional targets for pharmacological intervention. ADP-ribosylated p53 and NF-κB cannot interact with CRM1, and as a consequence, they cannot be exported from the nucleus to the cytosol. This post-translational modification machinery thus enables the integration of proteins into functional biological networks. It remains to be established whether mono-ADP-ribosylation in the cytosolic compartment can also affect protein localisation, as appears to be the case for Kapβ1.

Drug discovery approaches that target mono-ARTs thus show promise of highly favourable responses. Indeed, the role of this modification has already been linked to human disease, such as inflammation, diabetes, neurodegeneration, and cancer. Consideration of ARTD15 as a drug target has the potential to aid in the development of therapies that can target cancers and inflammation.

Through Kapβ1 mono-ADP-ribosylation, ARTD15 appears to represent a novel element in the regulatory mechanism of nucleocytoplasmic shuttling, and thus to have the potential to be viewed as a target in cancers that are characterised by protein mislocalisation, and also in cancers and other inflammatory diseases where the unfolded protein response (UPR) has a role. Indeed, ARTD15 might have a role in the UPR through its ADP-ribosylation of two components of the UPR: double-stranded RNA-dependent protein kinase (PKR)-like endoplasmic reticulum kinase (PERK), and inositol-requiring 1 (IRE1) (Jwa and Chang 2012). The release of ADP-ribosylated PERK and IRE1 from GRP78/BiP results in the activation of the kinase activity of PERK and both the kinase and nuclease activities of IRE1 (Jwa and Chang 2012). Thus ARTD15 can activate these endoplasmic-reticulum stress sensors during the UPR.

Of note, ARTD15 might have an additional role in the UPR through its ability to ADP-ribosylate Kapβ1. Indeed, Kapβ1 has been implicated in the regulation of the endoplasmic-reticulum quality control, as it promotes endoplasmic-reticulum-associated degradation (ERAD) (Zhong et al. 2011); thus, supporting the hypothesis that Kapβ1 has a functional role at the endoplasmic reticulum.

Future studies will address the role of ARTD15 and its ability to ADP-ribosylate proteins involved in the control of endoplasmic-reticulum homeostasis, and in cancers. In this respect, both the site of ADP-ribosylation on Kapβ1 and the ARTD15 catalytic site can be viewed as part of an innovative therapeutic strategy. While in general the development of new inhibitors specific for these novel ARTD family members should lead to the discovery of novel compounds with anticancer activities, compounds developed based on ARTD15 can be used to provide new insight into the mechanisms of nucleocytoplasmic shuttling, the UPR and cancer-regulatory pathways.

Acknowledgment This paper is dedicated to my husband, Tommaso, and to my children Marta and Valerio, who have suffered the consequences of my passion for research. I am grateful also to the many wonderful colleagues whom I have met during my life in science, here in Italy and abroad, as each of them has helped me to learn something new.

Conflict of interest: The author declare that there are no conflicts of interest.

References

Aitchison JD, Rout MP (2012) The yeast nuclear pore complex and transport through it. Genetics 190:855–883

Alber F, Dokudovskaya S, Veenhoff LM et al (2007) The molecular architecture of the nuclear pore complex. Nature 450:695–701

Ame JC, Spenlehauer C, de Murcia G (2004) The PARP superfamily. Bioessays 26:882–893

Baltimore D (2011) NF-kappaB is 25. Nat Immunol 12:683–685

Ben-Efraim I, Gerace L (2001) Gradient of increasing affinity of importin & #x03B2; for nucleoporins along the pathway of nuclear import. J Cell Biol 152:411–417

Bischoff FR, Klebe C, Kretschmer J, Wittinghofer A, Ponstingl H (1994) RanGAP1 induces GTPase activity of nuclear Ras-related Ran. Proc Natl Acad Sci USA 91:2587–2591

Bischoff FR, Ponstingl H (1991) Catalysis of guanine nucleotide exchange on Ran by the mitotic regulator RCC1. Nature 354:80–82

Borgese N, Fasana E (2011) Targeting pathways of C-tail-anchored proteins. Biochim Biophys Acta 1808:937–946

Brady CA, Attardi LD (2010) p53 at a glance. J Cell Sci 123:2527–2532

Cho SH, Ahn AK, Bhargava P et al (2011) Glycolytic rate and lymphomagenesis depend on PARP14, an ADP ribosyltransferase of the B aggressive lymphoma (BAL) family. Proc Natl Acad Sci USA 108:15972–15977

Ciciarello M, Mangiacasale R, Lavia P (2007) Spatial control of mitosis by the GTPase Ran. Cell Mol Life Sci 64:1891–1914

Ciciarello M, Mangiacasale R, Thibier C et al (2004) Importin & #x03B2; is transported to spindle poles during mitosis and regulates Ran-dependent spindle assembly factors in mammalian cells. J Cell Sci 117:6511–6522

Clarke PR, Zhang C (2008) Spatial and temporal coordination of mitosis by Ran GTPase. Nat Rev Mol Cell Biol 9:464–477

Conti E, Izaurralde E (2001) Nucleocytoplasmic transport enters the atomic age. Curr Opin Cell Biol 13:310–319

Corda D, Di Girolamo M (2003) Functional aspects of protein mono-ADP-ribosylation. EMBO J 22:1953–1958

Curtin NJ (2012) Poly(ADP-ribose) polymerase (PARP) and PARP inhibitors. In: Drug discovery today: disease models (Elsevier B.V.), pp e51–e58
D'Amours D, Desnoyers S, D'Silva I, Poirier GG (1999) Poly(ADP-ribosyl)ation reactions in the regulation of nuclear functions. Biochem J 342(Pt 2):249–268
Dani N, Barbosa AJ, Del Rio A, Di Girolamo M (2013) ADP-Ribosylated proteins as old and new drug targets for anticancer therapy: the example of ARF6. Curr Pharm Des 19:624–633
David-Pfeuty T, Chakrani F, Ory K, Nouvian-Dooghe Y (1996) Cell cycle-dependent regulation of nuclear p53 traffic occurs in one subclass of human tumor cells and in untransformed cells. Cell Growth Differ 7:1211–1225
Di Girolamo M, Dani N, Stilla A, Corda D (2005) Physiological relevance of the endogenous mono(ADP-ribosyl)ation of cellular proteins. Febs J 272:4565–4575
Di Girolamo M, Fabrizio G, Scarpa ES, Di Paola S (2014) NAD^+-dependent enzymes at the endoplasmic reticulum. Curr Top Med Chem 13:3001–3010
Di Paola S, Micaroni M, Di Tullio G, Buccione R, Di Girolamo M (2012) PARP16/ARTD15 is a novel endoplasmic-reticulum-associated mono-ADP-ribosyltransferase that interacts with, and modifies Karyopherin-β1. PLoS ONE 7:e37352
Fabbro M, Henderson BR (2003) Regulation of tumor suppressors by nuclear-cytoplasmic shuttling. Exp Cell Res 282:59–69
Fahrenkrog B, Aebi U (2003) The nuclear pore complex: nucleocytoplasmic transport and beyond. Nat Rev Mol Cell Biol 4:757–766
Feijs KL, Kleine H, Braczynski A et al (2013) ARTD10 substrate identification on protein microarrays: regulation of GSK3β by mono-ADP-ribosylation. Cell Commun Signal 11:5
Fischer HE, Lichtiger B, Glassman AB (1995) Implications of human T-lymphotropic virus type-I and type-II testing in donors and patients. Ann Clin Lab Sci 25:373–380
Fried H, Kutay U (2003) Nucleocytoplasmic transport: taking an inventory. Cell Mol Life Sci 60:1659–1688
Friedrich B, Quensel C, Sommer T, Hartmann E, Kohler M (2006) Nuclear localization signal and protein context both mediate importin & #x03B1; specificity of nuclear import substrates. Mol Cell Biol 26:8697–8709
Gall JG (1954) Observations on the nuclear membrane with the electron microscope. Exp Cell Res 7:197–200
Goenka S, Cho SH, Boothby M (2007) Collaborator of Stat6 (CoaSt6)-associated poly(ADP-ribose) polymerase activity modulates Stat6-dependent gene transcription. J Biol Chem 282:18732–18739
Goldfarb DS, Corbett AH, Mason DA, Harreman MT, Adam SA (2004) Importin & #x03B1: a multipurpose nuclear-transport receptor. Trends Cell Biol 14:505–514
Gorlich D, Kutay U (1999) Transport between the cell nucleus and the cytoplasm. Annu Rev Cell Dev Biol 15:607–660
Hadian K, Krappmann D (2011) Signals from the nucleus: activation of NF-kappaB by cytosolic ATM in the DNA damage response. Sci Signal 4:pe2
Hassa PO, Hottiger MO (2008) The diverse biological roles of mammalian PARPS, a small but powerful family of poly-ADP-ribose polymerases. Front Biosci 13:3046–3082
Hetzer M, Gruss OJ, Mattaj IW (2002) The Ran GTPase as a marker of chromosome position in spindle formation and nuclear envelope assembly. Nat Cell Biol 4:E177–184
Hobbs HH, Russell DW, Brown MS, Goldstein JL (1990) The LDL receptor locus in familial hypercholesterolemia: mutational analysis of a membrane protein. Annu Rev Genet 24:133–170
Hollingsworth TJ, Gross AK (2012) Defective trafficking of rhodopsin and its role in retinal degenerations. Int Rev Cell Mol Biol 293:1–44
Hottiger MO, Hassa PO, Luscher B, Schuler H, Koch-Nolte F (2010) Toward a unified nomenclature for mammalian ADP-ribosyltransferases. Trends Biochem Sci 35:208–219
Jwa M, Chang P (2012) PARP16 is a tail-anchored endoplasmic reticulum protein required for the PERK- and IRE1α-mediated unfolded protein response. Nat Cell Biol 14:1223–1230

Kalab P, Heald R (2008) The RanGTP gradient - a GPS for the mitotic spindle. J Cell Sci 121:1577–1586
Kalbfleisch T, Cambon A, Wattenberg BW (2007) A bioinformatics approach to identifying tail-anchored proteins in the human genome. Traffic 8:1687–1694
Kalderon D, Roberts BL, Richardson WD, Smith AE (1984) A short amino acid sequence able to specify nuclear location. Cell 39:499–509
Kameoka M, Ota K, Tetsuka T, Tanaka Y, Itaya A, Okamoto T, Yoshihara K (2000) Evidence for regulation of NF-kappaB by poly(ADP-ribose) polymerase. Biochem J 346(Pt 3):641–649
Kanai M, Hanashiro K, Kim SH et al (2007) Inhibition of Crm1-p53 interaction and nuclear export of p53 by poly(ADP-ribosyl)ation. Nat Cell Biol 9:1175–1183
Keeshan K, Cotter TG, McKenna SL (2003) Bcr-Abl upregulates cytosolic p21WAF-1/CIP-1 by a phosphoinositide-3-kinase (PI3K)-independent pathway. Br J Haematol 123:34–44
Koch-Nolte F, Adriouch S, Bannas P et al (2006) ADP-ribosylation of membrane proteins: unveiling the secrets of a crucial regulatory mechanism in mammalian cells. Ann Med 38:188–199
Koch-Nolte F, Kernstock S, Mueller-Dieckmann C, Weiss MS, Haag F (2008) Mammalian ADP-ribosyltransferases and ADP-ribosylhydrolases. Front Biosci 13:6716–6729
Komarova EA, Zelnick CR, Chin D et al (1997) Intracellular localization of p53 tumor suppressor protein in & #x03B3;-irradiated cells is cell cycle regulated and determined by the nucleus. Cancer Res 57:5217–5220
Kudo N, Wolff B, Sekimoto T et al (1998) Leptomycin B inhibition of signal-mediated nuclear export by direct binding to CRM1. Exp Cell Res 242:540–547
Kutay U, Guttinger S (2005) Leucine-rich nuclear-export signals: born to be weak. Trends Cell Biol 15:121–124
la Cour T, Kiemer L, Molgaard A, Gupta R, Skriver K, Brunak S (2004) Analysis and prediction of leucine-rich nuclear export signals. Protein Eng Des Sel 17:527–536
Lanford RE, Butel JS (1984) Construction and characterization of an SV40 mutant defective in nuclear transport of T antigen. Cell 37:801–813
Loschberger A, van de Linde S, Dabauvalle MC et al (2012) Super-resolution imaging visualizes the eightfold symmetry of gp210 proteins around the nuclear pore complex and resolves the central channel with nanometer resolution. J Cell Sci 125:570–575
Macara IG (2001) Transport into and out of the nucleus. Microbiol Mol Biol Rev 65:570–594
Maimon T, Elad N, Dahan I, Medalia O (2012) The human nuclear pore complex as revealed by cryo-electron tomography. Structure 20:998–1006
Malanga M, Althaus FR (2011) Noncovalent protein interaction with poly(ADP-ribose). Methods Mol Biol 780:67–82
Mattaj IW, Englmeier L (1998) Nucleocytoplasmic transport: the soluble phase. Annu Rev Biochem 67:265–306
Michael WM (2000) Nucleocytoplasmic shuttling signals: two for the price of one. Trends Cell Biol 10:46–50
Michael WM, Eder PS, Dreyfuss G (1997) The K nuclear shuttling domain: a novel signal for nuclear import and nuclear export in the hnRNP K protein. Embo J 16:3587–3598
Miwa M, Masutani M (2007) PolyADP-ribosylation and cancer. Cancer Sci 98:1528–1535
Miyamoto S (2011) Nuclear initiated NF-kappaB signaling: NEMO and ATM take center stage. Cell Res 21:116–130
Moll UM, LaQuaglia M, Benard J, Riou G (1995) Wild-type p53 protein undergoes cytoplasmic sequestration in undifferentiated neuroblastomas but not in differentiated tumors. Proc Natl Acad Sci USA 92:4407–4411
Moore MS, Blobel G (1994a) A G protein involved in nucleocytoplasmic transport: the role of Ran. Trends Biochem Sci 19:211–216
Moore MS, Blobel G (1994b) Purification of a Ran-interacting protein that is required for protein import into the nucleus. Proc Natl Acad Sci USA 91:10212–10216
Nakielny S, Dreyfuss G (1999) Transport of proteins and RNAs in and out of the nucleus. Cell 99:677–690

Oeckinghaus A, Ghosh S (2009) The NF-kappaB family of transcription factors and its regulation. Cold Spring Harb Perspect Biol 1:a000034
Otto H, Reche PA, Bazan F, Dittmar K, Haag F, Koch-Nolte F (2005) In silico characterization of the family of PARP-like poly(ADP-ribosyl)transferases (pARTs). BMC Genomics 6:139
Pante N, Kann M (2002) Nuclear pore complex is able to transport macromolecules with diameters of about 39 nm. Mol Biol Cell 13:425–434
Paschal BM, Delphin C, Gerace L (1996) Nucleotide-specific interaction of Ran/TC4 with nuclear transport factors NTF2 and p97. Proc Natl Acad Sci USA 93:7679–7683
Paschal BM, Gerace L (1995) Identification of NTF2, a cytosolic factor for nuclear import that interacts with nuclear pore complex protein p62. J Cell Biol 129:925–937
Peralta-Leal A, Rodriguez-Vargas JM, Aguilar-Quesada R et al (2009) PARP inhibitors: new partners in the therapy of cancer and inflammatory diseases. Free Radic Biol Med 47:13–26
Polo S, Confalonieri S, Salcini AE, Di Fiore PP (2003) EH and UIM: endocytosis and more. Sci STKE 2003, re17
Poon IK, Jans DA (2005) Regulation of nuclear transport: central role in development and transformation? Traffic 6:173–186
Poortinga G, Hannan KM, Snelling H et al (2004) MAD1 and c-MYC regulate UBF and rDNA transcription during granulocyte differentiation. Embo J 23:3325–3335
Prokocimer M, Peller S (2012) Cytoplasmic sequestration of wild-type p53 in a patient with therapy-related resistant AML: first report. Med Oncol 29:1148–1150
Quimby BB, Dasso M (2003) The small GTPase Ran: interpreting the signs. Curr Opin Cell Biol 15:338–344
Rapoport TA (2007) Protein translocation across the eukaryotic endoplasmic reticulum and bacterial plasma membranes. Nature 450:663–669
Rensen WM, Mangiacasale R, Ciciarello M, Lavia P (2008) The GTPase Ran: regulation of cell life and potential roles in cell transformation. Front Biosci 13:4097–4121
Ribbeck K, Lipowsky G, Kent HM, Stewart M, Gorlich D (1998) NTF2 mediates nuclear import of Ran. Embo J 17:6587–6598
Robbins J, Dilworth SM, Laskey RA, Dingwall C (1991) Two interdependent basic domains in nucleoplasmin nuclear targeting sequence: identification of a class of bipartite nuclear targeting sequence. Cell 64:615–623
Rosenthal F, Feijs KL, Frugier E et al (2013) Macrodomain-containing proteins are new mono-ADP-ribosylhydrolases. Nat Struct Mol Biol 20:502–507
Schnell DJ, Hebert DN (2003) Protein translocons: multifunctional mediators of protein translocation across membranes. Cell 112:491–505
Schreiber V, Dantzer F, Ame JC, de Murcia G (2006) Poly(ADP-ribose): novel functions for an old molecule. Nat Rev Mol Cell Biol 7:517–528
Seman M, Adriouch S, Haag F, Koch-Nolte F (2004) Ecto-ADP-ribosyltransferases (ARTs): emerging actors in cell communication and signaling. Curr Med Chem 11:857–872
Shaulsky G, Ben-Ze'ev A, Rotter V (1990) Subcellular distribution of the p53 protein during the cell cycle of Balb/c 3T3 cells. Oncogene 5:1707–1711
Shcherbik N, Haines DS (2004) Ub on the move. J Cell Biochem 93:11–19
Siomi H, Dreyfuss G (1995) A nuclear localization domain in the hnRNP A1 protein. J Cell Biol 129:551–560
Slade D, Dunstan MS, Barkauskaite E et al (2011) The structure and catalytic mechanism of a poly(ADP-ribose) glycohydrolase. Nature 477:616–620
Stewart M (2007) Molecular mechanism of the nuclear protein import cycle. Nat Rev Mol Cell Biol 8:195–208
Stommel JM, Marchenko ND, Jimenez GS, Moll UM, Hope TJ, Wahl GM (1999) A leucine-rich nuclear export signal in the p53 tetramerization domain: regulation of subcellular localization and p53 activity by NES masking. Embo J 18:1660–1672
Strambio-De-Castillia C, Niepel M, Rout MP (2010) The nuclear pore complex: bridging nuclear transport and gene regulation. Nat Rev Mol Cell Biol 11:490–501

Suntharalingam M, Wente SR (2003) Peering through the pore: nuclear pore complex structure, assembly, and function. Dev Cell 4:775–789

Tedeschi A, Ciciarello M, Mangiacasale R, Roscioli E, Rensen WM, Lavia P (2007) RANBP1 localizes a subset of mitotic regulatory factors on spindle microtubules and regulates chromosome segregation in human cells. J Cell Sci 120:3748–3761

Terry LJ, Shows EB, Wente SR (2007) Crossing the nuclear envelope: hierarchical regulation of nucleocytoplasmic transport. Science 318:1412–1416

Tsukaguchi H, Matsubara H, Taketani S, Mori Y, Seido T, Inada M (1995) Binding-, intracellular transport-, and biosynthesis-defective mutants of vasopressin type 2 receptor in patients with X-linked nephrogenic diabetes insipidus. J Clin Invest 96:2043–2050

Tulu US, Fagerstrom C, Ferenz NP, Wadsworth P (2006) Molecular requirements for kinetochore-associated microtubule formation in mammalian cells. Curr Biol 16:536–541

Vandromme M, Gauthier-Rouviere C, Lamb N, Fernandez A (1996) Regulation of transcription factor localization: fine-tuning of gene expression. Trends Biochem Sci 21:59–64

Verheugd P, Forst AH, Milke L, Herzog N, Feijs KL, Kremmer E, Kleine H, Luscher B (2013) Regulation of NF-kappaB signalling by the mono-ADP-ribosyltransferase ARTD10. Nat Commun 4:1683

Webster M, Witkin KL, Cohen-Fix O (2009) Sizing up the nucleus: nuclear shape, size and nuclear-envelope assembly. J Cell Sci 122:1477–1486

Weis K (2003) Regulating access to the genome: nucleocytoplasmic transport throughout the cell cycle. Cell 112:441–451

Welsh MJ, Smith AE (1993) Molecular mechanisms of CFTR chloride channel dysfunction in cystic fibrosis. Cell 73:1251–1254

Wen W, Meinkoth JL, Tsien RY, Taylor SS (1995) Identification of a signal for rapid export of proteins from the nucleus. Cell 82:463–473

Wickner W, Schekman R (2005) Protein translocation across biological membranes. Science 310:1452–1456

Wu D, Pan W (2010) GSK3: a multifaceted kinase in Wnt signaling. Trends Biochem Sci 35:161–168

Yang J, Aittomaki S, Pesu M, Carter K, Saarinen J, Kalkkinen N, Kieff E, Silvennoinen O (2002) Identification of p100 as a coactivator for STAT6 that bridges STAT6 with RNA polymerase II. Embo J 21:4950–4958

Yates SP, Taylor PL, Jorgensen R, Ferraris D, Zhang J, Andersen GR, Merrill AR (2005) Structure-function analysis of water-soluble inhibitors of the catalytic domain of exotoxin A from Pseudomonas aeruginosa. Biochem J 385:667–675

Yu M, Schreek S, Cerni C et al (2005) PARP-10, a novel Myc-interacting protein with poly(ADP-ribose) polymerase activity, inhibits transformation. Oncogene 24:1982–1993

Zerfaoui M, Errami Y, Naura AS et al (2010) Poly(ADP-ribose) polymerase-1 is a determining factor in Crm1-mediated nuclear export and retention of p65 NF-kappa B upon TLR4 stimulation. J Immunol 185:1894–1902

Zhong Y, Wang Y, Yang H, Ballar P, Lee JG, Ye Y, Monteiro MJ, Fang S (2011) Importin & #x03B2; Interacts with the Endoplasmic Reticulum-associated Degradation Machinery and Promotes Ubiquitination and Degradation of Mutant & #x03B1;1-Antitrypsin. J Biol Chem 286:33921–33930

Index

Current Topics in Microbiology and Immunology (2015) 384: 211–213
DOI: 10.1007/978-3-319-10771-4